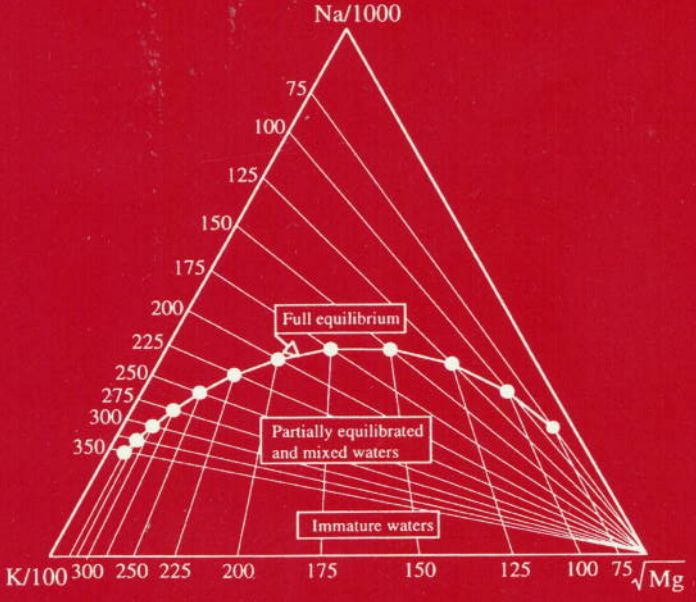

ISOTOPIC AND CHEMICAL TECHNIQUES IN GEOTHERMAL EXPLORATION, DEVELOPMENT AND USE

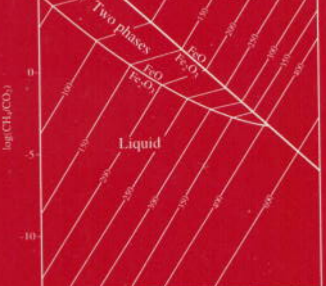

ISOTOPIC AND CHEMICAL TECHNIQUES IN GEOTHERMAL EXPLORATION, DEVELOPMENT AND USE

Edited by
Stefán Arnórsson

The following States are Members of the International Atomic Energy Agency:

AFGHANISTAN
ALBANIA
ALGERIA
ANGOLA
ARGENTINA
ARMENIA
AUSTRALIA
AUSTRIA
BANGLADESH
BELARUS
BELGIUM
BENIN
BOLIVIA
BOSNIA AND HERZEGOVINA
BRAZIL
BULGARIA
BURKINA FASO
CAMBODIA
CAMEROON
CANADA
CHILE
CHINA
COLOMBIA
COSTA RICA
COTE D'IVOIRE
CROATIA
CUBA
CYPRUS
CZECH REPUBLIC
DEMOCRATIC REPUBLIC OF THE CONGO
DENMARK
DOMINICAN REPUBLIC
ECUADOR
EGYPT
EL SALVADOR
ESTONIA
ETHIOPIA
FINLAND
FRANCE
GABON
GEORGIA
GERMANY
GHANA
GREECE
GUATEMALA
HAITI
HOLY SEE
HUNGARY
ICELAND
INDIA
INDONESIA
IRAN, ISLAMIC REPUBLIC OF
IRAQ
IRELAND
ISRAEL
ITALY
JAMAICA
JAPAN
JORDAN
KAZAKHSTAN
KENYA
KOREA, REPUBLIC OF
KUWAIT
LATVIA
LEBANON
LIBERIA
LIBYAN ARAB JAMAHIRIYA
LIECHTENSTEIN
LITHUANIA
LUXEMBOURG
MADAGASCAR
MALAYSIA
MALI
MALTA
MARSHALL ISLANDS
MAURITIUS
MEXICO
MONACO
MONGOLIA
MOROCCO
MYANMAR
NAMIBIA
NETHERLANDS
NEW ZEALAND
NICARAGUA
NIGER
NIGERIA
NORWAY
PAKISTAN
PANAMA
PARAGUAY
PERU
PHILIPPINES
POLAND
PORTUGAL
QATAR
REPUBLIC OF MOLDOVA
ROMANIA
RUSSIAN FEDERATION
SAUDI ARABIA
SENEGAL
SIERRA LEONE
SINGAPORE
SLOVAKIA
SLOVENIA
SOUTH AFRICA
SPAIN
SRI LANKA
SUDAN
SWEDEN
SWITZERLAND
SYRIAN ARAB REPUBLIC
THAILAND
THE FORMER YUGOSLAV REPUBLIC OF MACEDONIA
TUNISIA
TURKEY
UGANDA
UKRAINE
UNITED ARAB EMIRATES
UNITED KINGDOM OF GREAT BRITAIN AND NORTHERN IRELAND
UNITED REPUBLIC OF TANZANIA
UNITED STATES OF AMERICA
URUGUAY
UZBEKISTAN
VENEZUELA
VIET NAM
YEMEN
YUGOSLAVIA
ZAMBIA
ZIMBABWE

The Agency's Statute was approved on 23 October 1956 by the Conference on the Statute of the IAEA held at United Nations Headquarters, New York; it entered into force on 29 July 1957. The Headquarters of the Agency are situated in Vienna. Its principal objective is "to accelerate and enlarge the contribution of atomic energy to peace, health and prosperity throughout the world".

Printed by the IAEA in Austria
September 2000
STI/PUB/1086

ISOTOPIC AND CHEMICAL TECHNIQUES IN GEOTHERMAL EXPLORATION, DEVELOPMENT AND USE

SAMPLING METHODS, DATA HANDLING, INTERPRETATION

Edited by
Stefán Arnórsson

INTERNATIONAL ATOMIC ENERGY AGENCY
VIENNA, 2000

VIC Library Cataloguing in Publication Data

Isotopic and chemical techniques in geothermal exploration, development and use: sampling methods, data handling, interpretation / edited by Stefán Arnórsson.. — Vienna : International Atomic Energy Agency, 2000.
351 p. ; 24 cm.
STI/PUB/1086
ISBN 92–0–101600–X
Includes bibliographical references.

1. Geothermal resources — Sampling. 2. Radioisotopes in geology. I. Arnórsson, Stefán. II. International Atomic Energy Agency.

VICL 00–00248

FOREWORD

Since the eighties of the past century, the IAEA has been developing the applications of isotope and geochemical techniques applied to geothermal investigations. It has supported research on the development of isotope methods to geothermal development activities, with more emphasis on field applications, through its Technical Co-operation programmes. Twenty-five Member States have been recipients of assistance to undertake hydrological research and explore potential geothermal areas, manage reservoirs, protect the environment and establish laboratories in support of their energy programmes. This has resulted in intensive interaction with experts in industry and with Member States which use geothermal energy resources for electricity generation.

In 1995, an Advisory Group Meeting (AGM) was held on Isotope Applications in Geothermal Energy Development, with the participation of scientists from China, Ethiopia, Italy, Iceland, Indonesia, Japan, Mexico, New Zealand, Philippines, the Russian Federation, Switzerland, the United Kingdom and the USA. It was noted that the expanding applications of isotope techniques in geothermal operations, continuing IAEA technical co-operation on geothermal energy development and the increasing awareness for geothermal energy potential require a practical guide to facilitate field investigations as well as staff development in Member States. The meeting, therefore, recommended publication and dissemination of an updated manual of field methodologies on isotopes for sampling and data interpretation applied to geothermal investigations. This provided the IAEA an impetus to publish this book which was initially conceived in a Consultants Meeting on Instructional Manual on Methods for Isotope Sample Collection and Data Processing of Geothermal Fluids, organized in September 1997.

This book is designed as an instructional manual of essential nuclear and complementary methodologies for a multidisciplinary approach to geothermal exploration development and monitoring. It provides comprehensive procedures for carrying out isotope and geochemical investigations of geothermal systems, i.e. sampling, analysis and data interpretation. While it is intended for geoscientists working in various stages of geothermal projects, either in low or high enthalpy systems, this publication will also benefit those working in the cold water resources projects, where methods and principles of investigations are similar. The reader is also advised to consult the Agency's earlier two TECDOC publications on geothermal energy for case studies on exploration activities employing isotope techniques.

This book was edited by Stefán Arnórsson. Franco D'Amore made very important contributions to the text. In addition, the IAEA is grateful to L. Araguas-Araguas (Spain), M.A. Geyh (Germany) and scientists of the Philippine National Oil Company–Energy Development Corporation for reviewing the manuscripts.

EDITORIAL NOTE

CONTENTS

1. INTRODUCTION

Stefán Arnórsson

Geothermal energy is an important small energy resource whose exploitation has relatively insignificant environmental impact. The use of geothermal energy has proven to be cost effective in many countries where geological, hydrological and geophysical conditions are favourable to the formation of geothermal systems. This is particularly the case in active volcanic regions where geothermal gradients and rock permeabilities are high. However, economic geothermal reservoirs have also been discovered in sedimentary strata and fractured volcanics outside areas of recent volcanism.

Geothermal resources account for only a very small part of the world's present day energy consumption. They are, however, of high economic importance in many developing countries. The estimated world use of geothermal energy is summarized in Table 1.1. As may be deduced from this table, most countries exploiting geothermal resources have emphasized their use for electric power generation. Some countries, on the other hand, use geothermal water directly on a large scale, particularly for space heating.

The main factor determining the potential use of a particular geothermal resource is the reservoir temperature as summarized in Fig. 1.1.

The existence of geothermal reservoirs is manifested by the presence of hot springs and/or fumaroles. Exploration has, however, revealed that also hidden reservoirs exist. Sometimes there is little relationship between the distribution and intensity of surface geothermal activities only in an area and the extent and productivity of the underlying geothermal reservoir.

Geothermal exploration serves the purpose of locating geothermal areas favourable to development and to finding sites within them for drilling. This exploration includes geological mapping as well as geochemical and geophysical surveys. The principal purpose of geochemical surveys is to predict subsurface temperatures, to obtain information on the origin of the geothermal fluid and to understand subsurface flow directions. The basic philosophy behind geochemical prospecting for geothermal resources is that the concentrations of many components in the geothermal fluid, i.e. natural aqueous solutions and gaseous steam, reflect thermal conditions at depth. Studies in many drilled geothermal fields have shown that the aqueous concentrations of some chemical and isotopic components in well discharges are controlled by equilibrium with minerals in the aquifer rock. The aqueous concentrations of other components are, on the other

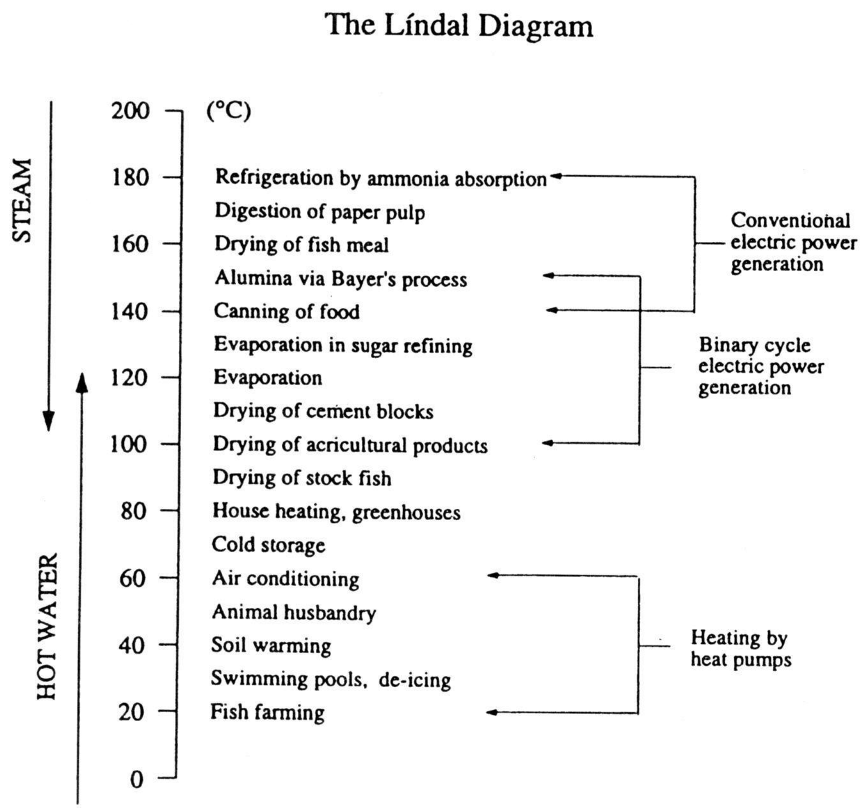

FIG. 1.1. Líndal diagram depicting the possible use of geothermal water and steam in relation to temperature.

hand, governed by their supply to the geothermal fluid. Equilibria between solution and minerals are generally temperature dependent in such a way that concentrations, or concentration ratios, of aqueous components change with temperature. The aqueous concentrations of chemical and isotopic components that have equilibrated with minerals in geothermal systems reflect, therefore, the temperature of the geothermal fluid. The same applies to isotopic equilibria between aqueous species.

In upflow zones of geothermal systems, the rising fluid often cools, either by conductive heat loss or by boiling, or by both. However, re-equilibration may be limited, partly because of the short residence time of the fluid in the upflow and partly because reaction rates decrease with decreasing temperatures. As a

TABLE 1.1. USE OF GEOTHERMAL ENERGY IN THE WORLD IN 1994, BY COUNTRY[a]

Country	Electric production		Direct use	
	Power (MW)	Annual use (GW·h)	Power (MW)	Annual use (GW·h)
China	28	98	2 143	5 527
Costa Rica	60	447		
El Salvador	105	419		
France	4	24	456	2 006
Georgia			245	2 136
Hungary			638	2 795
Iceland	50	265	1 443	5 878
Indonesia	309	1 048		
Italy	626	3 417		
Japan	299	1 722		
Kenya	45	348		
Macedonia			70	142
Mexico	753	5 877	28	74
New Zealand	286	2 193	264	1 837
Nicaragua	70	?		
Philippines	1 051	5 470		
Poland			63	206
Romania	2	?	137	765
Russian Federation	11	25	210	673
Serbia			80	660
Slovakia			100	502
Switzerland			110	243
Tunisia			90	788
Turkey	20	68	140	552
United States of America	2 817	16 491	1 874	3 859
Other countries		740	329	1 935
Total	6 543	37 952	9 047	33 514

[a] From Fridleifsson (1996).

result, the chemical and isotopic compositions of the fluid discharged at the surface can, and often do, reflect temperature conditions in the geothermal system below the zone of cooling in the upflow.

In some areas that are targets of geothermal exploration, there may be no surface manifestations. Geochemical techniques that involve identification of anomalies in the soil for components that are characteristically high in geothermal fluids, such as carbon dioxide or mercury, have been developed for such conditions. Sampling of fluids from shallow drillholes in such areas may be important.

Geochemistry plays an important role during geothermal exploration drillings and later development of geothermal reservoirs. Here, geochemistry furnishes data on the chemical properties of the discharged fluid, the level and temperature of producing aquifers in wells, and steam to water ratios in the reservoir. In this way, it contributes to the overall understanding of the production characteristics of the geothermal reservoir. It also quantifies scaling and corrosion tendencies.

After production has been initiated, geochemical monitoring is one of the most useful tools in mapping the response of the reservoir to the production load, including recharge, pressure drawdown and enhanced boiling. It is common to establish geochemical laboratory facilities at geothermal power plants to strengthen monitoring studies that contribute data pertinent to optimizing the economy of exploitation.

Geochemical studies of geothermal fluids essentially involve three steps:

(1) sampling;
(2) analysis;
(3) data interpretation.

Sampling involves some measurements on-site and appropriate treatment of the sample. In the case of natural manifestations, it also includes the selection of appropriate sampling sites. Upon storage, the chemical composition of the sample may change, at least with respect to some components. Later analysis — no matter how well done — will not give any correct information on the chemical and isotopic compositions of the geothermal fluid at the sampling site if sampling and sample treatment are inadequate. Interpretation of the analytical data suffers if either sampling or analysis, or both, are unsatisfactory. Sampling, analysis and data interpretation are generally most successful if the same person or the same team is involved in the whole process.

Once learned, sampling and analysis of geothermal fluids are routine procedures. On the other hand, interpretation of geochemical data never is, although many interpretation methods have been proposed and successfully used. No two geothermal fields are exactly alike. For this reason, studies in any particular field require an independent assessment of the geochemical data. The success of this independent assessment always rests to some extent on the background knowledge of the geochemist involved and on how well he can handle the subjects of physical chemistry, geochemistry, geology and hydrology, the first two disciplines being the most important.

Management of geochemical studies of geothermal fluids requires an expert with background knowledge in chemistry or geology (a chemist or a geochemist). Specifically, the disciplines in which skills are required are physical chemistry and/or geochemistry. The geochemical management essentially comprises four tasks:

(1) planning of specific activities such as geothermal exploration or monitoring studies of a reservoir under exploitation;
(2) supervision of sampling and sometimes also of analysis;
(3) data interpretation; and
(4) consultancy, i.e. providing recommendations to persons in charge of a specific project or operation.

This report focuses on the three stages of geochemical studies of geothermal fluids, i.e. sampling, analysis and data interpretation. In Chapters 2 to 6, some background information is provided on the strategy generally adopted in geothermal exploration and development and on the behaviour of chemical and isotopic components in the geothermal environment. Chapters 7 and 8 deal with the nature of surface thermal manifestations and sampling techniques while Chapter 9 focuses on analytical data handling and data presentation. The remaining chapters concentrate on data interpretation.

2. STRATEGY IN GEOTHERMAL EXPLORATION, DEVELOPMENT AND PRODUCTION

Stefán Arnórsson

As with Earth's mineral resources, an uncertainty is always involved with the success and economy of exploration and later development of geothermal resources. At the onset of geothermal exploration it is uncertain whether or not the efforts will result in economically, technically and environmentally feasible exploitation of the resource. The cause of the uncertainly lies in the extent of information available on the characteristics and the size of the anticipated geothermal resource. Geothermal exploration and development, therefore, invariably necessitate risk money that may end up as sunk cost if the exploration and development work yields a negative outcome, as far as the characteristics of the resource are concerned, so that exploitation cannot be realized.

Because of the uncertainty inherent in geothermal exploration and development, it has become common practice to divide the preparatory work into phases in an attempt to minimize cost and to maximize information for each phase. At the end of each phase, a decision is taken as to whether to continue or to terminate the development (Fig. 2.1). The phases are:

(1) Surface exploration to obtain indirect information on the extent of the geothermal reservoir, the subsurface temperatures and other features such as permeability control.
(2) Exploration drillings to obtain first direct information on reservoir temperature, pressure, permeability, reservoir fluid chemistry, etc.
(3) Appraisal (production) drillings to evaluate the characteristics of a prospective wellfield.
(4) Preliminary power plant design to analyse the economics of the project and to prepare a decision on building the plant.
(5) Financing, additional production drilling, preparation of tender documents, bidding and construction.

Geochemistry is extensively applied in all phases involved in geothermal exploration and development. It is also a major tool for monitoring studies. During the exploration phase, the task of geochemistry is largely twofold:

(1) To estimate subsurface temperatures by using isotope and chemical geothermometers as well as mixing models.
(2) To identify the source of the water, largely by using isotopic techniques.

During the exploration and appraisal drilling phases, geochemical investigations furnish various quantitative information including:

(1) the level of producing aquifers in wells and their temperature;
(2) the ratio of water to steam in the reservoir;

(3) assessment of the quality of water and steam in relation to the intended use and the environment;

(4) Scaling tendencies, both in production and injection wells and in surface equipment.

The results of exploration surveys and drillings are conveniently expressed in terms of conceptual models of the respective geothermal system. The model is updated as more information becomes available. Each time, the conceptual model summarizes the scientists' understanding of the geothermal system. It generally includes features such as distribution of aquifers, temperature, pressure and fluid flow.

Geothermal reservoirs are dynamic systems that will respond to the production load and, as a result, change their initial characteristics with time. These changes are basically due to pressure drop in the reservoir that will in turn lead to enhanced boiling (if the temperature is initially above 100°C) and enhanced recharge of new water into the reservoir. Data providing information on the long term response of a geothermal reservoir to production are necessary for specifying how the reservoir is best exploited economically and environmentally. These include physical, chemical and isotopic data.

Flow from wells decreases with time, often in a manner approaching exponential decline. The monitoring data are valuable for both timing and siting of replacement wells that are needed to make up for the decline in flow from existing production wells.

During the early years of geothermal utilization the waste fluid was generally disposed of by the least expensive method available. To minimize the environmental impact of geothermal exploitation, injection of the waste fluid has been adopted in many fields during the last one to two decades. Injection may also have the advantage of slowing down reduction in reservoir pressure and in this way increasing both the lifetime of individual wells and that of the wellfield as a whole. Injection may require the drilling of special wells, either within the geothermal reservoir or outside. Alternatively, production wells that turn out to be non-productive or very poor may be used for injection. At any rate, if injection is intended, this has to be taken into account during phase 3 in the development procedure for a geothermal resource (Fig. 2.1).

Geochemical monitoring studies focus largely on changes in well fluid compositions that result from boiling processes and recharge into the reservoir. They are principally used to:

(1) identify recharge into the reservoir of shallow cold water or of deeper hot water;

(2) assess boiling processes in producing aquifers;

1. Selection of area of interest
2. Report with plan on exploation

Decision on exploration

3. Geothermal exploration
   (Indirect information about size of area temperature and permeability)
4. Report on exploration results with recommendations for exploration drillings

Decision on exploration drillings

5. Exploration drilling and well testing
   (First direct information about temperature, pressure, lithology, permeability, fluid chemistry and well productivity. Revision of exploration data)
6. Report on results of exploration drillings with recommendations on the selection of a potential wellfield and appraisal drilings

Decision of appraisal drillings and preliminary design

7. Appraisal drillings, well measurements and testing
   (Further information on temperature, pressure and permeability in reservoir. Scaling and corrosion, tests, flow tests. First information on the production capacity of the reservoir and its response to the production load)
8. Preliminary engineering study of power plant
   (First assessment of power plant economy and preliminary design)

Decision on design

9. Production drillings, well measurements and testing
   (Provision of water/steam for power plant. Assessment of size and production characteristics of wellfield. Evaluation of productivity and longevity of wellfield by numerical simulation)
10. Engineering layout of power plant
   (design and economic analysis)

Engineering design of power plant

11. Further production drillings, well measurements and testing
   (Response of reservoir to exploitation)
12. Tender documents for construction
13. Construction
14. Production

Y = positive result

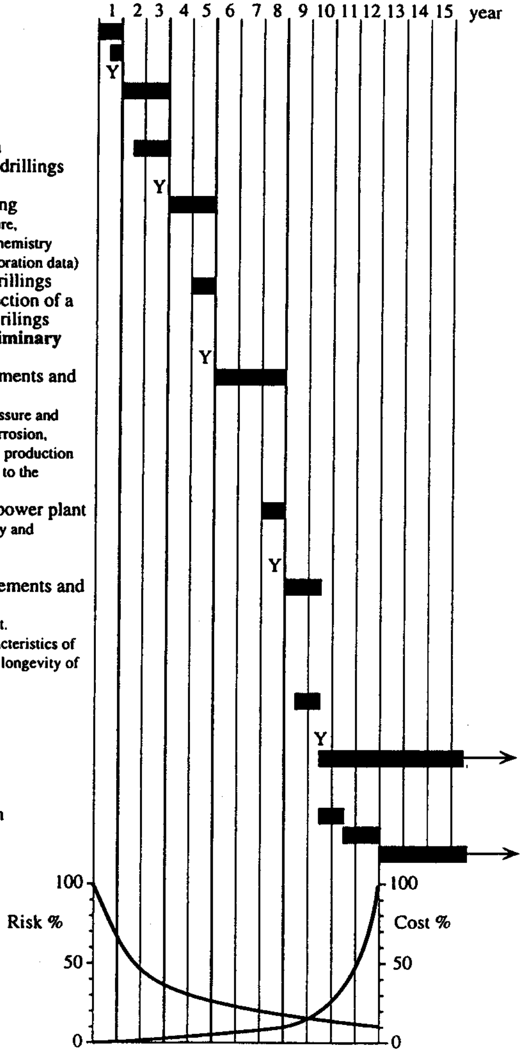

FIG. 2.1. Layout of strategy for geothermal exploration and development.

bicarbonate ions. Other homogeneous reactions are slow, such as those involving oxidation–reduction, e.g. reactions between dissolved sulphide and sulphate or carbon dioxide and methane. Equilibrium may, or may not, be closely approached between oxidized and reduced components of a particular element in groundwater systems, depending on the rate of the reaction, which is largely dictated by the temperature, and the temperature and pressure gradient across the system as well as by the fluid flow rate through it.

Early studies of geothermal fluid chemistry focused to a great extent on demonstrating whether or not chemical equilibrium was closely approached between the water and specific minerals. These studies involved comparing the concentrations of specific aqueous components with the solubility of hydrothermal minerals. This comparison was made at the aquifer temperature of wells because the solubility of most minerals is strongly temperature dependent. These early studies revealed that equilibrium was closely approached between the water and quartz in geothermal reservoirs, at least, if temperatures exceeded 180°C. At lower temperatures, equilibrium with chalcedony was approached. It was also shown that equilibrium was closely approached with calcite and later with Na and K feldspars, at least if temperatures exceeded some 100°C. In some systems equilibration with anhydrite and fluorite was attained. As improved thermodynamic data on aqueous species and minerals with more complex composition have become available in recent years that allow calculation of their solubilities, it has become possible to demonstrate that geothermal fluids are also close to equilibrium with complex Al silicates that exist as hydrothermal minerals in the geothermal systems.

When comparing well discharge compositions with the solubility of specific minerals with the purpose of demonstrating specific mineral–solution equilibrium/disequilibrium conditions in geothermal reservoirs, various simplifying assumptions are made in order to be able to make use of the concept of local equilibrium (Chapter 3.2). Firstly, specific models are adopted for calculation of reservoir fluid compositions (Chapter 12). This is, of course, relatively safe for hot water wells where the water discharged will be compositionally the same as the water in the aquifer, granting that no deposition from the water or dissolution from the rock has occurred during upflow in the well. The situation for mixed discharges of water and steam is more complicated. Here, boiling in producing aquifers and phase segregation may cause total well discharge composition and/or enthalpy to differ from any aquifer fluid composition and enthalpy (Chapter 12). Cooling of the water resulting from boiling by pressure drop may additionally bring about some mineral deposition or dissolution, Since dissolution of many rock forming minerals involves consumption of protons and release of cations into solution, together with silica, this dissolution process is conveniently described as a titration process, the water playing the role of the acid and the primary rock minerals the role of the base. Progressive rock mineral dissolution involves an increase in cation to proton ratios which is due to a decrease in hydrogen ion and/or an increase in the aqueous concentrations of the rock derived cations, or both. At equilibrium, cation/proton ratios will attain a particular value. This value will depend on the temperature and pressure of the system and the specific equilibrium (mineral) involved.

Since geothermal waters of a given temperature attain specific cation to proton ratios at equilibrium it is convenient to compute these ratios (Chapter 14) in order to assess the state of equilibrium of the water with respect to specific cations.

3.3. DEMONSTRATION/ASSUMPTION OF CHEMICAL EQUILIBRIUM

Thermodynamics does not deal with the rate of chemical reactions. The subject of reaction rates and reaction mechanisms belongs to kinetics, another major discipline of physical chemistry. In groundwater systems one may view chemical reactions as being of two types, homogeneous and heterogeneous. The former involves reactions between components in the aqueous phases but the latter reactions between components occupying the aqueous phase and some mineral or minerals of the rock. The rate of the latter type of reaction depends on the surface area between the phases as well as on temperature and the kinetic rate constant and how far the system departs from equilibrium. Rates of homogeneous reactions, on the other hand, only depend on temperature, the kinetic rate constant and departure from equilibrium. Since it is impossible for all practical purposes to measure or estimate with reasonable certainty the surface area between a mineral and the aqueous solution in a groundwater system, it is not possible with any confidence to estimate the time it takes for a given mineral–solution reaction to approach equilibrium to a given degree, even if the rate constant for this reaction is known. It should be emphasized here that exact equilibrium is only a hypothetical limiting case and as reactions proceed towards equilibrium their rate is reduced exponentially.

Some homogeneous reactions are fast and equilibrium can be closely approached within seconds, such as the reaction between hydrogen and as pyrite) and carbon (mostly as calcite) may be added in large amounts to altered rocks in the upflow zones of geothermal systems where boiling occurs. By contrast, the rock may become largely depleted of mobile elements such as chlorine and boron.

The overall water–rock interaction process in groundwater systems just described is a good example of an irreversible change. Yet, within parts of this system local equilibrium may be closely approached, at least for some components, i.e. a partial local equilibrium prevails.

The solubility of many primary silicate minerals of common rock types is pH dependent. Examples include olivines and pyroxenes as demonstrated below for Mg-olivine (forsterite) and CaMg-clinopyroxene (diopside):

$$Mg_2SiO_4 + 4H^+ = 2\ Mg^{2+} + H_4SiO_4^0 \quad (3.2)$$

and

$$CaMgSi_2O_6 + 4H^+ + 2H_2O = Ca^{2+} + Mg^{2+} + 2H_4SiO_4^0 \quad (3.3)$$

Other minerals display pH independent solubility in the pH range commonly observed in natural waters, such as the feldspars, as exemplified by albite below:

$$NaAlSi_3O_8 + 8H_2O = Na^+ + Al(OH)_4^- + 3H_4SiO_4^0 \quad (3.4)$$

At near neutral and alkaline pH, dissolved aluminium largely forms $Al(OH)_4^-$. In acid solution, on the other hand, dissolved aluminium largely occurs as Al^{3+}, in which case albite solubility becomes pH dependent:

$$NaAlSi_3O_8 + 4H_2O + 4H^+ = Na^+ + Al^{3+} + 3H_4SiO_4^0 \quad (3.5)$$

as is also the case in very alkaline water (pH > 10) when aqueous silica becomes considerably ionized, leading to

$$NaAlSi_3O_8 + 5H_2O + 3OH^- = Na^+ + Al(OH)_4^- + 3\ H_3SiO_4^0 \quad (3.6)$$

Mineral precipitation is also often pH related. An example is given by

$$Fe^{3+} + 3OH^- = Fe(OH)_3 \quad (3.7)$$

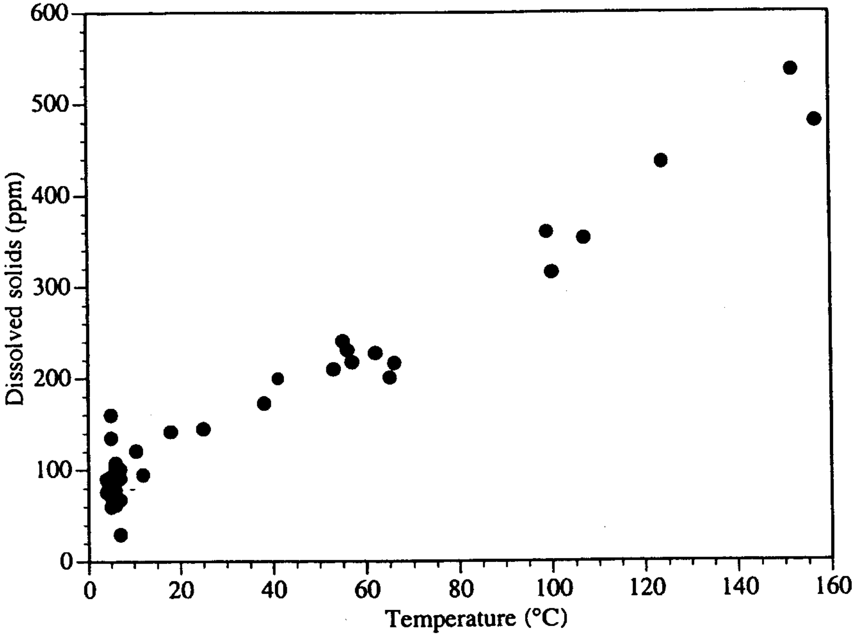

FIG. 3.1. Dissolved solids content, and surface and geothermal waters in the Hreppar-Land low temperature geothermal area in southern Iceland.

rock minerals that have formed in a high energy environment (such as minerals of igneous and high grade metamorphic rocks) are likely to be more soluble than hydrothermal minerals which form in a lower energy environment.

If secondary minerals are less soluble than the primary ones, the water will never reach saturation with the latter. Removal of dissolved constituents by precipitation of secondary minerals from the water ensures that the water remains undersaturated with the primary minerals. As a result, they will continue to dissolve, and the secondary minerals will continue to precipitate in their place. Given enough time the rock may be completely transformed mineralogically. During this process some material may be added to rock by the incoming water or may be extracted from it by the water leaving the system. However, for major rock components the hydrothermal alteration process is close to being isochemical. Trace elements may, on the other hand, be added to or subtracted from the rock in such amounts during the alteration process that their concentrations in the altered rock differ very much from those in the fresh rock. Thus, sulphur (mostly

(3) identify changes in the contribution of producing aquifers to the well output;
(4) quantify changes, if any, in scaling tendencies;
(5) quantify changes in water and steam quality; and
(6) revise conceptual reservoir models.

3. CHEMICAL REACTIONS AND CHEMICAL EQUILIBRIA

Stefán Arnórsson

3.1. SOME THERMODYNAMIC CONSIDERATIONS

Quantitative interpretation of the chemical and isotopic composition of geothermal fluids largely involves the application of chemical thermodynamics. *Thermodynamics,* which is one of the three disciplines of physical chemistry (the others are kinetics and quantum mechanics), involves the study of energy and its transformations. Chemical thermodynamics deals with the energy transformation associated with chemical reactions. It does not rest on the microscopic properties of matter but on measurable macroscopic properties such as volume, heat capacity, solubility, heat of reaction, temperature and pressure. The beauty and power of chemical thermodynamics lies in its ability to synthesize the numerous measured properties of matter into a unified framework through the application of mathematical thinking, allowing one to retrieve various thermodynamic parameters from the measurement of others.

Thermodynamics deals with systems, which may be regarded as a portion of matter separated from the rest of the observable universe by defined boundaries. These systems are either open, closed or isolated. An *open system* may exchange both matter and energy across its boundaries. On the other hand, a *closed system* allows energy, but not matter, to be transferred across its boundaries. An *isolated system* is entirely removed from its surroundings. Neither matter nor energy is allowed to flow across its boundaries.

Measurable properties of matter that describe its state are called *state variables.* Examples of state variables are temperature, pressure, volume and heat capacity. There are two kinds of state variable, intensive and extensive. *Intensive variables* are external to the thermodynamic system and independent of its matter, whereas the *extensive* ones are internal to the system, depending on the matter and its state in the system. Intensive variables include temperature and pressure while the extensive ones are the thermodynamic properties of matter such as volume, heat capacity, enthalpy and entropy.

A system is in a state of equilibrium if all the intensive variables are constant across the system. The equilibrium state is time and space invariant and, as the word equilibrium implies, a system at equilibrium has not tendency to change.

Some systems do not show any tendency to change although intensive variables, such as temperature, may vary across the system. Such systems are in a steady state. They are time invariant but not space invariant and can be open or closed, whereas the equilibrium system is an isolated one.

Further understanding of the equilibrium state is obtained by considerating reversible and irreversible changes. A chemical reaction that proceeds at a final rate is an *irreversible process*. It is called irreversible because it proceeds in one direction only. A reversible reaction, on the other hand, is an abstraction that can be closely approached but never totally realized in physical terms. To quote Nordstrom and Muñoz (1994): "In fact, reversibility is an alternative view of the equilibrium state; the impossibility of achieving a totally reversible process hinges on the paradox of achieving a process that is simultaneously at equilibrium state. One definition of a reversible process is a process that proceeds in such infinitely small stages that the system is at equilibrium for every step." In terms of molecular collision theory, chemical equilibrium is experienced when collision rates are equal in magnitude but opposite in direction for a particular chemical reaction.

Large systems on Earth are never at overall equilibrium. Geothermal systems and other groundwater systems provide a good example. On a short time scale, they may be regarded as steady state. Each part of the system remains unchanged. On the geological time-scale, on the other hand, geothermal systems are transient. Each system has a limited lifetime, and every part of the system changes, i.e. it evolves throughout its lifetime.

By considering groundwater convection from a recharge to a discharge area in a geothermal field, it becomes obvious that temperature, pressure and compositional gradients, or variations, exist across the system. It cannot be at overall equilibrium. Yet, numerous studies have indicated that equilibrium exists between fluids and minerals in geothermal systems. A more exact way of describing this would be to say that geochemical studies of geothermal systems indicate that the fluid is close to chemical equilibrium with some minerals in the rock.

The deduction of equilibrium between fluid and minerals in geothermal systems is based on the concept of local equilibrium. This concept assumes that one can isolate a small volume or part of a larger system so that equilibrium is maintained or, better, closely approached within this small volume and that all thermodynamic variables and relationships can be applied to this subsystem.

To define a chemical (thermodynamic) system completely, one must specify temperature, pressure and the concentration of all chemical components in this system (thermodynamics treats chemical and isotope components alike). However, if the system is at equilibrium, some of the variables are interrelated, as demonstrated by the Gibbs Phase Rule, and it is only necessary to define the independent variables in order to completely describe the system. The Gibbs Phase Rule is given by

$$P + F = C + 2 \tag{3.1}$$

where P and C stand for the number of phases and chemical components in the system and F is the number of independent variables. The phases of an equilibrated geothermal system are liquid water, the minerals with which it has equilibrated and steam, if present. A chemical component is a chemical species in the system that behaves independently. The number of chemical components in groundwater systems is maximally the total number element and isotopes in this system. If two isotopes or two elements freely substitute for each other in minerals (i.e. if they behave chemically or isotopically alike), they are appropriately classified as one component.

If equilibrium exists for all chemical and isotopic components in a system it may be shown that $P = C$, so the number of independent variables is two: the intensive variables temperature and pressure. Specifically for equilibrated geothermal systems, if both water and steam are present, the only independent variable is pressure. We have added one more phase without adding a component and from Eq. (3.1) we see that $F = 1$. When geothermal systems have two phases (water and steam are present), the pressure fixes the temperature of the system. It should be quite clear from physical considerations that it is not the temperature that fixes the pressure.

If a thermodynamic system has attained equilibrium for some components but not for others, it is said to be in a state of partial equilibrium. In order to define such a system completely it is necessary to specify, in addition to temperature and pressure, the concentrations of all the components that have not equilibrated (Box 3.1). In other words, the number of independent variables in the system is the number of non-equilibrated components plus two, i.e. temperature and pressure.

3.2. PROGRESSIVE WATER–ROCK INTERACTION

A groundwater system, such as a geothermal system, is characterized by a flow of fluid (water or steam or water–steam mixture) through a body of rock. This fluid will react with the rock chemically and, as is the case with any chemical reaction, change the system towards equilibrium. How closely equilibrium is approached at each point in the system (local equilibrium) depends on reaction rates and the rate of the through-flowing water. Reaction rates always increase with rising temperature. It is a useful rule of thumb to take reaction rates to increase two to three times for an increase in temperature by 10°C. Thus, an increase of 100°C increases reaction rates by 2^{10} to 3^{10}, or 1024 to 59 049 times. It is, thus, not surprising to observe that rocks are generally highly altered in high temperature geothermal systems ($t > 200°C$), whereas little alteration is observed in rocks close to the Earth's surface if they have never become appreciably heated after their formation.

In some geothermal systems a magmatic component may contribute to the chemical flux through the rock, in addition to the through-flowing water, and affect the questions of how closely equilibrium is approached.

It is generally accepted, as based on isotopic evidence, that geothermal waters are largely, if not solely, meteoric in origin. On the assumption that geothermal waters are, for all practical purposes, meteoric in origin, one may envisage progressive water–rock interaction towards equilibrium to proceed as meteoric water seeps into the ground and gains heat by contact with hot rock at depth. Rainwater, which is low in dissolved solids and slightly acid, is undersaturated with most, if not all, common minerals. This water, when it seeps into the soil and bedrock, will have the tendency to dissolve the rock minerals. In this process its dissolved solids content increases (Fig. 3.1). Reaction with organic material in the soil may also contribute to the dissolved matter in the water. As the dissolved solids content of the water increases owing to rock dissolution, the water approaches saturation (equilibrium) with the minerals of the rock. These minerals may indeed dissolve until the water becomes saturated with them. However, if the rock is igneous or high grade metamorphic, it is likely that the water will attain saturation with some other minerals that are less soluble than the primary ones before reaching saturation with the primary minerals of the rock. Primary changing the composition of the fluid as it moves through the aquifer and up the well to the wellhead where it is sampled.

The basic assumption underlying in testing mineral–solution equilibrium conditions, i.e. that the fluid discharged from a well was derived from a body of rock with specific composition, temperature and pressure, is at best an approximation. Most drilled geothermal reservoirs have very anisotropic permeability. When this is the case, the fluid discharged at any moment is a mixture of fluids that have travelled different distances through the rock from different sources, depending on the three dimensional distribution of permeabiilty in the formation. The different source areas within the reservoir may not satisfy the conditions implicit to the definition of local equilibrium as rock composition, temperature and pressure may not be the same.

The demonstration of a close approach to chemical equilibrium between specific aqueous components and hydrothermal minerals in geothermal systems resulted in the development of chemical and isotopic geothermometers. When applying geothermometers the situation with studies of well discharge chemistry is reversed. Equilibrium is assumed between specific aqueous solutes and minerals rather than an attempt is made to demonstrate this equilibrium by combining experimental and field data. As will be discussed in Chapter 10, the principal purpose of geothermometry is to estimate subsurface temperature in geothermal reservoirs from chemical analysis of hot spring and fumarole discharges, but geothermometry is also useful, in conjunction with temperature logging in wells, for locating the level of producing aquifers. It cannot be overemphasized that the assumptions of specific chemical and isotopic equilibria in geothermal reservoirs are subject to uncertainty, and so are the predicted geothermometry temperatures. How closely specific local chemical equilibria will be approached in a geothermal system depends on:

(1) the temperature of the system;
(2) the rate of fluxes of matter between phases and aqueous species in the system;
(3) the rate of fluxes of matter through the system; and
(4) the quantity of mass transfer required to reach equilibrium.

A geochemical study of a newly drilled geothermal field should always include a quantitative assessment of the chemical and isotopic compositions of the well fluids by analysing the overall state of chemical equilibrium in the reservoir.

3.4. THERMODYNAMIC TREATMENT OF EQUILIBRIUM

The free Gibbs energy (ΔG_r) of any chemical reaction is given by

$$\Delta G_r = \Delta G_r^0 + RT\ln Q \tag{3.8}$$

where ΔG_r^0 is the standard Gibbs energy of reaction (see Box 3.2), R is the gas constant, T the temperature in kelvin and Q the reaction quotient. The standard Gibbs energy of reaction is related to the equilibrium constant (K) by

$$RT\ln K = \mathrm{RT}\mathit{ln}\,Q \tag{3.9}$$

or $K = Q$ at equilibrium. If $K \neq Q$,, $\Delta G_r \neq 0$, and there is no equilibrium. Let us demonstrate this further by considering a reaction between albite and an aqueous solution:

$$NaAlSi_3O_8 + 8H_2O = Na^+ + Al(OH)_4^- + 3H_4SiO_4^0 \tag{3.4}$$

The reaction quotient, Q, for the reaction is given by

$$Q = \frac{a_{Na} \times a_{Al(OH)_4^-} \times a_{H_4SiO_4^0}^3}{a_{NaAlSi_3O_8} \times a_{H_2O}^8} \tag{3.10}$$

Here, a is the activity of the component indicated by the subscript, i.e. phases (albite, H_2O) and species (Na^+, $Al(OH)_4^-$ and $3H_4SiO_4^0$).

Sometimes, the term activity product (AP) is used instead of reaction quotient. When mineral–solution reactions are written with the mineral on the left hand side, $Q > K$ for a supersaturated solution and $Q < K$ for an undersaturated solution. The log of the Q/K ratio (log/Q/K) is called saturation index (SI). It is zero at equilibrium, positive for a supersaturated and negative for an undersaturated solution.

The activity of pure phases is 1. If the water that is involved in the reaction with albite is low in dissolved constituents (<1–2%), it can be regarded as almost pure, in which case its activity is close to 1, and Eq. (3.10) reduces to

$$Q = a_{Na^+} \times a_{Al(OH)_4^-} \times a_{H_4SiO_4^0}^3 \tag{3.10}$$

When studying whether a particular mineral–solution system is at equilibrium, thermodynamic data are needed on the respective equilibrium constant (K), and the value of the reaction quotient (Q) can be calculated from chemical analysis of the water. Such calculations are too complex or, better, too extensive for calculation 'by hand'. Aqueous speciation programmes are required for calculation of the activities of individual aqueous species and reaction quotients (see Sections 3.5 to 3.8 below).

The solubility constants for very many minerals can be calculated from published thermodynamic data on these minerals and the aqueous species that participate in the reaction (Boxes 3.3 and 3.4).

3.5. EFFECTS OF TEMPERATURE AND PRESSURE

The thermodynamic properties of substances change with temperature and pressure. The changes in enthalpy and entropy with temperature at a particular pressure are given by:

$$\left(\frac{\partial H}{\partial T}\right)_P = C_p \qquad (3.11)$$

and

$$\left(\frac{\partial S}{\partial T}\right)_P = \frac{C_p}{T} \qquad (3.12)$$

where H, S and C_p designate enthalpy, entropy and heat capacity, respectively. Replacing both enthalpy and entropy by their standard state counterparts for compound i yields:

$$\Delta H^0_{f,i,T} = \int_{T_r}^{T} C^0_{p,i} dT \qquad (3.13)$$

and

$$S^0_{i,T} = \int_{T_r}^{T} \frac{C^0_{p,i}}{T} dT \qquad (3.14)$$

Heat capacity varies with temperature. Experimental data are required to establish the C_p variations with temperature for compounds and reactions. A widely used heat capacity–temperature polynomial is given by

$$C^0_{p,i} = a + 2b \times T + c \times T^{-2} + g \times T^{-0.5} \tag{3.15}$$

However, other types of polynomial have been proposed but will not be considered here. The parameters a to g in Eq. (3.15) are temperature and pressure independent. Often it may be satisfactory to take one or more of these parameters to be equal to zero in describing the temperature dependence of heat capacity for compounds and reactions, at least, over a limited temperature range. Inserting the polynomial (3.15) into expressions (3.13) and (3.14) and integrating yields

$$\begin{aligned}\Delta H^0_{f,i,T} = \Delta H^0_{f,i,T_r} &+ a(T - T_r) + b(T^2 - T_r^2)\\ &- c(T^{-1} - T_r^{-1}) + \frac{f}{3}(T^3 - T_r^3) + \frac{g}{0.5}(T^{0.5} - T_r^{0.5})\end{aligned} \tag{3.13a}$$

$$\begin{aligned}S^0_{i,T} = S^0_{i,T_r} &+ a\ln(T / T_r) + 2b(T - T_r)\\ &- \frac{c}{2}(T^{-2} - T_r^{-2}) + \frac{f}{2}(T^2 - T_r^2) - \frac{g}{0.5}(T^{-0.5} - T_r^{-0.5})\end{aligned} \tag{3.14a}$$

where the integral constants in Eqs (3.13a) and (3.14a) are $\Delta H^0_{\mathrm{f},i,T_2}$ and $\Delta G^0_{i,T_r}$, respectively.

The variations in the Gibbs energy of compounds with temperature and pressure are given by

$$\left(\frac{\partial G}{\partial T}\right)_P = -S \tag{3.16}$$

and

$$\left(\frac{\partial G}{\partial T}\right)_T = V \tag{3.17}$$

Here, V designates the volume. The volume varies both with temperature and pressure. The temperature variation of the volume at constant pressure is called thermal expansivity, α, and is defined as

$$\alpha = \frac{1}{V}\left(\frac{\partial V}{\partial T}\right)_P \tag{3.18}$$

The change in volume by pressure is the compressibility, β, which is defined as

$$-\beta = \frac{1}{V}\left(\frac{\partial V}{\partial P}\right)_T \tag{3.19}$$

The negative sign ensures that β is positive because an increase of pressure (positive ∂P) brings about a reduction of volume (negative ∂V).

As can be seen from Eqs (3.14), (3.16) and (3.17), the change in the standard Gibbs energy of a compound i in going from temperature and pressure T_r and P_r to temperature T and pressure P is given by

$$\Delta G^0_{f,i,T,P} = -\int_{T_r}^{T}\int_{T_r}^{T} \frac{C^0_{p,i}}{T}\,dT + \int_{P_r}^{P} V_i^0\,dP \tag{3.20}$$

Solution of Eq. (3.20) requires solving a double integral which is somewhat tricky. This double integral is equal to

$$-\int_{T_r}^{T}\int_{T_r}^{T} \frac{C^0_{p,i}}{T}\,dT = \int_{T_r}^{T} C^0_{p,i}\,dT - T\int_{T_r}^{T} \frac{C^0_{p,i}}{T}\,dT \tag{3.21}$$

so that

$$\Delta G^0_{f,i,T,P} = -\int_{T_r}^{T} C^0_{p,i}\,dT - T\int_{T_r}^{T} \frac{C^0_{p,i}}{T}\,dT + \int_{P_r}^{P} V_i^0\,dP \tag{3.21a}$$

From Eqs (3.13), (3.13a), (3.14), (3.14a) and (3.21a), we see that

$$\begin{aligned}\Delta G^0_{f,i,T,P} = {} & \Delta H^0_{f,i,T_r} + a(T - T_r) + b(T^2 - T_r^0) \\ & - c(T^{-1} - T_r^{-1}) + \frac{f}{3}(T^3 - T_r^3) + \frac{g}{0.5}(T^{0.5} - T_r^{0.5}) \\ & - T\left[S^0_{i,T_r} + a\ln(T/T_r) + 2b(T - T_r) - \frac{c}{2}(T^{-2} - T_r^{-2})\right. \\ & \left. + \frac{f}{2}(T^2 - T_r^2) - \frac{g}{0.5}(T^{-0.5} - T_r^{-0.5})\right] + \int_{P_r}^{P} V_i^0\,dP\end{aligned} \tag{3.21b}$$

It is common practice to take the volumes, of both minerals and aqueous species, to be temperature and pressure independent, at least in the range occurring in geothermal systems. This is considered to be a satisfactory approximation in which case the pressure term in Eq. (3.21a) becomes

$$\int_{P_r}^{P} V_i^0 = V_i^0(P - P_r) \tag{3.22}$$

Substituting expression (3.22) into Eq. (3.21b) and rearranging yields

$$\begin{aligned}\Delta G^0_{f,i,T,P} = {} & \Delta H^0_{f,i,T_r,P_r} - TS^0_{i,T_r,P_r} \\ & + a\left[T - T_r - T(\ln T - \ln T_r)\right] + b\left[(T - T_r)(T_r - T)\right] \\ & + c\left[\frac{1}{T_r} - \frac{1}{2T} - \frac{T}{2T_r^2}\right] + f\left[\frac{TT_r^2}{2} - \frac{T^3}{6} - \frac{T_r^3}{3}\right] \\ & + g\left[4 \times T^{0.5} - \frac{2T}{T_r^{0.5}} - 2T_r^{0.5}\right] + V_i^0(P - P_r)\end{aligned} \tag{3.21c}$$

Sometimes, the first two terms on the right hand side of this equation are replaced by $\Delta G^0_{f,i,T_r,P_r} - S^0_{i,T_r,P_r}(T - T_r)$, which leads to

$$\begin{aligned}\Delta \bar{G}^0_{i,T,P} = {} & \Delta G^0_{f,i,T_r,P_r} - S^0_{i,T_r,P_r}(T - T_r) \\ & + a\left[T - T_r - T(\ln T - \ln T_r)\right] + b\left[(T - T_r)(T_r - T)\right] \\ & + c\left[\frac{1}{T_r} - \frac{1}{2T} - \frac{T}{2T_r^2}\right] + f\left[\frac{TT_r^2}{2} - \frac{T^3}{6} - \frac{T_r^3}{3}\right] \\ & + g\left[4 \times T^{0.5} - \frac{2T}{T_r^{0.5}} - 2T_r^{0.5}\right] + V_i^0(P - P_r)\end{aligned} \tag{3.23}$$

$\Delta G^0_{f,i,T,P}$ is called the standard molal Gibbs energy of formation at temperature T and pressure P, whereas $\Delta \bar{G}^0_{i,T,P}$ is the standard apparent Gibbs energy of compound i under the same conditions. The difference between the two energies is

$$\Delta G^0_{f,i,T,P} - \Delta \bar{G}^0_{i,T,P} = \Delta H^0_{f,i,T_r,P_r} - TS^0_{i,,T_r,P_r} - \Delta G^0_{f,i,T_r,P_r} \tag{3.24}$$

As

$$\Delta G^0_{f,i,T_r,P_r} = \Delta H^0_{f,i,T_r,P_r} - T\Delta S^0_{f,i,T_r,P_r} \tag{3.25}$$

we see that

$$\Delta G^0_{f,i,T,P} - \Delta \bar{G}^0_{i,T,P} = \mathrm{T}(\Delta S^0_{f,i,T_r,P_r} - S^0_{i,T_r,P_r}) \tag{3.25a}$$

It is convenient to use the apparent Gibbs energy for compounds because, when this is done, the form of Eq. (3.23) is exactly the same for compounds and reactions, i.e. for any reaction we have

$$\begin{aligned}\Delta G^0_{r,T,P} = {} & \Delta G^0_{r,T_r,P_r} - \Delta S^0_{r,T_r,P_r}(T - T_r) \\ & + \Delta a[T - T_r - T(\ln T - \ln T_r)] + \Delta b[(T - T_r)(T_r - T)] \qquad (3.26) \\ & + \Delta c\left[\frac{1}{T_r} - \frac{1}{2T} - \frac{T}{2T^2}\right] + \Delta f\left[\frac{TT_r^2}{2} - \frac{T^3}{6} - \frac{T_r^3}{3}\right] \\ & + \Delta g\left[4 \times T^{0.5} - \frac{2T}{T_r^{0.5}} - 2T_r^{0.5}\right] + \Delta V_i^0(P - P_r)\end{aligned}$$

Inspection of thermodynamic data for many minerals and aqueous species shows that pressure has little effect on their Gibbs energy in the range occurring in geothermal systems (1–200 bars), at least, compared to temperature. It is convenient to eliminate pressure as a variable, in which case the heat capacity parameters are valid either at 1 bar or at some other specified pressure. In the example given in Box 3.4, the heat capacity parameters reported are valid at 1 bar below 100°C and at vapour saturation pressures at higher temperatures.

3.6. AQUEOUS SPECIATION

When solids and gases dissolve in water, they react with the water molecules or between themselves to form various kinds of aqueous species such as free ions, ion pairs or hydrolysed ions. Some solid compounds form, at least partly, strong covalent bounds between elements. When such solids dissolve the covalent bonds do not break. Examples include covalent bonds between C and O in carbonates and S and O in sulphates. Aqueous species consisting of more than one covalent bond element are called complexes. Carbonate (HCO^3_-,CO_3^{--}) and sulphate (HSO_4^-, SO_4^{--}) are examples of complexes.

When salts dissolve in water and form ions, the cause is that it is energetically more favourable to have ions attached to water molecules than to have ions of opposite charge bonded together in a crystal. Water molecules possess the properties of a dipole, i.e. they carry small negative charges at one end and small positive ones at the other. Anions are attracted to the positive ends of water molecules and cations to the negative ones. Water molecules regularly oriented around a cation or an anion are said to be co-ordinated. There may be more than one layer of coordinated water molecules. The number of water molecules in the innermost layer depends on the size of the cation. In the example of silicon, Si^{4+}, which has a small radius (0.39 Å), only four water molecules are around. For the larger sodium ion (0.97 Å), there are six and for the very large caesium ion (1.87 Å) there are 12 water molecules. Anions are, in general, large so that they sho, a weaker tendency than cations to coordinate water molecules around themselves.

One or more of the water molecules surrounding a cation may lose a proton owing to the repulsive force of its positive charge on the positive charges of the protons in the co-ordinated water molecules. Cations reacting with water in this way are said to be hydrolysed. An example is given by Al:

$$Al^{3+} + H_2O = AlOH^{2+} + H^+ \qquad (3.27)$$

and

$$AlOH^{2+} + H_2O = Al(OH)_2^+ + H^+ \qquad (3.28)$$

$$Na(H_2O)_6^+ + Cl^- = NaCl(H_2O)_5^0 + H_2O \qquad (3.29)$$

Reactions between sodium and chloride ions in aqueous solution are generally expressed without explicitly denoting the involvement of the water molecules, i.e.

$$Na^+ + Cl^- = NaCl^0 \qquad (3.29a)$$

Hydrolysed cations are often referred to as hydroxide complexes, and the reaction is written as

$$Al^{3+} + OH^- = AlOH^{2+} \qquad (3.30)$$

or, written in terms of dissociation,

$$AlOH^{2+} = Al^{3+} + OH^- \qquad (3.30a)$$

i.e. expressed as the dissociation of a hydroxide complex.

The quantitative treatment of cation hydrolysis and ion pair formation is based on the concept of equilibrium between ions, hydrolysed ions and ion pairs. For reactions (3.29a) and (3.30a), we have

$$K_d = \frac{a_{\mathrm{Na^+}} a_{\mathrm{Cl^-}}}{a_{\mathrm{NaCl^0}}} \tag{3.31}$$

and

$$K_d = \frac{a_{\mathrm{Al^{3+}}} a_{\mathrm{OH^-}}}{a_{\mathrm{AlOH^{2+}}}} \tag{3.32}$$

3.7. CONCENTRATION AND ACTIVITY

Activity describes the thermodynamic behaviour of aqueous species. In a hypothetical solution of infinite dilution, activity becomes equal to concentration. In real solutions, activity deviates from concentration. This deviation is described by the activity coefficient, or

$$a_i = \gamma_i m_i \tag{3.33}$$

where a_i stands for the activity of aqueous species i (in mol · kg^{-1}) and γ_i and m_i stand for its activity coefficient (dimensionless quantity) and concentration (in mol · kg^{-1}), respectively.

The reason why a real solution deviates from an ideal (infinitely dilute) one is the interaction between species in solution. The amount of interaction depends on the types and numbers of aqueous species present in solution.

In geothermal chemistry an extended form of the Debye–Hückel equation is used to retrieve the values of the activity coefficients of individual aqueous species. This permits the conversion concentrations into activities according to Eq. (3.33). The extended Debye–Hückel equation is given by

$$\log \gamma_i = \frac{-A z_i^2 \sqrt{I}}{1 + \mathring{a}_i B \sqrt{I}} + \dot{b} I \tag{3.34}$$

Here, A and B are constants depending on the temperature and density of the water (Box 3.5), $\mathring{a}_i$ is the effective electrostatic radius of ion i, and I is the ionic strength of the solution. $\dot{b}$ is a constant depending on the salt content of the solution.

The approximation of taking $\dot{b}$ to be equal to zero is frequently made; in this case the activity coefficient of uncharged species ($z_i = 0$) is equal to unity, i.e. $a_i = m_i$.

Calculation of activity coefficients requires knowledge of the ionic strength of the solution. The ionic strength, I, is defined as

$$I = \frac{1}{2}\sum m_i z_i^2 \tag{3.35}$$

where m_i stands for the molal concentration of each ion and z_i its charge.

The ionic strength can be calculated approximately from analytical data. However, a precise calculation of the ionic strength requires an iteration process taking into account ion pairing.

3.8. CALCULATION OF AQUEOUS SPECIATION

Analyses of water and steam samples yield information on the concentration of the individual chemical components. Thermodynamic interpretations of the data with respect to equilibrium studies are, on the other hand, based on activities of the individual aqueous species. Therefore, an interpretation requires transformation of measured concentrations in activities.

Each analysed component can constitute more than one species. The relative abundance of interacting aqueous species is described by the equilibrium constants (dissociation constants). To calculate the activity of individual species: it is necessary to solve together two types of equation, mass balance equations, and dissociational equilibria. For natural waters for which 10 to 20 or more components are analysed, and having tens, if not hundreds of species, such calculations are very extensive and require chemical speciation computer programs. Box 3.6 provides a brief description of how to solve together these two types of equation. To keep the problem in Box 3.6 simple, only four components and 13 species are included.

BOX 3.1. INDEPENDENT VARIABLES IN GEOTHERMAL SYSTEMS

Most common analysis of geothermal well discharges includes only major chemical components in samples of water and steam as well as ^{2}H and ^{18}O. The major components in water samples include Si, B, Na, K, Ca, Mg, SO_4 (sulphate sulphur), H_2S (sulphide sulphur), CO_2 (carbonate carbon), NH_3, Cl, F, ^{2}H and ^{18}O. Occasionally Al, Fe and various trace elements are also analysed for. Although Mg, Fe and Al are minor components in the water, they are major components in the rock and, therefore, in the system. Additionally, pH is always measured. In gas samples, CO_2, H_2S, H_2, CH_4O_2 (not detectable in atmospherically uncominated samples), N_2, NH_3, Ar, ^{2}H and ^{18}O are most often determined. The total number of components analysed for in both phases, when Al, Fe and hydrogen ion (pH) are included, is 23. Observe that five elements are considered as constituting two components each: C (carbonate carbon and methane), N (nitrogen gas and ammonia), S (sulphate and sulphide sulphur), H (hydrogen ion and H_2 gas) and O (as O^{--} and O_2 gas). The components of these elements occur in two different oxidation states and, indeed, there are analytical methods for their separate determination. Of the 23 components analysed for, 13 are known to enter hydrothermal minerals as shown below. They are said to be compatible components.

Compatible component	Mineral	Compatible component	Mineral
Si	quartz, various silicates	Na	low-albite
K	K feldspar	Ca	calcite, anhydrite, fluorite
Mg	chlorite	Al	epidote, prehnite, chlorite
Fe	epidote, pyrite, pyrrhotite	SO_4	anhydrite
H_2S	pyrite, pyrrhotite	CO_2	calcite
F	fluorite	H (as OH)	chlorite, epidote, prehnite
O (as O^{2-})	most minerals		

BOX 3.1. (cont.)

Other components have no tendency to enter hydrothermal minerals. These include B, Cl, NH_3, H_2, O_2, N_2, CH_4 and Ar.

Mineral–solution equilibria fix the aqueous concentrations of the components entering the minerals. Mineral equilibria can also fix aqueous concentrations of other components, e.g.

$$FeS + H_2S = FeS_2 + H_2$$

fixes H_2 because other equilibria fix H_2S.

If there is equilibrium between two or more components in the aqueous phase that do not enter minerals, this equilibrium fixes their relative concentrations, e.g.

$$2NH_3 = N_2 + 3H_2$$
$$CO_2 + 4H_2 = CH_4 + 2H_2O$$
$$2H_2O = 2H_2 + O_2$$

and, if some of these components are fixed by mineral equilibria, the other components will be fixed through the relevant solute equilibria. Thus, O_2 is fixed by the last reaction as H_2 is fixed by mineral equilibria. CH_4 is also fixed – by the second reaction –, since CO_2 and H_2 are fixed by mineral equilibria. Neihter N_2 nor NH_3 enter the minerals. Equilibrium according to the first reaction fixes one component if the other is specified. Counting all the components fixed by chemical reactions, either between fluid and minerals, or between components in the aqueous phase, yields 17. There remain four components (B, Cl, Ar and either N_2 or NH_3) in addition to ^2H, ^{18}O. In order to describe the system fully one needs to specify temperature, pressure and the six components that are not fixed by equilibria.

Deuterium and ^{18}O react with the rock by exchange but do not equilibrate. They are, therefore, independent components. The exchange for ^2H is trivial, as the amount of hydrogen in the rock is trivial compared to the amount of hydrogen in the through-flowing water. The amount of ^{18}O exchange, on the other hand, can be quite large and is dictated by the amount of water–rock interaction in the system.

BOX 3.2. THE STANDARD STATE

It is not possible to determine the Gibbs energy and enthalpy of substances, only changes in these quantities associated with chemical reactions. By convention, the standard Gibbs energy and the standard enthalpy of the elements are taken to be zero at 25°C and 1 bar. When elements combine with themselves to form compounds which are stable at 25°C and 1 bar, like O_2 and H_2, their Gibbs energy and enthalpy are taken to be zero at these conditions. The standard Gibbs energy and standard enthalpy of compounds of two or more elements are relative to the values chosen for the elements and are termed standard Gibbs energy of formation from the elements and standard enthalpy of formation from the elements, respectively. They are symbolized byΔG_f^0 and ΔH_f^0, respectively.

The standard enthalpy of formation from the elements of compounds is determined experimentally. Consider the reaction:

$$2H_2 + O_2 = 2H_2O$$

The enthalpy of this reaction, as measured experimentally at 25°C and 1 bar, i.e. the standard enthalpy of the reaction (ΔH_f^0), is –571 660 J, i.e. –285 830 J per mol of water. The negatie value indicates that the reaction is exothermic, i.e. heat is given off. By definition, the standard enthalpies of hydrogen gas and oxygen gas are zero. For an isolated system (heat is conserved), we can write:

$$\Delta H_r^0 = 2 \times \Delta H_{f,H_2O}^0 - 2 \times \Delta H_{f,H_2}^0 - \Delta H_{f,O_2}^0 = -571\,660 \text{ J}$$

so $\Delta H_{f,H_2O}^0 = -285\,830 \text{ J} \cdot \text{mol}^{-1}$.

Let us assume that we can determine the equilibrium constant for the following reaction:

$$C + O_2 = CO_2$$

and that the log K value at 25°C and 1 bar is 69.092. From Eq. (3.9) we can calculate the Gibbs energy of the reaction as –394 375 J · mol^{-1}. Since

$$\Delta G_r^0 = \Delta G_{f,CO_2}^0 - \Delta G_{f,C}^0 - \Delta G_{f,O_2}^0$$

it follows that

BOX 3.2. (cont.)

$$-394\ 375 = \Delta G^0_{f,\mathrm{CO_2}} - 0 - 0$$

and $\Delta G^0_{\mathrm{f,\,CO_2}} = -394\ 375\ \mathrm{J \cdot mol^{-1}}$. By successive experiments one can retrieve the Gibbs energy and enthalpy of the formation values for other compounds.

Unlike Gibbs energy and enthalpy, it is possible to measure the absolute entropy of both elements and compounds. From the relationship

$$\frac{\partial S}{\partial T} = \frac{C_p}{T}$$

and the fact that $C_p \rightarrow 0$ for T → 0, it follows that $S \rightarrow 0$ for $T \rightarrow 0$. T is the temperature in kelvin. Thus, entropy of all substances is zero at $T = 0$. By experimentally determining the heat capacity (C_p) over a range of temperatures from near $T = 0$ to $T > 298.15$ K (25°C), a value for the standard absolute entropy (S^0) of substances at 25°C and 1 bar can be retrieved.

BOX 3.3. CALCULATION OF THE EQUILIBRIUM CONSTANT FOR MINERAL–SOLUTION REACTIONS AT 25°C AND 1 BAR

The standard Gibbs energy of formation from the elements (ΔG_f^0), standard enthalpy of formation from the elements (ΔH_f^0) and absolute entropy (S^0) of calcite ($CaCO_3$), liquid water (H_2O_l) and several aqueous species are as follows:

	ΔG_f^0	ΔH_f^0	S^0
$CaCO_3$	–1 128 295	–1 206 819	91.72
H_2O	–237 140	–285 830	69.95
H^+	0	0	0
Ca^{2+}	–552 791	–543 083	–56.48
$CO_{2,aq}$	–385 980	–413 508	118.45

We calculate the value of the equilibrium constant for the reaction:

$$CaCO_3 + 2H^+ = Ca^{2+} + CO_{2,aq} + H_2O$$

First, we have

$$\Delta G_r^0 = \sum_i \upsilon \Delta G_{f,i}^0$$

where υ represents the stoichiometric constant which is positive for products and negative for reactants,

$$\begin{aligned} \Delta G_r^0 &= \Delta G_{f,\mathrm{Ca}^{2+}}^0 + \Delta G_{f,\mathrm{CO}_{2,aq}}^0 + \Delta G_{f,\mathrm{H_2O}}^0 \\ &\quad - \Delta G_{f,\mathrm{CaCO_3}}^0 - 2 \times \Delta G_{f,\mathrm{H}^+}^0 = -47\,616\ \mathrm{J \cdot mol^{-1}} \end{aligned}$$

As

$$\Delta G_r^0 = -RT \ln K = -8.31441 \times 298.15 \times \ln(10) \times \log K$$

$$\log K = 8.342$$

Alternatively (if ΔG_f^0 were not given), log K could be obtained from the enthalpy and entropy data. We have

BOX 3.3. (cont.)

$$\Delta H_r^0 = \sum_i \upsilon \Delta H_{f,i}^0$$

and

$$\Delta S_r^0 = \sum_i \upsilon S_i^0$$

or

$$\Delta H_r^0 = \Delta H_{f,\mathrm{Ca}^{2+}}^0 + \Delta H_{f,\mathrm{CO}_{2,aq}}^0 + \Delta H_{f,\mathrm{H_2O_l}}^0 - \Delta H_{f,\mathrm{CaCO_3}}^0 - 2 \times \Delta H_{f,\mathrm{H}^+}^0 = -35\,602\ \mathrm{J \cdot mol^{-1}}$$

and

$$\Delta S_r^0 = S_{\mathrm{Ca}^{2+}}^0 + S_{\mathrm{CO}_{2,\mathrm{aq}}}^0 + S_{\mathrm{H_2O_l}}^0 - S_{\mathrm{CaCO_3}}^0 - 2 \times S_{\mathrm{H}^+}^0 = 40.20\ \mathrm{J \cdot mol^{-1} \cdot K^{-1}}$$

Finally,

$$\Delta G_r^0 = \Delta H_r^0 - T \times \Delta S_r^0 = -47\,588\ \mathrm{J \cdot mol^{-1}} \rightarrow \log K = 8.337$$

The log *K* numbers are the same for all practical purposes.

BOX 3.4. CALCULATION OF ENTHALPY, ENTROPY AND APPARENT GIBBS ENERGY AT ELEVATED TEMPERATURES AND PRESSURES

Below are thermodynamic data on albite ($NaAlSi_3O_8$), water and aqueous species that form when albite dissolves in water. The Gibbs energy, enthalpy and entropy data are at 25°C and 1 bar. Note that the heat capacity parameters b, c and g in Eq. (3.15) are taken to be zero:

	$\Delta G^0_{f,i}$	$\Delta H^0_{f,i}$	S^0_i	a	$f \times 10^6$
$NaAlSi_3O_8$	–3 713 160	–3 936 185	208.20	212.200	71.091
H_2O	–237 140	–285 830	69.95	75.585	–3.576
Na^+	–261 881	–240 300	58.41	81.302	–272.300
$Al(OH)_4^-$	–1 305 575	–1 500 690	111.12	300.129	–1 503.549
$H_4SiO_4^0$	–1 309 181	–1 460 238	178.85	298.343	–659.264

From the above data we calculate the enthalpy of formation of albite at 300°C. We have, from Eq. (3.13a),

$$\Delta H^0_{f,i,T} = -3\,936\,185 + 212.200(T - T_r) + \frac{71.091 \times 10^{-6}}{3}(T^3 - T_r^3)$$

Inserting 573.15 for T (= 300°C) and 298.15 for T_r (25°C) we obtain $\Delta H^0_{f,iT} = -3\,897\,023\ \mathrm{J \cdot mol^{-1}}$.

Next we calculate the Gibbs energy at 300°C for the following reaction:

$$NaAlSi_3O_8 + 8H_2O = Na^+ + Al(OH)_4^- + 3H_4SiO_4^0$$

First, the standard Gibbs energy of the reaction at T_r (25°C) is obtained from

$$\Delta G^0_r = \sum_i \upsilon \Delta G^0_{f,i} = -261\,881 - 1\,305\,575 + 3 \times (-1\,309\,181)$$

$$- 8 \times (-237\,140) - (-3\,713\,160) = 115\,281\ \mathrm{J \cdot mol^{-1}}$$

In a similar way, we calculate the entropy at T_r and Δa and Δf for the reaction:

$$\Delta S^0_r = 58.41 + 111.12 + 3 \times 178.85 - 8 \times 69.95 - 208.2 = -61.72\ \mathrm{J \cdot mol^{-1} \cdot K^{-1}}$$

BOX 3.4. (cont.)

$$\Delta a = 81.302 + 300.129 + 3 \times 298.343 - 8 \times 75.585 - 212.200$$
$$= 458.580 \text{ J} \cdot \text{mol}^{-1} \cdot \text{K}^{-1}$$

$$\Delta f = 10^{-6}\ [272.300 - 1503.549 - 3 \times (-659.264) - 8 \times (-3.576) - 71.091]$$
$$= -3798.124 \times 10^{-6} \text{ J} \cdot \text{mol}^{-1} \cdot \text{K}^{-3}$$

By inserting the values derived for the Gibbs energy and entropy at T_r and the values for the heat capacity parameters into Eq. (3.26) (remember that Δb, Δc and Δg are all equal to zero), the value for the Gibbs energy of the reaction is obtained: 126–808 J·mol^{-1}·K^{-1}.

Having performed these calculations, we insert the relevant equations into a spreadsheet and easily calculate, from the data at 25°C, the Gibbs energies and equilibrium constants for any desired reaction for which we have the necessary thermodynamic data.

BOX 3.5. CALCULATION OF ACTIVITY COEFFICIENTS

The effective ionic radii $å_i$ of some common ions are given below in ångström (10^{-8} cm):

9	H^+
8	Mg^{2+}, Be^{2+}
6	Li^+, Ca^{2+}, Cu^{2+}, Zn^{2+}, Mn^{2+}, Fe^{2+}, Ni^{2+}, Co^{2+}
5	Sr^{2+}, Ba^{2+}, Ra^{2+}, Cd^{2+}, Hg^{2+}, S^{2-}
4.5	Pb^{2+}, CO_3^{2-}, SO_3^{2-}
4–4.5	Na^+, HCO_3^-, $H_2PO_4^-$
4	SO_4^{2-}, HPO_4^{2-}
3.5	OH^-, F^-, HS^-
3	K^+, Cl^-, NO_2^-, NO_3^-
2.5	Rb^+, Cs^+, NH_4^+

The variation with temperature (0–350°C) in the values of the Debye–Hückel solvent parameters, *A* and *B*, are quite accurately described by the following equations:

$$A = \frac{1.824829238 \times 10^6 \rho^{0.5}}{(\varepsilon T)^{1.5}}$$

$$B = \frac{50.29158649 \times 10^8 \rho^{0.5}}{(\varepsilon T)^{0.5}}$$

where T is the temperature in kelvin, ρ the density of water and ε its dielectric constant. The values for ρ and ε can be obtained from steam tables and from Helgeson and Kirkham (1974), respectively.

A solution has the following composition (in ppm):

Na	1400	K	380	Ca	80	Mg	0.015
Cl	2200	SO_4	36	F	0.40		

Let us calculate the ionic strength of the solution. We first convert the concentration units to molalities and then insert the latter into Eq. (3.34):

BOX 3.5. (cont.)

$$I = \frac{1}{2}\left(\frac{1400}{23.00} + \frac{380}{39.10} + \frac{80}{40.08} \times 4 + \frac{0.015}{24.30} \times 4 + \frac{2600}{35.45} + \frac{36}{96.06} \times 4 + \frac{0.40}{20.00}\right)$$

$$\times 10^{-3} = 0.0770$$

Then, we calculate the activity coefficient for calcium ion (Ca^{2+}) at 200°C. According to Eq. (3.33), we have

$$\log \gamma_{Ca^{2+}} = \frac{-Az^2_{Ca^{2+}}\sqrt{I}}{1 + a_{C^{2+}} B\sqrt{I}} = \frac{-0.8099 \times 4 \times \sqrt{0.0770}}{1 + 6.0 \times 10^{-8} \times 0.3655 \times 10^{8} \times \sqrt{0.0770}} = -0.5589$$

$$\gamma_{Ca^{2+}} = 0.572$$

The value calculated above for the ionic strength is only approximate. In the above example, all components analysed for are assumed to form ions. This may not be case, particularly at elevated temperatures. Some of these components may form ion pairs with smaller charge than the simple ions or complexes (or even no chage), i.e. ion pairs such as $NaCl^0$ and $CaSO_4^0$. An accurate calculation of the ionic strength requires an iteration process such as that included in aqueous speciation programmes (Section 3.8), which takes into account the influence of ion pairing on the ionic strength.

BOX 3.6. CALCULATION OF AQUEOUS SPECIATION

Consider an aqueous solution containing Na, Ca, Cl and SO_4. In addition to H^+ and OH^+, the following aqueous species are present: Na^+, $NaCl^0$, $NaSO_4^-$, $NaOH^0$, Ca^{2+}, $CaCl^+$, $CaSO_4^0$, $CaOH^+$, Cl^-, SO_4^{2-}, HSO_4^-, i.e. 13 species in all. The mass balance equations (one for each component) are:

$$m_{\mathrm{Na}} = m_{\mathrm{Na^+}} + m_{\mathrm{NaCl^0}} + m_{\mathrm{NaSO_4^0}} + m_{\mathrm{NaOH^0}}$$

$$m_{\mathrm{Ca}} = m_{\mathrm{Ca^{2+}}} + m_{\mathrm{CaCl^+}} + m_{\mathrm{CaSO_4^0}} + m_{\mathrm{CaOH^0}}$$

$$m_{\mathrm{SO_4}} = m_{\mathrm{SO_4^{2-}}} + m_{\mathrm{HSO_4^-}} + m_{\mathrm{NaSO_4^-}} + m_{\mathrm{CaSO_4^0}}$$

$$m_{\mathrm{Cl}} = m_{\mathrm{Cl^-}} + m_{\mathrm{NaCl^0}} + m_{\mathrm{CaCl^+}}$$

where m_i represents concentration in mole · kg^{-1} of components/species i. The dissociation reactions are:

(1) $NaCl^0 = Na^+ + Cl^-$
(2) $NaSO_4^- = Na^+ + SO_4^{2-}$
(3) $NaOH^0 = Na^+ + OH^-$
(4) $CaCl^+ = Ca^{2+} + Cl^-$
(5) $CaSO_4^0 = Ca^{2+} + SO_4^{2-}$
(6) $CaOH^? = Ca^{2+} + Cl^-$
(7) $HSO_4^- = H^+ + SO_4^{-2}$
(8) $H_2O = H^+ + OH^-$

In order to identify all dissociation reactions, it is easiest to see which species can break down into simpler ones. The number of dissociational reactions is always equal to the number of species that can dissociate. The dissociation of water should not be forgotten.

The equilibrium constants for the dissociation reactions are:

$$(1)\ K_{\mathrm{NaCl^0}} = \frac{a_{\mathrm{Na^+}} a_{\mathrm{Cl^-}}}{a_{\mathrm{NaCl^0}}} \qquad (2)\ K_{\mathrm{NaSO_4^-}} = \frac{a_{\mathrm{Na^+}} a_{\mathrm{SO_4^{2-}}}}{a_{\mathrm{NaSO_4^0}}}$$

$$(3)\ K_{\mathrm{NaOH^0}} = \frac{a_{\mathrm{Na^+}} a_{\mathrm{OH^-}}}{a_{\mathrm{NaOH^0}}} \qquad (4)\ K_{\mathrm{CaCl^+}} = \frac{a_{\mathrm{Ca^{2+}}} a_{\mathrm{Cl^-}}}{a_{\mathrm{CaCl^+}}}$$

$$(5)\ K_{\mathrm{CaSO_4^0}} = \frac{a_{\mathrm{Ca^{2+}}} a_{\mathrm{SO_4^{2-}}}}{a_{\mathrm{CaSO_4^0}}} \qquad (6)\ K_{\mathrm{Ca^{+2}}} = \frac{a_{\mathrm{Ca^{2+}}} a_{\mathrm{OH^-}}}{a_{\mathrm{CaOH^+}}}$$

$$(7)\ K_{\mathrm{HSO_4^-}} = \frac{a_{\mathrm{H^+}} a_{\mathrm{SO_4^{2-}}}}{a_{\mathrm{HSO_4^-}}} \qquad (8)\ K_{\mathrm{H_2O}} = \frac{a_{\mathrm{H^+}} a_{\mathrm{OH^-}}}{a_{\mathrm{H_2O}}}$$

where a_i indicates the activity of the i-th species.

BOX 3.6. (cont.)

In order to obtain values for the concentrations of individual aqueous species, the mass balance and dissociation equilibrium reactions must be solved simultaneously. The total number of variables (equal to the total number of species) is 13. We have four mass balance equations and eight dissociational equilibria, or 12 equations in all. One more equation is needed. We could, for example, write a charge balance equation. The sum of all cation charges must be equal to the sum of all anion charges. It is, however, easier and more reliable to measure pH, in which case only 12 aqueous species are unknown and this is what we need.

It is easiest to replace the activities by the product of the activity coefficient and the concentration (see Eq. (3.33)). Then, for example, the dissociational equilibria described by expression (3) become

$$K_{NaOH^0} = \frac{m_{Na^+}\gamma_{Na^+}m_{OH^-}\gamma_{OH^-}}{m_{NaOH^0}\gamma_{NaOH^0}}$$

Again, for demonstration purposes, let us consider the solution for the mass balance equation for Cl. We have:

$$m_{Cl} = m_{Cl^-}\left[1 + \frac{m_{Na^+}\gamma_{Na^+}\gamma_{Cl^-}}{K_{NaCl^0}m_{NaCl^0}\gamma_{NaCl^0}} + \frac{m_{Ca^{2+}}\gamma_{Ca^{2+}}\gamma_{Cl^-}}{K_{CaCl^+}m_{CaCl^+}\gamma_{CaCl^+}}\right]$$

By writing similar values for the other components we are in a position to obtain a solution through an iterative process, i.e. by guessing the answer again and again until a solution is found that is numerically compatible with all the equations.

The ionic strength, I, for our system can be obtained from

$$I = \frac{1}{2}\left[m_{H^+} + m_{OH^-} + m_{Na} + m_{Ca} \times 4 + m_{Cl} + m_{SO_4} \times 4\right]$$

This allows the calculation of all activity coefficients.

Once the first iterative solution has been obtained it becomes apparent that the calculation of the ionic strength was only approximate. The components, as analysed, do not all form simple ions. The equation for the ionic strength becomes:

BOX 3.6. (cont.)

$$I = \frac{1}{2}\begin{bmatrix} m_{\mathrm{H}^+} + m_{\mathrm{OH}^-} + m_{\mathrm{Na}^+} + m_{\mathrm{Ca}^{+2}} \times 4 + m_{\mathrm{Cl}^-} + m_{\mathrm{SO}_4^{2-}} \times 4 \\ + m_{\mathrm{NaSO}_4^-} + m_{\mathrm{CaCl}^+} + m_{\mathrm{CaOH}^+} + m_{\mathrm{HSO}_4^-} \end{bmatrix}$$

and an updated value is obtained for the ionic strength and, subsequently, for the activity coefficients. The iterative procedure must be continued until the last solution gives an ionic strength that is so similar to the preceding one that the difference can be neglected.

4. REACTIVE AND CONSERVATIVE COMPONENTS

Stefán Arnórsson

The chemical and isotopic constituents in geothermal fluids have conveniently been classified into two groups, depending on their characteristics and the type of information they provide on the geothermal resource. The groups are *conservative* and *reactive* constituents. The *conservative constituents* have also been termed non-reactive, inert, incompatible or simply tracers. Once added to the fluid phase they remain there. The conservative constituents provide information on their own source as well as on the source of the fluid. Reactive constituents have also been termed geoindicators. They tend to equilibrate with other reactive constituents and/or the minerals of the rock in the geothermalsystem. They are useful in obtaining information on the physical state of geo-thermal reservoirs such as temperature and steam to water ratios.

By the concepts of chemical thermodynamics, conservative constituents have not equilibrated. They are independent variables. On the other hand, equilibrated reactive constituents do not constitute independent variables. They are simply a reflection of the state of the system (temperature, pressure and composition).

Some constituents (components) are said to be mobile, others immobile. Mobility and immobility refer to the ratio of a component between the fluid and the rock. For a mobile component, the concentration in the water is high relative to that in the rock. If the mobility is 100%, the respective component will only occupy the fluid phase given enough time for the fluid–rock interaction. Such a component is said to be conservative. Some reactive components can be highly mobile, such as Li in high temperature geothermal systems. When this is the case, it may be an acceptable approximation to regard the respective reactive component as a conservative one.

Rainwater with its low content of dissolved solids is undersaturated with most, if not all, minerals. In such water all components are conservative. At which point the various components may become reactive depends on the strength of later water–soil or water–rock interaction. This is usually the case with Ti, Fe and Al in the weathering zone and sometimes also with Mg. For low temperature waters, which have undergone limited reaction with the rock, othermajor components also become reactive. They include Si, Ca, Na, K, carbonate carbon and sometimes sulphate. The reactive nature of all these components really lies in their tendency to precipitate from solution, to form secondary minerals and to approach equilibrium locally with them.

Some components are conservative in geothermal systems because they only form soluble minerals and their sources of supply to the geothermal fluid are too limited to saturate with any mineral. Examples of such conservative components are Cl, B and Br. Other chemical constituents are truly chemically inert, such as the noble gases, whereas still other constituents react slowly and can, therefore, be regarded as conservative for all practical purposes. An example is N_2.

Deuterium (^2H) is the most widely used conservative isotope in geothermal studies. It is not inert but regarded as being highly mobile. Secondary minerals containing water certainly form and deuterium may fractionate considerably between these minerals and the water. It has, however, been convincingly argued that the amount of water held in secondary minerals is trivially low compared to the amount flowing through a given body of rock, and fractionation of deuterium between these phases will have a negligible effect on the deuterium content of the through-flowing water.

Some radioactive isotopes such as tritium (^3H) act as conservative components or tracers. Being radioactive with a known decay constant, tritium serves as a tool to determine the age of the water. Other isotopes that serve as tracers include ^{13}C, ^{40}Ar and ^3He.

Carbon-14 has been used to some extent to date geothermal waters. The main problem with interpreting the data stems from the dilution of the initial ^{14}C in the water by dead carbon from the rock or from magmatic emanations.

Waters with temperatures below about 100°C generally show very little oxygen shift, if any. When this is the case, ^{18}O can be used as a tracer like deuterium. On the other hand, waters that have attained higher temperatures have generally reacted sufficiently with the rock so as to produce a significant oxygen shift. When it is safe to assume that the oxygen shift is insignificant, the deuterium excess, d (defined as $\delta D - 8\delta^{18}O$), can be used to assess whether or not a particular geothermal water represents precipitation that has fallen under present day or different climatic conditions. The deuterium excess depends on the moisture saturation of the air in the source area.

Geochemists working in the field of geothermal geochemistry very often make the assumption that equilibrium prevails for a particular reaction, such as the reaction involving quartz and aqueous silica. Repeated assumptions of this kind sometimes seem to lead to the formation of a paradigm (a frame within which one thinks). The assumption develops into a fact, or rather a belief, that equilibrium must exist somewhere in the geothermal system for a specific reaction. Even the demonstration of specific mineral–solution equilibria by studies in some geothermal fields does not prove that such equilibria prevail in all geothermal fields. It must not be forgotten that the tool in quantitative geothermal geochemistry is physical chemistry (mostly thermodynamics, but also a little bit of kinetics), but not geothermometry or some models used to derive information about specific geothermal reservoir characteristics. It cannot be overempharized that the geochemist must always seek evidence for and against specific chemical equilibria involving reactive components (geoindicators). If the assumption of equilibrium is wrong, so is the conclusion from geoindicators about the state of a geothermal reservoir as deduced from the use of the geoindicators.

The authors of this book have had long experience in geothermal investigations and research. They have largely been working in geothermal fields in different kinds of geological setting. From observations, one of us has concluded that CO_2 partial pressures are externally fixed, i.e. CO_2 constitutes an independent variable. Another of the authors has concluded that aqueous CO_2 concentrations are fixed by equilibria with specific mineral buffers and, accordingly, CO_2 is a reactive component. Quite likely, both views are correct. The conclusions drawn by them from the study of specific geothermal systems are, strictly speaking, only valid for these systems and cannot be generalized to hold for all systems. Any geochemist working in an area that has been drilled should assess the state of the system (temperature, pressure and composition) and subsequently attempt to demonstrate which components have attained equilibrium and which not. The composition of the system is reflected in its alteration mineralogy. For some components such as Cl, B and ^2H — just to mention some — such an assessment is not relevant because they can be safely taken to be conservative, but for others, such as CO_2 or CH_4, it is a must (Box 4.1).

The concentrations, or better, activities of reactive components in equilibrated geothermal fluids depend on the minerals with which these components equilibrate. It is the composition of the rock, together with temperature and pressure, that determines which these minerals are. The composition of water or magmatic fluids entering the system may also contribute to mineral stability. Thus, to be exact, it is not the rock but the composition of the system that dictates which minerals form at a specific temperature and pressure.

In geothermal systems, pressure varies from about 1 bar at the surface to few hundreds of bars in the roots of these systems. Pressure variation within this range has a limited effect on mineral–solution equilibria and hence may be ignored. Thus, temperature and rock (system) composition effectively fix activities of reactive constituents at equilibrium. If the mineral or minerals that control the activity of a particular reactive component are stable over wide ranges of temperature and rock compositions, this reactive component has a wide applicability as a geoindicator. An example is provided by aqueous silica and quartz and by Na, K and alkali feldspars. The quartz and Na/K geothermometers are applicable in a wide variety of geological environments, from systems in basaltic terrain to water in rhyolite or clastic sediments, such as at Cerro Prieto in Mexico.

Sulphate is a reactive component in some geothermal systems but conservative in others. It is definitely reactive when aqueous sulphate precipitates with calcium to form anhydrite and equilibrium between this mineral and solution is closely approached. Equilibration is attained for anhydrite for, at least, some of the acid bisulphate waters in the Philippines. This is also the case for low and high temperature waters in basaltic rocks in Iceland if the water contains a significant component of sea water (>5%), as well as for shallow aquifers at Momotombo in Nicaragua. By contrast, deep aquifer waters (>250°C) at Momotombo are anhydrite undersaturated, as are some dilute geothermal waters in Iceland for all temperatures up to 350°C.

Some of the elements listed by Giggenbach (1991) as being conservative, such as Rb or Li, are not incompatible but highly mobile, at least in some geothermal systems. The degree of mobility may depend on the geological environment. In the geysir area in Iceland, there are strong gradients across the field in the concentrations of chloride of the hot spring waters. There is a good linear correlation between the concentration of the conservative elements, Cl and B (Fig. 4.1(a)), indicating that the variation in Cl is due to mixing of hot and cold water in the upflow. On the other hand, that Cl–Li relationship indicates that the mixing process leads to depletion in lithium (Fig. 4.1(b)), presumably because of its uptake into minerals that precipitate from the water as a result of the mixing process. The conclusion is inevitable that lithium does not act as conservative in the geothermal system of the geysir area in Iceland.

On the basis of the assumption that rock dissolution is stoichiometric, one can compare the aqueous concentrations of a conservative component and another component in order to see whether the latter is also conservative. If the ratio of the two components is the same in the water and in the rock, despite variable aqueous concentrations, both are conservative (Fig. 4.2(a)). If, on the other hand, the concentration of the test component relative to that of the conservative component is lower in the water than in the rock, this indicates a sink for the test component. It has been removed partly from the water, i.e. incorporated into a secondary mineral (Fig. 4.2(b)).

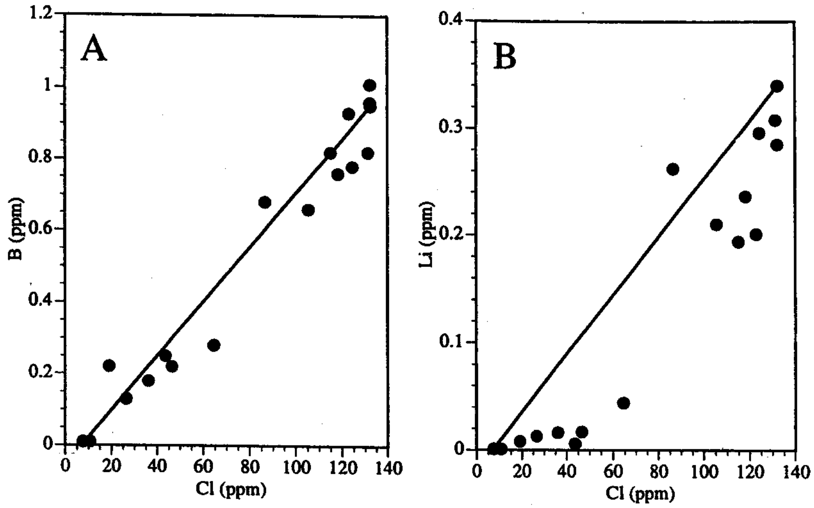

FIG. 4.1. Relationship between (A) Cl–B and (B) Cl–Li concentrations in thermal and cold waters from the geysir area, Iceland. A linear relationship is observed between the conservative components cl and B, indicating that their variation is due to mixing of hot and cold water in the upflow. This is, on the other hand, not the case for the relationship between Cl and Li. Evidently, the mixing process causes Li to be removed from the water.

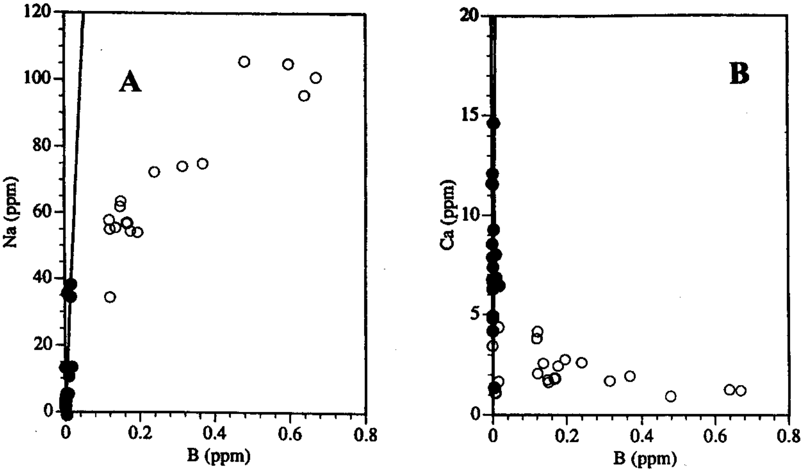

FIG. 4.2. Relationship between concentrations of (A) sodium and boron and (B) calcium and boron in surface and geothermal waters in the Hreppar Land low temperature area

in southern Iceland. Surface waters are shown as dots and geothermal waters as circles. the plotted element concentrations represent the net amount of these elements derived from the rock through its dissolution, i.e. the analysed aqueous concentrations have been corrected for contribution from the local precipitation. The lines represent Na/B and Ca/B concentrations in basaltic rocks in Iceland. It is observed that in surface waters this dissolution is near stoichiometric. As B is a conservative element this implies that Na and Ca also are in the surface environment. With progressive water–rock interaction (increasing B concentrations), it is seen that Na and, in particular, Ca are less mobile than B, most likely because they are removed from the water through precipitation of secondary minerals.

BOX 4.1. HOW DO WE DETERMINE WHETHER A COMPONENT IS CONSERVATIVE OR CONTROLLED BY SPECIFIC MINERAL–SOLUTION EQUILIBRIA?

There are essentially two methods: One is geological deduction and/or knowledge of mineral solubility. The other one relies on the correlation between two aqueous components, one of which is certainly conservative.

Deuterium is an example of a component that is taken to be conservative in geohydrological systems on the basis of geological deduction. The same applies to ^{18}O when this isotope is taken to be conservative (at temperatures of <100°C). Chloride is considered to be conservative because it only forms soluble salts and water–rock interaction experiments have shown that it is easily extracted from common types of volcanic rock into aqueous solution, indicating that it exists as soluble salts in these rocks.

BOX 4.1. (cont.)

There is, however, evidence from studies of very hot submarine geothermal systems that Cl may enter Al bearing amphiboles (hornblende), where it replaces OH. Under these conditions Cl is not conservative. The reason for this camouflage is that both Cl and OH are similar in size and have the same charge. Cl is somewhat larger than OH but not sufficiently so as to prevent it from replacing the latter at high temperatures, when the crystal lattice of hornblende is expanded and, therefore, more adaptable to permitting ions of different sizes to occupy particular sites in it. Hornblende is not expected to be a stable mineral in common rocks, igneous and sedimentary, until temperatures approaching 400°C. It is, therefore, satisfactory to take Cl to be conservative in all geothermal systems drilled so far.

A linear relationship between two components in mixed geothermal waters, where one component is certainly conservative, suggests that the other component is also conservative; at least this is how it has behaved after mixing has occurred. Data from the Landmannalaugar field in Iceland on the relationship between Cl and B, on the one hand, and Cl and ^{18}O, on the other hand, provide an example of such a linear relationship. Taking Cl to be conservative, which is considered perfectly safe, indicates that B and ^{18}O also are in the Landmannalaugar system, at least subsequent to mixing of hot and cooler water in the upflow.

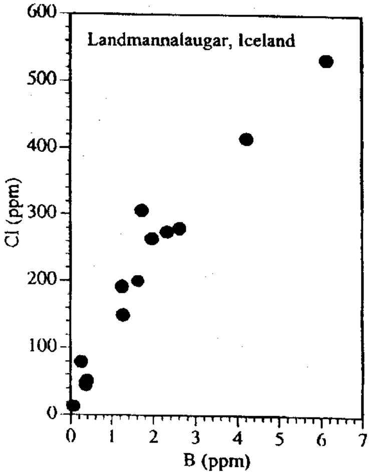

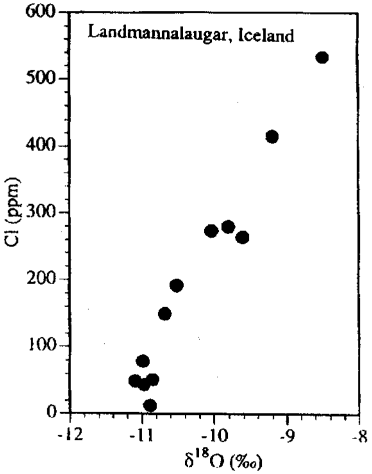

BOX 4.2. MINERAL STABILITY AS A FUNCTION OF TEMPERATURE, PRESSURE AND SYSTEM COMPOSITION

To demonstrate how alteration mineralogy depends on the composition of a given system (the composition of the rock), let us consider the triangular diagram below, which is valid at specified temperature and pressure.

The system under consideration consists of three components, C_1, C_2 and C_3. Possible phases in this system are indicated by P_1 to P_5. Tielines between minerals are based on geological observation, i.e. their association in rocks.

Next, we consider four hypothetical rock compositions, S_1 to S_4. The component composition of rock S_1 can be obtained by projecting this point onto the tielines between components C_1 and C_2 and between C_2 and C_3 (figure at bottom left). The projected points give the following ratios: $C_1/C_2 = 1.500$, $C_1/C_3 = 1.941$ and $C_2/C_3 = 1.273$. Further, $C_1 + C_2 + C_3 = 1$.

The relative proportions of the phases (minerals) in system S_1 can be obtained by the same approach. If we change the composition a little, as indicated by the short arrow pointing from S_1, we have changed the proportion of the minerals in the rock but the minerals themselves are the same as before. If, on the other hand, the rock composition had changed to S_2, it could no longer be represented by minerals P_1, P_2 and P_3. It would have to be represented by minerals P_1, P_2 and P_4. Similarly, rock composition S_3 would be represented by minerals P_2, P_4 and P_5. In other words, if we change the rock composition sufficiently, some minerals disappear and new ones appear instead. Some phases such as P_4 are stable over a wide range of composition. Other phases such as P_3 and P_5 are stable over a more limited compositional range.

Let us finally look at composition S_4. This composition falls on the tieline between P_1 and P_4. Here, four phases are stable. As three components are present, we can deduce, from the phase rule, that there is only one independent variable. If we have four phases, it is not possible to vary both temperature and pressure independently. It is only possible to vary one. If pressure is changed, temperature must change in a prescribed fashion, or vice versa.

Most minerals are stable over a range of temperatures and pressures. Only specific compositions allow the number of phases to be by one or

BOX 4.2. (cont.)

two greater than the number of components. If the latter is the case, then equilibrium fixes both temperature and pressure in addition to the reactive components.

Quartz and calcite are examples of minerals that are stable in rocks of geothermal systems of widely different composition. Fluorite, on the other hand, only appears to be stable in silicic rocks. Mineral stability also depends on temperature, as is exemplified in Figs 7.1 and 7.2 for well 15 at Nesjavellir in Iceland and for sandstones of the Cerro Prieto field, Mexico.

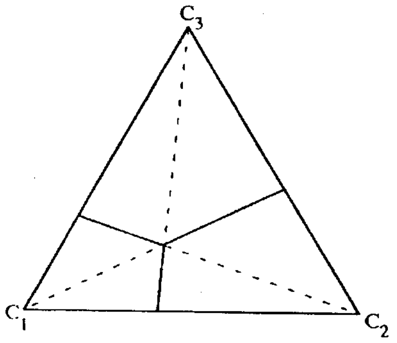

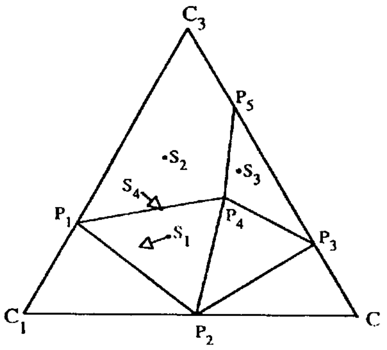

5. ISOTOPES FOR GEOTHERMAL INVESTIGATIONS

Jane Gerardo-Abaya, Franco D'Amore and Stefán Arnórsson

5.1. NOTATIONS

Isotopes are defined as any two or more species of atoms of a chemical element with the same atomic number and nearly identical chemical behaviour but with distinct atomic mass (i.e. mass number) and different physical properties. Some isotopes are stable whereas others are unstable or radioactive. As an example, an element such as hydrogen has three isotopes: the stable isotopes proton and deuterium as well as a radioactive isotope, tritium, symbolized as ^1H, ^2H and ^3H, respectively. Like hydrogen, oxygen also has three isotopes, ^{16}O, ^{17}O and ^{18}O. The number in the upper left corner indicates the mass of the particular element symbolized by a specific letter.

Unlike stable isotopes, radioactive isotopes break down into isotopes of other elements at a rate specified by its decay constant. For tritium, the half-life

TABLE 5.1. STABLE AND RADIOACTIVE ISOTOPES USED IN HYDROLOGICAL STUDIES

Stable isotopes		Radioactive isotopes	
Isotope	Substance	Isotope	Half-life (a)
Oxygen-18 (^{18}O)	H_2O	Krypton-85 (^{85}Kr)	10.8
Deuterium (^2H)		Tritium (^3H)	12.43
Carbon-13 (^{13}C)	HCO_3^-, CH_4	Silicon-32 (^{32}Si)	100
Deuterium (^2H)	H_2		
		Argon-39 (^{39}Ar)	269
Sulphur-34 (^{34}S) and	SO_4^{--}		
Oxygen-18 (^{18}O)		Carbon-14 (^{14}C)	5 730
Boron-11 (^{11}B)	$B(OH)_4^-$, $B(OH)_3^-$	Krypton-81 (^{81}Kr)	210 000
Chlorine-37 (^{37}Cl)	Cl, chlorinated hydrocarbons	Uranium-234 (^{234}U)	306 000
		Chlorine-36 (^{36}Cl)	306 000

is 13.43 a. Table 5.1 shows the commonly used stable and radioactive isotopes in hydrological investigations in geothermal systems.

The isotopic ratio, R, of an element in a particular substance is defined as the ratio of the number of atoms of a given isotope, A, to that of the most abundant isotope, B, of that element, or

$$R = \frac{A}{B} \tag{5.1}$$

For the purpose of illustration, if we take the isotopic ratio of deuterium to proton we obtain:

$$R_{3_{\mathrm{H}}} = \frac{^{2}H}{^{1}H} \tag{5.1a}$$

The isotopic ratio for deuterium and tritium to proton in sea water is 156×10^{-6} (Hagemann et al., 1970) and about 10^{-18}, respectively. For ^{18}O, this ratio is 2005×10^{-6} (Baertschi, 1976) and about five times lower for ^{17}O.

It is not easy to measure absolute isotopic ratios accurately, but differences in isotopic ratios between a particular sample and a standard can be measured accurately. For this reason isotopic concentrations are conveniently expressed in delta notation (δ) as parts per thousand, or

$$\delta = \frac{R_{\text{sample}} - R_{\text{standard}}}{R_{\text{standard}}} \times 1000 \tag{5.2}$$

where R stands for the isotopic ratio of the sample and standard, respectively. Thus, for example, if a water has a deuterium delta value ($\delta^{2}H$) of –50‰ this means that its deuterium content is 50‰, or 5%, lower than that of the standard. A positive delta value shows that the sample is more enriched in the respective isotope than the standard.

Different standards are used for the measurement of different isotopes. The standard that has been used for measuring delta values for the isotopes of oxygen and the stable isotopes of hydrogen is the Standard Mean Ocean Water (SMOW), while for sulphur it is troilite from the Canyon Diablo meteorite. For carbon the standard is PDB, a sample of fossil belemnite from the PeeDee Formation in North Carolina. Since the original supply of this standard has long been exhausted, the new reference standard is NBS-19, which is defined as $\delta^{13}C_{\text{NBS-19/V-PDB}} = 1.95$. All standards for stable isotope determinations can be obtained from the IAEA in Vienna.

The isotopic composition of SMOW represents a good average of the water in the oceans (Craig, 1961), which, with some 97% of the water present on the Earth's crust, has a fairly uniform isotopic composition (Friedman, 1953; Epstein and Mayeda, 1953). By definition SMOW has $\delta^{18}O = 0$ and $\delta^2H = 0$. The standard has been termed V-SMOW for practical purposes, where V stands for 'Vienna'. The SMOW defined by Craig is $\delta^2H = +0.2‰$ and $\delta^{18}O = +0.04‰$, with respect to V-SMOW.

Because of the different physical properties of isotopes of the same element, they display different reaction rates and different distribution in two chemical compounds or phases at equilibrium. As a result of their different physical properties, various physical processes can cause isotopic fractionation. Processes common in geothermal systems, such as evaporation, condensation, steam separation and mineral–solution reactions, produce isotopic fractionation. Like isotopic ratios, isotopic fractionation is expressed in δ notation. The fractionation is quantitatively described by the fractionation factor, α. It is defined as the ratio between the isotopic ratios in the different species or phases of a system:

$$\alpha = \frac{K}{n} \tag{5.3}$$

where n is the number of atoms exchanged in the reaction as written (normally, $n = 1$, making K equal to α, while α is a factor analogous to a distribution coefficient. It is temperature dependent and approaches unity at high temperatures.)

For an isotope exchange reaction as for ^{12}C and ^{13}C between CO_2 and CH_4, the reaction can be written as:

$$^{12}CO_2 + {}^{13}CH_4 = {}^{13}CO_2 + {}^{12}CH_4 \tag{5.4}$$

where the equilibrium constant, K, is given by

$$K = \frac{[^{13}CO_2][^{12}CH_4]}{[^{12}CO_2][^{13}CH_4]} \tag{5.5}$$

It is satisfactory to use measured concentrations rather than activities because the activity coefficients for isotopically substituted molecules can be taken to be equal to unity.

The equilibrium constant (fractionation factor) for any isotopic exchange is related to the ratio of the minor to the major isotope in species A and B by

$$\alpha_{A-B} = \frac{R_A}{R_B} \approx \frac{10^3 + \delta A}{10^3 + \delta B} \tag{5.6}$$

when δA and $\delta B << 1000$ (see Box 13.1).

The difference in isotopic fractionation between two phases, is Δ_{A-B}, is given by

$$\delta A - \delta B = \Delta_{A-B} \tag{5.7}$$

For small differences between δA and δB we have

$$\delta A - \delta B \approx 10^3 \ln \alpha_{A-B} \tag{5.8}$$

Radioactive isotopes, which are characterized by an unstable nucleus, decay into another element with time. The rate of decay is given by

$$-\frac{dN}{dt} = N\lambda \tag{5.9}$$

where N represents the number of radioactive nuclei of a particular kind in a compound at time t and l is the characteristic decay constant of the radioisotope. The decay may be any of the three following types of radiation:

(1) α decay, where the nucleus of the element emits an α particle and loses two protons and two electrons;
(2) β decay, where the nucleus of the element emits a β particle (nuclear electron), producing an element with the same mass;
(3) electron capture. The nucleus captures an electron by a process in which the inner layer produces an element of the same mass.

Rearranging Eq. (5.9) and integrating over the time interval between 0 and t, during which the number of radioactive nuclei in the compound decreases from N_0 to N, we obtain:

$$\ln \frac{N}{N_0} = -\lambda t \tag{5.10}$$

or

$$N = N_0 \, e^{-\lambda t} \tag{5.10a}$$

If the initial concentration of a radioactive isotope in a compound or a system, N_0, is known and the present concentration N measured, we can calculate the age of the system from Eq. (5.10).

The half-life ($t_{1/2}$) of a radioactive isotope is defined as the time required for one half the number of radioactive atoms in a compound to undergo decay, i.e. for N to become equal to $N_0/2$. Substituting $N_0/2$ for N in Eq. (5.10) leads to

$$t_{1/2} = \frac{\ln 2}{\lambda} = \frac{0.693}{\lambda} \tag{5.11}$$

The unit of radioactivity that had been used for years was one curie (Ci), which corresponds to 3.7×10^{-10} disintegrations per second, equivalent to the radioactivity of one gram of radium. The recommended unit at present is becquerel, equivalent to one decay per second (1 dps), i.e. $1/3.7 \times 10^{10}$ Ci.

5.2. USE OF ISOTOPES IN GEOTHERMAL INVESTIGATIONS

Nuclear techniques have become indispensable tools in geothermal investigations, for two reasons: (1) their isotope ratios are sensitive to changes in temperature, water–rock interaction and other physicochemical processes, such as mixing and steam separation, and (2) they are suitable as tracers for the origin of water and regional flow directions because the isotopes retain their physical and chemical characteristics. In many stages of geothermal development, stable isotopes such as ^{18}O and ^{2}H have distinct roles in defining the hydrological conditions and evaluating processes that affect the fluids. Radioactive isotopes such as ^{3}H, on the other hand, are applied in specific problems, as e.g. dating and detection of recent coldwater inflow into geothermal reservoirs.

The relative abundances of commonly applied isotopes in geothermal investigations were provided by Panichi and Gonfiantini (1976) and are shown in Table 5.2.

Various references provide detailed information on the properties of isotopes and their measurement. The reader is, therefore, advised to refer to these valuable materials for a comprehensive understanding of the principles of working with isotopes. Their characteristics and their behaviour are extensively discussed in IAEA (1981 and 1983) and for topics specific to geothermal systems in Henley et al. (1984) and UNITAR (1991). Some other references on the geochemistry of hydrothermal systems have, to a certain extent, integrated isotope applications. Other important papers reviewing the application of

TABLE 5.2. RELATIVE ABUNDANCES OF COMMONLY APPLIED ISOTOPES

Isotope	Abundance (%)	Isotope	Abundance (%)
^{1}H	99.985	^{16}O	99.76
$^{2}H = D$	0.015	^{17}O	0.04
^{3}H	10^{-15}–10^{-12}	^{18}O	0.20
^{12}C	98.89	^{32}S	95.0
^{13}C	1.11	^{33}S	0.76
^{14}C	1.2×10^{-10}	^{34}S	4.22

isotopes to geothermal systems are given by Craig (1963), Truesdell and Hulston (1980), Giggenbach et al. (1984) and Giggenbach (1991).

At a recent meeting at the IAEA, experts have evaluated the notable applications of different isotopes applicable in geothermal investigations. These are summarized in Box 5.1.

A beginner in the use of isotope techniques needs to become familiar with isotope notations and important associated terminologies. It is, however, considered advisable to expand the understanding of the principles, phenomena and other important isotopic characteristics by consulting literature that specifically deals with the subject. The remainder of this chapter describes the most important isotopic techniques employed for geothermal investigations. It aims at helping the reader start his work of applying isotope techniques in geothermal geochemistry.

5.3 ORIGIN OF GEOTHERMAL WATER

Geothermal fluids originate mainly from meteoric water (Craig, 1963). An important aspect of geothermal investigations is to determine the recharge to the geothermal systems. Craig (1963) established the isotopic characteristics ($\delta^{2}H$ and $\delta^{18}O$) of precipitation relating to latitude and altitude as well as to continental effects. Samples from higher latitudes and elevation or those collected further inland were progressively lighter (more negative values of δ). The values of $\delta^{2}H$ and $\delta^{18}O$ in precipitation were approximately related by the meteoric water line by

$$\delta^2H = 8\,\delta^{18}O + 10 \qquad (15.12)$$

The $\delta^{18}O$ values of geothermal waters are most often higher (less negative) than those of local meteoric waters, a trend in a $\delta^{18}O$ – δ^2H diagram which has been termed 'oxygen isotope shift' (Fig. 5.1). This has been interpreted as a result of isotopic exchange at high temperature between the water and the rock minerals which are richer in $\delta^{18}O$. The values of δ^2H are sometimes constant. Giggenbach (1992) has demonstrated that the values of δ^2H are also enriched and increase linearly with $\delta^{18}O$ in numerous geothermal and volcanic systems along convergent plate boundaries, depicting a mixing trend towards a possible

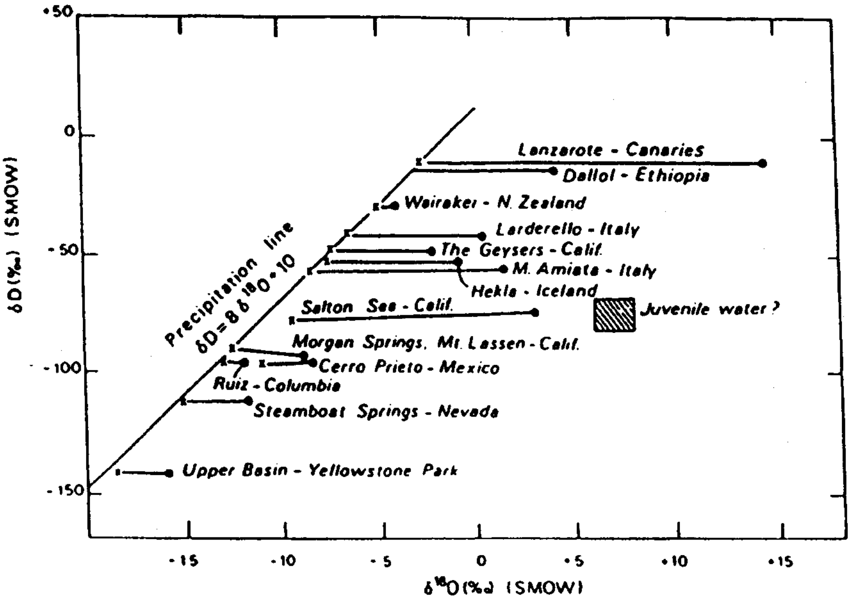

FIG. 5.1. Isotopic composition of water and steam from some of the important geothermal systems. × *indicates the isotopic composition of meteoric water, and* • *denotes the composition of the deep geothermal fluids. Sources of data are: Lanzarote (Arana and Panichi, 1974); Dallol (Gonfiantini et al., 1973); Larderello and Mt. Amiata (Panichi et al., 1974); Salton Sea (Craig, 1966); Ruiz (Arango et al., 1970) and other fields (Craig, 1963). After IAEA, 1981.*

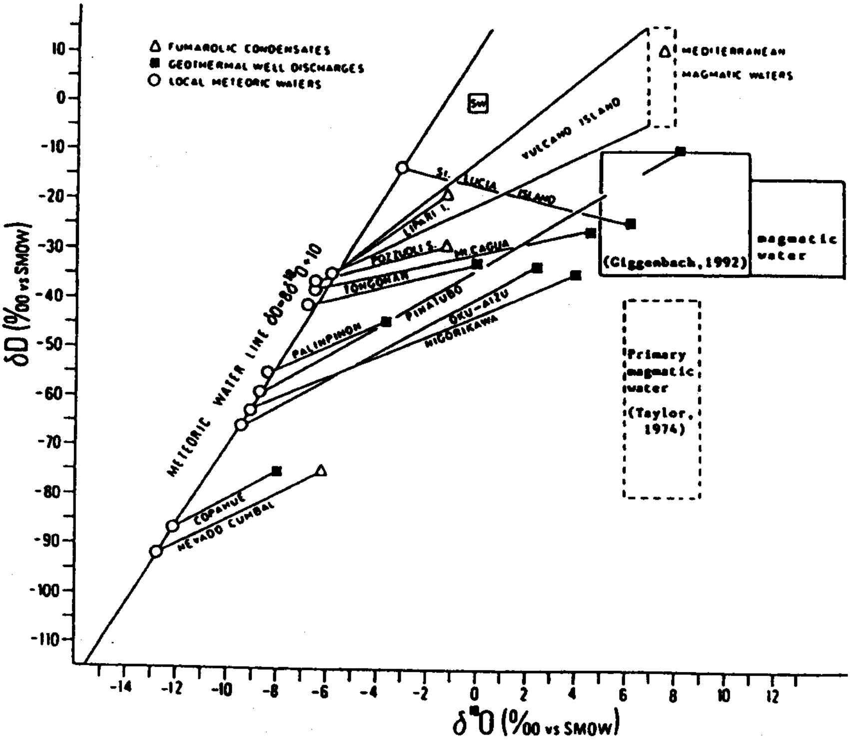

FIG. 5.2. Isotopic composition in some geothermal systems in different areas where enrichment in both $\delta^{18}O$ and δ^2H is indicated, due to mixing in different proportions between meteoric water (○) and geothermal fluids (■). Modified after Giggenbach, 1992.

common magmatic source having a $\delta^{18}O$ of +10 ± 2‰ and a δ^2H of −20 ± 10‰ (Fig. 5.2).

The applications of water isotopes in geothermal studies do not only involve tracing the origin of water. These isotopes are also useful in characterizing the boiling process and in monitoring the flow of injected fluids.

Oxygen-18 and deuterium have indicated mixing of injected water, geothermal fluids and meteoric water in the Palinpinon geothermal system, Philippines (Fig. 5.3).

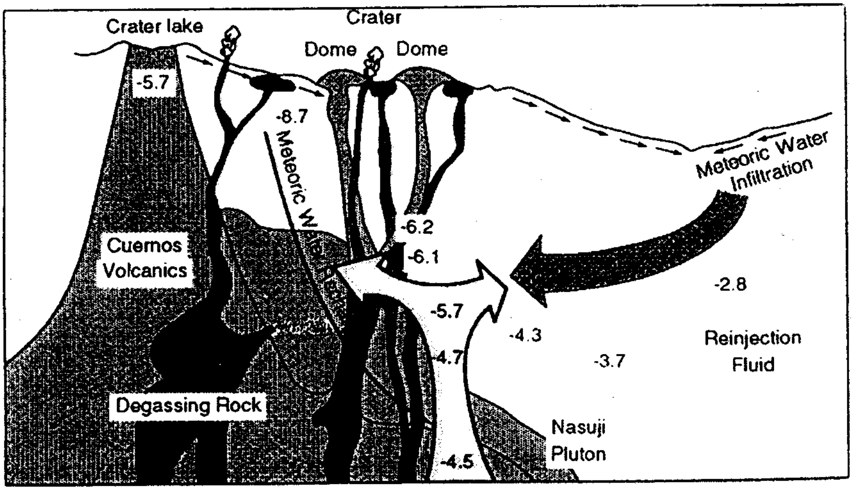

FIG. 5.3. Isotopes provide an indication of the mixing processes and dynamics of flow in the reservoir. A hydrogeochemical model of the Palinpinon geothermal system was conceptualized on the basis of the $\delta^{18}O$ composition (negative values in ‰) of the different bluid sources. the dark broad arrow indicates the movement of the isotopically enriched ($\delta^{18}O = -2.8$‰) injection water mixing with the upflowing geothermal fluid (light broad arrow). Meteoric water (thin arrows) also infiltrates some wells and causes depletion of stable isotopes.

5.4. STAGES OF GEOTHERMAL DEVELOPMENT WHERE ISOTOPES ARE EMPLOYED

Isotopes have become an essential part of major geothermal developments. Their use and interpretation are strengthened if complemented and combined with chemical techniques. Box 5.2 summarizes the various stages in geothermal exploration and development where isotopes, as experienced by various workers, have been found useful.

BOX 5.1. APPLICATION OF VARIOUS ISOTOPES IN GEOTHERMAL INVESTIGATIONS

^{18}O

The isotope ratio, $^{18}O/^{16}O$, is the most important isotope tracer in geothermal studies. It is used in the hydrology of hot and cold water, in SO_4–H_2O geothermometry, and as a tool to evaluate deep and shallow mixing as well as vapour separation processes. Because of the $\delta^{18}O$ shift in some systems, $\delta^{18}O$ distinguishes hot and cold waters more clearly than δ^2H. The equilibrium and kinetics of the $^{18}O(SO_4$–$H_2O)$ geothermometer has been well characterized relative to other isotope geothermometers. It is recommended for temperatures above 180°C.

^2H

The isotope ratio, $^2H/^1H$, is used with $^{18}O/^{16}O$ in hydrology. It indicates recharge (hot and cold) and the relative contribution of magmatic fluids. It forms the basis for the CH_4–H_2 and H_2–H_2O geothermometers. Together with $\delta^{18}O$ it is a valuable indicator for mixing and vapour separation processes. Unlike $\delta^{18}O$, δ^2H is hardly affected by exchange processes.

^3H

Its activity is established for use in dating of waters to indicate the depth of mixing processes. To avoid contamination, it should be used with great care as an artificial tracer of H_2O in liquid and vapour.

^{34}S

The ratio, $^{34}S/^{32}S$, is used in SO_4–H_2S geothermometry and to indicate sources of SO_4 acidity commonly encountered in geothermal systems associated with volcanism as well as for environmental studies to identify the origin of local acid rain. SO_4 also contains the isotope ^{18}O, which can be applied to trace the processes undergone by the fluids.

^{13}C and ^{14}C

$^{13}C/^{12}C$ can be useful to indicate sources of fluids (gas and liquid). CO_2–CH_4 geothermometry could potentially indicate the deepest geothermal temperatures

BOX 5.1. (cont.)

but its applicability and kinetics are poorly understood. ^{14}C is seldom useful in geothermal projects, because of the presence of large quantities of ^{14}C free volcanic CO_2 in most geothermal systems and exchange with $CaCO_3$.

^{3}He, ^{22}Ne, ^{36}Ar, ^{40}Ar and other noble gas isotopes

These isotopes are very useful in indicating the source (mantle, crust, subducted sediments or atmosphere) of associated fluids. Qualitatively, $^{3}He/^{4}He$ and $^{40}Ar/^{39}Ar$ indicate age of fluids except in systems hosted in U/Th poor basalts.

^{131}I

The activity of ^{131}I has been successful in tracing the flow of injected water in hot water geothermal reservoirs although it traces only the liquid phase flow. For high enthalpy systems, SF_6 or another vapour phase tracer is needed. SF_6 is not an isotope, but could provide a vapour phase artificial tracer for high enthalpy systems with partly or entirely steam producing geothermal reservoirs. Freon could also be used for these purposes, but it is ozone unfriendly, increasingly expensive and hard to obtain. Alcohol was tested in Mexico and indicated promising application as an alternative vapour phase tracer.

The following isotopes are potentially useful in geothermal projects:

^{223}Ra, ^{224}Ra, ^{226}Ra and ^{228}Ra

These radium isotopes have particular potential for investigating the extent of geothermal fluid–rock interaction. They also indicate the mixing of different sources of fluids, for example injection and primary geothermal fluids. However, field measurements and sampling are hampered by the short half-lives of ^{223}Ra and ^{224}Ra.

^{222}Rn

Along with Ra isotopes, radon can indicate fluid source and age if the processes are understood. Although this isotope has been studied for a long

BOX 5.1. (cont.)

time, it is still not well understood in reservoirs, so that its present use is limited. Radon occurs in reservoir fluid that is mostly associated with high enthalpy or recent discharge; in soil gases, Rn anomalies have been used to locate faults.

^{36}Cl

The systematics of ^{36}Cl are reasonably well understood, but the interpretation of individual systems needs further study. ^{36}Cl could provide indications of chloride (and fluid) age and therefore the size of geothermal reservoirs. ^{36}Cl is advantageous because the measuring technique by AMS has been fully established. The sampling method is simple and similar to chemical sampling (only 1 L of water is required), and it is applicable to CO_2 dominated systems. ^{36}Cl provides information on the underground processes as well as on the time ranges of Cl in the water cycle if the evolution of Cl is known.

However, it has some disadvantages. All sources of ^{36}Cl and Cl have to be evaluated (rain, shallow groundwaters, springs and others), particularly in geothermal systems that have significant dilution by brine Cl, which could cover the activity below the detection limit. A conceptual hydrological model, possibly from other (conventional) techniques, is required for the ^{36}Cl data to be interpreted. As ^{36}Cl is produced by water–rock interaction, it is also necessary to have other information such as the U and Th contents of rocks along the flow paths or of the reservoir rocks.

Thus, research is required to determine the ^{36}Cl fallout ratio of different latitudes from measurements in ice cores, Cl in precipitation and ^{36}Cl in shallow groundwater. ^{37}Cl may be useful for hydrology but also needs further study.

^{11}B and ^{87}Sr

Both isotopes have not been well tested but could distinguish subduction related magmatic heat sources (associated with marine sediments) from fluids of non-magmatic, hot spot or ridge magmatism origin. ^{87}Sr/^{86}Sr has been used to indicate source rocks of geothermal fluids.

BOX 5.1. (cont.)

^{39}Ar and ^{85}Kr

Both are probably too expensive to be analysed routinely but, like ^{36}Cl, could indicate fluid age. ^{85}Kr could replace tritium in dating young waters.

BOX 5.2. SUMMARY OF USE THE OF ISOTOPES FOR GEOTHERMAL EXPLORATION, DEVELOPMENT AND MONITORING STUDIES

Exploration

(1) Exploration starts with the assessment of existing surface manifestations and the search over wide areas for young volcanic rocks, hydrological conditions and structure that will allow geothermal reservoirs to form and remain. Radiometric isotope dating of volcanic rocks, as part of geologic studies, indicates potential heat sources. If fluids contain high ^{3}He and the rock is intermediate to silicic (with high U + Th), a young volcanic heat source is indicated along with a circulation system that can bring heat into near surface reservoirs.

(2) Once a favourable area is identified, existing fumarole and hot and cold spring fluids are analysed for chemical and isotopic (^{18}O, ^{2}H, ^{3}H and ^{13}C) compositions. These analyses are used to indicate possible recharge areas and to estimate reservoir temperatures through the use of geothermometers. Analyses of soil gases for constituents that may have originated in the geothermal reservoir may be useful in locating upflow zones. Although Hg and ^{222}Rn have been tested, the most reliable results have been obtained by using $^{13}C/^{12}C$ in CO_2 and the CO_2 concentration, which allow differentiation between normal soil with CO_2 of organic origin and CO_2 of magmatic or thermally metamorphosed limestone origin. The chemical and isotopic data are used to establish a geochemical model of the system. The presence of acid reservoir waters may be detected by a combination of chemical analyses and analyses of ^{34}S and ^{18}O of sulphate in acid hot spring waters to distinguish between shallow and deep acidity. At this time estimates can be made of the location of possible upflow and outflow areas.

Drilling

(3) The geochemical results, together with other exploration investigations, are useful in siting exploration wells. When a few wells have been drilled successfully and a decision has been made to proceed with development, a thorough baseline study should be carried out of the

BOX 5.2. (cont.)

geothermal fluid, local precipitation, cold surface waters and shallow groundwaters and particularly of waters used for drinking and agriculture, in order to be able to assess future changes in the isotopic composition that have resulted from exploitation of the geothermal resource in all these fluids. Meteorologic stations and rain collectors at different elevations for ^{18}O and ^{2}H analyses of local meteoric waters may be established at this time. This will allow for the calculation of the local meteoric water line and the isotopic altitude gradients, both of which provide fundamental information for identifying recharge areas. The method for collection of rain samples is described in detail in Box 8.14.

(4) After the first five to ten wells have been drilled, a complete isotopic and chemical study of well fluids is made to indicate the subsurface flow paths and show the locations of zones of upflow, outflow and marginal areas of mixing with cooler waters. In such a study, geothermometers, solute concentrations, gas concentrations and $\delta^{18}O$ values (because of the contrast between hot and cold waters) are particularly useful. It may be possible at this time to have some indication of the fluid homogeneity. With proper environmental safeguards, the drilled wells can be given extended testing to estimate flow rates and enthalpy, allowing power plant design and construction to proceed.

Monitoring

(5) As exploitation proceeds, changes in pressure, and fluid isotopic and chemical compositions can give indications of field capacity and the mode of response to fluid production. Inflow of cooler water can be predicted by isotopic and chemical changes. Fluid boiling, if close to wells, can cause formation plugging and, if widespread, result in a depletion of fluid and rapid pressure drop. Characteristic changes in enthalpy, isotope (^{18}O, ^{2}H) and chemical composition can indicate these reservoir production mechanisms early enough for proper reservoir management.

(6) Injection of condensate and separated brines is usually necessary for environmental reasons and to preserve the resource. Concern for early

BOX 5.2. (cont.)

breakthrough of cold injected fluid requires careful siting of injection wells. Natural tracers in injection fluid resulting from enrichment in ^{18}O and ^{2}H (as well as concentration of Cl and depletion in gas) during surface evaporation of wastewater or boiling of brine relative to the geothermal fluid provide a long term indication of the flow of injected fluids through the reservoir. Although tritium has been used as an artificial tracer, careful consideration should be given before such use because of its persistence and the masking of natural tritium levels which may still be useful for specific hydrologic applications such as dating young waters or indicating cool water incursion into the reservoir.

(7) In high enthalpy fields, reservoirs may be entirely or largely steam. These systems require vapour phase tracers. The only widely used radioactive vapour tracer is tritium, which requires long monitoring periods but prevents later detection of inflow of young waters containing 'natural' tritium. Alternate vapour phase tracers are also available.

(8) Isotope geothermometers could make a greater contribution to the study of production mechanisms if their kinetics were better known. Different geothermometers could then be used to indicate temperatures at different known distances from a producing well. The kinetics of isotopic fractionations among CO_2–CH_4–H_2–H_2O gases, as well as those of SO_4–H_2O–H_2S, still needs to be studied. Chemical and isotopic geothermometers have different rates of re-equilibration and indicate temperatures at different depths in a geothermal system. Certain isotopic geothermometers (^{18}O in SO_4 and H_2O; ^{13}C in CO_2 and CH_4) equilibrate more slowly than chemical geothermometers and indicate temperatures at and below depths reached by drillholes.

Miscellaneous

(9) Low to moderate temperature geothermal fluids which are used for direct heating can be studied by using established isotope hydrology techniques. The study of these fluids would be extended by testing of isotope geothermometers at lower temperatures. Scaling involving

BOX 5.2. (cont.)

sulphur compounds (FeS2, CaSO4) in high and low temperature reservoirs can be usefully studied through analyses of 34S.

(10) Finally, isotopes can make an important contribution to studies of the environmental impact of geothermal development. Monitoring possible leakage of brine from evaporation ponds by using artificial tracers and indication of the origin of local acid precipitation using ^{34}S may be important to maintaining the clean environmental reputation of geothermal energy.

6. THE SOURCE OF CHEMICAL AND ISOTOPIC COMPONENTS IN GEOTHERMAL FLUIDS

Stefán Arnórsson and Franco D'Amore

Geothermal fluids contain a large number of aqueous, gaseous and isotopic components in very variable concentrations. Many components exist as major constituents in geothermal waters although they occur only in trace amounts in common rock types.

The most important processes affecting geothermal fluid compositions include the overall irreversible dissolution of primary rock minerals and precipitation of secondary minerals. The dissolution process leads to increased concentrations of the aqueous components, including conservative species such as Cl, Br and B. Other components, brought into solution by primary rock mineral dissolution, are removed again by precipitation of secondary or hydrothermal minerals. As a result, the relative proportions of components in geothermal waters differ very much from those in common rock types. Components or elements which are largely reprecipitated are said to have low mobility; examples include Al, Mg and Fe. On the other hand, elements which are reprecipitated to a small extent are said to have high mobility; they include Li, Rb, Cs and many others. If elements once dissolved are not removed at all from the water, such as Cl, they are said to be conservative or incompatible. The conservative components are externally fixed, i.e. by their sources of supply to the geothermal fluid. By contrast, components that precipitate to form hydrothermal minerals are internally fixed and, if they come close to equilibrium with the hydrothermal minerals, their aqueous concentrations are quantitatively fixed by the solubility of these minerals.

The classic rock dissolution experiments by Ellis and Mahon (1964, 1967) showed that some elements such as Cl and B, occurring in trace amounts in common volcanic rocks, are easily dissolved so that they become major components in the aqueous phase. Most of the Cl and B could be dissolved from such rocks without significantly altering the primary minerals. On the basis of this observation, Ellis and Mahon (1967) concluded that these highly mobile elements were not contained in the crystal lattice of the primary rock minerals but existed as soluble salts on their surfaces.

Chlorine and boron, together with many other elements, exist in magmas as fugitive components — chlorine as HCl, boron probably as borates, sulphur as SO_2, carbon as CO_2, and, to a lesser extent, as CO, fluorine as HF, and hydrogen as H_2O and H_2. The fugitive compounds tend to leave the magma by the process of degassing. The extent of degassing depends on many factors such as their initial concentration in the magma, the external pressure, the rate of ascent of the magma, its viscosity and its rate of solidificaton. Rapidly solidified magma will tend to trap these fugitive compounds. Evidence for this is certainly provided by analysis of volcanic glass. Helium, which has very low solubility in magma, is detectable in basaltic glass (Poreda et al., 1992) and basaltic glass is higher in sulphur than crystallized basalt and gabbro (Gunnlaugsson, 1977). The fugitive components may react with the glass within which they are enclosed or with the crystals between which they were trapped. For example, one would expect HCl to change into soluble chloride salts by exchanging H for cations in the rock.

One of the impacts of the experimental work done by Ellis and Mahon (1964, 1967) on rock dissolution was their demonstration that no magmatic supply was required to account for the composition of geothermal waters. All that was required was interaction of the water with the reservoir rock. However, the close association of many active geothermal systems with volcanoes and with magma chambers below geothermal systems, as identified by geophysical methods, strongly indicates that magmas are a potential source for, at least, some fugitive components in geothermal systems. White (1970) pointed out that it was difficult to account for the mass output of chloride from geothermal systems, such as Wairakei, throughout their lifetime by rock leaching alone because it would involve such a huge volume of rock. A concentration process, such as that of magma degassing, would be required.

Probably the best example of contribution of fugitive components from a magmatic source to an overlying geothermal system is provided by Krafla in northeast Iceland. At the end of 1975, a volcanic episode that lasted until 1984 started within the fissure swarm of the Krafla central volcano. In this period nine small volcanic eruptions occurred. They were associated with rhythmic inflation and deflation of the volcano (Björnsson et al., 1977). After each eruption a new inflation period began. This inflation period ended by a rapid deflation when the next eruption was about to take place. The inflation period was considered to be caused by flow of magma into two magma chambers in the roots of the volcano and the deflation period by discharge of magma from these chambers into the fissure swarm running through the volcano (Einarsson, 1978). Sometimes discharge from the magma chambers resulted in the formation of dykes filling tensional fissures only, but sometimes the magma reached the surface, leading to a volcanic eruption. A few months after the first eruption had occurred, the gas content, particularly CO_2, of the only discharging well in the area at that time rose sharply (Ármannsson et al., 1982). Later on this rise was observed in fumaroles over the whole area. About 22 years after the outbreak of the first eruption at Krafla, the geothermal steam both from many wells and fumaroles still remains high in CO_2.

It does not matter whether the source of conservative elements to geothermal waters is the rock with which the water interacts or degassing of the magma heat source, or whether these elements are carried into the system by the recharging water, which is the case with geothermal sea water. In any case the conservative elements are externally fixed, i.e. by their sources of supply, but not by reactions within the system involving precipitation of secondary minerals, that is reactions which remove constituents from the water.

Hydrothermal alteration of common types of igneous rock does not involve large changes in the chemical composition of the rock. It is roughly isochemical. A logical conclusion from this observation is that neither much chemical transport into the system from external sources is involved nor chemical transport by the outflowing water. Yet, some elements show large changes, either depletion or enrichment. Soluble elements, such as Cl and B, are almost completely removed from common igneous rocks during their hydrothermal alteration. Other elements, which are contained within the crystal lattices of the primary minerals, such as Ge and Li, may also be largely removed during the alteration process (Arnórsson, 1984; Shaw and Sturchio, 1992). By contrast, some elements, notably C, S and H, occur in higher concentrations in hydrothermally altered rocks than in their fresh counterparts. Carbon occurs mostly as calcite, sulphur as pyrite and other sulphides and hydrogen in water and/or hydroxide bearing minerals. In Icelandic geothermal systems sulphur concentrations in the rock of upflow zones where boiling occurs may be as high as 2–5% (Fig. 6.1), whereas in basaltic glass it is only 0.08% and in holocrystalline basalt as low as 0.01–0.02% (Gunnlaugsson, 1977). Carbon concentration in upflow zones may be as high as 1% (Björnsson et al., 1972) but in basalt it is about 0.012% on average (Sveinbjörnsdóttir et al., 1995). It is considered that the elevated S and C concentrations in the boiling zone of some Icelandic geothermal systems are due to a supply from a degassing magmatic heat source. Rock leaching to account for the accumulation of S and C would require a volume of rock 100 times greater than that of the upflow. This volume seems unduly large.

Early work on hydrogen and oxygen isotopes in geothermal waters from several fields in the world carried out by Craig et al. (1956) showed that the δ^2H values of the geothermal waters were the same as those of local precipitation in each area, whereas $\delta^{18}O$ values were less negative (Fig. 5.1). According to Craig et al. (1956), deuterium results indicated that the geothermal waters were local

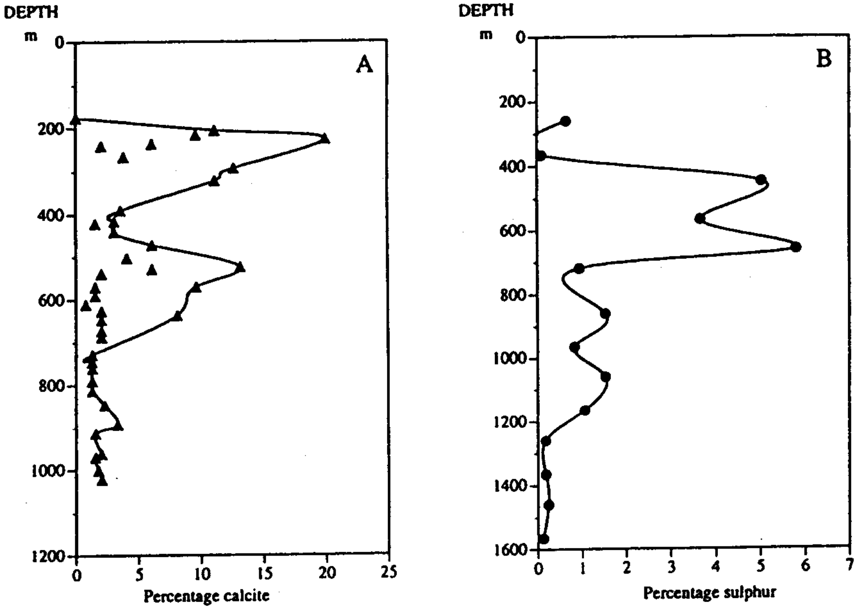

FIG. 6.1. Distribution of (A) calcite and (B) sulphur in altered rock in two high temperature wells in Iceland, Reykjanes 8 and Krafla 3; based on Tómasson and Kristmannsdóttir (1972) and Gunnlaugsson (1977), respectively.

precipitation that had infiltrated to deep levels, where they gained heat by contact with hot rock. The departure of the $\delta^{18}O$ values from the meteoric line, the oxygen shift, was explained by exchange of ^{18}O with the rock.

Since the pioneering work of Craig et al. (1956) enormous data have accumulated on the ^2H and ^{18}O composition of all kinds of natural waters. In some geothermal fields it is observed that geothermal waters have more positive values for both δ^2H and $\delta^{18}O$ than local precipitation (Giggenbach, 1992), whereas in other areas the δ^2H and $\delta^{18}O$ values are more negative (Arnórsson, 1995a). Elevated δ^2H values of geothermal waters, in relation to local precipitation, have been explained by the presence of a component of magmatic water, termed andesitic water, in the geothermal water (Giggenbach, 1992). In fact, the deuterium and oxygen isotope composition of geothermal waters associated with andesitic volcanism were explained by Giggenbach as mixing of andesitic water

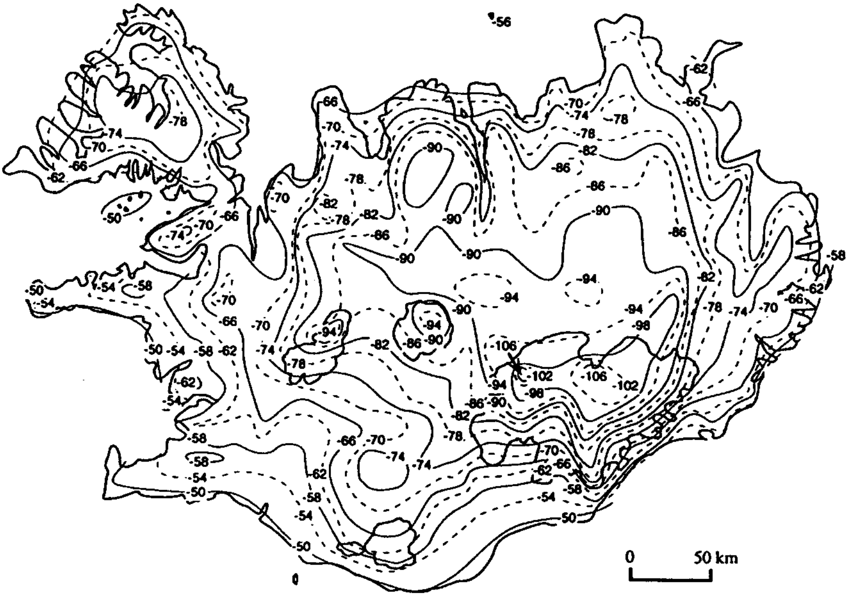

FIG. 6.2. Map showing the distribution of deuterium in present day precipitation in Iceland. From Árnason (1977a).

and local precipitation. The source of the andesitic water is thought to be a mixture of sea water incorporated into altered oceanic crust and juvenile water.

The low deuterium content of geothermal waters in relation to local precipitation has been explained by distant source areas on higher ground inland where the deuterium content of the precipitation is lower (more negative) than that in the respective geothermal fields (Árnason, 1977a). In his classic isotopic studies on natural waters in Iceland, Árnason (1977a) extensively sampled the country waters from local streams and springs, considered to be representative of the average deuterium content of the local precipitation, to construct a map showing how the deuterium content of the precipitation varied across the country (Fig. 6.2).

By drawing a line perpendicular to topographic contours from a particular geothermal field until the deuterium content of the geothermal water matched with the value of the precipitation, he defined what he considered to be the groundwater flow from the recharge area to that geothermal field (Fig. 6.3).

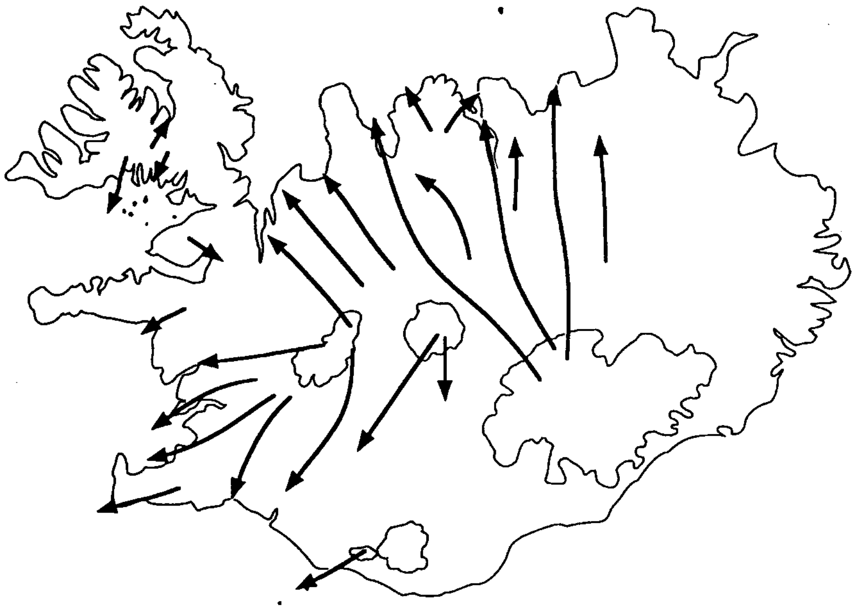

FIG. 6.3. Subsurface flow of water from recharge areas to geothermal fields according to the interpretation of deuterium data in meteoric and geothermal waters by Árnason (1977a). The arrow heads coincide with a particular geothermal field, and the tail of the same arrow to the recharge area for that geothermal field.

Deuterium data for geothermal waters having more negative values than that of local precipitation have also been explained by the presence of an 'ice age' component in these waters, i.e. the geothermal water contains a component of water that is more than some 10 000 years old, i.e. water from the last glaciation. Because of the colder climate at that time, precipitation would have been more depleted in deuterium than today's precipitation at any specific location. Since the climatic shift at the end of the last glaciation was severe on high latitudes but small in equatorial regions, the presence of 'ice age' water in geothermal water in high latitudes would shift the δ^2H to much more negative values, whereas such shifts would be slight in low latitude areas.

The deuterium excess for the global meteoric line is ten. This excess depends on the average moisture in the source area of the precipitation, being lower in moist areas and higher in dry areas. Thus, by the south coast of Iceland, which is an area of high average air moisture with high rainfall from southerly air masses, it is 3.5 (Sveinbjörnsdóttir et al., 1995), whereas in the eastern part of the Mediterranean it is greater than 20 (Nuti, 1991). The deuterium excess may be used as a tracer for waters which do not display significant oxygen shift. According to Arnórsson et al. (1995), geothermal waters with temperatures of less than about 80°C in the basaltic terrain in Iceland do not show any significant oxygen shift. Some geothermal waters, such as those in the Laugarnes field within the city of Reykjavík in Iceland, have a deuterium excess of 14 to 16, which is significantly higher than that of today's precipitation in the area, indicating, thus, that the geothermal water must have fallen as precipitation under climatic conditions that differ from those of today.

It should be evident from the discussion above that it is by no means straightforward to apply deuterium as a tracer to trace the origin of geothermal waters. A particular geothermal water may contain a component of magmatic water that will affect its deuterium composition or a component of precipitation that fell under climatic conditions differing from those of today. In both cases it is not valid to use a map showing geographic variations in the deuterium content of today's precipitation to locate the recharge areas to hot waters in geothermal fields.

Helium isotopes provide information on the source of geothermal fluids. High $^3He/^4He$ ratios are indicative of mantle contribution to the geothermal fluid. On the other hand, low ratios indicate a crustal source of radiogenic ^4He. It may be difficult to delineate the mechanism by which high ^3He is transported to the geothermal fluid. The helium could be derived from a deep source via diffusion, degassing of magma in relatively shallow chambers or dissolution from the rock with which the water interacts. In all cases the ultimate source of ^3He is the same, namely the mantle.

The ratio of $^{34}S/^{32}S$ differs considerably between ocean water and common rock types. For this reason sulphur isotope ratios have been used to distinguish between marine and rock leaching sources (Thorssander, 1986). For precipitation and waters that have reacted only to a small extent with the rock, $\delta^{34}S$ is useful to identify, the contribution from seawater spray and aerosols to the dissolved sulphate in the water, on the one hand, and anthropological sources or the rock, on the other hand.

7. GEOTHERMAL MANIFESTATIONS AND HYDROTHERMAL ALTERATION

Franco D'Amore, Stefán Arnórsson

The existence of geothermal systems is most often, but not always, revealed by certain surface manifestations which include thermal springs, fumaroles and hydrothermal alteration of the soil or exposed rocks. The geochemical characteristics of these manifestations, in particular the chemical and isotopic composition of discharged water and steam, provide information, such as subsurface temperatures, on various features of the underlying geothermal system. These manifestations are the subject of geochemical exploration surveys.

Hydrothermal alteration of the rock at depth, both its intensity and the types of hydrothermal minerals that have formed as well as fluid inclusions, provide information on various characteristics of the geothermal reservoir including temperature distribution and its thermal history. Some secondary minerals, such as quartz, calcite and pyrite, precipitate readily from solution when extensive boiling occurs. Accordingly, abundant quartz, calcite and pyrite in hydrothermally altered rocks is indicative of extensive boiling. Abundant adularia (K feldspar) is known to coincide with zones of high permeability.

Studies of hydrothermal alteration are important in delineating geothermal reservoir characteristics during the exploration and appraisal drilling phases. They are based on petrological examination of drill chips and cores. As alteration is intimately linked to chemical and isotopic reactions that influence geothermal fluid compositions, a brief summary of the nature of hydrothermal alteration processes will be given in the two last sections of this chapter although hydrothermal alteration studies are not covered by this book.

7.1. THERMAL SPRINGS

In the uppermost few metres of the soil or bedrock, temperature varies seasonally. However, because of the poor thermal conductivity of rocks and rock derived material, seasonal fluctuations in air temperature are seldom detectable one to two metres below the surface. Below this zone, temperatures increase linearly with depth, at least if not disturbed by flow of groundwater.

Water in springs is thermal if its temperature is higher than the average annual temperature in the area where it occurs. It is, however, common to take a spring to be thermal if its temperature exceeds the average temperature of the warmest month in the area.

One of the main characteristics of thermal springs, as compared with non-thermal springs and surface waters, is stability in temperature and flow. Thermal springs are often said to be warm if their temperature is below some 45°C but hot if their temperature is higher. Thermal expansion of water is quite insignificant in the range of 0–45°C. As a result, circulation of low temperature groundwater is driven by hydrostatic head. On the other hand, at higher temperatures, particularly above about 100°C, thermal expansion contributes more and more to driving groundwater circulation. It leads to a pressure gradient between a colder and, therefore, denser groundwater column and a hotter and, therefore, lighter groundwater column. Groundwater circulation driven by the pressure gradient of water of different densities is said to be density driven. The extent of density driven convection is dictated by geothermal gradient and permeability. For geothermal systems with temperatures in excess of some 60–80°C, it may not be necessary to have hydrostatic head to drive the circulation of the groundwater. It may be solely density driven.

It is noteworthy that flow rates of springs in Iceland with temperatures below some 50°C are generally low, and flow rates increase with rising temperature. This has been attributed to increasing contribution of density driven groundwater convection (Bödvarsson, 1982). If warm springs have high flow rates (tens of litres per second) in spite of low temperatures, they are suspected to be a mixture of hot and cold groundwater.

When geothermal water above 100°C rises to form springs it boils subsurface unless the flow rate is so low that it cools by conduction to sub-boiling temperature in the upflow. The temperature of boiling springs is determined by the boiling point of water at the respective atmospheric pressure. Springs that periodically boil explosively are called geysers, after the spring Geysir in Iceland, which means a spouter or erupter. Periodic boiling results from subsurface steam formation in the channels feeding geysers. The steam that forms results in much expansion of the rising fluid causing the water above to be rapidly expelled, thus reducing pressure and enhancing the boiling. The eruption of a geyser ceases when the water in the fractures immediately below it has all been expelled.

Perpetual geysers are rare but magnificent geothermal manifestations. Because of their beauty and tourist attraction they constitute an important resource as they are. Examples of magnificent geysers include Old Faithful in Yellowstone National Park, Wyoming, United States of America, and the

Bibilong boiling spouter in Namling County of the Tibetan autonomous region. Old Faithful erupts very regularly and spouts water some 50 m into the air. The Bibilong geyser continuously bursts from a steep cliff and obliquely jets more than ten metres into the air.

The chemical composition of boiling springs differs from that of the aquifer water below the first level of boiling. The spring water is depleted in gas but has become enriched in its dissolved solids content as a result of the steam loss. These processes must be taken into account when interpreting chemical and isotopic data from boiling springs with respect to subsurface temperatures and some other features of the underlying geothermal system, as discussed in various later chapters of this book. In contrast to boiling springs, the water in non-boiled spring waters is the same as that in the feeding aquifer, except for modifications caused by reactions in the upflow and eventual mixing with cold water.

7.2. FUMAROLES AND STEAM HEATED WATERS

Thermal springs demonstrate that the table of the hot groundwater coincides with the Earth's surface. When this groundwater table is below the surface and temperatures are higher than boiling at atmospheric pressure, surface manifestations are expressed as fumaroles, sometimes called steam vents. When deposits of native sulphur have formed around fumaroles they are termed solfataras. The boiled hot water is discharged off subsurface. The level of the water table in any area is largely dictated by topography and rock permeability but also by the amount of precipitation. Thus, fumaroles are more common on high ground than on low ground as well as where geothermal systems occur in young and, therefore, permeable volcanics.

In many geothermal areas fumaroles characterize the geothermal manifestations on high ground but hot springs do the same thing on low ground. The hot springs discharge boiled water that has flowed laterally from an upflow as determined by the hydraulic gradient. This distribution of thermal manifestations is a characteristic feature of many geothermal systems associated with andesitic volcanoes such as Amatitlán in Guatemala, Ahuachapán and Berlín in El Salvador and Tongonán as well as other geothermal areas in the Philippines.

When the geothermal water boils subsurface, it is largely degassed and the gases are discharged to the surface with the steam. The gas content of steam in fumaroles provides various kinds of information about the characteristics of the underlying geothermal system such as reservoir temperatures and the direction of subsurface water flow.

Fumarole steam above liquid dominated reservoirs is always saturated. On the other hand, fumarole steam in vapour dominated systems as well as steam discharged within or in the vicinity of craters of active volcanoes may be superheated. For example, Japanese and Soviet scientists sampled fumaroles on Japanese islands and Kamchatka, where the temperature was over 700°C. The same order of temperature has been registered on the islands of Vulcano and Stromboli, Italy.

Rising geothermal steam may condense partly or completely in surface waters. When this occurs, steam heated hot springs form. If a limited amount of water is available the surface water may be heated to the boiling point. Boiling of this water and the associated alteration of the soil and rock into clay leads to the development of mud pools, mud pots and mud volcanoes.

Clearly, steam heated waters have never been in the deep geothermal system. Their isotopic and chemical composition does not, therefore, reflect the physical conditions that characterize this system. Their isotopic and chemical composition is determined by isotopic and chemical reactions occurring at the surface and by the gas and isotopic composition of the rising steam and the initial surface water as well as by vaporization of the steam heated water. For this reason, sampling these manifestations does not serve any geothermal exploration purpose. Steam heated waters can often be identified as such by geological-hydrological observation. Chemically, they are characterized by low chloride content (similar to that of local surface water), high sulphate content (up to 2000 ppm), low pH (often between 2 and 4) and Na/K ratios similar to those of the rock which they have altered.

In some areas, both in volcanic and non-volcanic regions, dry gas, which is almost pure CO_2, is discharged from the ground. These manifestations may or may not be associated with geothermal reservoirs.

Hydrothermal (phreatic) craters manifest explosive subsurface boiling. Craters of this kind may be tens of metres in diameter. They may be triggered by earthquakes which cause a sudden change of permeability. Examples of hydrothermal explosions include those occurring in the Qupu geothermal area, Tibet, in 1975 and in the Yunnan province of China in 1976. Hydrothermal explosions may also occur as a result of poor cementing or insufficient casing of wells. Shallow casing may lead to the outflow of fluid from a deep high pressure aquifer into a shallow one where the pressure exerted by the deep aquifer exceeds the lithostatic pressure.

7.3. HYDROTHERMAL ALTERATION

The chemical and isotopic reactions between geothermal fluids and rocks influence not only the composition of the fluid but also the composition and the mineralogy of the rock. As was explained in Section 3.2, progressive reaction between water and rock leads to dissolution of the primary rock minerals and deposition from the fluids of secondary or hydrothermal minerals. From general thermodynamic considerations, it can be concluded that the types of hydrothermal mineral that form depend on the temperature, pressure and chemical composition of the system. It has, however, been shown that pressure in the range occurring in geothermal systems (1–200 bars, corresponding to 0–3000 m depth) has little effect on mineral stability. Accordingly, alteration mineralogy is largely dictated by temperature and system, i.e. rock composition. Many studies have shown that geothermal fluids closely approach chemical equilibrium with hydrothermal minerals in geothermal systems, at least, if temperatures exceed about 100°C (Giggenbach, 1981; Arnórsson et al., 1983a), and sometimes at lower temperatures (Arnórsson and Andrésdóttir, 1995).

Some groundwater systems, including geothermal systems, are said to be rock dominated. This implies that the mass of the inflowing and outflowing fluid is small compared to the mass of rock it flows through. In a rock dominated system the hydrothermal minerals that form in response to fluid–rock interaction are determined by the temperature of the system and the composition of the rock. In some geothermal fluids the inflowing water may be sea water. Also, some geothermal systems receive gaseous components from their magmatic heat source. This external supply of chemical components to the geothermal system influences the system composition and may affect, in addition to the composition of the rock, the type of hydrothermal minerals deposited from the fluid. As an example, it can be mentioned that anhydrite is an abundant hydrothermal mineral in geothermal basalt–seawater systems in Iceland with temperatures in excess of some 100°C, whereas it is not scarce or present in basalt–meteoric water geothermal systems. In some Philippine geothermal fields, acid alteration zones that have been identified are characterized by minerals such as diaspore, kaolinite and anhydrite (Reyes, 1991). This alteration is attributed to acidic fluids resulting from supply of acids such as HCl and SO_2 by degassing of the magmatic heat source.

Some hydrothermal minerals form solid solutions. Examples include epidote and chlorite. Epidote has the formula $Ca_2Al_2(Al,Fe)Si_3O_{12}(OH)$, where aluminium occupies three types of crystallographic sites. In one of these sites ferric iron substitutes easily for aluminium. Epidotes contain variable amounts of aluminium and ferric iron, depending on the composition of the system (rock type) in which they form. Basaltic rock is high in iron and, as a result, epidote in such rock is iron rich, often approaching $Ca_2Al_2FeSi_3O_{12}(OH)$ in composition. On the other hand, silicic rocks such as rhyolites are low in iron and so are epidotes they host, sometimes close to $Ca_2Al_3Si_3O_{12}(OH)$ in composition. Chlorite ($(Mg,Fe)_5Al_2Si_3O_{10}(OH)_8$) is another example of a common, solid solution hydrothermal mineral. It is a mixture of two end members where Mg and Fe substitute for each other: Mg chlorite ($Mg_5Al_2Si_3O_{10}(OH)_8$) and daphnite ($Fe_5Al_2Si_3O_{10}(OH)_8$).

Solid solution minerals can adapt to some extent to changes in rock composition by changing their composition, thus increasing their stability range. As a result, epidote and chlorite are widespread as alteration minerals in geothermal systems hosted by rocks of basaltic to rhyolitic composition.

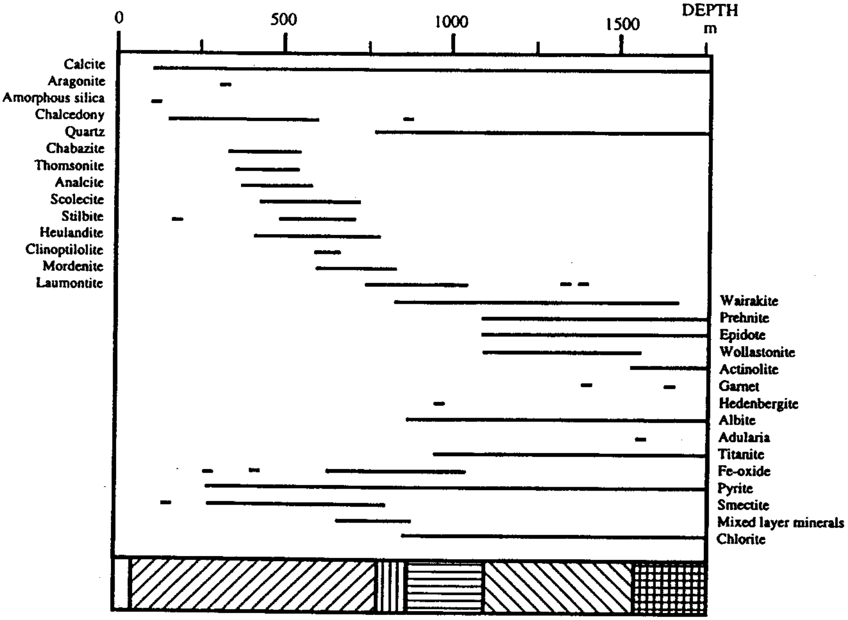

FIG. 7.1. Depth distribution of hydrothermal minerals in rocks penetrated by well 15 at Nesjavellir, Iceland. Mineral zones are shown at the bottom. Their shading is the same as in Fig. 7.3. From Steingrímsson et al. (1986).

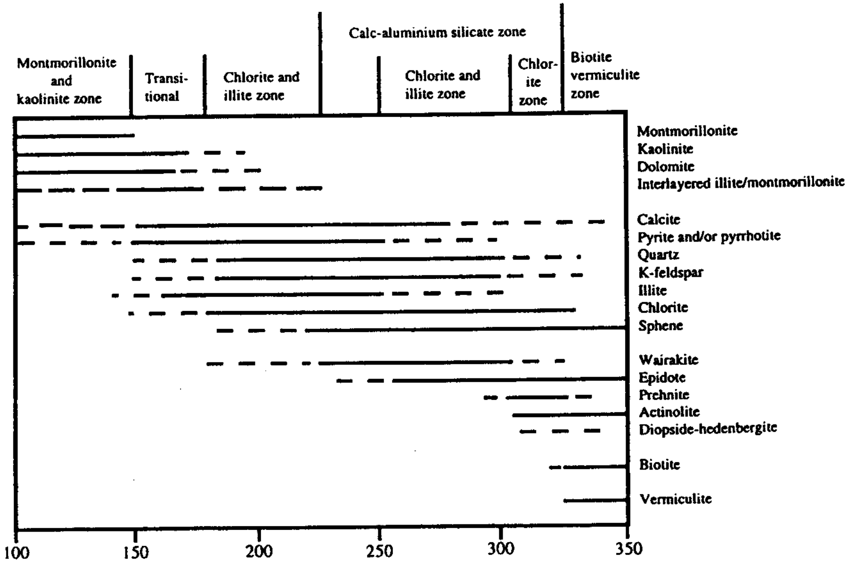

FIG. 7.2. Temperature range for the occurrenc of hydrothermal minerals in the sandstones of the Cerro Prieto geothermal field, Mexico.

For rocks of a given composition, alteration minerals largely reflect the system temperature at the time of their formation as their stability is practically independent of pressure. Some alteration minerals have a wide temperature stability range, such as quartz, calcite and pyrite, whereas other minerals are stable only over a limited temperature range as many zeolites, prehnite, epidote and chlorite, just to mention a few. Figures 7.1 and 7.2 show the depth/temperature distribution of hydrothermal minerals in basaltic rocks penetrated by well 15 at Nesjavellir in Iceland and in the sandstones of the Cerro Prieto field, Mexico. In both fields the range of temperature is about the same. Accordingly, differences in the alteration mineralogy are mostly due to differences in rock composition.

Studies of alteration in drilled geothermal fields provide information on formation temperatures both in vertical and horizontal directions. Often the alteration mineralogy matches well the measured temperature distribution. In some cases, however, the mineralogy indicates a different temperature pattern. When

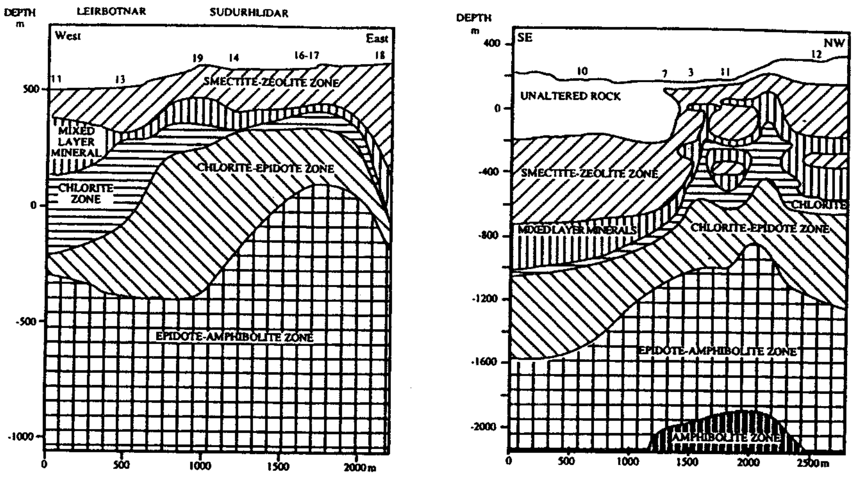

FIG. 7.3. Hydrothermal alteration zonation in the Krafla (left) and Nesjavellir (right) geothermal reservoirs in Iceland. From Ármannsson et al. (1987) and Franzson (1988), respectively. The numbers on the top of each section represent the wells on which the sections are based. Numbers on Y axis show metres above or below sealevel.

this is the case, it is taken to indicate that the geothermal system has evolved with respect to temperature and that the alteration pattern reflects temperatures that existed in the system sometime in the past. In the Laugarnes field within the city of Reykjavík in Iceland, the presence of epidote, chlorite and some other hydrothermal minerals reflects formation temperatures of about 250°C (Arnórsson, 1995a). The maximum measured downhole temperature at 3000 m depth is 160°C. The alteration mineralogy is taken to indicate that the Laugarnes system was of the high temperature type sometime in the past but has cooled down after it had been cut from its presumed magmatic heat source in conjunction with its drifting out of the active volcanic belt. It has developed into a low temperature system in the process.

Sometimes, measured temperatures in wells do not yield correct information on the temperature depth distribution in the system, but mineral zonation may. There are essentially two reasons for this. One is that two or more aquifers penetrated by the well do not have the same pressure potential. When this occurs fluid will flow in the well under shut-in conditions from the aquifer with the highest pressure potential and into the aquifers with lower pressure potentials. The temperature in the well between aquifers will be determined by the temperature of the highest pressure potential aquifer.

If a well intersects a boiling aquifer the temperature in a shut-in well above this aquifer tends to be adjusted to the boiling point curve with depth. Steam from the aquifer entering the well will rise. If water at some level is below the boiling point, the steam will condense and heat the water in the process. Steam will continue to rise and condense until the whole water column has been heated to the boiling point. Steam may still continue to ascend to form a steam cap under the wellhead and push the water level in the well down. Steady state conditions are reached when steam condensation by conductive heat loss balances the flow of steam from the boiling aquifer.

Certain hydrothermal minerals, which have a limited temperature stability range, have been used to map alteration zones in geothermal systems. In the basaltic environment in Iceland, essentially five mineral zones, named after the index mineral, have been distinguished (Fig. 7.3). The sixth zone, the amphibolite zone, has only been identified in the hottest wells at Nesjavellir (Fig. 7.3). Similar, yet somewhat different zones have been recognized in sandstones of the Cerro Prieto field, Mexico (Fig. 7.2). In the Hakone geothermal field in Japan, four zones have been distinguished on the basis of the most prominent layer silicates, namely kaolinite, smectite, smectite–chlorite and chlorite zones.

It is possible to infer the shape of the geothermal reservoir and upflow zones from the shape of the mineral zones in extensively drilled geothermal fields. The plunging down of the mineral zones towards east in the Krafla field (Fig. 7.3) indicates that one is approaching the boundary of the geothermal reservoir at well 18. It is evident from the mineral zonation at Nesjavellir that the major upflow is in the vicinity of well 11.

7.4. ACID SURFACE LEACHING AND MINERAL DEPOSITION

A special type of alteration is produced on the surface in geothermal fields where steam containing H_2S condenses in surface water. In the process a steam heated surface water forms. The H_2S in the rising steam reacts with the oxygen dissolved in the water or directly with the oxygen of the atmosphere. Partial oxidation leads to the formation of native sulphur, but complete oxidation leads to the formation of sulphuric acid:

$$H_2S + \frac{1}{2}O_2 = S + H_2O \tag{7.1}$$

and

$$H_2S + 2O_2 = 2H^+ + SO_4^{2-} \tag{7.2}$$

Sulphuric acid is a strong acid that is completely dissociated for all practical purposes as indicated by reaction (7.2). Steam heated waters may attain a pH as low as 1.

The acid steam heated waters are strongly undersaturated with most common rock forming minerals. As a result, soil and rock are extensively dissolved and undergo drastic chemical changes and complex mineralogical transformation. The minerals present depend on the original rock and the extent to which leaching has progressed. The final product is commonly kaolinite, amorphous silica and anatase with smaller and variable amounts of many other minerals such as native sulphur, gypsum and pyrite or haematite. The native sulphur originates from partial oxidation of the H_2S in the rising steam, and gypsum from its complete oxidation and subsequent reaction with calcium dissolved from the rock.

Acid surface leached soil around fumaroles often forms very conspicuous thermal manifestations. Sometimes the acid leached ground only reaches to a depth of one to two metres and seldom to more than a depth of a few tens of metres.

The H_2S concentrations in fumarole steam are affected by several processes. First, they are affected by the H_2S of the parent hot water and, secondly, by its reaction with the wallrock in the upflow. Additionally, near surface oxidation of H_2S may lower its concentration in the steam. The H_2S concentration in geothermal reservoir waters is determined by temperature dependent equilibria with specific minerals; it increases with rising aquifer temperature. For this reason, H_2S concentrations in fumarole steam tend to be positively related to the temperature of the source aquifer for that steam.

Long or slow passage of the steam to the surface from the source aquifer is associated with removal of H_2S from the steam. Accordingly, steam in marginal fumaroles of geothermal fields may be low in H_2S but is relatively higher in CO_2; alteration around such fumaroles may be limited. By contrast, alteration tends to be more prominent above major upflow zones which pass relatively H_2S rich steam to the surface.

The degree of alteration in geothermal areas caused by steam heated waters not only depends on the amount of H_2S in the steam but also on rock type, precipitation and longevity of the geothermal activity. Basaltic rock, in particular basaltic glass, is very susceptible to alteration. Increased precipitation supplying oxygenated water enhances the alteration process.

Siliceous and calcareous sinters are common in many geothermal areas. Silica sinters are composed of amorphous silica. Thermal waters which have reached saturation with amorphous silica precipitate this phase readily. For boiling hot (100°C) springs, amorphous silica saturation is reached when dissolved silica concentrations (as SiO_2) are about 380 ppm. As will be discussed in Chapter 10, such silica concentrations correspond with subsurface temperatures of about 220°C. Thus, the presence of silica sinter deposits indicates temperatures well in excess of 200°C in the underlying geothermal system.

Carbonate sinters (travertine) are deposited from thermal waters high in dissolved CO_2 in response to surface or near surface CO_2 degassing of the water. Travertine and siliceous sinters form heaps, layers and terraces around the springs and along the streams flowing from them. Sometimes, they create very spectacular structures such as large mounds resembling waterfalls as the Mammoth springs of the Yellowstone National Park in Wyoming. At Pamukkale in Turkey, water pools have developed on splendidly white travertine mounds. In the Longma hot spring area in the northern Tibetan hinterland, a wonderful 'stone forest' of travertine has formed. Owing to the dry air in the area, the thermal water evaporates rapidly at the spring vents, and the precipitated travertine forms columns of varying height around each vent. Several tens of travertine columns exist in the area. Commonly, they are 2 to 3 m high but the tallest one reaches 7 m. Thermal water still emerges from the tops of some of the lower columns.

Salt efflorescent precipitates are sometimes associated with pools and lakes fed by geothermal fluids. Such waters and the associated salt deposits often contain very high concentrations of boron and the rare alkali elements as well as Li. Often, they also contain double sulphates, sulphur and clay. Sometimes, they are high in mercury and arsenic. The salt efflorescence is usually a spectacular phenomenon.

8. SAMPLING OF GEOTHERMAL FLUIDS: ON-SITE MEASUREMENTS AND SAMPLE TREATMENT

Stefán Arnórsson and Franco D'Amore

8.1. OBJECTIVES

The objective of any geothermal exploration and development programme is to determine at the lowest possible cost the economic and environmental feasibility of exploiting a particular geothermal resource. The objective of monitoring studies after exploitation has started is to map the response of the geothermal reservoir to the production load in order to maximize the quality of its exploitation. Geochemical techniques applied during the various stages of exploration and evaluation of geothermal resources, as well as monitoring studies, are particularly important because of the information they provide at relatively low cost.

During the exploration phase geochemical data are used to:

(1) Evaluate the origin of the geothermal fluids;
(2) Determine the compositional characteristics of the geothermal fluids in relation to those of the surface and groundwater;
(3) Estimate subsurface temperatures and subsurface gas partial pressures;
(4) Define the chemical properties of the fluid with respect to environmental issues, scaling, corrosion and other technical aspects;
(5) Delineate a hydro-geochemical model of the geothermal system showing, as far as possible, the distribution of subsurface temperatures and directions of groundwater flow.

During the exploration and appraisal (production) drilling phases, geochemical data on the composition of the discharged fluids provide information on:

(6) The quality of the geothermal fluid for the intended use, and environmental issues;
(7) The temperature and level of producing horizons in wells (in conjunction with logging data);
(8) Steam to water ratios in producing aquifers;
(9) Scaling and corrosion tendencies.

Additionally, the drillhole data should be used to:

(10) Quantitatively explain the composition of the geothermal fluid (solution–mineral equilibria);
(11) Identify the sources of conservative components;
(12) Specify some operational conditions and the conditions for injecting waste fluids;
(13) Improve the conceptual hydro-geochemical model of the geothermal reservoir.

When exploitation has started, water and steam samples from wells should be sampled and analysed at regular intervals in order to:

(14) Evaluate boiling processes in the aquifer of producing wells;
(15) Map changes in aquifer temperatures and aquifer steam to water ratios;
(16) Map recharge (hot or cold water) into the reservoir.

Essentially conservative components (Chapter 4) are used to specify the origin of the fluids but reactive components are employed to characterize the various physical properties of the reservoir. Data on many trace elements are needed for assessing the environmental impact of exploitation. The components to be analysed in samples depend on the purpose of the respective geochemical study, as will be discussed in the following section.

8.2. SELECTION OF ELEMENTS AND COMPONENTS FOR ANALYSIS

The chemical and isotopic components that are generally analysed for in water and steam samples during geochemical exploration, well testing and monitoring studies are listed in Box 8.1. Each of the chemical and isotopic components provides information, which may relate to the source of the geothermal fluid or some components in it (e.g. δ^2H, $\delta^{18}O$, δ^3He, $\delta^{34}S$, $\delta^{13}C$, Cl, B), its age (^3H, ^{14}C), physical reservoir characteristics such as temperature and boiling (Si, Na, K, Ca, CO_2, H_2S, H_2 and many more), control of fluid compositions by equilibria with hydrothermal minerals (pH, Al, As, Fe, Ti, Mg, SO_4, F, Si, Na, K, Ca, CO_2, H_2S, H_2 and many more) or the quality of the fluid with respect to the kind of exploitation involved and the environment (e.g. Si, Al, Cl, B, As, Cd, Cu, Hg, Mn, Pb, Zn and many more). The choice of components to be analysed calls for specific sample treatment and specific sample volumes, depending on the analytical technique to be used. Which components are selected depends, to a certain an extent, on the knowledge of the geochemist as regards data interpretation but partly also on the cost involved or on the available analytical facilities. Successful sampling and analysis depend on the background knowledge in analytical chemistry and data interpretation of those who plan and carry out this sampling.

During the exploration phase, the emphasis is on components that provide information on physical reservoir characteristics and the source of the fluid. For well testing, the same components are of interest, in addition to those which relate to the quality of fluid for its intended use, as well as environmental issues. Monitoring studies mostly require data pertaining to physical reservoir characteristics.

Determination of isotope ratios in certain compounds ($\delta^{18}O$ in water and sulphate, $\delta^{2}H$ in water and hydrogen gas, $\delta^{34}S$ in sulphate and sulphide, $\delta^{13}C$ in CO_2, CH_4, HCO_3 and H_2CO_3 (dissolved CO_2)) provides information on temperature (isotope geothermometers) in geothermal systems and on the sources of the compounds hosting these isotopes.

To improve the understanding of the origin of some components in geothermal fluids, it is useful to analyse the hydrothermally altered rock of the geothermal reservoir as well as fresh rock of the same kind. Depletion of an element in the altered rock as compared to fresh rock, or an increase in its concentration, provides information on the water–rock interaction and/or supply to the rock from an external source. The difference in the $\delta^{18}O$ content of fresh and altered rocks is a measure of water–rock ratios. Cl and B concentrations in fresh and altered rock provide information on the potential of the rock as a source for these elements in the water. Large additions of an element to the altered rock (see, e.g., Fig. 6.1) point to an external source. Water–rock interaction experiments may also furnish useful data to improve the understanding of the nature of geothermal reservoirs.

Studies that require data on rock chemistry and water–rock interaction experiments are not routine parts of geothermal exploration, development and monitoring investigations. They are generally regarded as parts of basic research.

8.3. SELECTION OF SITES FOR SAMPLING OF THERMAL WATERS FOR GEOCHEMICAL EXPLORATION

Geological mapping and geochemical reconnaissance surveys usually constitute the first phase of geothermal exploration programmes. When planning a sampling programme for geothermal fluids, as part of an exploration programme, it is necessary to have a map showing the distribution of the thermal manifestations in the area to be investigated as well as temperatures and flow rates of the springs. If flow rates are not measured as part of the geological mapping, they should be estimated. All available data on the chemistry of the thermal fluids should be assembled. It is not possible to give any general guideline on the number of samples to be collected from a particular area, as this will depend on its size and the number of geothermal manifestations.

Sampling of surface waters and of non-thermal springs form an inherent part of any geochemical exploration survey. Deuterium and ^{18}O isotope data on these waters serve to determine the isotopic composition of local precipitation and to indicate the origin of the geothermal fluid. The chemical composition of the non-thermal waters is necessary for evaluating possible mixing of thermal with cold water in upflow zones (Chapter 11). These data are also useful in delineating how the waters change chemically with rising temperature from an overall disequilibrium towards equilibrium with hydrothermal minerals.

8.4. SAMPLING OF SURFACE WATERS, SPRINGS AND HOT AND COLD WATER WELLS

When a sampling point has been selected,

(1) the sample site should be described,
(2) on-site measurements should be carried out, and
(3) a sample should be collected and treated according to the elements to be determined as well as the analytical technique.

The description of the site should include the nature of the emergence point. Is the outlet well defined, not visible, or does the spring form a pool? Does the water issue from the bedrock, through and organic soil cover, etc.? Whenever possible, the spring location should be related to tectonic or other geological structures, rock type and topography.

Measurements to be carried out on-site include:

(1) The flow rate, which, if not measured, should be estimated.

Upon rapid expansion at the surface it may become slightly superheated. As already mentioned (Chapter 7), fumarole steam in the vicinity of active volcanoes may be strongly superheated. Although such fumaroles are of great geochemical interest, they will not be discussed here as they are of limited interest for geothermal exploration.

Warm, moist air emerging from hot ground may look like a fumarole. Temperature measurement will reveal that it is not. For this reason it is recommended to have a thermometer when collecting samples from fumaroles and to measure the temperature so as to eliminate any uncertainty about the nature of the discharge.

Steaming ground may look very conspicuous from a distance. However, closer inspection may reveal that the discharging steam is diffuse and that it is difficult to find any well defined vents. This is particularly the case when the steam issues in highly permeable formations such as young lavas. Experience shows that such discharges may be difficult, if not impossible, to sample. Slight restriction to flow in the tubing and the valve of the sampling bulb may give rise to a diversion of the steam in the fumarole to be sampled towards another outlet. The best fumarole sampling points form small, well defined holes through which steam discharges at considerable velocity. Such holes are especially found where the ground has been intensely altered by acid surface leaching. Sampling from boiling mud pools is not advisable. The steam passing through them may have lost some H_2S and picked up atmospheric gases.

When sampling fumarole steam, the main concern is usually to avoid air contamination of the sample. Generally, the presence of oxygen in geothermal steam is taken as evidence of atmospheric contamination. However, oxygen in fumarole steam may have originated from degassing of steam heated water and could really be present in the steam. In well discharges, on the other hand, the presence of oxygen in gas samples can safely be considered to be a measure of atmospheric contamination. Atmospheric contamination reduces the value of data on N_2 and Ar. It also tends to yield low values for H_2S because the atmospheric oxygen easily oxidizes it, especially when the acid gases (CO_2 and H_2S) are collected into alkaline solution.

As with water samples, it is not possible to give any general rules on the number of gas (steam) samples to be collected from a particular geothermal field for a geochemical exploration survey. This number will depend on the size of the area and the number of fumarole and gaseous thermal spring manifestations. If many fumaroles occur within a relatively small area, at least several of them should be sampled within one such area to reveal whether or not the gas content of the steam is homogeneous rather than to assume that one sample from such a cluster of fumaroles is representative. Homogenous composition indicates that the steam composition is controlled by deep seated processes rather than shallow ones.

8.6. SAMPLING OF WET STEAM WELLS

To collect samples of water from the wellhead separator of wet steam wells it is necessary that a 0.5 in. socket has been welded at a low point on the separator body to which a 0.5 in. stainless steel ball valve should be fitted. For steam sample collection, another 0.5 in. socket with a 0.5 in. ball valve should have been welded on the steam line from the separator. Its location is not of importance, and it need not be more than one to two metres away from the separator.

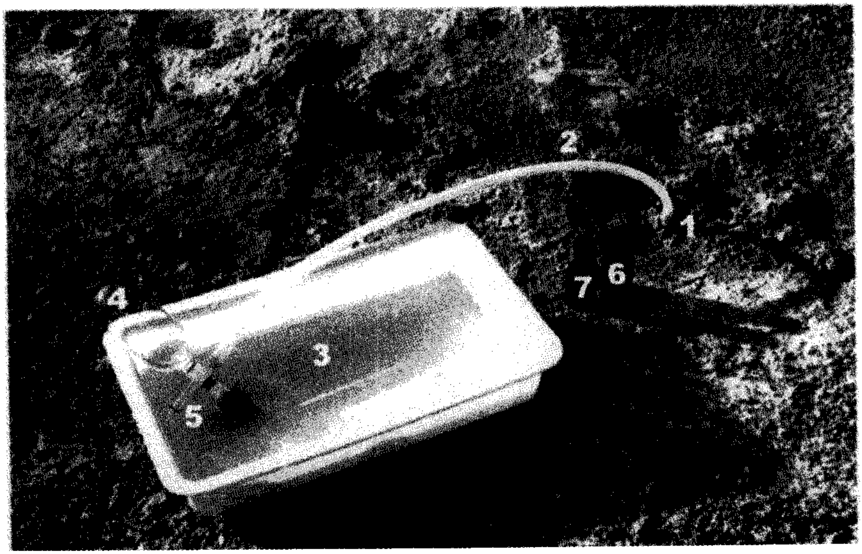

FIG. 8.2. View of apparatus for sampling fumaroles into a pre-evacuated sampling bulb. (1) Funnel covered with clay; (2) tubing; (3) tray with water for cooling; (4) gas sampling bulb; (5) tubing clamp; (6 and 7) two 50 mL sample bottles for (a) δ^2H and $\delta^{18}O$ and (b) NH_3.

If two-phase pipelines are used to convey the well fluid to a separator station and no steam separator has been installed at an exploration well being tested, a 0.5 in. socket with a 0.5 in. ball valve must be welded on the two-phase pipeline close to the wellhead. The socket should be in the middle of the pipe in a horizontal position. Its location is not critical except that it should be close to the wellhead and at least 2 m from any bend or restriction in the pipe. To keep the screw thread of the ball valve clean, a cap should be screwed on it between sampling activities. The same applies, of course, to the sample ball valves, if a wellhead separator has been installed on the wellhead.

A Webre separator (Fig. 8.5) must be used if samples are to be collected from a two-phase pipeline. In sampling with the Webre separator it is important that steam samples are not contaminated with brine and, in particular, brine

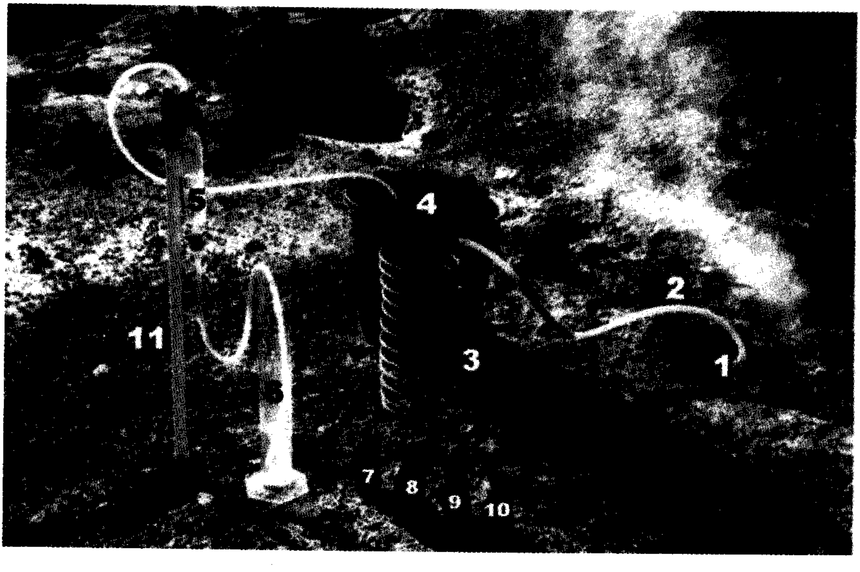

FIG. 8.3. View of apparatus required for sampling separately non-condensible gases and condensed steam. (1) Funnel covered with clay; (2) tubing; (3) cooling coil; (4) bucket with cold water; (5) gas sampling bulb with stopcocks at both ends; (6) measuring cylinder; (7 to 10) 50 mL glass bottles for collection of samples for (a) δ^2H and $\delta^{18}O$, (b) NH_3, (c) CO_2 and (d) H_2S; (11) stake peg.

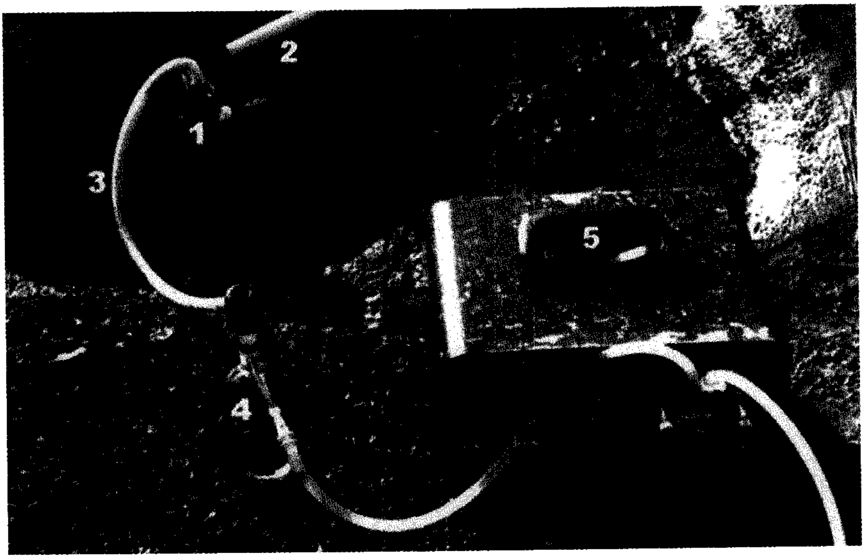

FIG. 8.4. Sampling of a gas phase from a hot water pool. (1) Funnel which has been placed over the stream of gas; (2) stake peg with clamp to fasten funnel; (3) tubing; (4) evacuated sampling bulb; (5) sampling pump for sucking up water from the pool into the funnel and tubing to displace air (a hand vacuum pump may also be used).

samples are not contaminated with steam. Whether a brine component is present or not in the steam can be verified by analysing Cl in the condensate. If steam comes with the water, so does a gas phase, which can easily be verified by placing the end of the tubing conveying the cooled water from the separator into water to see if gas bubbles emerge. If they do, steam is coming with the water. If they do not, the water sample is as it should be. A detailed description of the sampling procedure using a Webre separator is given in Box 8.13.

A cooling coil must be used to prevent boiling when collecting water samples from the Webre separator. The flow from the separator should be adjusted in such a way that cooling to about 30°C can be achieved, at least when collecting samples into glass bottles for pH, total carbonate and isotope measurements. This intensive cooling is not required when collecting samples into plastic bottles for determination of other components.

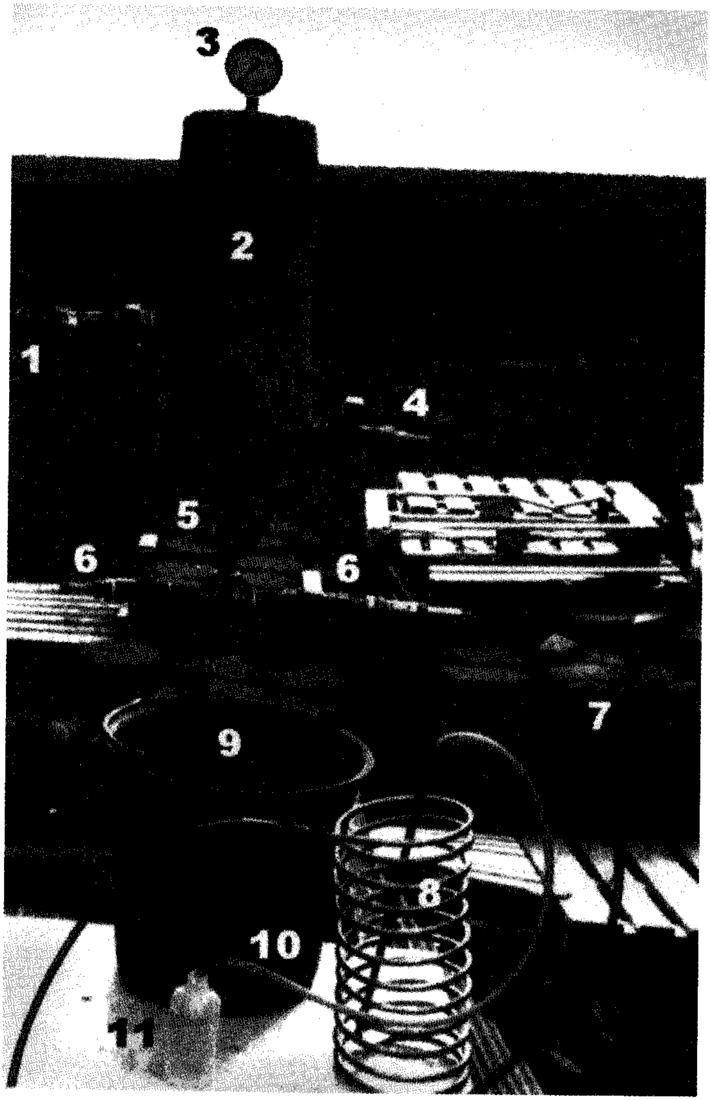

FIG. 8.5. Webre separator for collecting water and steam samples from wet steam wells: (1) valve connecting separator to 1/2 in.socket on two phase flow pipe; (2) Webre separator; (3) pressure gauge; (4) water sampling valve; (5) valve for adjusting steam flow; (6) steam outlet valves; (7) high pressure tubing for connecting separator and cooling coil; (8) cooling coil; (9) bucket with cold water; (10) tubing from cooling coil with non-return valve (not shown); (11) sample bottle.

A cooling coil may also be used to collect steam samples, although this is not necessary. Cooling may also be done by pouring water onto the gas sampling ulb during collection or immersing it directly into cold water. In both cases an atmospheric non-return valve must be fitted on the tubing between the cooling coil and the gas sampling bulb, or between the separator and the gas sampling bulb, to ensure that pressure does not build up in the bulb that may cause the tubing to come off or the bulb to explode.

If a separator has been installed at each wellhead, the Webre separator is not necessary, and the cooling coil can be fitted directly on the respective ball valves. If a coil is not used for steam samples, the ¼ in. silicone tubing with the one way atmospheric valve is connected directly on the ½ in. ball valve on the steam line.

The flow pattern of water–steam mixtures depends on the relative volume of the phases and their velocity. When the steam dominates the volume, the water tends to occur as droplets in the steam phase. This pattern of flow is the most favourable one for separation and sample collection. When the volume fraction of water increases, the flow may become annular, the water may flow at the bottom of horizontal pipes and the steam at the top, or the water may come in slugs. These flow patterns, in particular slug flow, make separation more difficult as they lead to variable flow of water and steam into the Webre separator, thus upsetting the adjustment of the valves on the separator.

It may not be possible to collect with a Webre separator steam free water samples from wells with high discharge enthalpy (>2500 kJ/kg). The Webre separator cannot be adjusted to discharge water only through the water valve. When this is the case it is best to collect the water sample from the weirbox, if available. The disadvantage of collecting water samples from the weirbox of wells with low water flow rates is that the water may have evaporated substantially, thus changing its composition, especially the isotopic content.

It is recommended to use the Webre separator, if possible, to collect water and steam samples at the same pressure rather than collecting the water sample from the weirbox and the steam sample from a pressurized pipeline. This makes assessment of total discharge and reservoir fluid compositions easier and more reliable. However, for trace element analysis, it may be beneficial to collect a special sample from the weirbox in order to avoid contamination. Contamination is considered to be more likely from the valves and the Webre separator than from pipelines which the water has flowed through undisturbed for some time.

8.7. GENERAL INFORMATION ON MATERIAL SELECTION, ACID WASHING AND REASONS FOR SAMPLE TREATMENT

All information relevant to the characteristics of the sampling site and results of measurements on-site should be written down in a field notebook. A convenient numbering system should be adapted to identify all samples throughout all types of analysis to be made. One possibility is to give samples from a specific area a three letter code followed by a number incorporating year of sampling and number. For example: GEY-98-0121 means samples from the Geyser field collected in 1998, being sample number 121 for that year.

Sample bottles have not been specified here except for their size. High density polyethylene bottles are convenient. If they are being reused they should be soaked in acid bath of 5% ultrapure HNO_3 for 24 hours and then thoroughly rinsed with deionized water. Reused vials for nutrient salts should be well rinsed with 1 M HCl followed by washing in ample deionized water. Use glass bottles of amber glass and rinse them with deionized water.

Plastic bottles are much more widely used for the storage of water samples for inorganic analyses than glass bottles. Compared to glass bottles they are cheaper and less fragile. On the other hand, the disadvantage of plastic is that its porosity is high enough to allow some evaporation when samples are stored for long periods of time. This is why samples for isotopes, pH and carbonate analyses should be collected into glass bottles.

Solid particles suspended in water samples may react with the water upon storage of the samples and in that way change their composition. For this reason it is necessary to filter samples upon collection. In particular, acidified samples must be filtered because the pH of an acidified sample is as low as 1. At this low pH, the water has the tendency to effectively dissolve any dust, rock or other particles that would be present in an unfiltered sample. The acidificaton serves two purposes. One is to prevent precipitation of solids that could occur during sample storage, such as precipitation of ferric hydroxide or of calcium carbonate from waters rich is CO_2. Secondly, acidification prevents adsorption of ions onto the walls of the sample bottle.

One of us has had good experience with using battery driven (12 V) filtering pumps for collecting water samples. This allows water to be sucked up directly from the spring or surface water to be sampled and then pressed through the filter straight into the sampling vessel without any contact with the As the sample is pressurized after entering the pump, degassing is not a problem.

It is considered best to add a little $HgCl_2$ solution to samples collected for carbon isotope analysis. This will kill any bacteria in the sample that are so small that they pass the filter membrane, thus preventing any growth of organisms that would affect the carbon isotopic content of dissolved carbonate. This treatment is, of course, also possible for the nutrient salt samples. However, the mercury introduced into the sample could affect the performance of the cadmium reducing column in the auto-analyser. It is, therefore, considered better to put these samples into a cooling box immediately after sampling and freeze them as soon as possible. In this way, growth of bacteria or other organisms affecting the aqueous concentrations of the nutrient salts is prevented.

The parameters that are probably most often determined with the poorest precision and the least care is pH and total carbonate. Very often alkalinity is measured instead of total carbonate. Alkalinity is defined as the reaction of a water sample against acid from its pH to a pH of about 4.5, or, more precisely, to a pH corresponding to the equivalent point where $H^+ = HCO_3^-$. This point represents the maximum slope on a graph of pH (x-axis) versus titre (mL 0.1 M HCl solution, y axis). Most often it lies between a pH of 4 and 5, the precise value depending on the concentration of dissolved carbonate. For most surface waters the only base reacting against the acid added to the sample is bicarbonate. For such waters it is a good approximation to take the milliequivalents of acid added to be equal to HCO_3^-. This is, however, not valid for very many geothermal waters, because bases other than bicarbonate affect their alkalinity. For data interpretation it is of interest to determine total carbonate but not alkalinity. Accordingly, it is recommended to adapt an analytical method that fulfils the requirements for data interpretation, such as that described in Box 8.6 for total carbonate measurement. Geothermal exploration surveys generally include sampling and analysis of both surface waters and thermal springs. It would be awkward to use two analytical procedures for these two types of water, i.e. to determine total carbonate in geothermal waters by the method described in Box 8.6 and to determine alkalinity in surface waters. However, as pointed out in that box, determination of total carbonate in samples low in that component (less than about 0.5 mmoles/kg) is not as accurate when titrating to a pH of 3.80 as when titrating to the equivalent point. It is recommended, therefore, to titrate to the equivalent point for such samples. Interference may be corrected for theoretically, or by back-titration (see Box 8.6). Theoretical correction involves calculation of the extent bases present in the sample other than carbonate have reacted with the acid added. The correction is based on the analytical concentration of these bases. If back-titration is selected, the sample should be further titrated to about pH = 3.80 before degassing it with respect to CO_2. Then the pH should be adjusted to the pH of the equivalent point and finally back-titrated to pH = 8.30.

It is common to use alkalinity as a measure of the extent of reaction water has with the rock according to the process involving uptake of CO_2 from the atmosphere and its conversion into bicarbonate, but this is an approximation not acceptable for many types of water. Sulphur, in the form of sulphate, often occurs in groundwaters in substantial concentrations relative to bicarbonate, and many elements of low mobility, such as iron and aluminium, are reprecipitated as hydroxides; this does not show up as changes in bicarbonate concentrations although considerable water–rock interaction is involved.

BOX 8.1. CHEMICAL AND ISOTOPIC COMPONENTS ANALYSED IN WATER AND STEAM SAMPLES FOR GEOCHEMICAL STUDIES OF GEOTHERMAL RESOURCES

I. EXPLORATION SURVEYS

A. Water samples

Generally analysed: pH, Si, B, Na, K, Ca, Mg, CO_2 (total carbonate carbon), SO_4, H_2S, Cl, F, Li, conductivity, δ^2H and $\delta^{18}O$.

Specific: It is recommended also to analyse for Al and Fe, at least, if analysis of some other elements is performed by ICP-AES emission spectrography. Most minerals contain iron or aluminium, or both, and data on these elements expand the possibilities of quantitative interpretation of the data by studying specific mineral–solution equilibrium conditions.

For specific purposes, selected samples may also be collected for analysis of Br, I, Li, NH_4, Rb, Cs, various trace metals (As, Ba, Cd, Co, Cr, Cu, Hg, Mn, Mo, Ni, P, Pb, Sr, Ti, Zn), nutrient salts (NH_3, NO_2^-, NO_3^- and PO_4^{3-}) and isotopes, in particular, $\delta^{13}C$, ^{14}C and ^3H, but occasionally also $\delta^{18}O$ in H_2O and SO_4 as well as $\delta^{34}S$ and $\delta^{36}Cl$. Further, redox measurements (Eh) may provide useful information as well as direct determination of Fe^{2+} and Fe^{3+}.

B. Steam (gas) samples

Generally analysed: CO_2, H_2S, NH_3, H_2, CH_4, N_2, O_2 and Ar.

Specific: Helium is often analysed for, and occasionally the other inert gases (Ne, Kr, Xn and Rn) are determined in selected samples together with the heavier hydrocarbons as well as δ^3He. The purpose of such analyses is scientific, except for δ^3He, which provides information on the magmatic contribution to the geothermal fluid rather than aiming at specifying some geothermal resource characteristics. At times, measurements of δ^2H in H_2 and CH_4, and of $\delta^{13}C$ in CO_2 and CH_4, are carried out for geothermometry purposes.

BOX 8.1. (cont.)

II. WELL TESTING

Generally analysed: As for exploration surveys.
Specific: As for exploration surveys.

III. MONITORING STUDIES

It is advisable to collect water samples frequently, or every two to three months, from wet steam wells for monitoring studies and to analyse only for a few components such as Si, B, Na, K, Ca, Mg, SO_4 and Cl.

It is considered sufficient to collect water and steam samples once or twice a year for complete analyses of major components and isotopes as specified above for exploration surveys.

For hot water wells, sampling once or twice a year is generally regarded satisfactory for analyses of major chemical components and isotopes.

BOX 8.2. CRITERIA FOR SELECTING SPRINGS AND FUMAROLES FOR SAMPLING

The following criteria are recommended when selecting springs and fumaroles for sampling:

(1) high temperature
(2) high flow rate
(3) neutral to alkaline pH
(4) high electric conductivity
(5) location
(6) well defined outlet.

When fumaroles and mud pools or springs of muddy water are located close to each other, the fumaroles should be sampled preferentially. Most likely the muddy springs represent steam heated water. On-site pH measurement will help in identifying steam heated waters.

When making a final selection of a sample site in the field, it is convenient to measure the temperature of the water and its electric conductivity. The spring with the highest temperature and the highest conductivity should be selected.

Samples should be collected as far as possible from narrow vents rather than large pools. Exposure of the thermal water to the atmosphere in large pools may cause changes in its chemistry and isotope composition.

If a cluster of springs or fumaroles with variable flow rates and temperature occurs within a relatively small area, they should be sampled such as to cover the whole temperature range. It is advisable to collect many samples from at least one or two clusters. This will reveal whether or not the geothermal fluid is relatively homogeneous within each cluster. Homogeneous composition points to a common deep source. Variable composition, on the other hand, indicates the effect of some near surface processes, such as mixing, which should be evaluated.

BOX 8.3. APPARATUS AND REAGENTS REQUIRED FOR SAMPLING OF SURFACE WATERS, SPRINGS AND HOT AND COLD WATER WELLS

APPARATUS

(1) Silicone tubing (1/4 in. diameter, one about 5 m long and another about 2 m long).
(2) Plastic funnel (about 10 cm in diameter). The longer tubing is placed on the funnel.
(3) Plastic can (about 1 L).
(4) Plastic bucket (about 10 L).
(5) 1/8 in. or 1/4 in. cooling coil of stainless steel (type 316) — total length about 5 m. It is most convenient to curl the steel pipe into a coil of about 15 cm diameter so that it fits into the bucket.
(6) It is advisable to have hose clamps, a screw driver and a small wrench for connecting the tubing and the cooling coil and the tubing onto the sampling pump (see item (10) below).
(7) Digital thermometer.
(8) Marking pen.
(9) Cooling box (for nutrient salt samples).
(10) Battery and 12 V driven sampling pump (optional) and/or a vacuum hand pump and filtering apparatus.
(11) Pocket size GPS instrument to determine the geographic co-ordinates of sample sites.
(12) Additional tools that are required or often come handy include forceps and/or thin disposable plastic gloves to handle the filter membranes, pliers, fittings to connect tubings to taps on wellheads, a good pocket knife, a small shovel, a light backpack, thick rubber gloves, rubber boots, a large container of known volume for measurements of discharge, and a stopwatch, if flow is to be measured.

REAGENTS AND EQUIPMENT FOR FIELD CHEMICAL PRETREATMENT

(13) Concentrated nitric acid (HNO_3), ultrapure.
(14) Filter membrane (0.1 mm) of cellulose nitrate or cellulose acetate.

BOX 8.3. (cont.)

Often filter membranes of 0.2 or 0.45 mm may be considered adequate.

(15) 1 mL pipette.

(16) Tips for 1 mL pipette.

(17) Distilled (deionized) water (required for cleaning filtering apparatus and also if a sample for silica determination is diluted to prevent its polymerization).

(18) 50 mL volumetric flask, 5 mL pipette and tips for this pipette. Only required if a sample for silica determination is diluted to prevent its polymerization.

(19) 2% zinc acetate solution [$(CH_3COO)_2Zn$]. Dissolve 2 g in 100 mL of deionized water. Only required for special samples collected for SO_4 determination when the water contains >1 ppm H_2S.

(20) 1% $HgCl_2$ solution: Dissolve 1 g $HgCl_2$ in 100 mL deionized water.

(21) A plastic drop dispenser. Only required if samples are collected for carbon isotope determination, $\delta^{13}C$ and ^{14}C.

BOX 8.4. RECOMMENDED SAMPLE VOLUMES AND SAMPLE TREATMENT FOR ANALYSIS OF SELECTED PARAMETERS IN WATER SAMPLES ACCORDING TO ANALYTICAL INSTRUMENTS AND METHODS

pH meter, automatic titrator: pH, total carbonate.

One 50 mL glass bottle for pH, one 250 mL glass bottle for total carbonate.

No treatment, except for unclear water, which must be filtered. Store in glass.

Ion chromatograph: Cl, F, SO_4, sometimes Na, K, NH_4 and Br.

Optical spectrophotometer: Si, B

Selective electrodes: Cl, F, NH_3

One 200 mL plastic bottle.

Filter using 0.1 µm cellulose nitrate or cellulose acetate filter membrane.

Do not acidify.

Inductively coupled plasma atomic emission spectrograph (ICP-AES): Si, B, Na, K, Ca, Mg, Fe, Al, S (if H_2S is low, the analysed sulphur is taken to be SO_4), various trace elements such Mn, Sr and Ba.

One 200 mL plastic bottle.

Filter using 0.1 µm cellulose nitrate or cellulose acetate filter membrane.

Acidify with 1 mL concentrate ultrapure HNO_3.

Atomic absorption spectrophotometer (AAS): Si, Na, K, Ca, Mg, Al, Li, Rb, Cs and many more trace elements.

One 500 mL plastic bottle.

Same treatment as for ICP-AES, except add 1 mL of the acid to 500 mL sample.

Inductively coupled plasma mass spectrograph (ICP-MS): Many trace elements including Al, As, Ba, Cd, Co, Cr, Cu, Hg, Mn, Mo, Ni, P, Pb, Sr, Ti, Zn.

One 100 mL plastic bottle.

BOX 8.4. (cont.)

Same treatment as for ICP-AES except add 1 mL of the acid to 100 mL sample.

Autoanalyser: NH_3, NO_2, NO_3, PO_4.

Four 20 mL plastic vials, one for each component.

Filter using 0.1 mm cellulose nitrate or cellulose acetate filter membrane.

Put immediately into a cooling box. Freeze as soon as possible.

NB: Fill the vials about 3/4 to allow for extra space when the samples freeze.

Titration with $BaClO_4$ (with thorin as indicator): SO_4. For samples high in H_2S (>1 ppm).

One 100 mL plastic bottle.

Filter. Add 1 mL of 2% $Hg(CH_3COO)_2$ solution to 100 mL sample.

Optical spectrophotometer: Si as SiO_2 > 100 ppm.

One 100 mL plastic bottle.

Filter using 0.1 μm cellulose nitrate or cellulose acetate filter membrane. Dilute sample with deionized water so that the final concentration will be <100 ppm SiO_2.

Mass spectrometer: δ^2H and $\delta^{18}O$, $\delta^{34}S$.

One 50 mL glass bottle. If also determining $\delta^{18}O$ in SO_4 and $\delta^{34}S$, one 250 mL glass bottle.

Filter if not clear. No other treatment.

The quantity of sulphur for sulphate isotope analysis must be ≥2 mg.

Mass spectrometer: $\delta^{13}C$, ^{14}C.

One 1000 mL glass bottle.

Filter if not clear. Add 4 to 5 drops of 1% $HgCl_2$ solution.

Radioactive counting: Tritium (^3H).

One 500 mL plastic bottle.

Filter if not clear. No treatment.

Optical spectrophotometer: Fe^{2+}, Fe^{3+}. (see Box 8.10).

Two 50 mL glass bottles, one for Fe^{2+} and one for total iron.

BOX 8.5. PROCEDURE FOR WATER SAMPLING FOR SPRINGS EMERGING ON A SLOPE

(1) Immerse the funnel so the water flows into the tubing. Use a siphon if necessary. Make sure that air bubbles do not adhere to the inner surface of the tubing. If the flow rate is low and the water has become turbid when putting the funnel in place, wait until the water flowing from the tubing appears clear.

(2) Connect the cooling coil to the tubing and place it into the bucket that should be full of cold water (Fig. 8.1). Control the flow such that the water cools to at least about 30°C. (Cooling is only required for samples collected into glass bottles if their temperature exceeds 30–40°C). Allow water to flow from the cooling coil into two 50 mL and one 250 mL glass bottles (for measurement of δ^2H, $\delta^{18}O$, pH and total carbonate). Filter only if the water is not clear. It is necessary to cool these samples so that later contraction of the water, as it cools in airtight glass bottles, does not create low pressure leading to degassing of the water and evaporation.

(3) Disconnect the cooling coil. Allow the water to flow into a can, filter sample into one 200 mL plastic bottle (untreated sample for determination of Cl, B, F, etc.).

(4) Filter sample into another 200 mL plastic bottle, acidify it with 1 mL of concentrated ultrapure HNO_3 and shake to mix; or collect 500 mL into a plastic bottle and acidify with 1 mL concentrated ultrapure HNO_3 (see Box 8.4 for analytical method).

(5) If trace elements are to be analysed, filter sample into a 100 mL plastic bottle, acidify with 1 mL of concentrated ultrapure HNO_3 and shake to mix.

(6) Collect filtered samples into four 20 mL plastic vials, if nutrient salts (NH_3, NO_2, NO_3 and PO_4) are to be determined.

(7) Allow filtered water to flow into a 100 mL plastic bottle until it is almost full. Add 2 mL of 2% zinc acetate solution. Mix well and fill the bottle. This sample should only be taken of waters containing >1 ppm H_2S for measurement of SO_4.

(8) Dilute filtered sample with deionized water so $SiO_2 < 100$ ppm (see Box 8.4). Needed for colorimetric analysis but also for other methods for saline waters (≥ seawater salinity).

BOX 8.5. (cont.)

(9) H_2S should be determined on the sampling site. See analytical procedure in Box 8.7.

(10) O_2, if to be determined, should also be analysed on-site or, alternatively, at the end of each sampling day (see procedure in Box 8.8).

(11) Eh, if to be determined, must be measured on the sampling site (see Box 8.9).

(12) Water and air temperatures should be measured, and the flow rate should be either measured or estimated. Sample site should be described (see text).

FOR SPRINGS WITH WATER LEVEL BELOW SURROUNDING GROUND, STREAMS, RIVERS AND LAKES

(1) Scoop water with a can from the spring, stream or river and use that water to collect, filter and treat samples as described above for springs on slopes.

(2) For those samples that are collected into glass bottles and need to be cooled, connect the tubing and funnel to the cooling coil. Insert the coil into the bucket containing cold water. Pour water from the can into the funnel and hold it in the air to ensure flow through the cooling coil. One to two litres of the water should be flushed through the tubing and cooling coil before collecting the samples. Otherwise proceed as described above. Water may also be sucked up by using a sampling pump and pumped through the cooling coil.

WELLS

(1) For flowing wells the procedure is the same as for springs on slopes, except that the tubing on the funnel is now connected to a valve on the wellhead with the appropriate fittings. It is important to flush very well before sampling in order to minimize contamination from the valve.

(2) For non-flowing wells the procedure is the same as for streams.

BOX 8.6. MEASUREMENT OF pH AND TOTAL CARBONATE

pH

pH is measured with a portable pH meter, at least if determined in the field. Preferably use a meter and electrode with a rapid response. When measuring high pH waters (>9), it is necessary to use an electrode that is not sensitive to sodium interference up to pH values as high as 11.

EQUIPMENT AND BUFFERS

(1) pH meter.
(2) Fast response combined pH electrode (at least when using a portable meter).
(3) Three buffer solutions: acetate buffer (pH = 4.66 at 25°C), phosphate buffer (pH = 6.88 at 25°C), borax buffer (pH = 9.18 at 25°C); and for high pH waters (>9.0) a fourth buffer solution should be used, with a pH of around 10 at 25°C. Observe that the pH of the buffer solutions is temperature dependent. This must be taken into account when calibrating the pH meter.
(4) A 50 mL glass bottle with airtight lid (one for each sample, see Box 8.4).
(5) Four 50 mL polyethene jars with lid.
(6) Deionized water.
(7) Thermometer.

PROCEDURE (if the measurement is carried out some time after sampling)

(1) The electrode should always be rinsed well with deionized water when moving it from one solution into another. Immerse the electrode into the phosphate buffer. Wait until stable reading is obtained and then adjust the reading to the value of the buffer at the temperature of the solution.
(2) Measure the acetate buffer. Adjust the slope to obtain a correct reading at the buffer temperature.
(3) Then measure the borate buffer (and the high pH buffer). The meter should now give a correct reading (within 0.01–0.02 pH units). If the pH reading gives too a low value, it is likely that the sodium ion in the

BOX 8.6. (cont.)

buffer is interfering or that the response of the electrode is not sufficiently rapid, because of its inadequate performance.
(4) Finally, check that the phosphate buffer gives the correct reading. If not, re-adjust the meter and repeat the calibration.
(5) Immerse the electrode into the pH glass sample bottle. It is advisable to make a hole through a tap that fits the pH sample bottles. The hole should be just big enough for the electrode. By screwing the lid tight, contact of the sample with the air during measurement is minimal.
(6) Wait until stable reading is obtained. This may take as long as 10 min, depending on the type and condition of the electrode and the pH of the sample. Ordinarily, stable reading is obtained within 1 min.

PROCEDURE (if the measurement is carried out at the sampling site)

(1) Transfer a sample of water to a 50 mL polyethylene jar and screw the lid on. A special hole should have been made through the lid through which the glass electrode just fits. Place the jar into the water which is to be sampled. Fill three other jars with the buffer solutions and place them also into the water. Wait until the buffers have reached the same temperature as the water (within about 2°C).
(2) Continue as described under items 1 to 6 in the procedure above. Measure the pH of the sample in the jar.

TOTAL CARBONATE

Total carbonate is determined by titration with 0.1M HCl solution from pH 8.30 to pH 3.80 using a pH meter. The measurement is generally carried out in conjunction with the pH measurement described above in this box. For waters low in total carbonate (<20 ppm) the lower pH value should not be adhered to as the titration end-point (see below).

EQUIPMENT AND REAGENTS

(1) pH meter.

BOX 8.6. (cont.)

(2) Combined pH electrode or separate pH and reference electrodes.
(3) 150 mL pyrex beaker.
(4) One 50 mL and one 100 mL volumetric flask.
(5) 2 mL microburette calibrated at 0.002 mL.
(6) 1 mL pipette.
(7) 0.1 M HCl standard solution. Prepare from 1 N Titrisol.
(8) 0.1 M NaOH standard solution. Prepare from 1 N Titrisol.
(9) Hydrogen peroxide, analytical reagent grade.
(10) 1 M HCl solution. Mix 20 mL of concentrated HCl (sp.gr. 1.19), analytical reagent grade, with 200 mL of deionized water. Only required when titrating samples of steam condensate collected into alkaline solution.
(11) Deionized water.
(12) N_2 gas (pressurized cylinder).

PROCEDURE (WATER SAMPLES)

(1) Parallel with the pH measurement, if not carried out on the sampling site, adjust the sample pH to about 9 by adding 0.1 M HCl or 0.1 M NaOH solution from the 1 mL pipette. Then adjust the pH accurately to 8.30 by the HCl solution from the microburette.
(2) Titrate from pH 8.30 to pH 3.80 with the standard 0.1 M HCl solution using the microburette. Record the titre (titre A).
(3) $CO_2 = \frac{\text{titre A} \times 4400}{\text{mL sample}} - (6.97 + 1.182H_2S + 0.0088SiO_2 + 0.100B)$

where CO_2 represents total carbonate carbon expressed as ppm. Other component concentrations in the equation are also in ppm. The interfering effects of SiO_2, H_2S and B have here been calculated on the basis of their analysis as well as the interference from water (6.97) required to titrate pure water from pH 8.30 to pH 3.80.

Alternatively, to correct for interference, continue as follows:

(4) Bubble N_2 through the sample for 10 min.

BOX 8.6. (cont.)

(5) Titrate back to pH 8.30 with the 0.1 M NaOH solution. Record the titre (titre B).

(6) $CO_2 = \frac{(\text{titre A} - \text{titre B}) \times 4400}{\text{mL sample}}$

PROCEDURE (STEAM CONDENSATE)

(1) Extract 1 mL aliquot of the alkaline solution from the gas sampling bulb and pour into the 150 mL beaker. Add 2–5 drops of the hydrogen peroxide, mix well and leave for 1 min.
(2) Adjust the pH to 8.30. First add some 1 M HCl solution. When the pH is 9.0–9.5, add the 0.1 M HCl standard solution from the microburette to adjust the pH accurately to 8.30.
(3) Titrate with the 0.1 M HCl standard solution to pH 3.80 (titre A).

(4) $CO_2 = \frac{(\text{titre A}) \times 4400}{\text{mL sample}} - 6.97.$ As before, CO_2 is total carbonate in ppm.

NOTES ON THE METHOD AND CHANGES IN pH AND CARBONATE DURING SAMPLE STORAGE

The only aqueous species whose activity is routinely measured directly is H^+. The activity of H^+ changes with temperature. In contrast, elemental concentrations in water samples do not change with temperature. The change in pH of natural waters with temperature largely depends on which acids buffer the pH and how the dissociation constant of this acid varies with temperature. For example, the dissociation constant of aqueous silica (silicic acid) changes very much with temperature below 100°C. At 25°C the logarithm of the dissociation constant is –9.91. At 20°C it is 10.02 and at 0°C it is 10.48 . If a water pH were 9.91 at 25°C and were solely buffered by silica, the pH would be 10.02 at 20°C and 10.48 at 0°C. In contrast to silicic acid, the dissociation constant of carbonic acid varies little with temperature around 25°C. Its value (logarithm) at 25°C is –6.35. If a water sample had a pH of 6.35 and were

BOX 8.6. (cont.)

solely buffered by carbonic acid, the pH of this water would change little with temperature around 25°C.

The temperature dependence of H^+ activity (pH) demands that the temperature of the pH measurement be recorded. The temperature of the electrode, test samples and buffers must be the same. It is the problem of maintaining constant temperature of instrument, buffers and sample that makes accurate pH measurements in the field difficult and time consuming. Experience has shown the pH measurement is generally most accurate if samples are stored in airtight glass bottles and if the procedure is carried out in the laboratory, even several days after sampling.

Some waters contain relatively high concentrations of iron. If these waters are oxygenated, the iron tends to be precipitated as $Fe(OH)_3$. This precipitation, which removes OH^+ from solution, will change the pH, the magnitude depending on the pH buffer capacity of the water and the quantity of precipitate. The only way to determine the pH of iron rich oxygenated waters accurately is to measure it on-site.

If pH is to be measured directly at the elevated temperature of a thermal spring water, it is necessary to allow the electrode to equilibrate thermally and heat the buffer solutions to the temperature of the thermal water, e.g. by immersing jars containing them into the water and calibrating the pH meter using the heated buffers.

At a pH of 8.30 almost 100% of the dissolved carbonate occurs as HCO_3^-. At pH 3.80 it has all been converted to CO_2. Thus, the equivalent of acid added is equivalent to the total carbonate carbon. Bases other than bicarbonate may react with the acid added. Their interference must be corrected for. In geothermal waters the interference of these acids, especially from boron and silica, may far outweigh the amount of acid required to titrate the HCO_3^-.

There are two ways by which this interference can be corrected. One is theoretical, involving the calculation of the equivalence concentrations of the interfering bases in solution from their analysis and the pH measurement. Alternatively, the sample can be backtitrated after expelling the CO_2 by blowing N_2 solution through it. The advantage of the first method it that it corrects for H_2S, whereas the second does not. The theoretical correction is

BOX 8.6. (cont.)

recommended for waters containing low boron but high H_2S. When backtitrating, correct theoretically for H_2S.

Alkalinity is frequently determined instead of total carbonate. This involves titrating the sample from its pH to the equivalent point where $H^+ = HCO_3^-$. This point, which represents the maximum slope on a pH (x axis) versus titre (mL 0.1 M HCl solution, y axis) curve, occurs around pH 4–5, the precise value depending on the concentration of dissolved carbonate. Alkalinity titration to the equivalent point is good for very dilute water with low dissolved total carbonate because the second end-point is more precise than the 3.80 pH end-point. The sample may be titrated from its pH or pH = 8.30. If the first choice is selected, a correction must be made for any HCO_3^- that occurs as $H_2CO_3^0$ at the initial pH of the water.

BOX 8.7. MEASUREMENT OF H_2S

APPARATUS AND REAGENTS

(1) 2 mL microburette calibrated at 0.002 mL intervals.
(2) 50 mL Erlenmeyer flask.
(3) Pipettes, 5 mL and 0–1 mL (adjustable).
(4) 50 mL volumetric flask.
(5) Glass rod.
(6) Acetone.
(7) 5 M NaOH solution. Dissolve 200 g of NaOH in 1 L of deionized water.
(8) Dithizone.
(9) 0.001 M mercuric acetate [$Hg(CH_3COO)_2$] standard solution. Dissolve 0.3187 g of $Hg(CH_3COO)_2$ in 1 L of deionized water. Store in a dark bottle in the dark. The solution is stable for 1 year.
(10) Deionized water.

PROCEDURE

(1) Pipette 5 mL of the 5 M NaOH solution and 5 mL of acetone into the Erlenmeyer flask.
(2) Add 1–50 mL of sample. If the sample aliqout is <10 mL, add deionized water to make the total 'sample' volume about 10 mL.
(3) With the glass rod, add a tiny crystal of dithizone. The solution should be very pale yellow and only one phase.
(4) Titrate with the standard $Hg(CH_3COO)_2$ solution to a pink end-point. Record the titre.
(5) $$H_2S\,(\text{ppm}) = \frac{\text{mL } 0.001\text{ M } Hg(CH_3COO)_2 \text{ solution} \times 34}{\text{mL sample}}$$

If H_2S is <0.3 ppm, it is best to take a 50 mL sample aliquot. If H_2S concentration is approximately in the range 0.3–5.0 ppm, take 10 mL aliquot. If H_2S > 5 ppm, it is best to take a sample aliqout of <10 mL and as little as 0.05 mL for condensate rich in H_2S (see discussion below).

BOX 8.7. (cont.)

NOTES ON THE METHOD

The method is based on reacting Hg^{2+} with sulphide (S^{2-}) in alkaline solution to precipitate HgS, which is black. When all the sulphide has reacted, Hg^{2+} reacts with the dithizone to form a pink Hg dithizonate complex. The sensitivity of the method is about 0.01 ppm when using a 50 mL sample aliquot. It is best to use as little dithizone as possible to make the end-point as sharp as possible.

It serves three purposes to make the sample strongly alkaline. Firstly, dithizone is yellow in alkaline solution making the end-point from yellow to pink sharp. Secondly, HgS precipitates readily from alkaline solution. Thirdly, H_2S will not be lost during titration.

Dithizone does not dissolve in water but dissolves in acetone, which in turn dissolves in water.

If H_2S is high in the sample the yellow colour changes gradually to brown, making the end-point indistinct. This is the reason for taking a small aliquot for H_2S rich samples. The titre should not be more than about 2 mL.

H_2S is easily lost from the sample upon storage by degassing and/or oxidation. The H_2S could be preserved by precipitating it as ZnS with $Zn(CH_3COO)_2$. However, on-site titration is preferred as it only takes a few minutes. If possible, do not cool the sample. Otherwise, use a stainless steel cooling coil to minimize H_2S loss during sampling.

BOX 8.8. MEASUREMENT OF DISSOLVED OXYGEN BY WINKLER TITRATION

REAGENTS

(1) 30% manganese chloride solution: Dissolve 30 g of $MnCl_2 \cdot 2H_2O$ (or 40 g of $MnCl_2 \cdot 5H_2O$) in distilled water and dilute to 100 mL. Store in glass bottle.

(2) Alkaline iodide solution: Dissolve 30 g of KOH in about 30 mL of deionized water and 60 g of KI in about 60 mL of deionized water. Mix the solutions. The volume should be about 100 mL. Both solutions are about saturated so it may be difficult to dissolve the solids. As a result there may be some precipitate in the bottle but this does not matter. Upon storage the solution sometimes turns brown, probably because of formation of I_2 but that does not seem to interfere.

(3) Sulphuric acid solution: Mix 50 mL of concentrated acid (sp. gr. 1.98) and 50 mL of deionized water. Carefully pour the acid into the water because the solution becomes very hot and may effervesce. Store in glass.

(4) 1% starch solution: Dissolve 1 g of water soluble starch in 100 mL of deionized water. It is necessary to heat the solution to make the starch dissolve. Filter the solution using very coarse filter paper. Coffee filters are handy. If the solution is not filtered small particles in it sometimes make it difficult to detect the titration end-point accurately.

(5) 0.1 M sodium thiosulphate standard solution: Dissolve 24.85 g of $Na_2S_2O_3 \cdot 5H_2O$ in deionized water and dilute to 1000 mL in a volumetric flask.

(6) 0.001667 M iodate standard solution: Dissolve 356.7 mg of KIO_3 in deionized water and dilute to 1000 mL in a volumetric flask.

APPARATUS

(1) Special bottles for O_2 sampling and analysis, about 50 mL.
(2) Magnetic stirrer (battery driven) and magnet.
(3) Two 0.5 mL pipettes.
(4) Tips for 0.5 mL pipettes.

BOX 8.8. (cont.)

(5) 2 mL microburette calibrated at 0.002 mL intervals.
(6) Cooling coil, tubing, funnel, bucket (see Box 8.3).

SAMPLE COLLECTION

Non-thermal water from springs, streams, rivers and lakes

(1) It is essential to select a site where no air bubbles are visible, which is often the case where current is swift in streams.
(2) Prepare sampling by opening the bottles containing the 30% manganese chloride and the alkaline iodide solutions. Put tips on both of the 0.5 mL pipettes.
(3) Insert the oxygen bottles into the water and rinse two to three times. Immerse the bottles well, allow them to fill up and make sure that no air bubbles are visible on their inside. Pull the bottles out.
(4) Quickly add 0.5 mL of the manganese chloride solution. Expel it at the bottom of the bottle. Make sure that no air is pipetted with the solution.
(5) Add 0.5 mL of the alkaline iodide solution, also to the bottom of the bottle. Again make sure that no air is pipetted with the solution into the bottle.
(6) Place the tap onto the bottle immediately. Make sure that it is tight. Turn the bottle upside down and mix thoroughly. The sample may be titrated immediately or at the end of the day.

Hot water drillholes

(1) Connect the silicone tubing well onto a valve on the borehole. Flush the tubing and the cooling coil for several minutes at good flow in order to make sure that no air bubbles adhere to the walls of the tubing and the cooing coil.
(2) Place the cooling coil into the bucket, which should be full of cold water.
(3) Allow cooled water to flow into the oxygen flask by placing the end of the tubing connected to the cooling coil to the bottom of the bottle.

BOX 8.8. (cont.)

Allow the water to flow for about one minute after the bottle is full so as to replace the water that initially entered it and contacted air .

(4) Continue as described under items (4) to (6) above for non-thermal waters.

Thermal springs

(1) Place the funnel with the tubing attached deep into the water. Make sure, when water flows through the tubing, that no air bubbles adhere to its wall. Proceed according to items (2) to (4) above for drillholes.

(2) If it is not possible to make water flow through the tubing, insert the oxygen flask into the hot water (see sampling of cold water above).

ANALYSIS

(1) Prepare the titration by placing new tips on the two 0.5 mL pipettes and by filling the 2 mL microburette with the standard thiosulphate solution. Open the glass bottles with the sulphuric acid and the starch solutions. Make the magnetic stirrer ready.

(2) Open the oxygen flask, add immediately 0.5 mL of the sulphuric acid solution and insert the magnetic stirrer. Make it rotate fast so that the manganese hydroxides dissolve rapidly and the solution mixes well.

(3) Titrate the sample, which now appears brown (if there was any oxygen in it), with the 0.1 M thiosulphate standard solution until the brown colour has become faint (0.6–0.7 mL for air saturated cold water).

(4) Add 0.5 mL of the starch solution. This should turn the solution purple blue. Continue titrating until the colour disappears; samples containing no dissolved oxygen but small amounts of H_2S may not turn purple blue upon addition of the starch solution; $O_2 = 0$.

(5) The concentration of O_2 is:

$$O_2(\text{ppm}) = \frac{(\text{molality } Na_2S_2O_3 \text{ solution})\,(\text{mL } Na_2S_2O_3 \text{ solution} - \text{blank}^b) \times 32\,000}{(\text{mL sample}) \times 4}$$

$$O_2(\text{mL STP}^a) = \frac{(\text{molality } Na_2S_2O_3 \text{ solution})\,(\text{mL } Na_2S_2O_3 \text{ solution} - \text{blank}^b) \times 24\,400}{(\text{mL sample}) \times 4}$$

BOX 8.8. (cont.)

[a] STP indicates standard temperature and pressure, i.e. volume at 25°C and 1 bar.

[b] As discussed below there is usually a little oxygen in the reagent solutions used for the O_2 analysis, and it is necessary to make a correction for that. Such correction corresponds to a given amount of thiosulphate solution required to titrate the O_2 in the reagent solutions.

The number of mL of each sample is determined by weighing the empty oxygen bottle. Fill it with water, then weigh again. The difference of the two weights in grams is equal to the volume of the bottle in mL. The actual sample is 1 mL less than this volume, i.e. the amount of manganese chloride and alkaline iodide solutions added (0.5 + 0.5 = 1 mL). However, by taking the sample to be equal to the volume of the bottle and determining the O_2 in the reagent blank (see below), an appropriate correction can be made.

STANDARDIZATION OF THIOSULPHATE SOLUTION

It is necessary to standardize the sodium thiosulphate solution by titration with standard KIO_3 solution.

(1) Add about 50 mL of deionized water to a 100 mL beaker. Then add 1 mL of the sulphuric acid solution by pipette.
(2) Add 0.5 mL of the manganese chloride solution and mix well.
(3) Add 0.5 mL of the alkaline iodide solution and mix again.
(4) Finally, add 10 mL of the standard KIO_3 solution. The solution now becomes yellow.
(5) Add 1 mL of 1% starch solution.
(6) Titrate with the thiosulphate solution until the purple iodine colour disappears.
(7) The concentration of the thiosulphate solution (m_s) is:

$$m_s = \frac{0.1}{\text{mL } Na_2S_2O_3 \text{ solution}}$$

BOX 8.8. (cont.)

DETERMINATION OF BLANK REAGENT

Titrate cold tap water three times by adding usual, double and triple amounts of all the reagents to the sample.

Observe that the bottle with the double dose of reagent has 1 mL less tap water in it than the sample with the ordinary reagent dose (0.5 mL manganese chloride solution + 0.5 mL alkaline iodide solution) and the sample with the triple dose has 2 mL less.

Plot the number of mL of each titre against the dose added (single, double, triple).

Define a line through these data points. Its slope gives the difference between the O_2 concentration in the sample and the reagents.

This difference corresponds to the value for the blank (see items (6) and (7) under ANALYSIS above) if the volume of the sample bottle is taken to represent the volume of the sample.

NOTES ON THE METHOD

Measurement of dissolved oxygen in water by Winkler titration is based on the following reactions:

$$2\mathrm{Mn}^{2+} + 4\mathrm{OH}^- = 2\mathrm{Mn(OH)}_2 \qquad (1)$$

$$2\mathrm{Mn(OH)}_2 + \frac{1}{2}\mathrm{O}_2 + \mathrm{H}_2\mathrm{O} = 2\mathrm{Mn(OH)}_3 \qquad (2)$$

By adding the $MnCl_2$ and alkaline KI solutions to the sample, divalent manganese hydroxide is precipitated. Dissolved O_2 in the sample oxidizes this hydroxide to trivalent manganese hydroxide, i.e. $Mn(OH)_3$. The trivalent manganese hydroxide is brown. Observe also that a large excess of iodide is added to the solution.

By acidifying the sample with sulphuric acid the manganese hydroxides are dissolved. Simultaneously trivalent manganese is reduced to divalent and I^- oxidized to I_2.

BOX 8.8. (cont.)

$$2Mn(OH)_3 + 6H^+ + 2I^- = 2Mn^{2+} + I_2 + 6H_2O \tag{3}$$

The iodine reacts with the iodide in the solution to form iodate ion (I_3^-):

$$I_2 + I^- = I_3^- \tag{4}$$

The iodate ion produces yellowish colour but the starch turns it purple blue. The iodate ion is converted into iodide ion by reacting it with thiosulphate:

$$I_3^- + 2S_2O_3^{2-} = 3I^- + S_4O_6^{2-} \tag{5}$$

By adding together reactions (1) to (5) above we obtain

$$\frac{1}{2}O_2 + 2H^+ + 2S_2O_3^{2-} = H_2O_6^{2-} \tag{6}$$

Thus, it takes four moles of thiosulphate to consume one mole of O_2.

The Winkler titration is very precise, to within 0.002 mL of thiosulphate solution, which corresponds to about 0.03 ppm O_2 for a sample bottle of 50 mL. The main problem with this method is atmospheric contamination. Oxygen is very rapidly dissolved in water exposed to the atmosphere. This method is, therefore, difficult for thermal waters containing no or very little oxygen. It may be better to use special ampoules for such waters that are available for different ranges of concentrations or a dissolved oxygen meter with selective membrane electrode.

The main concern with oxygen in thermal waters is its corrosive nature that can be quite severe when such water is piped in black steel for direct heating.

BOX 8.9. MEASUREMENT OF REDOX POTENTIAL (Eh)

APPARATUS

(1) Voltmeter (pH meter).
(2) Platinum electrode.
(3) One 20 mL plastic vial with airtight lid for measuring test solution (usually comes with the platinum electrode).
(4) Digital thermometer.

PROCEDURE

(1) Pour the plastic vial full of untreated sample.
(2) Immediately immerse the electrode and ensure that the lid is tight. Keep the plastic vial immersed in the water. Measure the temperature of the test solution to ensure that it is the same as that of the water. Alternatively, the electrode may be immersed directly into the water to be measured.
(3) Take a voltage reading when the meter has stabilized (this may take 5 to 10 min depending on the time it takes for the meter to stabilize thermally with the environment).

NOTES ON REDOX POTENTIAL MEASUREMENTS

Unlike pH measurement systems, oxidation–redox potential systems cannot be standardized against buffers. After setting the millivolt range on the instrument make the following checks to ensure correct electrode performance: Add sufficient pH7 buffer to immerse the electrode and stir the solution using a magnetic stirrer. Add a sufficient quantity of quinhydrone crystals to saturate the solution. Immerse the electrode into the solution and measure the potential. It should have the following values (within ±10 mV) at the following temperatures: +92 mV (20°C), +86 mV (25°C), +79 mV (30°C). Remove the electrode and rinse thoroughly with deionized water. Make up a second saturated quinhydrone solution in pH4 buffer. The millivolt potential should now read as: +268 (20°C), 263 (25°C) and +258 (30°C). If the system potentials are correct, rinse the electrode well with deionized water. The electrode can now be used to measure the Eh of test solutions.

BOX 8.9. (cont.)

Theoretically, the mV difference between the two solutions should be 177 mV. If, on the other hand, deviation from this difference exceeds 10 mV, the electrodes should be cleaned in aqua regia (three volumes concentrated HCl and one volume concentrated HNO_3). The aqua regia solution is very corrosive and must, therefore, be handled with utmost care. After cleaning, repeat measurements. Note that quinhydrone solutions are not stable. Therefore, discharge them after use.

Measurement of redox potential is usually not routinely carried out as part of geochemical investigations of geothermal fluids. However, such measurements provide important information about the redox state of the fluid and allow evaluation of whether or not specific redox equilibria are closely approached. The general experience is that there is no univeral Eh for non-thermal and warm waters, i.e different redox couples such as Fe^{2+}/Fe^{3+}, O_2/pH and NH_3/NO_3 yield different redox potentials, and they also differ from the measured value. Therefore, equilibrium does not prevail with respect to redox potential in non-thermal and warm waters. With rising temperature, there is a general convergence towards an overall redox equilibrium. This is, however, not easy to verify by direct measurement for boiled waters because cooling by boiling upsets any redox equilibrium as does degassing of the water. Both cooling and boiling affect the pH of the water, and boiling also its content of gaseous constituents.

When measuring the redox potential it is necessary to carry out the measurement at the temperature of the water and record this temperature. It is not possible to calculate the redox potential at other temperatures because, as already stated, it cannot be assumed that a specific redox couple buffers the Eh.

BOX 8.10. MEASUREMENT OF FERROUS AND TOTAL IRON WITH TPTZ

APPARATUS

(1) One adjustable micropipette, 0–0.2 mL, and one 1 mL pipette.
(2) Tips for pipettes.
(3) Two 50 mL brown glass bottles (for each sample).

REAGENTS AND STANDARDS

(1) 6M hydrochloric acid. Dilute 54 mL of concentrated hydrochloric acid (sp. gr. 1.19) to 100 mL with deionized water.
(2) 2M sodium hydroxide solution. Dissolve 8 g sodium hydroxide in 100 mL of deionized water.
(3) Ascorbic acid. Dissolve 7 g ascorbic acid in 100 mL of deionized water. Make up a new solution as soon as it starts turning yellow.
(4) TPTZ solution. Add 0.5 mL concentrated hydrochloric acid (sp. gr. 1.19) to 0.08 g of 2,4,6-tripyridyl-1,3,4-triazine and dilute to 100 mL with deionized water.
(5) Ammonium acetate solution. Dissolve 5 g ammonium acetate in 100 mL of deionized water.
(6) Make standards of desired concentrations from $FeCl_3$ standard solution in hydrochloric acid. For a good quality spectrophotometer, the lowest standard should be 1 or 2 ppb but the highest 500 ppb.

STANDARDS

(1) Pour about 45 mL of $FeCl_3$ standard solution into eight 50 mL brown glass bottles containing 0, 1, 2, 5, 10, 50, 200 and 500 ppb of Fe.
(2) Continue as described under items (2) to (7) in the procedure below.

PROCEDURE (DETERMINATION OF TOTAL IRON)

(1) Add about 45 mL of filtered sample to a 50 mL brown glass bottle.
(2) Add 0.06 mL 6M HCl solution.
(3) Add 0.10 mL 2M NaOH solution.

BOX 8.10. (cont.)

(4) Add 1 mL of the ascorbic acid solution. Shake well and wait for at least 30 s.
(5) Add 1 mL of the TPTZ solution.
(6) Add 1 mL of the ammonium acetate solution. Mix well.
(7) Fill the the bottle with filtered sample. Mix well.
(8) Measure absorbance at 595 μm.

PROCEDURE (DETERMINATION OF FE^{2+})

(Reagents for determination of ferrous iron must be added during sampling and analysis carried out within 10 h.)

(1) Add about 45 mL of filtered sample to a 50 mL brown glass bottle.
(2) Add 0.06 mL 6M HCl solution.
(3) Add 0.10 mL 2M NaOH solution.
(4) Add 1 mL of the TPTZ solution.
(5) Add 1 mL of the ammonium acetate solution. Mix well.
(6) Fill the the bottle with filtered sample. Mix well.
(7) Measure absorbance at 595 μm within 10 h after adding reagents.

NOTES ON THE METHOD

Ferrous ion (Fe^{2+}) forms a violet complex with 2,4,6-tripyridyl-1,3,4-triazine (TPTZ) at pH3.5–5.8. To determine total iron concentrations, ascorbic acid is added to reduce ferric to ferrous iron. Without adding ascorbic acid, Fe^{2+} is only complexed with TPTZ. Acetate is added to prevent reduction of ferric to ferrous iron after preparation.

BOX 8.11. PREPARATION WORK FOR SAMPLING FUMAROLES, STEAM IN WELLS AND GASES FROM THERMAL SPRINGS

TYPES OF BULBS

The type of gas sampling bulbs to be used is important. For fumaroles and steam wells, we recommend bulbs with one stopcock of teflon with two O rings to tighten the space between the stopcock and the glass in which it is positioned and a third O ring by the tip of the stopcock that presses against the glass in the neck of the bulb as it is closed (see Fig. 8.2). Teflon stopcocks without O rings are not recommended. They tend to leak. Classic bulbs with glass stopcocks that need to be lubricated are not recommended either. They are more difficult to handle than bulbs with teflon stopcocks, especially when collecting samples into alkaline solution.

Use of bulbs with two teflon stopcocks (one at each end) with or without a septum has some advantages. It permits evacuating the bulbs at the sampling site by expelling air from the bulb by passing through it steam from the fumarole or well to be sampled. This permits a test of how good steam flow can be maintained from the fumarole and into the bulb, an information important for finding out whether samples free of air contamination can be collected. These bulbs are also convenient when sampling gas from springs and fumaroles by collecting the dry gas and condensed steam separately.

EVACUATION OF BULBS

If collecting gas from fumaroles or wells into alkaline solution, the gas sampling bulbs should be evacuated in the laboratory before being taken into the field.

(1) Add 50 mL of freshly prepared 4 M NaOH solution to the glass sampling bulb (dissolve 80 g of NaOH pellets in deionized water and dilute to 500 mL) or 10 mL of freshly prepared 50% w/v KOH solution (dissolve 100 g of KOH pellets in 100 g of water). It is advantageous to add a pH indicator, such as alizarin blue, to the alkaline solution. Below pH11, this blue indicator turns purple red. To ensure quantitative

dissolution of CO_2 and H_2S in the alkaline solution, its pH must not become less than about 10.

(2) Evacuate the bulb using a vacuum pump. Allow the solution to boil for 1 to 2 min. This ensures that air is completely expelled from the bulb. Vacuum equal to the vapour pressure of the alkaline solution can easily be attained.

(3) Always shake each bulb when packing for a field trip. A 'hammering' sound, when the solution bounces against the wall of the bulb, indicates vacuum in the bulb.

MEASUREMENT OF SAMPLE SIZE COLLECTED AND CORRECTION OF CO_2 AND H_2S CONCENTRATIONS IN STEAM

It is necessary to record the volume of both gas and steam sampled in order to calculate the concentration of the various gases in the steam.

(1) First weigh all the gas sampling bulbs when empty and dry. Then fill them with water and weigh again. The difference of the two weights gives the grams of water in each bulb, which is equal to the volume of the bulb in millilitres (V_{eb}):

$$Wt_{fb} - Wt_{eb} = V_{eb} \tag{1}$$

Here, Wt_{fb} is the weight of the bulb when full of water and Wt_{eb} is the weight of the empty bulb in grams.

(2) After having evacuated the bulb, weigh it. Record the weight (Wt_{Nb}).

(3) Collect the sample and weigh the bulb again. The difference of the weight of the bulb with the sample and with the alkaline solution (Wt_{Nb}) only gives the weight of steam collected (Wt_s). This weight is, of course, practically the same as the volume of the condensed steam, $Wt_s = V_s$:

$$Wt_{gb} - Wt_{Nb} = Wt_s \tag{2}$$

BOX 8.11. (cont.)

The subscripts gb, Nb and s denote bulb with sample, bulb with NaOH or KOH solution, and sample, respectively.

(4) The volume of gas sampled (V_s) is equal to:

$$V_g = V_{eb} - V_N - V_s \tag{3}$$

Here, V_{eb} is the volume of the empty bulb and V_N and V_s are the volumes of the alkaline solution added and the condensed steam collected, respectively.

Since the pressure in the bulb has not yet been measured the quantity of gas is not known. The product of volume and pressure of a gas or a gas phase at a given temperature is a measure of the moles of gas. Hence

$$\frac{(V_d + V_g)P_s}{24.4} = m_g \tag{4}$$

where V_d and V_g denote the volumes of the dead space in the evacuated line of the gas chromatograph used for analysis and of the sample, respectively, in mL. P is pressure in bars, measured when the sampling bulb is opened for the first time into the evacuated line of the gas chromatograph. mg represents mmoles of gas sampled (excluding CO_2 and H_2S, i.e. the gases which dissolve in the alkaline solution). 24.4 is the volume in litres of one mole (or millilitres of one millimole) of ideal gas at STP (standard temperature and pressure), i.e. 25°C and 1 bar pressure.

Finally, calculate the number of mmoles of gas per kg of steam. This is obtained from:

$$\text{mmol gas / kg steam} = \frac{m_g}{m^s} \times 1000 \tag{5}$$

where m_g designates, as before, mmoles of gas sampled and m^s is the millilitres (grams) of steam sampled.

Chromatographic analysis gives the relative amounts of the gases in the gas phase (dry gas), and this analysis, together with Eq. (5) above, yields the concentration of each of the dry gases in the steam.

BOX 8.11. (cont.)

When the gas analysis has been completed, the condensate can be extracted from the bulb and analysed for CO_2 and H_2S according to the procedures given in Boxes 8.6 and 8.7. In order to obtain the concentrations of these gases in the steam collected, the measured concentrations need to be corrected for dilution by the alkaline solution. The corrected concentrations of these gases in the steam (m_g^s) are given by

$$m_g^s = \frac{m^s + V_N}{m^s} \qquad (6)$$

BOX 8.12. APPARATUS AND SAMPLING PROCEDURE FOR SAMPLING FUMAROLES AND GASES FROM THERMAL SPRINGS

APPARATUS

(1) Gas sampling bulb, about 300 mL.
(2) Two plastic funnels, one about 10 cm in diameter and the other about 20 cm.
(3) ¼ in. silicone tubing, at least three pieces about 1, 2 and 4 m long.
(4) Stake peg.
(5) 1 in. diameter stainless steel pipe or quartz tube.
(6) Tray or small bucket of plastic for cooling water and small shovel.
(7) Digital thermometer.
(8) Hand vacuum pump. Only required for sampling gas from springs.
(9) Copper tubing, about 1 cm diameter and 30 to 40 cm long for each sample, and clippers. Required for analysis of noble gases.

Items (10) to (14) below are only required for the alternative sampling procedure.

(10) Measuring cylinder, about 500 mL.
(11) 2% zinc acetate solution. Dissolve 4 g $Zn(CH_3COO)_2$ in 200 mL of deionized water.
(12) 40% sodium hydroxide solution. Dissolve 200 g in deionized water and dilute to 500 mL.
(13) About 200 mL gas washing bottle.
(14) Two stoppers of silicone rubber with ¼ in. glass tubes running through them for closing the gas washing bottle. One tube should be long enough to run down to the bottom of the gas washing bottle but the other should end just below the stopper.

SAMPLING PROCEDURE FOR FUMAROLES

(1) After having selected a sampling point, turn the funnel upside down over the discharge and cover it well with clay or soil in order to avoid atmospheric contamination. Depending on the nature of the fumarole sampling site, it may be considered feasible to insert the stake peg into

BOX 8.12. (cont.)

the ground to create a hole for the steam flow followed by insertion of the stainless steel pipe. Make sure that the hole outside the pipe is well sealed with clay and/or soil. A view of the sampling apparatus is shown in Fig. 8.2.

(2) Fill the tray/bucket with cold water.

(3) Connect the bulb and allow the steam to flow through the tubing and the tee piece of the bulb for 1 to 2 min (use the shortest tubing possible) to expel any air. Close the far end of the tee piece with a clamp, open the bulb and turn it upside down to allow the entering steam to bubble through the alkaline solution. Immerse the bulb into the cold water or pour cold water over it every now and then to condense the steam and cool the sample.

(4) When the steam flow has decreased substantially, close the sampling bulb. Sampling is complete. Avoid collecting steam until flow is very much reduced. This causes risk of some backflow of alkaline solution plus condensate into the tubing and substantial steam condensation in the tubing, which would give too high gas concentrations in the steam. This sample is suitable for analysis of CO_2, H_2S, H_2, CH_4, N_2, O_2 and Ar.

(5) Connect another sampling bulb to the tubing (with stopcock at both ends). Allow steam to flow through it for a few minutes to expel air. Close the far end stopcock of the bulb, cool and collect a little over 100 mL of condensate. Disconnect the bulb and pour the condensate into two 50 mL glass bottles. One is for NH_3 analysis and the other for δ^2H and $\delta^{18}O$.

(6) For analysis of noble gases, connect a copper tube to the tubing from the funnel/pipe. Allow steam to flow through it for 1 to 2 min. Press the pipe together at the far end with the clippers and then at the end by the tubing.

ALTERNATIVE SAMPLING PROCEDURE FOR FUMAROLES

(1) Items (1) and (2) are as on the previous page (see also Fig. 8.3).

(2) Connect a sampling bulb having stopcocks at both ends to the tubing conveying the steam from the fumarole and put about 30 cm long tubing on the far end of the bulb. Have both stopcocks open.

BOX 8.12. (cont.)

(3) Collect condensate into the bulb until the bulb is full and the condensate is flowing from the tubing.

(4) Place the 30 cm tubing to the bottom of the measuring cylinder (or connect it to the measuring gas wash bottle).

(5) Turn bulb upside down, collect gas and expel the condensate into the measuring cylinder.

(6) When the gas sampling bulb has been filled with gas, close its lower stopcock first and then the upper stopcock. Measure the volume of condensate collected. This sample is for analysis of all non-condensable gases and isotopes (H_2, CH_4, N_2, O_2, CO, Rn, the noble gases and heavier hydrocarbons, δ^3He, δ^2H in H_2 and CH_4, $\delta^{13}C$ in CO_2 and CH_4).

(7) For analysis of H_2S, add 5mL of 2% zinc acetate solution to a 50 mL glass bottle and pour condensate into it until full. Fix the cap firmly.

(8) For analysis of CO_2, pipette 5 mL of the 40% NaOH solution into another 50 mL glass bottle and pour condensate into it until it is full.

(9) Collect condensate into two more 50 mL glass bottles for measurement of NH_3, δ^2H and $\delta^{18}O$.

SAMPLING PROCEDURE FOR GAS IN THERMAL SPRINGS

(1) Place the funnel with the required length of tubing on it upside down over the stream of gas from the spring water. Use the stake peg and clamps to ensure that it sits in a stable position (see Fig. 8.4).

(2) Connect an evacuated gas sampling bulb to the silicone tubing which is connected to the funnel.

(3) Attach the hand vacuum pump to the tee piece of the bulb with a short piece of tubing and suck up water until the space under the funnel, the tubing and the tee piece are completely full of water.

(4) Close the tubing to the hand vacuum pump with a clamp and disconnect it.

(5) Allow gas to collect under the funnel.

(6) Shake the tubing occasionally to allow the gas accumulating under the funnel to replace the water in the tubing that simultaneously percolates down in the tubing.

BOX 8.12. (cont.)

(7) When the tubing and the space under the funnel are full of gas, open the bulb carefully to suck in gas until the water level has risen to the top of the funnel. Then close.

(8) Repeat until no more gas sucks into the bulb, which can be observed by no rise in the water level under the funnel when the bulb is open. Close bulb and disconnect. The sample can be used for analyses as the dry gas sample under the alternative procedure above.

ALTERNATIVE SAMPLING PROCEDURE FOR GAS IN THERMAL SPRINGS

(1) Place funnel over gas stream as described in procedure above.

(2) Connect a gas sampling bulb with stopcocks at both ends to the tubing attached to the funnel.

(3) Connect a water trap to the gas sampling bulb using a short silicone tubing (20–30 cm) and a hand vacuum pump to that bottle.

(4) Open both stopcocks and suck up water from the spring until the bulb is full of water.

(5) Close the stopcock on the bulb next to the water trap and disconnect the trap.

(6) Allow gas to collect under the funnel and shake the tubing occasionally to allow the gas cumulating under the funnel to replace the water in the tubing.

(7) When the tubing and the space under the funnel are full of gas, turn the gas sampling bulb upside down. Connect 20–30 cm long silicone tubing to the lower stopcock on the bulb and place its open end to the bottom of a measuring cylinder. Open the upper stopcock. Then carefully open the lower stopcock on the bulb and allow water to flow through the short tubing into the measuring cylinder until the water level has just reached the top of the funnel. Repeat until all water has been displaced from the sampling bulb. Disconnect the bulb. The sample can be used for analyses as the dry gas sample under the alternative procedure for fumaroles above.

BOX 8.12. (cont.)

DRY GAS MANIFESTATIONS

Dry gas manifestions are known in some areas, i.e. a gas phase flows out of the ground at low temperatures. To sample such manifestations, a hole should be dug into the ground. The funnel with the connected tubing is placed upside down into the hole over the stream of gas and the hole filled up to seal the funnel as well as possible. Digging of the hole may introduce a lot of air into the soil. For this reason, the gas should be allowed to flow through the tubing attached to the funnel for some time (even several hours) before sampling is commenced.

NOTES ON THE SAMPLING METHODS

Simultaneous sampling of steam and gases into an evacuated gas bulb is convenient for analysis of CO_2, H_2S, H_2, CH_4, N_2, O_2 and Ar. For analysis of isotopes, CO, Rn, the noble gases and heavier hydrocarbons, the alternative sampling procedure is to be used where the condensate and the dry phase are collected separately. This latter method is necessary for CO determination.

It is only possible to measure the relative gas concentrations in dry gas samples if the volume of condensate collected into the measuring cylinder is measured (see item (6) under alternative sampling procedure for fumaroles in this box).

By subtracting the volume of the bulb from the measured condensate, volume one obtains the volume of condensate that comes with one bulb of gas at atmospheric pressure. Measurement of N_2 in both types of sample also makes it possible to calculate the concentrations in the steam of all the gases analysed for in the dry gas sample.

Use evacuated sampling bulbs to collect samples of dry gas manifestations. Sampling simply involves connecting an evacuated bulb to the tubing from the funnel, opening it only slightly to restrict the flow of gas so as to reduce the risk of sucking in air from the soil.

When collecting dry gas and condensate separately, CO_2 and H_2S must be determined in both the dry gas and the condensate samples, as they will only partly dissolve in the condensate.

BOX 8.12. (cont.)

There is always some steam condensation in the tubing. However, if the steam flow is sufficiently high, droplets which form inside the tubing are swept with the flowing steam into the bulb.

The time of sampling is variable, depending on the steam and gas flow. For fumaroles it is on average some half an hour, but it may only take a few minutes to collect dry gas from thermal springs, at least if the gas flow rate is high.

Determination of isotopic ratios in gas components and of the noble gases and heavier hydrocarbons is only carried out in special laboratories. Their analysis does not form a regular part of geothermal investigations. However, the isotopic ratios of hydrogen and carbon in H_2, H_2O, CO_2 and CH_4 provide valuable information on subsurface temperatures and on the origin of the geothermal fluid, as does δ^3He.

Borosilicate glass is inadequate for collecting samples for He and He isotope measurements. The helium diffuses through the glass and is lost. Either copper tubing or bulbs of special aluminium silicate glass are required.

BOX 8.13. APPARATUS REQUIRED FOR SAMPLING WET STEAM WELL DISCHARGES

EQUIPMENT

(1) Thermally insulated stainless steel (type 316) Webre separator with a pressure gauge (Fig. 8.5).
(2) Stainless steel (type 316) cooling coil: diameter 6–8 mm, total length about 6 m. It is most convenient to curl a steel pipe into a coil of about 15 cm diameter so that it fits into the bucket.
(3) High pressure tubing to connect separator and cooling coil. Steel wire tubing with inner teflon lining fitted with stainless steel speed connectors to facilitate connection is handy.
(4) Evacuated gas sampling bulb, about 300 mL, containing 50 mL 4 M NaOH solution or 10 mL of 50% weight/volume KOH solution.
(5) Silicone tubing (1/4 in. diameter) about 1 m long with an atmospheric non-return valve. To be placed directly on the steam valve of the Webre separator or on the far end of the cooling coil.
(6) Apparatus listed under items (3)–(4) and (6)–(11) in Box 8.3.
(7) Additional tools that are required or often come handy include forceps and/or thin disposable plastic gloves to handle the filter membranes, pliers, screwdriver, wrenches, fittings to connect tubings to valves on wellheads, a good pocket knife and thick rubber gloves.

REAGENTS AND APPARATUS

The same reagents and chemistry equipment are required as listed for water samples in Box 8.3.

SAMPLING PROCEDURE USING A WEBRE SEPARATOR

(1) Connect the Webre separator onto the ½ in. valve on the pipe next to the wellhead.
(2) Connect the cooling coil to the Webre separator.
(3) Fill the bucket with cold water.
(4) Open the valve on the pipe fully as well as all the valves on the Webre separator and flush well for several minutes.

BOX 8.13. (cont.)

(5) Close all valves on the Webre separator and take a pressure reading on the separator.

For steam sample

(6) Open the water outlet valve well but the steam outlet valve only slightly. This ensures that dry steam is discharged from the steam valve. This adjustment causes the water level to be low in the separator and all the water and some of the steam entering the separator to discharge through the water valve. Check that the steam is dry, i.e. free from water droplets. If no droplets are present the discharge nearest to the outlet is not visible. If not dry, close the steam valve partially and/or open more the water valve. Wait until stabilized flow under the new adjustment has been obtained.

(7) Connect an evacuated gas sampling bulb to the ¼ in. silicone tubing, which has a non-return atmospheric valve on it, to the steam valve of the separator. Open the bulb and immerse into cold water in the bucket. Collect a sample until a sufficient quantity has been obtained. Stop before most of the steam from the separator discharges through the non-return valve.

Alternatively:

(a) Connect the cooling coil to the separator. Wait until condensate has flowed from the coil for 1 to 2 min.

(b) Connect an evacuated gas sampling bulb to the cooling coil with the short piece of ¼ in. silicone tubing with the non-return valve on it. Open the bulb and collect a sufficient quantity of sample.

(c) In both cases, separately collect a condensate sample into two 50 mL glass bottles for measurement of NH_3 and of δ^2H and $\delta^{18}O$.

For water sample

(8) The separator adjustment should be 'reversed'. The steam valve should be well opened but the water valve only slightly. With this adjustment

BOX 8.13. (cont.)

the water level in the separator is high and very wet steam is discharged from the steam valve. All of the steam and some of the water entering the separator discharge through this valve.

(9) Connect the cooling coil and immerse it into cold water in the bucket. Wait until cooled water has flowed for 2 to 3 min from the cooling coil. Put the 1 m long ¼ in. silicone tubing with the non-return valve on it on the far end of the cooling coil. Make sure that no gas bubbles are discharged with the water. Visible gas bubbles indicate that some steam is discharging from the water valve. If so, readjust the separator valves by closing more the water valve and/or opening more the steam valve so that water free from steam comes through the water valve.

(10) Collect and treat samples as described in Box 8.5 for water samples. It is important to cool samples collected into glass bottles to, at least, about 30°C.

SOME NOTES

It is essential to use gas sampling bulbs that are safely airtight so that they can be safely stored before analysis in the laboratory. Place either 10 mL of 50% weight/volume freshly prepared KOH solution (low in carbonate) or 50 mL of freshly prepared 4 M NaOH into the bulbs and evacuate them before going into the field (see Box 8.11).

Water and steam samples from each well should always be collected on the same occasion. For interpretation they should be regarded as one sample and labelled as one sample.

Sampling pressure (in the Webre separator or in the wellhead separator) must be recorded during sampling. The Webre separator must be fitted with a pressure gauge. Read the pressure when the outlets of the separator are closed. Make sure that pressure does not fall appreciably when opening and adjusting the separator for sampling. This should be done by restricting the flow from the separator. A value for the discharge enthalpy must also accompany the analytical data on the water and steam samples for interpretation of these data. The sampling pressure to be recorded is that read on the separator during sampling.

BOX 8.13. (cont.)

When collecting samples from wellhead separators, the procedure is exactly the same as described above for steam and water samples using a Webre separator, respectively, except that the tubing with the one way atmospheric valve is connected directly to valves on the separator body (for water samples) and on the steam line (for steam samples).

BOX 8.14. PROCEDURE FOR CUMULATIVE MONTHLY SAMPLING OF PRECIPITATION FOR ISOTOPIC ANALYSES

To obtain reliable isotopic data from rain, it is essential that the sampling procedure described below is followed in detail. Above all, evaporation should be avoided, because this strongly affects the isotopic composition of the water sample. Thus, if a cumulative monthly sample is being obtained, the rainwater which accumulates in the collector before sampling at the end of each month should be protected against evaporation with paraffin oil (liquid petrolatum). It is, therefore, essential to use airtight bottles to preserve, ship and store the precipitation samples collected for isotopic analysis. It is also advisable to use the high density polyethylene bottles provided by the International Atomic Energy Agency (IAEA), which have been checked for their tightness and the consistency of isotopic measurements after several months of storage. The bottles provided by the IAEA have a volume of 0.5 L (for tritium analysis) and 50 mL (for ^{2}H and ^{18}O), which are considered the optimal amounts of water required for isotopic analysis. The following procedure must be observed:

(1) Each sample must represent the cumulative precipitation for a one month period, beginning on the first day of the month and continuing until the end of the month. The monthly amount of rain should be recorded by using the rain gauge which normally is set up near to the rain collector. In the absence of a rain gauge, the monthly amount of rain can also be determined as follows: total amount (in L) of rainwater collected in the vessel, measured in a graduated cylinder divided by area of funnel (in m^2). The resulting value already represents the amount of precipitation in mm. It is important to know the monthly amount of rain (in mm) so that the weighted annual isotopic value of rainfall can be calculated.

(2) The rain water is collected through a funnel into a plastic vessel, called rain collector (~ 5 L capacity), which is left in an open space for the whole month. The vessel can be a recycled but very clean plastic container found in chemical labs. It is advisable to use those with built-in faucets to facilitate sampling at the end of the month. Otherwise, it is important to modify the vessel as indicated in the attached sketch. The collector is completely covered with aluminium foil or styrofoam to

BOX 8.14. (cont.)

avoid evaporation through its walls. It is necessary to put paraffin oil, available in a pharmacy as liquid petrolatum, in the rain collector to prevent evaporation of the accumulating water. The paraffin oil layer floating over the water should have a thickness of about 0.5 cm. The tip of the funnel should not touch the upper surface of the oil layer (see attached design for further reference). This set-up can be protected by a fence and raised (about 1 m) from the ground.

(3) At the end of the month, the rain collector must be shaken to mix the sample abefore filling the bottles to be sent for analysis. The collector should not, however, be aggressively shaken, to prevent the oil from forming an emulsion with water which later would make its separation difficult. Instead, the oil must be left to float on top of the water before filling the sampling bottles. The water sample is collected in the IAEA plastic sampling bottles by opening the faucet (if available) at the bottom of the collector (see sketch). The bottles should always be labelled immediately after filling with water sample. The operations described above should be carried out as rapidly as possible, in order to reduce the time during which the sample is exposed to the atmosphere and, thus, to the risk of evaporation. When the bottles with samples are filled, the collector should be dried again before using it for the next month's precipitation sampling.

(4) Always be sure to use the bottles provided by the IAEA, and ensure that the double cap is securely tightened. Sharp objects (e.g. screws, nails, wood splinters) in the box should not be used when samples are sent to the laboratory for analyses. These objects can puncture the plastic bottles. Data reflecting name and altitude of the sampling station as well as the amount of rain in the particular month should accompany the sample. If available, the mean monthly air temperature at ground level from a nearby meteorological station should also be reported.

BOX 8.14. (cont.)

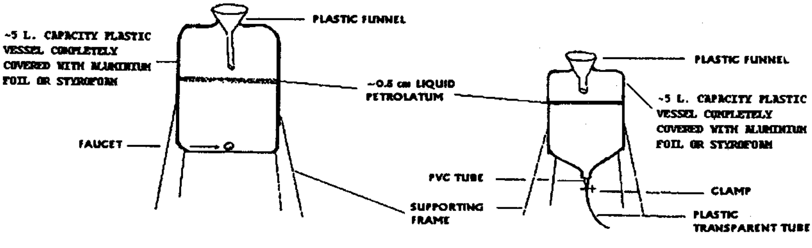

OPTION A

OPTION B

SET UP FOR CUMULATIVE SAMPLING OF PRECIPITATION FOR ISOTOPIC ANALYSIS

9. PRESENTATION OF ANALYTICAL RESULTS, ANALYTICAL PRECISION AND ACCURACY

Stefán Arnórsson

Samples of water and gas from geothermal manifestations and wells are analysed for a variety of purposes. Most analyses are carried out for geochemical purposes, i.e. with the aim of quantifying the geothermal reservoir characteristics, both initially and later when the exploitation may have induced changes in the initial natural state of the reservoir. Geochemical analyses are, however, also required to characterize the quality of the fluid for the intended use and for environmental considerations.

For some chemical constituents samples need to be treated as already discussed in Chapter 8, and some components must either be determined on-site or shortly after sampling because the concentrations of these components in the sample tend to change upon storage. The minimum chemical analytical facilities required for geochemists working on geothermal projects relate to sampling and analysis of those components that must be carried out during or shortly after sampling. In water samples, this includes pH, CO_2 (total carbonate carbon), H_2S, NH_3, O_2, Fe^{2+} and Fe^{3+}. It is not considered feasible to have an external laboratory to do gas analysis (CO_2, H_2S, NH_3, H_2, CH_4, N_2, O_2 and Ar), at least, if the samples need to be shipped, owing to risk of breaking the bulbs during shipment. One should have gas analysis carried out very soon after sampling so that resampling can be carried out if the analysis reveals an unacceptable amount of air contamination.

Instrumentation for major element analysis of water samples as well as analysis of trace elements has become much more sophisticated and expensive during the last two decades, demanding, for economic reasons, that a large number of samples be analysed on each instrument. This has led to the development of geochemical analytical service facilities in several countries that are contracted for geochemical analysis in favour of setting up analytical facilities for individual projects. For isotopic analyses, some of which require both expensive and sophisticated apparatus, this has been common practice for a long time.

In this report we do not deal with analytical procedures other than those required to be carried out in the field. It should, however, be realized that the analytical method to be adopted calls for specific sample treatment and sample volume. Therefore, it is necessary to know at the time of sampling which analytical methods are to be used, as was already discussed (Chapter 8).

9.1 ANALYTICAL PRECISION AND ACCURACY

Nature often seems to control accurately the concentrations of chemical constituents in natural waters, and small variations can often be useful indicators of differences or changes in processes. This calls for accurate analysis.

A good example of the value of accurate analysis is provided by data on sodium and potassium from water discharged from a wet steam well at Nesjavellir in Iceland (Fig. 9.1). The samples were analysed by atomic absorption spectroscopy, on the one hand, and by ion chromatography, on the other. The first analytical method indicated some scatter without any observable trend with time, and some variations in the Na/K ratio and, therefore, in the Na/K geothermometry temperatures. The ion chromatography analysis showed, on the other hand, a very slight but steady rise in the concentrations of both Na and K during the first year of discharge but, thereafter, the concentrations have remained practically constant. Na/K ratios were remarkably constant so that Na/K geothermometry temperatures only varied by 1 °C. The data from the ion chromatograph analysis revealed slightly increased vaporization of the reservoir water during the first year of discharge, an important observation, whereas the atomic absorption data failed to do so because of analytical imprecision.

It is important to keep statistical control of both analytical accuracy and analytical precision. Accuracy refers to how accurately a component is determined in absolute terms. On the other hand, precision is relative, referring to how accurately differences in component concentrations are determined. To control accuracy, it is necessary to analyse a standard of natural water together with every batch of samples. To control precision, all components should be analysed in duplicate.

If concentration levels are rather similar, it is acceptable to present differences between duplicate samples in terms of concentration. If variation, on the other hand, is large, as is generally the case for natural waters, even from the same field, it is better to express differences between duplicate samples in relative terms, i.e. on a percentage basis.

The percentage difference (*%M*) of duplicate determination is given by

$$\%M = \frac{|M_2 - M_1|}{(M_1 + M_2)/2} \times 100 \tag{9.1}$$

where M_l and M_2 represent each of the two determinations. When this has been done for all samples analysed together in one batch, the average of $\%M$ ($\%\overline{M}$) should be calculated from

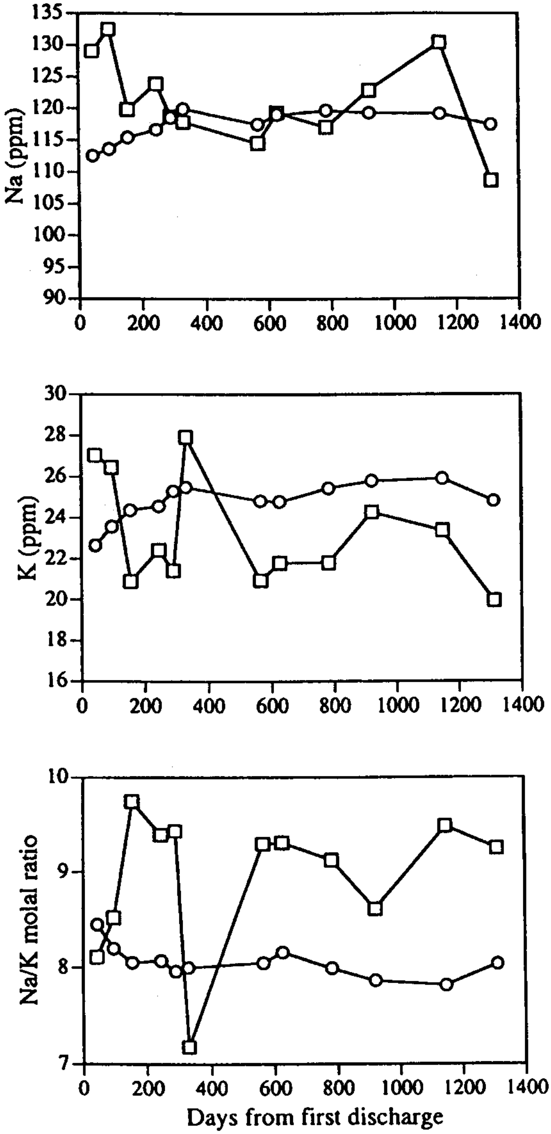

FIG. 9.1. Variation with time in Na and K concentrations and Na/K ratios in the discharge from well 6 at Nesjavellir. Circles and squares denote ion chromatography and atomic absorption analyses, respectively. The concentrations refer to a separation pressure of 15 bar abs.

$$\%\overline{M} = \sum \frac{\%M}{n} \tag{9.2}$$

and the standard deviation, σ, from

$$\sigma = \sqrt{\frac{(\%\overline{M} - \%M_1)^2 + (\%\overline{M} - \%M_2)^2 + \ldots.(\%\overline{M} - \%M_n)^2}{n-1}} \tag{9.3}$$

where n stands for the number of samples analysed in each batch. Both $\%M$ and σ are easily calculated with the aid of spreadsheets.

The analytical precision at the 95% confidence level, A_p, is given by

$$A_p = \%M + 2\sigma \tag{9.4}$$

Granting that analytical error is at random, this implies that the difference between one out of every 20 duplicate samples is greater than indicated by Eq. (9.4).

Table 9.1 gives the mean percentage difference and standard deviation based on duplicate analysis of some components in geothermal water samples.

Sometimes, only the standard deviation is reported with chemical and isotope analysis. For completely random distribution of the analytical error, the mean deviation of duplicate analysis is just about the same as the standard deviation.

It is common practice to analyse samples more than twice for a particular component if the difference in $\%M$ is regarded as unduly large. When this is the case the analytial result to be reported should be the average of all the determinations unless it can be shown that one or more determination was truly faulty but not statistical. Components in samples that have been determined more than twice should not be included when calculating $\%M$ and σ.

Analytical precision, of course, depends on the method used but also on the analyst and the component concentration. Errors increase when the detection limit for any analytical method is approached (see footnotes in Table 9.1). Depending on their concentrations, it is often convenient to report two statistical values for analytical precision for some components.

Accuracy should be good for most major components routinely determined in samples of geothermal fluids. It is not considered necessary to maintain statistical control of analytical accuracy. It is sufficient to run a standard of a

TABLE 9.1. EXAMPLE OF REPORTED ANALYTICAL METHODS AND PRECISION FOR ANALYSIS OF GEOTHERMAL WATERS (from Arnórsson et al., 1983a)

Component	Analytical method	Mean deviation	Standard deviation
pH	pH meter	0.03	0.03
SiO_2	Spectrophotometric, yellow silicomolybdic acid	2.7%	1.8%
B	Spectrophotometric, methylene blue fluoroborate	3.8%[a]	2.8%
Na	Atomic absorption spectrometry	1.9%	1.6%
K	Atomic absorption spectrometry	3.0%	2.0%
Ca	Atomic absorption spectrometry	2.0%	1.6%
Mg	Atomic absorption spectrometry	5.3%[b]	5.5%
Fe	Co-precipitation with oxine, tannic acid and thionalide followed by XRF analysis	26.2%	23.5%
Al	Spectrophotometric, catechol violet	2.8%[c]	4.7%
CO_2^c	Titration with 0.1N HCl using pH meter	4.3%[d]	3.7%[d]
SO_4	Titration with $BaClO_4$ using thorin indicator	1.4%[e]	1.6%[e]
H_2S	Titration with $(CH_3COO)_2Hg$ using dithizone as indicator	7.8%[f]	8.2%
Cl	Mohr titration	1.8%	1.7%
F	Ion sensitive electrode	3.6%	2.6%

[a] 10% at concentration levels below 0.1 ppm.

[b] Below 0.01 ppm, the average analytical error was ±0.001 ppm.

[c] For samples containing less than 0.1 ppm, the average difference of duplicate samples was 0.007 ppm and always within 0.02 ppm.

[d] For concentrations below 10 ppm, the mean and standard deviations were 1.5 and 1.1 ppm, respectively.

[e] Mean and standard deviations were 0.5 ppm at concentrations below 10 ppm.

[f] At concentrations below 0.1 ppm, the mean and standard deviations were 0.01 ppm.

natural sample with every batch of samples in order to check if the analytical value obtained on this standard is within acceptable limits when read against calibration standards. An acceptable limit is $\%\overline{M}$ for the respective analytical batch.

It is common practice to calculate the charge balance of water analysis. For first class analysis, the difference in the sum of cations charges should be within 5% of the sum of anion charges. However, 10% difference is generally regarded as satisfactory. For very saline and extremely dilute water, where acceptable analytical errors are larger than for more common salinities, a charge balance of more than 10% may be acceptable. Charge balance is, of course, only of value to check on the results of the major ions in solution. It is not a check of precision of minor ions nor of neutral species.

Sometimes, the cause of a poor charge balance is that one or more major ions have not been analysed for. This is, e.g., known for waters heavily polluted with artificial fertilizes when the nutrient salts were not analysed.

A further check of overall analytical accuracy involves determination of evaporated residue and comparison of its value with the sum of all dissolved solids. Gaseous species should not be included in this sum. However, the fraction of the total carbonate that exists as HCO_3^- should be included.

9.2 PRESENTATION OF ANALYTICAL RESULTS

Interpretation of chemical and isotopic data on geothermal fluids sometimes rests directly on analytical concentrations. It is, however, more common that the analytical data require some handling before they can be interpreted for specific purposes. Often primary data on conservative components (tracers) can be used directly. On the other hand, most interpretation of reactive components, such as evaluation of mineral saturation and scaling tendencies, requires computation of species activities.

It is always important to tabulate, with the chemical and isotopic analysis, measurement of those physical parameters that are required for the handling and interpretation of the chemical and isotopic data (Tables 9.2 and 9.3). In the case of analytical data (both chemical and isotopic) on water and steam samples from wet steam wells, it is necessary to report measured enthalpy as well as sampling pressure, for both the water and steam samples. If these data are not available, calculation to reservoir chemistry cannot be done, thus limiting the value of the geochemical data.

Discharge enthalpy may not have been measured when geochemical samples are collected. When this is the case it is necessary to study variations in the measured discharge enthalpy of the respective well and deduce from these measurements the value of the discharge enthalpy at the time of sampling,

TABLE 9.2. DATA FROM WET-STEAM WELLS REQUIRED FOR CALCULATION OF RESERVOIR FLUID CHEMISTRY

Physical data: Sampling pressure, well discharge enthalpy (if water and steam samples are collected at different pressures, this must be reported)

Chemical data:

Water sample: pH and the concentrations of Si, B, Na, K, Ca, Mg, CO_2 (total carbonate carbon), SO_4, H_2S, Cl, F, δ^2H and $\delta^{18}O$ and possibly some other elements and isotopes

Steam sample: δ^2H and $\delta^{18}O$ as well as CO_2, H_2S, H_2, CH_4, N_2, O_2, Ar and possibly some other gases. It is important to report the concentration of the gases in the steam phase. It is not sufficient to report their relative (i.e. volume %) concentrations.

It is desirable to have data on temperature logs and circulation losses together with the geochemical data. The physical data provide information on the level of the producing aquifer. This information is useful when selecting the aquifer temperature for chemical speciation calculations. It also allows a comparison between geothermometry results and measured downhole temperatures.

---

e.g. by selecting the measurement that is nearest in time or by interpolation (average) of the last and first enthalpy measurements before and after sampling.

In geothermal development it is, we regret to say, much too common that geochemists and well logging experts do not collaborate closely and exchange data. Temperature logging carried out during heating-up of wells is commonly used to identify permeable horizons that are expected to be producing aquifers. The same kind of information is obtained from fluid circulation losses during drilling. Temperature measurements carried out after the respective well has recovered thermally provides information on the temperature of the permeable horizons. Geothermometry, which is based on data on the fluid composition, also provides information on aquifer temperatures. Comparisons of the two measurements are important and essential for maximizing information provided by the geochemical data.

TABLE 9.3. EXAMPLE OF CHEMICAL AND ISOTOPIC ANALYSIS WITH NECESSARY PHYSICAL DATA FOR A WET–STEAM WELL (well at Momotombo, Nicaragua)

Water sample (conc.: ppm)		*Steam sample* (conc.: mmol/kg)	
pH/°C	7.92/25	CO_2	354.3
SiO_2	453	H_2S	7.63
B	28.0	H_2	1.065
Na	1645	CH_4	0.840
K	214.0	O_2	0.000
Ca	47.5	N_2	19.29
Mg	0.09	Ar	0.017
Al	0.23	δ^2H	–52.3
Fe	0.360	$\delta^{18}O$	–6.61
ΣCO_2	22.9		
H_2S	1.53	*Physical and other data:*	
SO_4	99.1	Sample No.	NIC-0057
NH_3	0.58	Date of sampling	12.11.96
Cl	2954	Well depth	442
Diss. solids	5466	Discharge enthalpy (kJ/kg)	1138
δ^2H	–47.1	Sampling pressure for water (bar abs.)	1.0
$\delta^{18}O$	–3.23	Sampling pressure for steam (bar abs.)	5.5
		Steam flow rate (kg/s)	7.2
		Temp. of aquifers[a] (°C/depth in m)	210/423

[a] From downhole logging

BOX 9.1. INTERPRETATION OF TEMPERATURE LOGGING DATA DURING AND AFTER THERMAL RECOVERY OF A GEOTHERMAL WELL

The figure below shows the thermal recovery of well 18 at Nesjavellir and well 16 at Reykir in Mosfellssveit in Iceland after cold water had been pumped into them during completion tests.

The two breaks in the temperature profile for the Nesjavellir well (indicated by arrows) represent the aquifers. After thermal recovery of the well, the temperature of these two aquifers is about the same. The very sharp temperature drop above the upper aquifer suggests that water enters the well from the deeper aquifer, ascends in the well and flows into the upper aquifer. This indicates that the deeper aquifer has higher pressure potential. Because of flow into the upper aquifer, the measured temperature in the well does not give an indication of its initial temperature. On the other hand, the temperature logging gives the correct temperature of the deeper aquifer.

The negative temperature peak (shown by the arrow) at about 700 m depth in the well at Reykir corresponds with a permeable horizon. It is considered that water was lost into the formation at this level, causing the slow heating. It is expected that this horizon represents a potential aquifer. The temperature of this aquifer is close to 100°C as shown by the temperature profile measured after thermal recovery of the well.

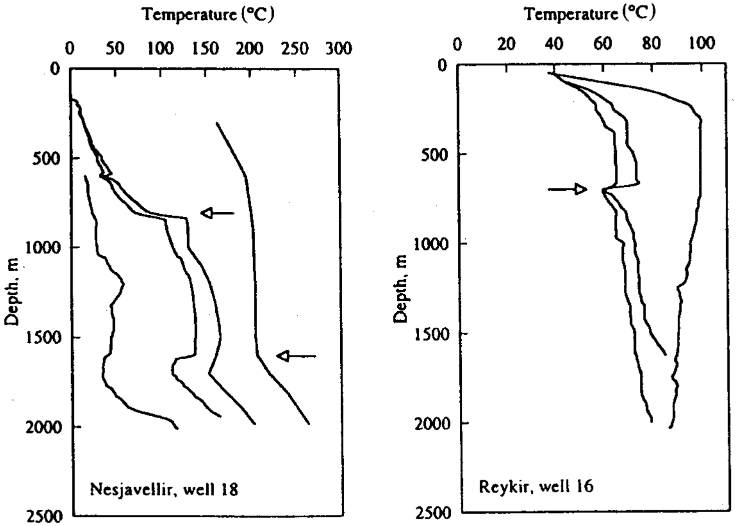

10. GEOTHERMOMETRY

Franco D'Amore and Stefán Arnórsson

Chemical and isotope geothermometers probably constitute the most important geochemical tool for the exploration and development of geothermal resources. They are also very important during exploitation in monitoring the response of geothermal reservoirs to the production load.

During the exploration phase, geothermometry is used to estimate subsurface temperatures, i.e. temperatures expected to be encountered by drillings, using the chemical and isotopic composition of hot spring and fumarole discharges. During the later phases in geothermal development and monitoring, geothermometry has been successfully applied to interpret the composition of well discharges with respect to locating the levels of producing horizons in the wells. Geothermometry is also useful in elucidating chemical reactions occurring in the zone of depressurization around wells that result from boiling and/or cooling by recharging cold water.

Geothermometers have been classified into three groups:

(1) Water or solute geothermometers;
(2) steam or gas geothermometers;
(3) isotope geothermometers;

Water and steam geothermometers are collectively termed chemical geothermometers.

During the ascent of geothermal waters from a deep reservoir to the surface, they may cool by conductive heat loss as they travel through cooler rocks or by boiling because of decreasing hydrostatic head. Cooling by conduction does not by itself cause any changes in the chemical and isotopic composition of the water. Yet, the cooling may change its degree of saturation with respect to both primary and secondary minerals. As a result, conductive cooling can bring about some modification in the chemical composition of the ascending water by mineral dissolution or precipitation. Boiling invariably causes changes in the composition of rising geothermal waters. These include degassing and an increase in the solute content of the water due to steam loss. The boiling mechanism affects the gas content of the steam that forms. The principal application of chemical and isotopic geothermometers during geothermal exploration involves estimation of reservoir temperatures below the zone of cooling. When applying these geothermometers it is invariably assumed that no changes in water composition occur in conjunction with conductive cooling; boiling is taken to be adiabatic.

The amount of conductive heat loss of ascending geothermal waters is proportional to the distance travelled and inversely proportional to the flow rate. For vertical pipe flow, Truesdell et al. (1977) have calculated that temperatures are reduced by half for waters flowing at 0.4 $L{\cdot}s^{-1}$ from a 1 km deep reservoir. Conductive cooling can be expected to be important for isolated springs with flow of less than 1 $L{\cdot}s^{-1}$. In the case of closely spaced springs, in trying to envisage the amount of conductive cooling in the upflow, the aggregate flow should be considered.

When geothermometers are applied to estimate subsurface or aquifer temperatures, a basic assumption is always made, namely that temperature dependent chemical or isotopic equilibria prevail in the source aquifer. Further, as stated above, the approximation is made that chemical and isotopic reactions do not significantly modify the composition of the fluid as it ascends from the source aquifer to the point of sampling, whether it be a thermal spring, fumarole or wellhead.

The assumption of equilibrium is not necessarily always true, and certainly is neither a law of physical chemistry nor a geochemical fact for all areas. Although equilibrium has been demonstrated by studies of well discharge chemistry and alteration mineralogy in some areas, it need not be so in all areas. However, as more and more information has accumulated from geothermal fields worldwide indicating that specific mineral–solution or solute–solute equilibria always prevail, it is, of course, logical to extend that information into a general working hypothesis. Thus, equilibrium between quartz and solution as well as between alkali feldspars and solution is invariably attained in geothermal reservoirs, at least, when temperatures exceed about 150–180°C. Accordingly, the application of the quartz and the Na/K geothermometers to high temperature geothermal reservoirs can be regarded as thoroughly established.

Experience shows that results for different chemical and isotope geothermometers sometimes compare well for a particular discharge although sometimes large differences are seen. Good conformity between individual geothermometers is usually taken to indicate that the assumption of equilibrium is valid and that faith can be put into the results. Discrepancy in results, on the other hand, is indicative of disequilibrium. A discrepancy may, however, be utilized to quantify various processes in geothermal systems such as boiling and mixing with cooler water in upflow zones. Therefore, differences in the results of individual geothermometers need not be a negative outcome for their interpretation.

It is to be emphasized that different geothermometers are valid in different temperature ranges. They equilibrate at different rates and respond differently to cooling and boiling in upflow zones. When interpreting temperature values derived from the various chemical and isotope geothermometers, it is important to have a sound understanding of the chemical and isotope processes involved as well as of the basic assumptions and simplifying approximations made. The task of the geochemist when interpreting chemical and isotopic data with respect to geothermometry is more than inserting analytical values into specific geothermometry equations. The geochemist's role is rather to verify or disprove the validity of the assumptions and approximations made when using specific geothermometry equations.

10.1 WATER GEOTHERMOMETERS

Many water geothermometers were developed from the mid-1960s to the mid-1980s. The most important ones are the silica (quartz and chalcedony), Na/K and Na–K–Ca geothermometers. Others that have been developed are based on Na/Li, Li/Mg, K/Mg ratios and Na–K–Mg relationships. Theoretically any cation ratio and any uncharged aqueous species concentration can be used as a geothermometer as along as equilibrium prevails (Arnórsson and Svavarsson, 1985).

Two methods have been used to calibrate the above mentioned water geothermometers. One is theoretical and the other empirical or geochemical. Theoretical calibration is based on experiments in the laboratory to establish values for equilibrium constants for specific mineral–solution reactions on which the geothermometry equation is based. An example is quartz. The calibration of this geothermometer is based on experimentally determined quartz solubility in water. Geochemical or empirical calibration involves correlating specific aqueous component concentrations in well discharges with their aquifer temperature. The Na/K, Na–K–Ca and many other cation ratio geothermometers have been calibrated in this way. Yet, a new theoretical calibration is now available for the Na/K (albite/K feldspar) geothermometer (Arnórsson et al., 1998).

A temperature equation for a geothermometer is a temperature equation for a specific equilibrium constant referring to a specific mineral–solution reaction. For quartz the reaction is:

$$SiO_{qtz} + 2H_2O = H_4SiO_4^0 \qquad (10.1)$$

The equilibrium constant for this reaction is given by:

$$K_{qrz} = \frac{[\mathrm{H_4SiO_4^0}]}{[\mathrm{quartz}][\mathrm{H_2O}]^2} \tag{10.2}$$

where brackets indicate the activity of the respective species and phases. The activity of pure phases is equal to 1. In general, quartz does not contain impurities to any significant amount and, if the water is dilute, its activity is close to 1, in which case Eq. (10.2) reduces to:

$$K_{qtz} \approx [\mathrm{H_4SiO_4^0}] \tag{10.2a}$$

Sea water contains about 3.5% of dissolved salts and 96.5% water. The activity of water in sea water is about equal to its mole fraction. The mole fraction of all salts in sea water is calculated to be 0.02 so that the mole fraction of water is 0.98. Therefore, $[\mathrm{H_2O}] = 0.98$ and $[\mathrm{H_2O}]^2 = 0.96$. As the equilibrium constant for the reaction takes a fixed value at any specific temperature and pressure, it can be deduced from Eq. (10.2) that the solubility of pure quartz in sea water is 96% of that in pure water at any temperature.

An expression of the form of the van't Hoff equation has been widely used to express the temperature dependence of equilibrium constants including geothermometry equations. The equation is

$$\frac{\partial \ln K}{\partial (1/T)} = \frac{-\Delta H_r^0}{R} \tag{10.3}$$

where K is the equilibrium constant, T the temperature in kelvin, ΔH_r^0 the enthalpy of the reaction and R the gas constant. For many silicate–water reactions, it is a good approximation, at least up to about 250°C, to take the enthalpy of such reactions to be constant. This implies that the heat capacity for the reaction $(\Delta C_{p,r}^0)$ is zero. For these conditions and replacing the natural logarithm by $\log_{10}$, Eq. (10.3) simplifies to

$$\log K = \frac{1}{T}\frac{-\Delta H_r^0}{R \times 2.303} \tag{10.3a}$$

In other words, the equilibrium constant changes linearly with the reciprocal of the absolute temperature. The slope of the line is $-\Delta H_r^0/R \times 2.303$. This calibration is particularly useful when experimental or drillhole data, which are used to calibrate geothermometers, only cover a limited temperature range and need to be extrapolated, either to lower or higher temperatures. It was also very useful before the age of computers to linearly regress data, but now it is not.

The rate of equilibration for the various water geothermometers differs as deduced from field observations. However, hard facts about the reactions rates are limited except for quartz and chalcedony. Chalcedony and quartz come close to equilibrium with aqueous silica within hours or days at temperatures exceeding 0°C and 150°C, respectively. The precise rate, of course, depends on the surface area between the respective minerals and solution. By contrast, equilibration with quartz is slow at low temperatures, in particular below 50°C. The Li/Mg and K/Mg cation geothermometers re-equilibrate rapidly, at least compared with the silica and the Na/K geothermometers, in upflow zones of geothermal systems where cooling occurs. Water salinity also affects the rate of re-equilibration in upflow zones. For the silica minerals, it increases with increasing water salinity but the opposite seems to be the case for the cation geothermometers.

10.1.1 Silica geothermometers

Several calibrations have been proposed for the quartz and chalcedony geothermometers. Solubility equations for the various silica minerals are given in Box 10.1. For chalcedony the temperature–solubility equations are practically the same. It is recommended to use the one given by Fournier (1977). It is based on solubility experiments above 125°C and extrapolation to lower temperatures. The equation by Arnórsson et al. (1983b), on the other hand, is based on drillhole data from Iceland.

Extensive experimental data have been produced on quartz at one bar below 100°C and at vapour saturation pressures at higher temperatures. They have been summarized by Gunnarsson and Arnórsson (1998). There is some disagreement between the experimental results below 100°C and above 250°C (Fig. 10.1). The solubility equation proposed by Fournier and Potter (1982) has been most widely used for chemical geothermometry. However, the more recent solubility equation proposed by Gunnarsson and Arnórsson (1998) and Arnórsson et al. (1998a) is considered better because it relies on a wider experimental database. This new equation indicates similar solubility in the temperature range of 100–250°C but higher and lower solubility at lower and higher temperatures, respectively (Fig. 10.2). The quartz solubility equation, which indicates lower solubility above 250°C (Arnórsson et al., 1998a), yields

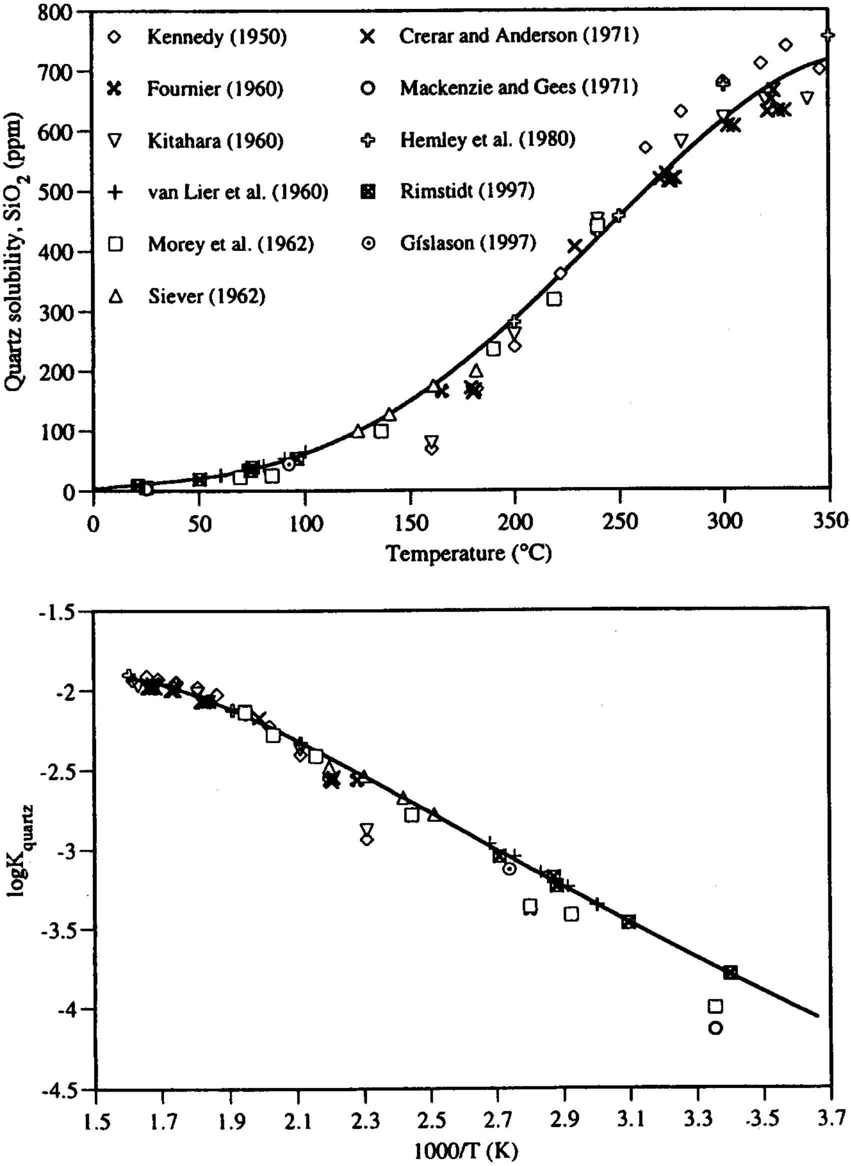

FIG. 10.1. Experimental data on quartz solubility in pure water.

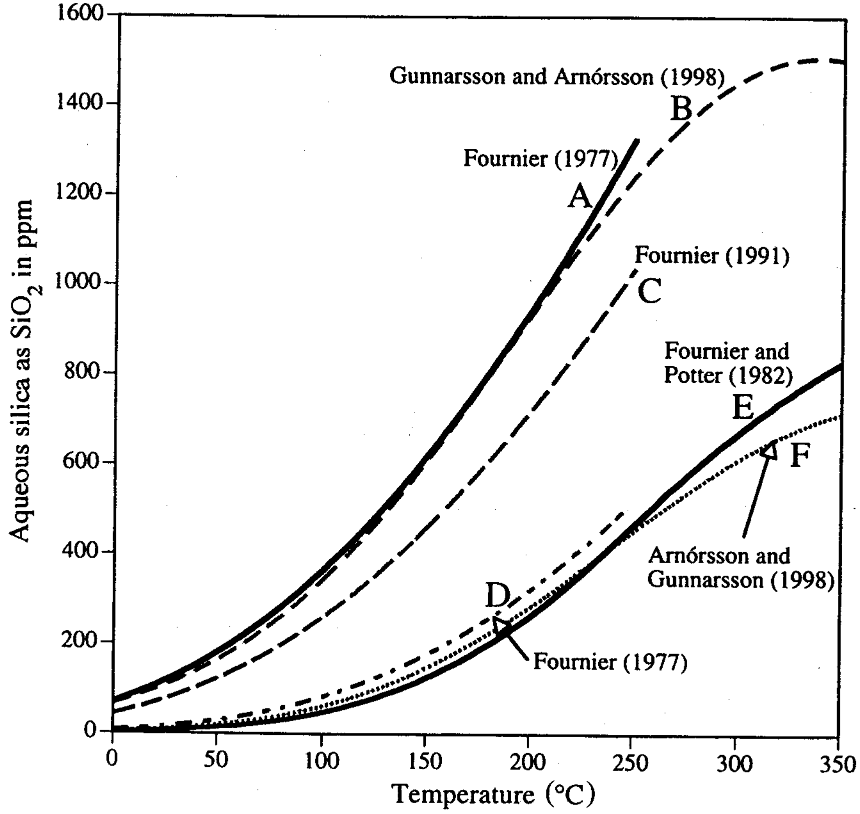

FIG. 10.2. The solubility of quartz, chalcedony, opal and amorphous silica in water at 1 bar below 100°C and at the vapour pressure of the solution at higher temperatures. A and B: armorphous silica. C: opal. D: chalcedony. E and F: quartz. The sources of the data are shown in the figure.

higher quartz equilibrium temperatures, the difference increasing with rising temperature and reaching 30°C at 350°C.

When calculating temperatures from the silica content of natural water assuming equilibrium with either quartz or chalcedony, the temperatures are termed quartz equilibrium and chalcedony equilibrium temperatures, respectively.

There are several known silica polymorphs in nature. They are: quartz, amorphous silica, moganite, tridymite, cristobalite, coesite and stichovite. Chalcedony is a variety of quartz, being composed of very fine quartz crystals, in fact so fine that their surface energy contributes to their solubility, explaining why chalcedony is more soluble than quartz (Walther and Helgeson, 1977). Detailed studies of natural chalcedony grains have shown that they are a mixture of two silica polymorphs, quartz and moganite (Gíslason et al., 1996). Moganite has never been found pure in nature. As a result, it has been difficult to measure its solubility. Initially, experimental solutions probably attain saturation with moganite, which is more soluble than quartz but stable conditions are not attained, and the aqueous silica gradually falls and approaches equilibrium with quartz. Simultaneously, the moganite is progressively destroyed. Gíslason et al. (1996) have used a rate of solution experiment to calculate the moganite solubility (Box 10.1).

The silica phases of interest for geochemical studies of geothermal fluids are quartz, chalcedony and amorphous silica and probably also moganite, at least when it has become possible to determine its solubility experimentally with accuracy.

Arnórsson (1975) concluded that geothermal waters in Iceland equilibrated with chalcedony below 180°C but with quartz at higher temperatures. Occasionally, groundwaters equilibrate with amorphous silica. In most known geothermal systems the silica minerals with which the aqueous silica approaches equilibrium are precipitated from solution. They are secondary. Which silica mineral constitutes the controlling phase for aqueous silica concentrations depends on the rate of two counteracting processes, dissolution of the primary silicate minerals of the rock and precipitation of a silica mineral. The rate of dissolution of the primary rock minerals depends on their properties and how reactive the water is, which is largely controlled by its pH. Low pH waters, such as CO_2 rich waters, tend to dissolve silicate minerals so rapidly that neither quartz nor chalcedony precipitation copes with it for kinetic reasons, at least at low temperatures (<50°C), but amorphous silica does. For this reason, such waters tend to equilibrate with amorphous silica.

Minerals of volcanic rocks, such as basalt, dissolve relatively rapidly. As a result, silica is released rapidly into solution when water reacts with such rocks. At low temperatures the rate of quartz precipitation does not cope with the rate of silica release into solution by the dissolving primary minerals and the water tends to equilibrate with chalcedony. At temperatures above about 180°C, on the other hand, equilibration with quartz is attained but the quartz precipitation rate is very much enhanced by rise of temperature, as demonstrated experimentally. In mature sedimentary rocks, which contain less reactive minerals than volcanic rocks, equilibration with quartz may be experienced at temperatures of even less than 100°C, the reason being the slower rate of silica release into solution as compared to volcanic rock systems. At present, it seems to be the best choice to assume equilibrium with chalcedony for geothermal systems in volcanic rocks if the chalcedony equilibrium temperature is less than 180°C. On the other hand, equilibrium with quartz should be assumed if the chalcedony equilibrium temperature is >180°C.

Amorphous silica precipitates readily from solution. As a result, geothermal spring waters are seldom amorphous silica supersaturated. The precipitate of the amorphous silica forms sinters around the spring vents. The solubility of amorphous silica at 100°C is about 350 ppm. This corresponds to a quartz equilibrium temperature of about 220°C. As a result, a subsurface temperature of about 220°C may be regarded as an upper roof for the quartz geothermometer. If the quartz geothermometer indicates subsurface temperatures of some 220°C but the cation geothermometers show a substantially higher temperature, the calculated quartz equilibrium temperature should be regarded as being low, because of presumed precipitation of silica from solution to form amorphous silica.

The solubility reactions for silica minerals are invariably expressed as:

$$SiO_{2,solid} + 2H_2O = H_4SiO_4^0 \qquad (10.1a)$$

However, $H_4SiO_4^0$ is not the only queous silica species in natural waters. $H_4SiO_4^0$ is a weak acid which dissociates, if the pH of the water is high enough, to yield $H_3SiO_4^-$:

$$H_4SiO_4^0 = H^+ + H_3SiO_4^- \qquad (10.4)$$

Analysis of silica in aqueous solution yields the total silica concentration, generally expressed as ppm SiO_2, which includes both un-ionized ($H_4SiO_4^0$) and ionized ($H_3SiO_4^-$) silica. The dissociation constant for silicic acid is about 10^{-10} at 25°C. Thus, at a pH of 10 ($H^+ = 10^{-10}$) the concentration of unionized silica equals that of ionized silica:

$$\frac{[H^+][H_3SiO_4^-]}{[H_4SiO_4^0]} = K_{H_4SiO_4^0} \qquad (10.5)$$

and

$$\frac{[H_3SiO_4^-]}{H_4SiO_4^0]} = \frac{K_{H_4SiO_4^0}}{[H^+]} = \frac{10^{-10}}{10^{-10}} = 1 \qquad (10.5a)$$

In waters with a pH in excess of 9, as measured at 25°C, a significant fraction (>10%) of the analysed total silica exists in solution as $H_3SiO_4^-$. In calculating quartz or chalcedony equilibrium temperatures for such high pH waters, the analysed silica concentrations need to be corrected to retrieve the fraction in solution that occurs as $H_4SiO_4^-$. This can be done approximately by solving together the following mass balance equation and Eq. (10.5):

$$[H_4SiO_4^{-1}] + [H_3SiO_4^-] = SiO_{2,anal} \qquad (10.6)$$

to yield

$$H_4SiO_4^0 = \frac{SiO_{2,anal}}{\frac{K_{H_4SiO_4^0}}{H^+} - 1} \qquad (10.7)$$

The temperature dependence of the dissociation constant for silicic acid is given by:

$$\log K_{H_4SiO_4^0} = -2549/T - 15.36 \times 10^{-6}T^2 \qquad (10.8)$$

By calculating the value of this constant at the temperature at which the pH is measured, the concentration of $H_4SiO_4^0$ (unionized silica) can be retrieved from the measured pH and total silica concentration of the water with the aid of Eq. (10.7). To obtain a value for the silica (quartz or chalcedony) equilibrium temperature, the value for the unionized silica (as SiO_2 in ppm) may be inserted into the respective silica geothermometry equation in Box 10.1.

Geothermal waters may boil in the upflow of geothermal systems if reservoir temperatures exceed 100°C. The boiling causes the concentrations of aqueous solutes to increase in proportion to the steam formation. It also causes the pH of the water to increase because the weak acids dissolved in the water, CO_2 and H_2S, are transferred into the steam phase. Although boiled water in hot springs may have such a high pH that a substantial fraction of the dissolved silica is ionized at the temperature of the spring, the calculated pH under reservoir conditions for all types of water, dilute to saline, is so low that practically all the silica is in an un-ionized form ($H_4SiO_4^0$), at least, if temperatures exceed 180°C. Therefore, it is appropriate to use total analysed silica instead of the calculated un-ionized silica to estimate the silica equilibrium temperature. In other words, if the total silica concentration of a spring indicates a temperature of more than 180°C, this geothermometry result should be used rather than the one obtained from the calculated un-ionized silica concentration in the spring water.

As was stated above, boiling causes the concentrations of aqueous solutes to increase in proportion to the steam formation. This also increases the aqueous silica concentrations, which leads to an overestimation of the silica equilibrium temperature. The equations in Box 10.1, which are valid for steam loss by adiabatic boiling to 100°C, should be used to estimate silica temperatures for boiling hot springs. It has been pointed out (White, 1976) that precipitation of silica from solution occurs in conjunction with boiling, thus causing the silica concentration to be lower in springs than anticipated in their concentration in parent reservoir water. This precipitation counteracts the increase in the silica concentration caused by the boiling. Therefore, the silica geothermometry equations, which do not involve boiling, may give just as good a picture of subsurface temperatures as the equations that take it into account. Accordingly, it is concluded that both types of equation should be used to calculate the silica temperatures and that the actual temperature in the feeding aquifer to the respective hot springs may lie between the two extremes.

10.1.2. Na-K geothermometer

Na/K ratios in geothermal waters were initially used to locate the major upflow zone in the Wairakei geothermal field in New Zealand (Ellis and Wilson, 1961), the lowest ratios being closest to the major upflow. Already at this time, the opinion was expressed that the Na/K ratios of geothermal waters were probably controlled by the equilibrium between the geothermal water and alkali feldspars.

Very many geochemical (empirical) calibrations have been proposed for the Na/K geothermometer (Box 10.2). They reflect two things: many researchers have observed that Na/K ratios of geothermal waters relate to water temperature and that thermodynamic data have not been sufficiently accurate for theoretical calibration, or minerals other than feldspars are involved in the control of aqueous Na/K ratios.

Reactions between alkali feldspars and Na and K in aqueous solution have often been described as exchange reactions. At the temperature prevailing in geothermal systems (<350°C), this is probably not true, at least in the sense that Na and K do not exchange for each other and equilibrate with a mixed alkali feldspar. The reaction in question involves simultaneous equilibrium between Na^+ and K^+ in solution and quite pure albite and K feldspar. Both the feldspars are probably highly ordered with respect to Al and Si, i.e. low albite and microcline (Arnórsson and Stefánsson, 1998). The reaction involved is appropriately expressed as:

$$NaAlSi_3O_8 + K^+ = KAlSi_3O_8 + Na^+ \tag{10.9}$$

the equilibrium constant being

$$K_{alkali\ field} = \frac{[Na^+]}{[K^+]} \tag{10.10}$$

as the respective feldspars are almost pure, i.e. their activity is ~1.

Very extensive studies of hydrothermally altered rocks and of metamorphic rocks in metamorphic facies of lower grade than the amphibolite facies have revealed that their alkali feldspars are quite pure albite and pure K feldspar, respectively. In the amphibolite facies and higher grade metamorphic rocks, corresponding to formation temperatures in excess of some 400°C and characterized by the appearance of Al bearing amphibole (hornblende), the plagioclase begins to contain some calcium. With increasing formation temperature its calcium content rises (see, e.g. Miyashiro, 1994). K feldspars in metamorphic rocks persist into the granulite facies, i.e. up to melting temperatures. There is, thus, no logic in postulating that Na/K ratios in geothermal waters are controlled by exchange reactions with a single alkali feldspar of mixed composition.

Both albite and K feldspar (adularia) are characteristic secondary minerals in hydrothermally altered rocks of geothermal systems that occur in volcanic rocks ranging from basaltic to silicic in composition. However, these feldspars need not form as secondary minerals in all geothermal systems irrespective of the rock type they are hosted in. It has indeed been postulated that Na/K ratios in geothermal waters associated with sedimentary rocks are controlled by exchange equilibria with clays rather than alkali feldspars:

$$\begin{aligned} &Na_{0.33}Al_{2.33}Si_{3.67}O_{10}(OH)_2 + 0.33K^+ \\ &\quad = K_{0.33}Al_{2.33}Si_{3.67}O_{10}(OH)_2 + 0.33Na^+ \end{aligned} \tag{10.11}$$

Arnórsson and Stefánsson (1998) have recently assessed experimental thermodynamic data on feldspars from which Arnórsson et al. (1998a) have retrieved a new calibration for the Na-K geothermometer. This theoretical equation (see Box 10.2) compares well with the empirical equations proposed by Truesdell (1976) and Arnórsson et al. (1983b) (Fig. 10.3). It somewhat departs, on the other hand, from the equations proposed by Fournier (1979) and

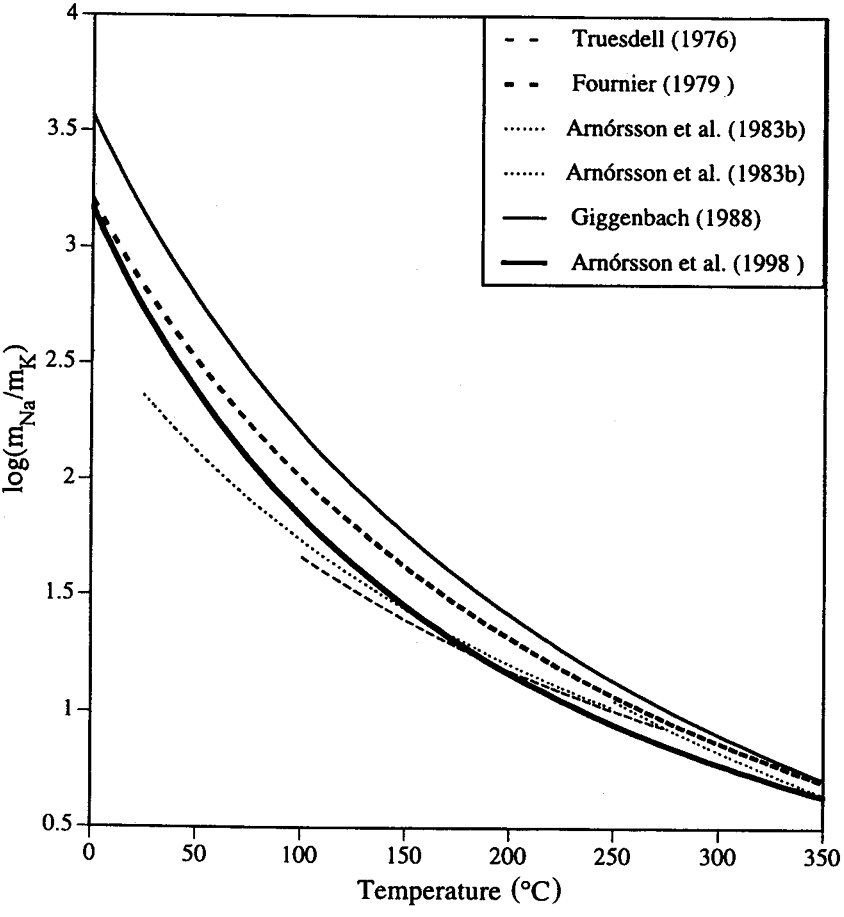

FIG. 10.3. Proposed temperature curves for the Na–K geothermometer as indicated (see equations in Box 10.2).

Giggenbach (1988). Fournier's (1979) calibration is empirical whereas that of Giggenbach (1988) is based on thermodynamic data on low albite and K feldspar presented by Bowers et al. (1984). It is considered that their data are less reliable than the calorimetric data selected by Arnórsson and Stefánsson (1998), which are, therefore, preferred.

As was discussed in Section 3.2, the overall process of hydrothermal alteration is irreversible where primary rock minerals are continuously being dissolved and secondary minerals precipitated. An inevitable consequence of this is that the waters must always be somewhat supersaturated with respect to the secondary minerals. Otherwise they would have no tendency to form by precipitation from solution. As shown in the figure in Box 14.5, for low albite, thermal and non-thermal groundwaters in the area of Skagafjördur, Iceland, are supersaturated with respect to this mineral. They are just about equally supersaturated with respect to microcline. As a result, they are calculated to be at simultaneous equilibrium with both of the alkali feldspars. The reason is that the supersaturation is caused by excessive aluminium in solution.

The solubilities of both low albite and microcline (fully ordered K feldspar with respect to Al and Si) decrease with decreasing temperatures. As a result, these feldspars tend to precipitate in upflow zones of geothermal systems where the water cools either by conduction or boiling or both. Since the concentrations of aluminium in geothermal waters are invariably much lower than those of sodium and potassium, the availability of aluminum is a controlling factor for the feldspar precipitation. Even if the feldspars re-equilibrated in response to cooling, this would have a small effect on the Na/K ratio of the water. It is assumed that this is the main cause of the apparent slow re-equilibration of the Na/K geothermometer. Aqueous Na/Al and K/Al ratios increase with increasing water salinity. As a result, Na/K ratios are less affected by alkali feldspar precipitation from saline waters than corresponding precipitation from dilute waters causing saline waters to apparently respond more slowly to cooling than dilute waters.

Although albite and K feldspar are widespread as secondary minerals in rocks of geothermal systems of quite variable composition, they do not form in all types of rock subjected to hydrothermal alteration. As a result, there is no universal Na/K geothermometer. It is, however, concluded that the Na/K geothermometer based on assumed equilibrium with low albite and microcline (Arnórsson and Stefánsson, 1998) is valid in volcanic rocks ranging from basaltic to silicic in composition, as well as in immature sedimentary rocks, such as greywackes, which are roughly andesitic in composition. It will depend on the temperature of the water, its residence time underground and the sources of supply of acids to the water how close it comes to equilibrium with the two feldspars. In the old groundwaters in Skagafjördur, Iceland, equilibrium is closely approached at temperatures as low as 20°C. In CO_2 rich waters in Iceland, on the other hand, no close approach to equilibrium appears to be attained at temperatures much below 150°C.

10.1.3. Na–K–Ca geothermometer

The Na–K–Ca geothermometer, developed by Fournier and Truesdell (1973), has been very successful. It is empirically calibrated. The main advantage of the Na–K–Ca geothermometer in comparison with the quartz geothermometer, and especially the Na/K geothermometer, is that it does not give high and misleading results for cold and slightly thermal, non-equilibrated waters.

The reactions involved may be expressed as

$$\begin{aligned} &K^+ + Na_{0.667}Ca_{0.167} - \text{solid} \\ &\quad = 0.667Na^+ + 0.167Ca^{2+} + K - \text{solid} \end{aligned} \tag{10.12}$$

and

$$\begin{aligned} &K^+ + 0.333Na^+ + Ca_{0.667} - \text{solid} \\ &\quad = 0.667Ca^{2+} + KNa_{0.333} - \text{solid} \end{aligned} \tag{10.13}$$

The equilibrium constant for these reaction has the following general form:

$$\log K = \log(\text{Na/K}) + \beta\log(\text{Ca}^{0.5}/\text{Na}) \tag{10.14}$$

where β is 1/3 (0.333) for reaction (10.12) and 4/3 (1.333) for reaction (10.13). Fournier and Truesdell (1973) proposed that a value for β of 4/3 should be used if that value yielded a Na–K–Ca temperature of <100°C. If, on the other hand, this β yielded >100°C, the value should be taken to be 1/3 and the Na–K–Ca temperature should be recalculated to give what was considered to be the best value. β should also be taken to be 1/3 if log ($Ca^{0.5}/Na$) is negative.

It is not known which minerals are involved in controlling the relative abundance of Na, K and Ca in natural waters, i.e. the Na–K–Ca geothermometer, but several have been proposed, including clays, micas and feldspars.

Two empirical corrections have been proposed to the Na–K–Ca geothermometer, one involving CO_2 partial pressure (Pâces, 1975) and the other the Mg content of the water (Fournier and Potter, 1979, Box 10.3). The magnesium correction to the Na–K–Ca geothermometer is generally only significant for waters of low temperature. The CO_2 correction involves the addition of a term I to the equilibrium constant, or

$$\log K = \log (\mathrm{Na/K}) + \beta \log (\mathrm{Ca}^{0.5}/\mathrm{Na}) + \mathrm{I} \tag{10.15}$$

where

$$\mathrm{I} = -1.36 - 0.253 \log P_{CO_2} \tag{10.16}$$

The problem with the CO_2 correction involves estimation of the CO_2 partial pressure. One possibility is to use an equation relating the CO_2 partial pressure to the temperature:

$$\log P_{CO_2} = -3.78 + 0.0168t \tag{10.17}$$

where the pressure is in bars and the temperature (t) in °C. This relationship assumes that the CO_2 partial pressure is controlled by equilibrium of CO_2 with a specific mineral buffer, which may be expressed as:

$$\mathrm{CaAl - silicate} + K - \mathrm{feldspar} + \mathrm{CO_2} = \mathrm{K - mica + calcite} \tag{10.18}$$

Another possibility is to use the relative abundance of CO_2, CO and H_2 in the gas phase:

$$CO_2 + H_2 = CO + H_2O \tag{10.19}$$

From this geobarometry reaction, it is seen that the CO_2 partial pressure is proportional to the ratio of the partial pressures of CO to H_2. The equilibrium constant for this reaction varies insignificantly with temperature. Between 130° and 320°C, the CO_2 partial pressure can be described by:

$$\log P_{CO_2} = 3.52(\pm 0.2) + \log\left(\frac{CO}{H_2}\right) \tag{10.20}$$

where gas concentrations are in mole percentage of dry gas and CO_2 partial pressure is in bars.

A third possibility of estimating CO_2 partial pressures is to take potassium to calcium ratios along with CO_2 partial pressures to be fixed by the following reaction:

$$3\text{K} - \text{feldspar} + CO_2 + Ca^{2+} = \text{K} - \text{mica} + \text{calcite} + 2K^+ \tag{10.21}$$

leading to

$$\log P_{CO_2} = \log (m_K^2/m_{Ca}) - 3.0 \tag{10.22}$$

allowing the CO_2 partial pressure to be determined from the K/Ca ratio of the water.

Reactions (10.18), (10.19) and (10.21) are based on the assumption that specific equilibria control CO_2 partial pressures. Generally it is observed that Eq. (10.19), which involves gas equilibria, yields higher values for the CO_2 partial pressures than the other two reactions that involve mineral equilibria.

10.1.4. Na–K–Mg geothermometer

Giggenbach (1988) proposed the following temperature equation for the K–Mg geothermometer:

$$t(°\text{C}) = \frac{4410}{14.00 - \log(m_K^2/m_{Mg})} - 273.15 \tag{10.23}$$

The calibration was based on a calculated equilibrium constant for the following reaction:

$$\begin{aligned} &2.8\text{K} - \text{feldspar} + 1.6\text{water} + Mg^{2+} \\ &\quad = 0.8\text{K} - \text{mica} + 0.2\text{chlorite} + 5.4\text{quartz} + 2K^+ \end{aligned} \tag{10.24}$$

using thermodynamic data on the minerals from Helgeson et al. (1978). Further, Giggenbach (1988) used data on low albite and microcline from Bowers et al. (1984) to retrieve a temperature equation for the Na–K geothermometer:

$$t(°\text{C}) = \frac{1390}{1.75 - \log(m_{Na}/m_K)} - 273.15 \tag{10.25}$$

The respective K, Na and Mg concentrations in Eqs (10.23) and (10.25) are in ppm.

By combining these two ratios, Giggenbach (1988) plotted into a triangular diagram the relative distribution of Na, K and Mg in water at equilibrium at different temperatures with the minerals of Eqs (10.9) and (10.24) (Box 10.4).

It is often observed that the Na–K and K–Mg geothermometers give different results. This was interpreted by Giggenbach (1988) as being due to variable departure from equilibrium for the two reactions. Clearly, the K/Mg geothermometer responds faster than the Na/K ratio to decrease of temperature in upflow zones. Accordingly, the K/Mg geothermometer tends to give lower temperatures than the Na/K geothermometer.

In the context of the Na–K–Mg geothermometer, it is to be emphasized that the hydrothermal alteration process, which involves water–rock interaction, is an overall irreversible reaction involving dissolution of primary rock minerals and precipitation of secondary ones (Chapter 3.2). Cold waters seeping into the ground are undersaturated with most primary minerals of volcanic rocks and, therefore, tend to dissolve them. The Na/K ratio of such waters is similar to that of the enclosing rock while Mg concentrations tend to be relatively high. Progressive interaction between water and rock towards equilibrium changes Na/K ratios towards equilibrium with feldspars. At the same time, both Na and K concentrations almost invariably increase. Similarly, Mg concentrations decrease because Mg is incorporated into precipitating minerals such as smectite and chlorite. These processes cause K/Mg ratios to increase strongly as groundwater reacts progressively with the rock towards equilibrium with secondary minerals.

When ascending geothermal waters cool without boiling, their pH decreases. Both the decreases in temperature and pH cause the water to become increasingly undersaturated with primary igneous rock minerals, thus enhancing their rate of dissolution and causing their K/Mg ratios to become lower. The aqueous Na/K ratio tends to change towards this ratio in the rock. For this reason, geothermal waters, which have cooled and reacted much in the upflow, show quite different temperature values for the Na–K and K–Mg geothermometers, the latter indicating lower temperatures.

On the basis of the relative abundance of Na, K and Mg in natural waters Giggenbach (1988) classified them as 'immature', 'partially equilibrated or mixed' and 'fully equilibrated', meaning progressive reaction towards equilibrium as one moves from immature waters to fully equilibrated ones, 'fully equilibrated' meaning equilibrated with respect to all the components in question. The advantage of the Na–K–Mg geothermometer is that it helps distinguish equilibrated from disequilibrated waters. Its disadvantage, on the other hand, lies in the apparent reactivity of Mg minerals causing aqueous Mg concentrations to change rapidly in response to changing temperature, thus responding effectively to cooling in the upflow unlike the more slowly responding geothermometers such as the quartz and the Na/K geothermometers. After all, the usefulness of all geothermometers lies in their slow response to changing temperature in upflow zones. However, the reactions involved must not be so slow that equilibrium is generally not attained in geothermal reservoirs.

The methodology of constructing the Na–K–Mg geoindicator diagram is described in detail in Box 10.4. The choice of the Na/K geothermometry equation used for the construction of this diagram considerably affects the estimated subsurface temperature. Giggenbach (1988) used thermodynamic data on microcline and low albite from Bowers et al. (1984) to retrieve a temperature equation for the Na/K ratio. For any particular Na/K ratio, this equation yields a higher temperature than most other Na–K geothermometry equations, the difference being as much as 50°C. For data interpretation involving use of the Na–K–Mg triangular diagram, it is important to analyse the effect of the selected Na–K geothermometry equation on the estimated subsurface temperature.

10.1.5. Other cation geothermometers

Several cation ratio geothermometers other than those just described have been developed (Box 10.2). Tonani (1980) proposed to use $Na/Ca^{0.5}$ and $K/Ca^{0.5}$ ratios as geothermometers. Apparently, they have not been used much for geothermal exploration. They seem to be affected by CO_2 partial pressure. The precipitation of calcium as carbonates in upflow zones, which occurs when boiling takes place, tends to lead to high subsurface temperature estimates by these geothermometers.

Kharaka and Mariner (1989) proposed a geothermometer based on Li/Mg ratios. When applying this geothermometer to thermal spring waters of a particular area, the indicated temperatures tend to be much lower than those observed in drillholes except possibly for systems in metamorphic and granitic terrain. The reason for the difference is that the spring waters contain significantly higher Mg than the well waters. As already discussed in Section 10.1.4 on the Na–K–Mg geothermometer, geothermal waters easily pick up Mg from the wallrock during cooling in upflow zones, with the result that any geothermometer involving Mg tends to give low temperature estimates. As Mg is very low in geothermal reservoir waters, relatively little reaction with the wallrock in the upflow is required to alter the aqueous Mg concentration significantly.

When the results of the K–Mg and Li–Mg geothermometers agree well with those of the quartz, Na–K and Na–K–Mg geothermometers, it is considered reliable to assume that equilibrium has been attained for the Mg bearing geothermometers at the indicated geothermometry temperature, implying also that there has been little water–rock interaction in the upflow. This tends to be the case when boiling is extensive, causing pH to become relatively high, in which case the water is not reactive, i.e. not highly undersaturated with the primary rock minerals. On the other hand, if boiling does not occur so that the water retains its CO_2, pH stays lower making the water more reactive, which tends to cause aqueous Mg concentrations to increase in the upflow.

Fouillac and Michard (1981) were the first to propose Na/Li aqueous ratios as a geothermometer. Later on, Kharaka et al. (1982) presented a new calibration for this geothermometer. In both cases the calibration was empirical, based on drillhole data. Because of their different geochemical properties, it is not expected that Li substitutes for Na in hydrothermal or other minerals. In view of its crystal radius, Li is likely to substitute Mg.

The Na/Li geothermometer appears to be sensitive to the total dissolved solids of the water and to the rock type. Since Li is a minor constituent in a geothermal fluid and Na is a major one, slight changes in Li concentrations during the ascent of the fluid can greatly affect the Na/Li ratio.

10.2 STEAM (GAS) GEOTHERMOMETERS

In many geothermal fields, surface manifestations consist only of hot ground, acid surface waters and fumaroles. In these fields the thermal groundwater table is subsurface. When this is the case, water geothermometers cannot be applied. This has called for the development of steam (gas) geothermometers for geothermal exploration. The first gas geothermometer developed is that of D'Amore and Panichi (1980). Later geochemical methods involving gas chemistry have been developed to estimate steam to water ratios in geothermal reservoirs (e.g. D'Amore and Truesdell, 1985; Arnórsson et al., 1990), as discussed in Chapter 15.

There are essentially three types of steam geothermometers, those based on:

(1) gas–gas equilibria;

(2) mineral–gas equilibria involving H_2S, H_2 and CH_4 but assuming CO_2 to be externally fixed according to empirical methods;
(3) mineral–gas equilibria.

The first two groups of geothermometer require only data on the relative abundance of gaseous components in a gas phase, whereas the third group calls for information on gas concentrations in steam.

The thermodynamic properties of gases of geothermal interest and their solubility in water are accurately known. Thus, gas–gas geothermometers are theoretically and accurately calibrated. It is, of course, clear that the calibration of the geothermometer of D'Amore and Panichi (1980) is partially empirical, i.e. with respect to the selection of CO_2 partial pressure. Both empirical and theoretical calibrations have been used for the mineral–gas geothermometers (Nehring and D'Amore, 1984; Arnórsson and Gunnlaugsson, 1985; Giggenbach, 1991; Arnórsson et al., 1998b).

In three respects, steam geothermometry is more difficult to handle than water geothermometry. Firstly, gas concentrations in geothermal reservoir fluids are affected by the ratio of steam to water of that fluid. Secondly, the gas content of fumarole steam is affected by the boiling mechanism in the upflow, steam condensation and the separation pressure of the steam from parent water. Thirdly, the flux of gaseous components into geothermal systems from their magmatic heat source may be quite significant and influence how closely gas–gas and mineral–gas equilibria are approached in specific aquifers. The components of water geothermometers are, on the other hand, with few exceptions solely derived from the enclosing rocks. Only if the recharging fluid is saline, as is the case with sea water, are some aqueous components of water geothermometers externally derived.

Giggenbach (1991) presents a gas geothermometer based on CO, CO_2 and CH_4 concentrations according to the reaction:

$$3CO_2 + CH_4 = 4CO + 2H_2O \tag{10.26}$$

Rather than lumping the three carbon gas species into a complex, multicomponent equilibrium expression, Giggenbach (1991) chose to use a graph relating CH_4/CO_2 and CO/CO_2 ratios to temperature according to the above reaction (Fig. 10.4). The graph is based on the assumption that the redox potential of the system is controlled by the di- and trivalent iron of the rock and is valid for single liquid systems, boiling systems and vapour dominated systems.

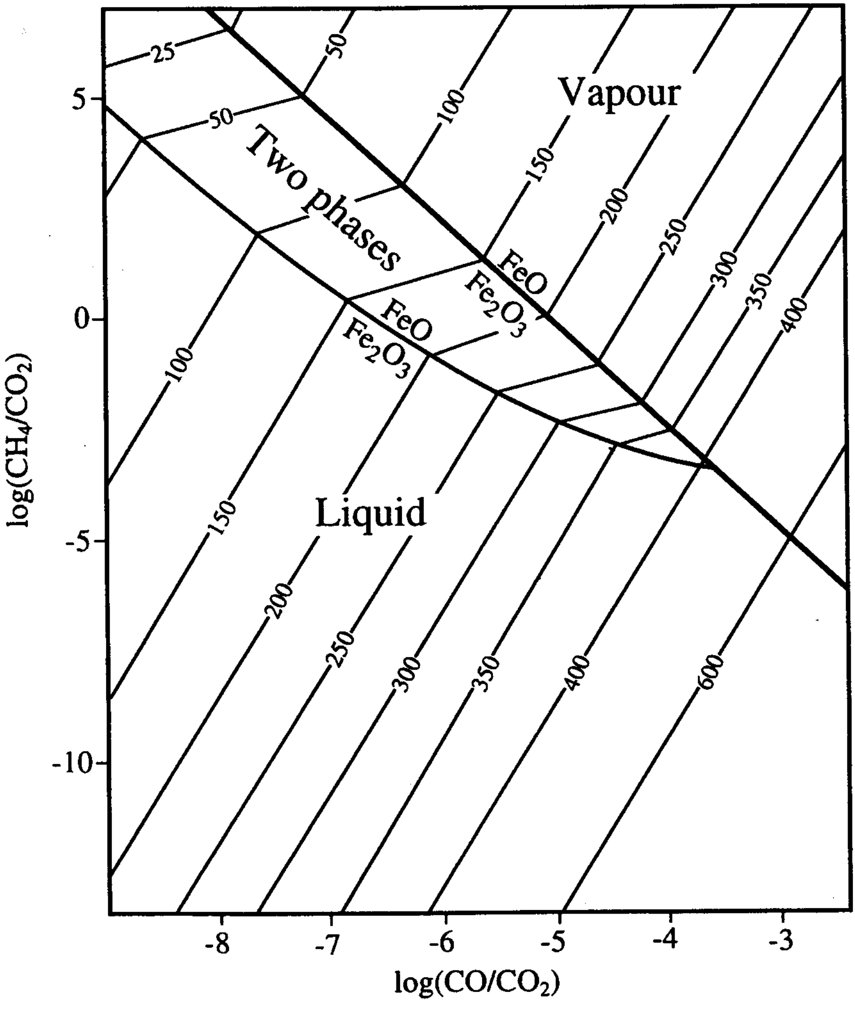

FIG. 10.4. The CO–CO_2–CH_4 geothermometry diagram of Giggenbach (1991). Subsurface temperatures are estimated from analysed CO, CO_2 and CH_4 concentrations by finding a common temperature for the two ratios.

Analysis of practically all aqueous species involves determination of elemental concentrations. The only major exceptions are SO_4 and H_2S. Special examples include Fe^{2+} and Fe^{3+}, as well as tri- and pentavalent arsenic. In contrast, gaseous species such as CO_2, CH_4 and CO as well as H_2S and SO_2 are generally determined as such. The carbon and sulphur of these gases occur in different oxidation states. The same applies to the above mentioned aqueous components, as well as to H_2 and H^+, which are separately determined. The possibility of separately analysing components of the same element in different oxidation states obviously indicates that the respective oxidation–redox reactions are slow. Otherwise, the analysis of these components would not provide any specific equilibrium conditions, merely those of the temperature of the analysis. Since redox reactions are slow, such as those involving geothermal gases, it may always be questioned whether such redox equilibria are closely approached in geothermal systems. It is important to demonstrate whether or not this is generally the case by sampling and analysing well discharges derived from sub-boiling aquifers. If the aquifer is sub-boiling, it is straightforward to calculate the aquifer concentrations of each gas component and assess from knowledge of the aquifer temperature whether equilibrium is attained or not.

Arnórsson (1986) developed a method of correcting for the effect of steam condensation in the upflow below fumaroles on the results of those gas geothermometers that are based on gas concentrations in steam. Geothermometers based on gas ratios are not affected by steam condensation. For this reason, it is advantageous to use gas ratios. In the case of geothermometers using gas concentrations, it is best to take a ratio of this gas to another gas, such as argon, that has only an atmospheric source. In this case, it can be assumed with reasonable confidence that its concentration in the deep geothermal fluid equals that of air saturated water. This approach was taken by Giggenbach (1991) and Arnórsson et al. (1998b).

No specific recommendations can be given as to which steam geothermometers should be used for a specific geothermal field. Use all of them, compare the results and, with the aid of the mode of calibration, attempt to assess which geothermometers yield the most reliable information.

10.3 MULTIPLE MINERAL EQUILIBRIUM APPROACH

One method of estimating subsurface temperatures in geothermal systems involves calculation of reaction quotients from analytical data on the thermal waters for a set of minerals over a range of temperature in order to see at which temperature equilibrium exists between the water and these minerals (Figs 10.5 and 10.6). Reed and Spycher (1984) proposed this approach. The choice of minerals should, of course, include those known to occur as hydrothermal minerals in the geothermal system under study or in geothermal systems in general, but in particular those occurring in the same type of rock as the system under exploration. Minerals that should always be considered include quartz or chalcedony, the alkali feldspars (albite and microcline), calcite, in some cases anhydrite, fluorite and/or zeolites, smectite, chlorite, wairakite, prehnite, epidote and mica. Even pyrite, pyrrhotite and magnetite should also be considered for high temperature geothermal systems. If many minerals indicate about the same equilibrium temperature, the average of the equilibrium temperature for the set of these minerals can be regarded as the best estimate of the subsurface temperature. Aqueous speciation programmes are required to calculate values for the respective mineral saturation indices.

One of the advantages of this approach is that it serves to distinguish between equilibrated and non-equilibrated waters. A large range of temperatures is observed for non-equilibrated waters (Fig.10.6), whereas conformity with respect to mineral saturation temperature is generally good for equilibrated waters (Fig. 10.5).

10.4. DISCUSSION ON CHEMICAL GEOTHERMOMETERS

Basic thermodynamic considerations reveal that there are at most two independent variables in multiphase systems of a given composition at equilibrium. This fact may be derived from one of the basic statements of chemical thermodynamics:

$$dG = \left(\frac{\partial G}{\partial T}\right)_{P,n} dT + \left(\frac{\partial G}{\partial P}\right)_{T,n} dP + \left(\frac{\partial G}{\partial n}\right)_{P,T} dn \qquad (10.27)$$

At equilibrium, dG (the Gibbs energy of a system) is zero, and for a system of a given composition at equilibrium, the last term (chemical potential) on the right hand side of Eq. (10.27) is also zero. For such a system, there are only two intensive variables, temperature and pressure. Ideally, one can calculate the values of both temperature and pressure by specifying a value for two equilibrium constants in the system. In fact, any two equilibrium constants, such

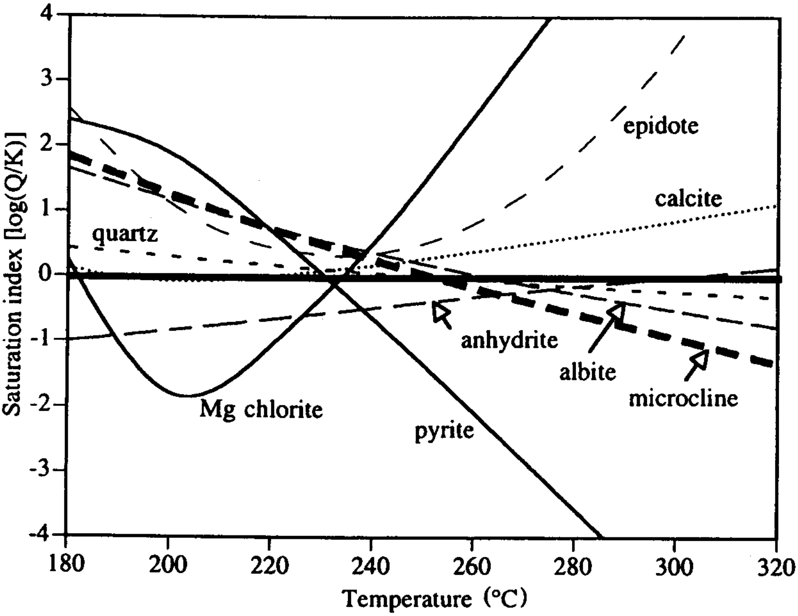

FIG. 10.5. Mineral saturation diagram for well 9 at Krafla, Iceland. It is seen that the aquifer is close to saturation with all the minerals at 230–250°C, except for anhydrite. The aquifer temperature for this well is 230°C.

as equilibrium between quartz and solution and alkali feldspars and solution, can be used.

As already mentioned (Chapter 4), the pressure in the range occurring in geothermal systems has little effect on, at least, most equilibrium constants. Therefore, one equilibrium constant alone can be used to retrieve a value for the only effective intensive variable, temperature.

Probably all geothermal systems are not at overall equilibrium. Some components, such as Cl and B, do not occur in sufficiently high concentrations in the fluid phase to precipitate and form minerals. They only occur in the fluid phase and, therefore, there cannot be equilibrium between phases for these components. Their concentrations in the fluid phase are governed by their sources of supply to that phase.

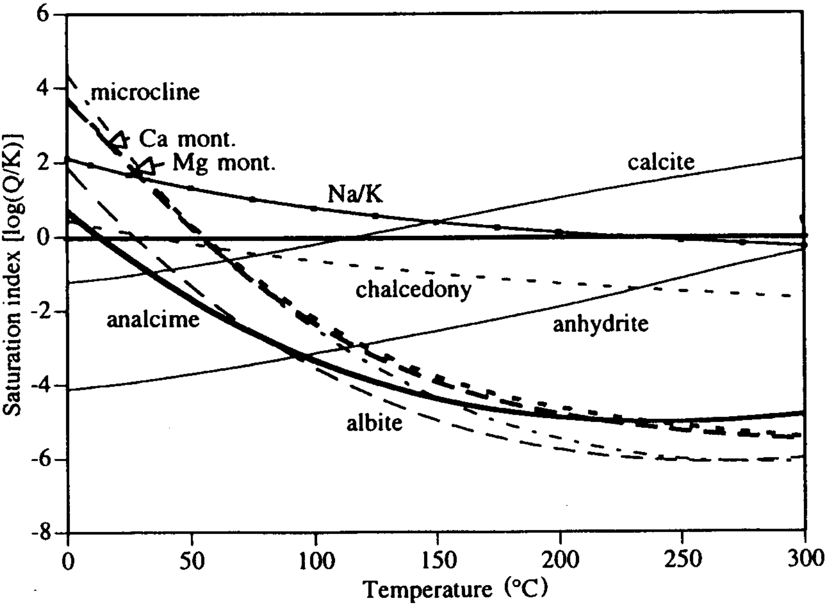

FIG. 10.6. Saturation state of surface water (Svartá river in northern Iceland) with respect to selected common hydrothermal minerals, as indicated. Na/K designates albite–microcline equilibrium. It is seen that equilibrium does not prevail within a narrow range of temperature as is the case with the geothermal water in Fig. 10.5, indicating overall disequilibrium conditions.

Chemical reactions and chemical equilibria involve species activities, not component concentrations. The use of chemical geothermometers based on analysed concentrations of specific components, therefore, involves an approximation that takes activity to be equal to concentration. For the silica and the gas geothermometers, this is a good approximation since the activities of neutral aqueous species ($H_4SiO_4^0$ and gaseous species) do not depart much from unity. It is only for high pH waters (>9 at 25°C) that the analysed silica cannot be taken to represent $[H_4SiO_4^0]$ as discussed in Section 10.1.1.

It is a good approximation to take Na and K concentrations to represent Na^+ and K^+ activities for the Na/K geothermometer, because almost all of both aqueous Na and K occurs as free ions and the activity coefficients of these ions are similar at all temperatures so that

$$\frac{m_{\mathrm{Na}}}{m_{\mathrm{K}}} \approx \frac{[\mathrm{Na}^+]}{[\mathrm{K}^+]} \qquad (10.28)$$

where brackets denote activities. For geothermometers involving divalent ions, the assumption of taking elemental concentrations to represent specific ion activity will produce a larger error. The problem is not circumvented by empirical calibration. Such a calibration must simply be reflected in a larger scatter of the data points when drillhole data of water of different salinities and pH are used for calibration. Salinity affects the relationship between activity and concentration (activity coefficients). Together, these variables affect the ratio between the free ion concentration and element concentration. In other words, at any temperature, salinity and pH affect the relative abundances of the various aqueous species concentrations hosting a particular element.

Geothermometers do not necessarily provide information on maximum temperatures in geothermal reservoirs. At best they indicate the temperature of the source aquifer where equilibrium was last attained. If this source aquifer is shallow, geothermometers will not provide information on deeper, and possibly hotter, regions in the reservoir.

It is sometimes regarded as a fact that equilibrium for specific reactions is always attained in geothermal reservoirs. However, if equilibrium has not been demonstrated, this is not a fact but an assumption. When very high temperatures are indicated as is sometimes the case for gas–gas equilibria involving CO_2, CH_4 and H_2, or $\delta^{13}C$ values in CO_2 and CH_4, to be discussed in the following section, this need not reflect very high temperature in the roots of the geothermal system. It might just as well reflect chemical or isotopic disequilibrium conditions.

10.5 ISOTOPE GEOTHERMOMETERS

Fractionation of the isotopes of light elements between compounds is quite significant and temperature dependent. This has made it possible to use the distribution of the stable isotopes of H, C and O between aqueous and gaseous compounds as geothermometers. Isotopic fractionation factors are generally symbolized by α. The general expression for isotopic fractionation between two compounds, *A* and *B*, is the following:

$$1000 \ln \alpha_{AB} = \delta_A - \delta_B \qquad (10.29)$$

where δ_A and δ_B designate the respective isotopic ratios in compounds A and B, respectively (see Eq. (5.2)).

Four isotopic geothermometers have been developed and quite extensively used. They are based on the following exchange reactions:

$$^{12}CO_2 + {}^{13}CH_4 = {}^{13}CO_2 + {}^{12}CH_4 \qquad (10.30)$$

$$CH_3D + H_2O = HDO + CH_4 \qquad (10.31)$$

$$HD + H_2O = H_2 + HDO \qquad (10.32)$$

$$S^{16}O_4 + H_2{}^{18}O = S^{16}O_3{}^{18}O + H_2{}^{16}O \qquad (10.33)$$

Thus, the first geothermometer is based on $\delta^{13}C$ values in CO_2 and CH_4, the second and third on δ^2H in CH_4 and steam and in H_2 and steam, respectively. The fourth geothermometer uses $\delta^{18}O$ in aqueous SO_4 and liquid water.

The distribution of sulphur isotopes ($\delta^{34}S$) between SO_4 and H_2S has also been used as a geothermometer:

$$^{32}SO_4 + H_2{}^{34}S = {}^{34}SO_4 + H_2{}^{32}S \qquad (10.34)$$

Oxygen isotopes partition strongly between water and CO_2 according to:

$$C^{16}O_2 + H_2{}^{18}O = C^{16}O^{18}O + H_2{}^{16}O \qquad (10.35)$$

The kinetics for this reaction is fast, even at low temperatures, so re-equilibration upon changes in temperature occurs rapidly. For this reason, this isotopic reaction does not constitute a useful geothermometer.

The $\delta^{34}S$ isotope geothermometer (Eq. (10.34)) is applicable to relatively low temperature waters if the residence time of the water exceeds some 500 years. The oxygen isotope geothermometer involving sulphate and water is also useful for predicting subsurface temperatures in systems of quite low temperatures (~100°C). If oxidation of sulphide to sulphate occurs in upflow zones, this geothermometer yields anomalously high temperature estimates.

The three remaining isotope geothermometers are largely useful for high temperature geothermal systems. At times, because of low concentrations of either CH_4 or H_2, or both, it may be difficult though to determine their isotopic ratios.

It is well known that methane concentrations increase substantially in the upflow of some high-temperature geothermal systems in Iceland. Early formed methane will be isotopically very light. For isotopic equilibrium to be closely approached, chemical equilibrium must first be attained followed by redistribution of the isotopes to isotopic equilibrium. The slowest isotopic reaction is that involving the distribution of ^{12}C and ^{13}C between CO_2 and CH_4 (Lyon, 1974).

Oxygen isotopes fractionate considerably between hydrothermal minerals. Accordingly, they could be used as geothermometers to estimate mineral formation temperatures in geothermal systems. This has not been used much in geothermal investigations, probably mainly because it is time consuming and expensive. Among common hydrothermal minerals, the fractionation factor is largest between quartz and magnetite. Quartz is invariably the most ^{18}O enriched mineral and magnetite the most ^{18}O deficient (Becker and Clayton, 1976). The following equation describes well the experimental data on $\delta^{18}O$ in quartz and magnetite in the temperature range of 0–450°C:

$$1000\ln \alpha = 4.80 \times 10^6/T^2 \tag{10.36}$$

where

$$1000\ln \alpha = \delta^{18}O_{(\mathrm{quartz})} - \delta^{18}O_{(\mathrm{magnetite})} \tag{10.37}$$

Unified isotopic equilibria are generally not observed in geothermal systems, i.e. the different isotope geothermometers yield different temperature values. This discrepancy may be due to different rates of re-equilibration as deep geothermal fluids ascend and cool, to gas reactions which either increase or decrease specific gas concentrations and in this way upset isotopic equilibria, or to the fact that isotopic equilibrium has never been attained, at least for some of the reactions.

10.5.1. Carbon dioxide and methane isotope geothermometers

The carbon isotope equilibrium fractionation factors between carbon dioxide and methane at different temperatures have been calculated from spectroscopic data by Bottinga (1969) and Richet et al. (1977). The temperature equation is given in Box 10.6.

Lyon and Hulston (1984) found that the temperature of isotopic equilibrium could be estimated within 2°C over the temperature range 150–500 °C, using the following equation (Eq. (2) in Box 10.6):

$$t(^\circ\mathrm{C}) = \frac{15790}{1000 \ln \alpha + 9.0} - 273 \qquad (10.38)$$

Craig (1963) was the first to use this geothermometer to evaluate temperatures at deep levels in some geothermal fields in the USA. Since then, this isotope geothermometer has been applied in most of the major geothermal fields in the world (e.g. Hulston and McCabe, 1962; Nakai, 1968; Panichi et al., 1979; Lyon and Hulston, 1984; Nuti et al., 1985).

Generally the carbon dioxide–methane isotope geothermometer indicates temperatures which are 50–150°C higher than those encountered in drillholes. This has been taken to indicate that this geothermometer, which responds slowly, reflects temperatures at deeper levels than those penetrated by drillholes.

10.5.2 The methane–hydrogen gas isotope geothermometer

The theoretical temperature equation for the isotopic fractionation for this geothermometer was retrieved by Bottinga (1969) and later by Richet et al. (1977) and is shown by Eq. (3) in Box 10.6. The experimental data of Craig (1975) give a significantly different equation (Box 10.6, Eq. (4)).

Gunter and Musgrave (1971) applied this geothermometer to estimate the underground temperature in the vapour dominated part of the Yellowstone National Park geothermal system. They obtained a value of only 105°C. Lyon (1974) and Craig (1975) estimated subsurface temperatures at Broadlands, New Zealand, and Imperial Valley, California, respectively, using the δ^2H methane–hydrogen geothermometer. Their estimates are 20–40°C higher than the values measured in drillholes in these areas. Panichi et al. (1979) and Nuti et al. (1985) obtained temperatures that are 50°–100°C higher than those encountered in drillholes in the Larderello and Phlegraean fields, again indicating the tendency for these geothermometers to reflect temperatures at deep levels in geothermal systems, or alternatively that equilibrium is not attained for this reaction but only approached from the 'high temperature side'.

10.5.3. Water–hydrogen gas isotopic geothermometer

This geothermometer has been theoretically calibrated by Richet et al. (1977). It is possible to use either measured δ^2H in steam or water in conjunction with the δ^2H in H_2 to calculate the equilibrium temperature value (see Box 10.6).

The hydrogen–water isotope exchange equilibrium constant has not only been calculated on the basis of theoretical considerations but also determined experimentally. This isotope geothermometer appears to be the best among the isotope geothermometers, at least in the sense that it predicts subsurface temperatures actually encountered in deep drillholes. Árnason (1977b) applied this geothermometer extensively to estimate subsurface temperatures in geothermal systems in Iceland. In these systems, which are hosted in basaltic rocks, hydrogen gas occurs in measurable concentrations at aquifer temperatures as low as 130°C. Árnason (1977b) generally obtained temperatures similar to those measured in drillholes, where they were available, but conformity with chemical geothermometers was good in other areas. However, at Reykjanes, a geothermal system characterized by geothermal sea water, he obtained δ^2H hydrogen–water temperatures in excess of 400°C. This result emphasizes that chemical reactions involving the formation of hydrogen gas need to be evaluated when interpreting the results of this isotope geothermometer. At Reykjanes, hydrogen gas concentrations are much lower than those in meteoric water geothermal systems in Iceland and are thought to be controlled by a different mineral buffer (Arnórsson and Gunnlaugsson, 1985).

10.5.4. Sulphate–water oxygen isotope geothermometer

It may not be possible to apply gas isotope geothermometers in some liquid dominated geothermal systems during the exploration phase because of lack of natural gas manifestations. This may also be the case during later drilling development phases because of low concentrations of gases, in particular H_2 and CH_4, in well discharges. In such fields the sulphate–liquid water $\delta^{18}O$ pair may prove very useful. The ^{18}O fraction factor between liquid water and sulphate has been determined experimentally by Lloyd (1968) (Eq. (7) in Box 10.6) and by Mizutani and Rafter (1969) (Eq. (8) in Box 10.6). The discrepancy between these two equations is less than 10°C.

The isotope exchange reaction rate for this pair is regulated by temperature and is inversely proportional to the aquifer water pH. At pH equal to 7, the time required to reach 90% equilibrium is 500 years at 100°C and decreases to two years at 300°C. The range of aquifer pH in most medium and high temperature geothermal systems and the fluid residence time are sufficiently long for close approach to isotopic equilibrium for this geothermometer.

The drawback with the sulphate–liquid water $\delta^{18}O$ isotope geothermometer is that mixing with sulphate bearing shallow groundwaters and oxidation of H_2S may modify the isotopic composition of the dissolved sulphate so that it no longer reflects that of the deep geothermal sulphate. Water isotopic composition may also be affected by evaporation or mixing with shallow ground water.

10.5.5. Sulphate– hydrogen sulphide geothermometer

This geothermometer has only been applied to estimate temperatures in New Zealand geothermal fields. The results obtained were inconsistent, sometimes clearly indicating lack of isotopic equilibrium between the components in question. The temperature dependence of the isotopic distribution, as given by Kusakabe (1974) (Box 10.6, Eq. (9)), needs to be verified experimentally.

10.5.6. Carbon dioxide–water isotopic geothermometer

The theoretical calibration of this geothermometer, as calculated by Richet et al. (1977), is given in Box 10.6, Eqs (10) and (11). This geothermometer yields equilibrium temperatures in the Larderello field, Italy, very similar to those measured at the wellhead, reflecting, as was stated above, the high reaction rate for the respective isotope exchange.

BOX 10.1. TEMPERATURE EQUATIONS FOR THE SILICA GEOTHERMOMETERS

S represents silica concentration as SiO_2 in mg/kg

Geothermometer	Equation (t in °C)	Range (°C)	Source
Quartz	$\frac{1309}{5.19 - \log S} - 273.15$	25–250	Fournier (1977)
Quartz[a]	$\frac{1522}{5.75 - \log S} - 273.15$	25–250	Fournier (1977)
Quartz	$-42.2 + 0.28831S - 3.6686 \times 10^{-4}S^2 + 3.1665 \times 10^{-7}S^3 + 77.034\log S$	25–900	Fournier and Potter (1982)
Quartz[a,b]	$-53.5 + 0.11236S - 0.5559 \times 10^{-4}S^2 + 0.1772 \times 10^{-7}S^3 + 88.390\log S$		Fournier and Potter (1982)
Quartz	$-55.3 + 0.3659S - 5.3954 \times 10^{-4}S^2 + 5.5132 \times 10^{-7}S^3 + 74.360\log S$	0–350	Arnórsson et al. (1988a)
Quartz[a]	$-66.9 + 0.1378S - 4.9727 \times 10^{-5}S^2 + 1.0468 \times 10^{-8}S^3 + 87.841\log S$	0–350	Arnórsson et al. (1988a)
Chalcedony	$\frac{1032}{4.69 - \log S} - 273.15$	0–250	Fournier (1977)
Chalcedony	$\frac{1112}{4.91 - \log S} - 273.15$		Arnoórsson et al. (1983b)
Moganite[c]	$-30.7 + 0.53113S + 1.2578 \times 10^{-4}S^2 - 5.9241 \times 10^{-7}S^3 + 19.576\log S$	0–200	Gíslason et al. (1996)
α-Crisobalite	$\frac{1000}{4.78 - \log S} - 273.15$		Fournier (1977)

BOX 10.1. (cont.)

Geothermometer	Equation (t in °C)	Range (°C)	Source
Opal	$\frac{781}{4.51-\log S}-273.15$	25–250	Fournier (1991)
Amorph. silica	$\frac{731}{4.52-\log S}-273.15$	25–250	Fournier (1977)
Amoorph. silica[d]	$-121.6 + 0.2694S - 1.8101 \times 10^{-4}S^2 + 7.5221 \times 10^{-8}S^3 + 55.114\log S$	0–350	This study

[a] Silica concentrations in water initially in equilibrium with quartz after adiabatic boiling to 100°C.

[b] As presented by Arnórsson (1985).

[c] The present equation was retrieved from the values for the equilibrium constant given by Gíslason et al. (1996).

[d] Based on Gunnarsson and Arnórsson (1998).

BOX 10.2. TEMPERATURE EQUATIONS FOR CATION GEOTHERMOMETERS

Concentrations are in ppm if not otherwise specified.

Geothermometer	Equation (*t* in °C)	Range (°C)	Source
Na-K	$\frac{856}{0.857 + \log(Na/K)} - 273.15$	100–275	Truesdell (1976)
Na-K	$\frac{1217}{1.438 + \log(Na/K)} - 273.15$		Fournier (1979)
Na-K	$\frac{833}{0.780 + \log(Na/K)} - 273.15$		Tonani (1980)
Na-K	$\frac{933}{0.993 + \log(Na/K)} - 273.15$	25–250	Arnórsson et al. (1983b)
Na-K	$\frac{1319}{1.699 + \log(Na/K)} - 273.15$	250–350	Arnórsson et al. (1983b)
Na-K	$\frac{1178}{1.470 + \log(Na/K)} - 273.15$		Nieva and Nieva (1987)
Na-K	$\frac{1390}{1.750 + \log(Na/K)} - 273.15$		Giggenbach et al. (1988)
Na-K[a]	$733.6 - 770.551Y + 378.189Y^2 - 95.753Y^3 + 9.544Y^4$	0–350	Arnórsson et al. (1998)
K-Mg[b]	$\frac{2330}{7.35 + \log(K^2/Mg)} - 273.15$		Fournier (1991)
K-Mg[c]	$\frac{1077}{4.033 + \log(K^2/Mg)} - 273.15$		Fournier (1991)
K-Mg	$\frac{4410}{14.0 + \log(K^2/Mg)} - 273.15$		Giggenbach (1988)

BOX. 10.2. (cont.)

Geothermometer	Equation (t in °C)	Source
Li-Mg	$\frac{2200}{5.470 - \log(\mathrm{Li}/\mathrm{Mg}^{0.5})} - 273.15$	Kharaka and Mariner (1989)
Na-Li	$\frac{1590}{0.779 + \log(\mathrm{Na}/\mathrm{Li})} - 273.15$	Kharaka et al. (1982)
Na-Li[d,e]	$\frac{1000}{0.389 + \log(\mathrm{Na}/\mathrm{Li})} - 273.15$	Fouillac and Michard (1981)
Na-Li[e,f]	$\frac{1195}{0.130 + \log(\mathrm{Na}/\mathrm{Li}^{0.5})} - 273.15$	Fouillac and Michard (1981)
Na-Ca	$\frac{1096.7}{3.08 - \log(\mathrm{Na}/\mathrm{Ca}^{0.5})} - 273.15$	Tonani (1980)
K-Ca	$\frac{1930}{3.861 - \log(\mathrm{K}/\mathrm{Ca}^{0.5})} - 273.15$	Tonani (1980)
Na-K-Ca[g]	$\frac{1647}{\log(\mathrm{Na}/\mathrm{K}) + \beta \log(\mathrm{Ca}^{0.5}/\mathrm{Na}) + 2.24} - 273.15$	Fournier and Truesdell (1973)

[a] Y designates the logarithm of the molal ratio of Na/K.

[b] For log (K^2/Mg) > 1.25.

[c] For log (K^2/Mg) < 1.25.

[d] Valid for Cl concentrations of <0.3 mol/kg.

[e] Concentrations are in mmol/kg.

[f] Valid for Cl concentrations of >0.3 mol/kg.

[g] Concentrations are in mol/kg. $\beta = 4/3$ for $t < 100$°C and 1/3 for $t > 100$°C and for log ($Ca^{0.5}/Na$) < 0.

BOX 10.3. MAGNESIUM CORRECTION TO THE Na–K–Ca GEOTHERMOMETER

In the equations, C_x represents the concentration in ppm of component x:

$$R = \frac{C_{\mathrm{Mg}}}{C_{\mathrm{Mg}} + 0.61C_{\mathrm{Ca}} + 0.31C_{\mathrm{K}}} \times 1000$$

For 1.5 < R < 5, the Mg correction (Δt_{Mg} in °C) is:

$$\Delta t_{\mathrm{Mg}} = -1.03 + 59.971\log R + 145.05(\log R)^2 - 36\,711(\log R)^2/T$$
$$-1.67 \times 10^7 \log \mathrm{T}R/T^2$$

For 5 < R < 50,

$$\Delta t_{\mathrm{Mg}} = 10.66 - 4.7472\log R + 325.87(\log R)^2 - 1.032 \times 10^5(\log R)^2/T$$
$$-1.968 \times 10^7 \log R/T^2 + 1.605 \times 10^7(\log R)^3/T^2$$

We do not apply a Mg correction if Δt is negative or $R < 1.5$.

The above Mg correction is applicable only for waters which have a calculated Na–K–Ca temperature of >70°C.

If R > 50, select the measured spring temperature.

T represents the calculated Na–K–Ca temperature in kelvin.

BOX 10.4. CONSTRUCTION OF THE Na–K–Mg GEOINDICATOR TRIANGULAR DIAGRAM

(1) Select a temperature equation for the Na/K geothermometer (we recommend the equation of Arnórsson et al. (1998a)).

(2) Calculate Na/K ratios at an interval of 25°C from 75° to 350°C. If you choose the geothermometry equation of Arnórsson et al. (1998a), use the following formula to compute the Na/K ratios:

$$\begin{aligned}\log(\mathrm{Na/K}) = &-17.944 - 6427/T^2 + 2095.8/T \\ &- 0.811\times10^{-6}T^2 + 5.482\log T\end{aligned} \qquad (1)$$

where T is in kelvin and Na/K in ppm. Divide the ratio by 10. For example, at 75°C a value of 7.219 is obtained.

(3) Calculate the Na fraction (NaF) for this ratio:

$$\mathrm{Na_F} = \frac{1}{1+\dfrac{1}{(\mathrm{Na/K})\times 10}} = 0.878 \qquad (2)$$

(4) The following $\mathrm{Na_F}$ values were obtained for the selected temperatures: 0.803 (100°C), 0.717 (125°C), 0.627 (150°C), 0.541 (175°C), 0.465 (200°C), 0.399 (225°C), 0.344 (250°C), 0.298 (275°C), 0.260 (300°C), 0.229 (325°C) and 0.203 (350°C).

(5) Treat K/Mg ratios in the same way. By rearranging the K–Mg geothermometry equation of Giggenbach, we obtain:

$$\log(\mathrm{K^2/Mg}) = \frac{-4410}{T} + 14.00 \qquad (3)$$

Again calculate the K fraction (K_F) at 75°C. The $\log(\mathrm{K^2/Mg})$ ratio is −1.333 and from

$$K_F = \frac{1}{1+\dfrac{1}{\mathrm{K/Mg}^{0.5}\times 100}} = 0.044 \qquad (4)$$

BOX. 10.4. (cont.)

Observe that on the Na–K–Mg diagram the relative abundance of potassium and magnesium is expessed as K/Mg$^{0.5}$ and not as K^2/Mg as is done in the geothermometry equation. We have

$$\log(K/\sqrt{Mg}) = \frac{-2205}{T} + 7.00 \qquad (3a)$$

(6) The following K_F values were obtained at the temperatures selected above: 0.110 (100°C), 0.225 (125°C), 0.381 (150°C), 0.546 (175°C), 0.686 (200°C), 0.789 (225°C), 0.859 (250°C), 0.905 (275°C), 0.934 (300°C), 0.954 (325°C) and 0.967 (350°C).

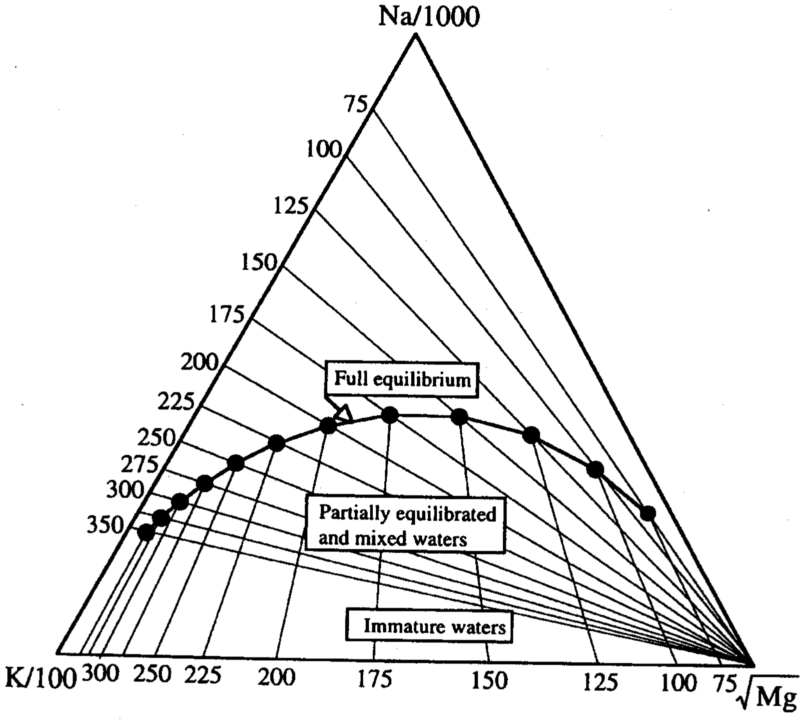

BOX 10.4. (cont.)

(7) Next draw a set of lines of equal Na/K ratios from the Mg apex of the triangle to the calculated respective Na_F values on the Na–K tie line on the triangle.

(8) Draw comparable lines for equal $K/Mg^{0.5}$ ratios. In order not to make the diagram too overcrowded, do not draw these lines all the way to the Na apex but only to the point of intersection with the respective Na–K line of equal temperature.

(9) Calculate the co-ordinates for the point of intersection of lines of equal temperature. We have:

$$\mathrm{Na}_T + \mathrm{K}_T + \mathrm{Mg}_T = 1 \tag{5}$$

where the subscript T indicates the fraction of the respective component on the triangular diagram:

$$\frac{\mathrm{Na}_T}{\mathrm{K}_T} = \frac{f_{\mathrm{NaK}}(T)}{10} \rightarrow \mathrm{Na}_\mathrm{T} = \frac{\mathrm{K}_T f_{\mathrm{NaK}}(T)}{10} \tag{6}$$

$$\frac{\mathrm{K}_T}{\sqrt{\mathrm{Mg}_T}} = \frac{f_{\mathrm{KMg}}(T)}{100} \rightarrow \sqrt{\mathrm{Mg}_T} = \frac{100\mathrm{K}_T}{f_{\mathrm{KMg}}(T)} \tag{7}$$

where $f_{\mathrm{NaK}}(T)$ and $f_{\mathrm{KMg}}(T)$ represent the temperature equations for the Na/K and K/Mg geothermometers, respectively. Inserting Eqs (6) and (7) into Eq. (5) yields:

$$\mathrm{K}_T = \frac{f_{\mathrm{NaK}}(T)}{10} + 1 + \frac{100}{f_{\mathrm{KMg}}(T)} \tag{8}$$

After having obtained a value for K_T, values for Na_T and $\sqrt{Mg_T}$ can be obtained from Eqs (6) and (7).

(10) Finally draw a curve through the points of intersection of equal temperature for Na/K ratios, on the one hand, and $K/Mg^{0.5}$, on the other. This curve represents equilibrium for all three ions, Na, K and Mg, according to reactions (10.9) and (10.24).

BOX 10.4. (cont.)

To use the diagrams, plot your data points into them using the following relationships:

(1) $S = Na/1000 + K/100 + Mg^{0.5}$

(2) $Na_F = Na/1000 \times S$

(3) $Mg_F = Mg^{0.5}/S$

For a population of data points from a particular area, it is possible to deduce with the aid of the Na–K–Mg diagram in this box whether specific samples are (1) immature, (2) partly equilibrated or mixed or (3) fully equilibrated.

BOX 10.5. TEMPERATURE EQUATIONS FOR STEAM (GAS) GEOTHERMOMETERS

(1) The gas geothermometer of D'Amore and Panichi (1980) (concentrations in vol. %):

$$t(^\circ\mathrm{C}) = \frac{24\,775}{2\log(\mathrm{CH_4/CO_2}) - 6\log(\mathrm{H_2/CO_2}) - 3\log(\mathrm{H_2S/CO_2}) + 7\log \mathrm{P(CO_2)} + 36.05} - 273.15 \tag{1}$$

This geothermometer is based on the assumption that CO_2 partial pressures are externally fixed and that equilibrium exists for the following reactions:

$$\mathrm{C + CO_2 + 6H_2 = 2CH_4 + 2H_2O} \tag{2}$$

and

$$\mathrm{CaSO_4 + FeS_2 + 3H_2O + CO_2 = CaCO_3 + \tfrac{1}{3}Fe_3O_4 + 3H_2S + \tfrac{7}{3}O_2} \tag{3}$$

The first reaction involves elemental carbon (graphite) while the second involves anhydrite ($CaSO_4$), pyrite (FeS_2) and magnetite (Fe_3O_4) in addition to the various gases. The temperature dependences of the equilibrium constants for these reactions are described by:

$$\log K_2 = 6.82 + \frac{11\,801}{T} - 7.11 \times \log T \tag{3}$$

and

$$\log K_3 = 23.68 - \frac{62\,220}{T} \tag{4}$$

where the subscripts 2 and 3 refer to the respective equation numbers.

The oxygen partial pressure, which enters Eq. (3), was empirically related to the temperature by

BOX 10.5. (cont.)

$$\log P(O_2) = 8.20 - \frac{23\,643}{T} \qquad (6)$$

In Eqs (4) to (6), the temperature is in kelvin.

The selection of a value for the CO_2 partial pressure was based on the relative amount of CO_2 in the gas phase:

If $CO_2 < 75\% \rightarrow P(CO_2) = 0.1$ (atm)
If $CO_2 > 75\% \rightarrow P(CO_2) = 1$ (atm)
If $CO_2 > 75\%$ and $CH_4 > 2H_2$ and $H_2S > 2H_2 \rightarrow P(CO_2) = 10$ (atm)

The method of selecting the CO_2 partial pressure is rather arbitrary and cannot be expected to fully suit all fields. However, this geothermometer, when applied to fumaroles, yields temperature values for many geothermal reservoirs that match well those encountered in drillholes. Although not attempted by D'Amore and Panichi (1980), values for $P(CO_2)$ may be estimated by a variety of models.

(2) Gas geothermometers of Nehring and D'Amore (1984) (gas concentration in log(mmol/kg)):

Geothermometer		Temperature range	
H_2-CO_2	$(t°C) = 190.3 + 55.97Q_{HC} - 0.14Q_{HC}^2$ where $Q_{HC} = \log H_2 + \frac{1}{2} \log CO_2$	?	(7)
H_2S-CO_2	$(t°C) = 194.3 + 56.44Q_{SC} + 1.53Q_{SC}^2$ where $Q_{SC} = \log H_2S + \frac{1}{6} \log CO_2$	?	(8)

These geothermometers are based the following reactions, respectively:

$$\tfrac{1}{2} C + H_2O = H_2 + \tfrac{1}{2} CO_2 \qquad (9)$$

and

$$\tfrac{1}{2} FeS_2 + \tfrac{1}{6} C + H_2O = \tfrac{1}{6} Fe_3O_4 + \tfrac{1}{6} CO_2 + H_2S \qquad (10)$$

BOX 10.5. (cont.)

(3) Steam geothermometers of Arnórsson and Gunnlaugsson (1985) (gas concentrations are in log(mmol/kg). Q designates the logarithm of the respective gas concentration or gas ratio):

Geothermometer	Temperature equation	Remarks	
CO_2	$t(°C) = -44.1 + 269.25Q - 76.88Q^2 + 9.52Q^3$	All waters	(11)
H_2S	$t(°C) = 246.7 + 44.8Q$	All waters above 300°C	(12)
H_2	$t(°C) = 277.2 + 20.99Q$	and waters in the range	(13)
CO_2/H_2	$t(°C) = 341.7 - 28.57Q$	200–300°C for	(14)
H_2S/H_2	$t(°C) = 304.1 - 39.48Q$	Cl > 500 ppm.	
H_2S	$t(°C) = 173.2 + 65.04Q$	All waters below 200°C	(15)
H_2	$t(°C) = 212.2 + 38.59Q$	and waters in the range	(16)
CO_2/H_2	$t(°C) = 311.7 - 66.72Q$	200–300°C for Cl <500ppm.	(17)

4. Gas geothermometers of Giggenbach (1991) (gas concentrations are in mole per cent):

Geothermometer	Temperature equation	
H_2/Ar	$t(°C) = 70(2.5 + \log(H_2/Ar))$	(18)
CO_2/Ar	$\log(CO_2/Ar) = -0.04 + 0.0277T + 2048/T$ where T is in kelvin.	(19)
CH_4/CO_2	$t(°C) = \dfrac{4625}{10.4 + \log(CH_4/CO_2)} - 273.15$	(20)

The calibration of the H_2/Ar geothermometer is based on the assumption that the ferrous to ferric ratio in the rock fixes the H_2/H_2O fugacity ratio. In addition, Ar concentrations are taken to correspond with that of air saturated water at 25°C.

In calibrating the CO_2/Ar geothermometer, the same reasoning was used for Ar as for the H_2/Ar geothermometer. CO_2 was considered to be buffered by the following reaction:

$$CaAl_2 - \text{silicate} + K - \text{feldspar} + CO_2 = K - \text{mica} + \text{calcite} \qquad (21)$$

BOX 10.5. (cont)

where

$$\log P_{CO_2} = 0.0168t - 3.78 \qquad (22)$$

t is in centigrades.

5. Steam geothermometers of Arnórsson et al. (1998b) (gas concentrations are in mmol/kg):

The temperature equations for these geothermometers are based on thermodynamic data for the following reactions:

$$2Ca_2Al_3Si_3O_{12}(OH) + 2CaCO_3 + 3SiO_2 + 2H_2O$$
$$= 3Ca_2Al_2Si_3O_{10}(OH)_2 + 2CO_{2,aq} \qquad (23)$$
$$FeS_2 + FeS + 2Ca_2Al_2Si_3O_{10}(OH)_2 + 2H_2O$$
$$= 2Ca_2Al_2FeSi_3O_{12}(OH) + 3H_2S_{aq} \qquad (24)$$
$$4FeS + 2Ca_2Al_2Si_3O_{10}(OH)_2 + 2H_2O$$
$$= 2Ca_2Al_2FeSi_3O_{12}(OH) + 2FeS_2 + 3H_{2,aq} \qquad (25)$$

For reservoir waters, the gas geothermometry temperatures according to these reactions are:

Gas	Temperature equation (kelvin)	Temperature range	
CO_2	$\log CO_2 = k_0 + 5.520 - 412.50/T + 0.0144T - 5.029\log T$	(>230°C)	(26)
H_2S	$\log H_2S = k_0 + 16.451 - 3635.08/T + 0.00839T - 6.074\log T$	(>150°C)	(27)
H_2	$\log H_2 = k_0 + 17.266 - 4587.39/T + 0.00547T - 5.356\log T$	(>150°C)	(28)

The value of k_0 is determined by the composition (activity) of the minerals with which the respective gases equilibrate.

Using reaction (23) for temperatures >230°C, drillhole data at lower temperatures and k_0 values as discussed below, the following temperature equation is valid for CO_2:

$$\log CO_2 = 6.236 - 4606.63/T - 0.00537T + 2.386\log T \qquad (>100°C) \qquad (29)$$

BOX 10.5. (cont.)

The values of k_0 in Eqs (26) to (28) were taken by Arnórsson et al. (1998a) to be –0.523 for the CO_2 reaction and +0.104 for the H_2S and H_2 reactions. These values correspond with clinozoisite and epidote activities of 0.3 and 0.7, respectively, but unit activity of all other minerals and water. The following gas geothermometry equations which are valid for gases in steam at atmospheric pressure (100°C) were, thus, obtained:

CO_2 $\quad t(^\circ\mathrm{C}) = 4.724Q^3 - 11.068Q^2 + 72.012Q + 121.8$ (30)

H_2S $\quad t(^\circ\mathrm{C}) = 4.811Q^2 + 66.152Q + 177.6$ (31)

H2 $\quad t(^\circ\mathrm{C}) = 6.630Q^3 + 5.836Q^2 + 56.168Q + 227.1$ (32)

where Q = log mmol/kg of gas.

The above selected epidote and clinozoisite compositions are representative of basaltic rocks. For other mineral compositions, other k_0 values must be selected. With k_0 values selected for a particular geothermal field, the respective log(gas) values can be derived from Eqs (26) to (28) for reservoir waters. By doing this, e.g. at 5°C intervals up to 350°C, the values can be refitted to yield an equation of log(gas) as has been done above.

On the assumption that N_2 and Ar concentrations in geothermal reservoir waters are equal to those in air saturated water at 5°C, the following steam geothermometry equations were obtained from Eqs (26) to (28) by taking their ratio to N_2 and Ar:

CO_2/N_2 $\quad t(^\circ\mathrm{C}) = 1.739Q^3 + 7.599Q^2 + 48.751Q + 173.2$ (33)

H_2S/Ar $\quad t(^\circ\mathrm{C}) = 4.108Q^2 + 42.265Q + 137.6$ (34)

H_2/Ar $\quad t(^\circ\mathrm{C}) = 0.640Q^2 + 43.260Q + 170.0$ (35)

Q represents the logarithm of the respective gas ratio.

BOX 10.6. TEMPERATURE EQUATIONS FOR ISOTOPE GEOTHERMOMETERS

Temperature is in kelvin.

Reaction: $^{12}CO_2 + {}^{13}CH_4 = {}^{13}CO_2 + {}^{12}CH_4$

Temperature equation: $1000\ln \alpha = 15.25 \times 10^3/T + 2.432 \times 10^6/T^2 - 9.56$ (1)

(valid in the range 100–400°C)

$$t(°C) = \frac{15\,790}{1000\ln\alpha + 9.0} - 273 \quad (2)$$

(valid in the range 150–500°C)

Reaction: $CH_3D + H_2 = HD + CH_4$

Temperature equation: $1000\ln \alpha = 288.9 \times 103/T + 31.86 \times 10^6/T^2 - 238.28$

(valid in the range 100–400°C) (3)

and

$1000\ln \alpha = 181.27 \times 10^6/T^2 - 8.95 \times 10^{12}/T^4 - 90.9$ (4)

(valid for $t > 200$°C)

Reaction: $HD + H_2O = H_2 + HDO$

Temperature equation: $1000\ln \alpha = 396.8 \times 10^3/T + 11.76 \times 10^6/T^2 - 217.3$ (5)

(valid in the range 100–400°C for equilibrium between H_2 and steam)

and

$1000\ln \alpha = 396.8 \times 10^3/T + 25.196 \times 10^6/T^2 - 284$

(valid in the range 100–400°C for equilibrium between H_2 and liquid water)

Reaction: $S^{16}O_4 + H_2{}^{18}O = S^{16}O_3{}^{18}O + H_2{}^{16}O$ (7)

Temperature equation: $1000\ln \alpha = 3.25 \times 10^6/T^2 - 5.6$

and

$1000\ln \alpha = 2.88 \times 10^6/T^2 - 4.1$ (8)

(valid in the range 100–350°C)

Reaction: $^{32}SO_4 + H_2{}^{34}S = {}^{34}SO_4 + H_2{}^{32}S$

BOX 10.6. (cont.)

Temperature equation: $1000\ln \alpha = 6.04 \times 10^6/T^2 + 2.6$ (1)

(valid for t >150°C) (9)

Reaction: $C^{16}O_2 + H_2{}^{18}O = C^{16}O^{18}O + H_2{}^{16}O$

Temperature equation: $1000\ln \alpha = 7.849 \times 10^3/T + 2.941 \times 10^6/T^2 - 887.$ (10)

(valid in the range 100–400°C for equilibrium between CO_2 and steam)

and

$1000\ln \alpha = -18.29 \times 10^3/T + 7.626 \times 10^6/T^2 + 19.6$ (11)

(valid in the range 100–400°C for equilibrium between CO_2 and water)

11. MIXING PROCESS IN UPFLOW ZONES AND MIXING MODELS

Stefán Arnórsson

11.1. MIXING PROCESSES

The use of chemical and isotopic geothermometers to estimate subsurface temperatures from the composition of surface discharges is based on the notion that geothermal fluids may cool in upflow zones either conductively or by boiling due to depressurization, or by both processes. However, hot waters ascending from a geothermal reservoir may also cool by mixing in the upflow with shallow, relatively cold water. When this is the case geothermometers may yield misleading results.

Mixing of geothermal water with cold water may occur after a variable amount of conductive cooling of the hot water and before, during or after boiling. Mixing is most prone to occur where there is a change of permeability. Drillings have shown that the pressure potential in the upflow of many geothermal systems is lower than in the enveloping cold groundwater body. When this is the case, cold groundwater tends to enter the geothermal system and mix with the rising hot water. At the boundaries of geothermal systems where hot and cold waters meet, local mixing brings about mineral deposition that reduces permeability and seals off the hot and cold groundwater systems. This seal impedes incursion of cold water into the geothermal system, thus reducing the likelihood of mixing.

Since cold waters are most often lower in dissolved solids than geothermal waters, mixing is often referred to as dilution. Large variations in the temperature and flow rates of thermal springs in a particular field that can be linked with parallel variations in the concentrations of non-reactive components in the water, such as Cl (see Chapter 4), usually constitute the best evidence that mixing has occurred.

Local cold waters frequently differ in their δ^2H and $\delta^{18}O$ content from geothermal waters. This tends to be the case for δ^2H when the geothermal water originates as precipitation in a distant recharge area. The $\delta^{18}O$ content of geothermal waters is often displaced from the meteoric line towards higher values (less negative) as a result of exchange of ^{18}O between water and rock, but all common rock types are richer in ^{18}O than natural waters. The magnitude of the oxygen shift depends on the extent of the water–rock interaction. There appears to be a crude relationship between the temperature of geothermal waters and their ^{18}O shift. Generally, increasing temperatures enhance chemical reaction rates including reactions involving water and rock, thus increasing the ^{18}O isotope shift. Mixing of geothermal water with local cold water may manifest itself in a linear relationship between the δ values for ^{2}H and ^{18}O or between these values and the aqueous concentrations of conservative elements such as Cl.

Mixing,such as conductive cooling and boiling, can upset chemical equilibria between water and rock minerals, thus causing a tendency for the water to change composition after mixing with respect to reactive chemical components. On the other hand, the concentrations of non-reactive components in mixed waters are determined by their content in the hot and cold water components in that mixture and their relative proportions.

Geothermal systems often coincide with permeability anomalies and are often located in fractured rocks. As a result, the permeability of their host rock may be highly anisotropic. Anisotropy in permeability has important implications for mixing processes. Waters emerging in springs or discharging from drillholes and derived from a system with anisotopic permeability are inevitably a mixture of many water components that have originated in different places and travelled through different distances to the spring or well. In addition, the time for travel has differed among these components. Any schematic two dimensional sketch of water flow from a recharge area to a geothermal system with a single major upflow or mixing at a specific point must at best be a gross simplification. Only when groundwater advection in aquifers is driven by hydraulic head can overpressure be expected to prevail throughout the advective aquifer. Such an overpressure will, of course, impede mixing with water from the adjacent rock for that part of the hot water that issues from fractures to form natural springs.

In the present context, mixing of geothermal and cold water and the application of the mixing model to estimate subsurface temperatures in geothermal systems refers to mixing of two components of quite different compositions in such a way that the concentrations of reactive components do not change much after mixing has occurred. Mixing of this kind is likely to be confined to upflow zones. Mixing at deep levels in geothermal reservoirs is likely to be completely masked for reactive constituents through re-equilibration of these constituents subsequent to mixing, in which case application of geothermometers is appropriate to estimating subsurface temperatures rather than the mixing models discussed below.

11.2. MIXING MODELS

Mixing models have been developed to allow estimation of the hot water component in mixed waters emerging in springs or discharged from shallow drillholes. There are essentially three kinds of mixing model:

(1) The chloride–enthalpy mixing model;
(2) The silica–enthalpy warm spring mixing model;
(3) The silica–carbonate mixing model.

The first model has probably been most widely used.

When applying mixing models to estimating subsurface temperatures, several simplifying assumptions are made. Conservation of mass and heat is always assumed, both during and after mixing. Thus, it is assumed that chemical reactions occurring after mixing are insignificant and do not modify the water composition.

It is necessary to establish that the sampled and analysed waters are truly mixed before applying mixing models to estimate reservoir temperatures. Assuming mixing for unmixed waters and applying mixing models can yield erroneous results which are generally too high.

Recognition of mixed water on the basis of the chemical composition of a single sample is generally not convincing. A much stronger case is made for mixing of hot and cold water in the upflow zone of a particular geothermal system, when the mixing process can be identified and quantified by consideration of samples from many springs and surface waters. Linear relationships between the concentrations of conservative components, such as between Cl and B or Cl and δ^2H, are generally considered to constitute the best evidence for mixing. A linear relationship between Cl and $\delta^{18}O$ has also proved to be useful in cases where hot waters show a significant oxygen shift. In the last two examples mentioned, $\delta^{18}O$ is used as a conservative component. A near linear relationship between chloride and silica has been observed for variably mixed waters in some geothermal fields. Such a relationship implies that silica behaves as a conservative component after mixing. In other words, the mixed water neither precipitates silica nor dissolves it from the rock to any extent. Such a behaviour for silica is indeed assumed when using the silica–enthalpy warm spring and the silica–carbonate mixing models. Conservative behaviour of silica is also assumed when quartz equilibrium temperatures are used to create a chloride–enthalpy mixing model.

When initially developed, mixing models were aimed at estimating subsurface temperatures in geothermal reservoirs on the basis of the chemical composition of spring discharges. However, mixing models, at least the chloride–enthalpy mixing model, have also been applied to well discharges. It is considered questionable to use such data to estimate the temperature of a hot water component in geothermal reservoirs, certainly in the case of deep wells. For boiling reservoirs this is not logical. Here, pressure, i.e. depth within the system, determines the temperature.

Waters of high temperature (>200°C) are generally relatively rich in carbon dioxide. When cold water mixes with such waters to such an extent that boiling does not occur, the mixture becomes acid. The reason is that the dissociation of carbonic acid (dissolved carbon dioxide) increases with temperature decreasing below about 200°C. Acid waters high in dissolved carbon dioxide are likely to be far removed from equilibrium with both primary and secondary rock forming minerals and, as a result, quite reactive. The protons added to the water through the mixing process stimulate dissolution of many minerals, resulting in a drastic change in the relative concentrations of the major cations, or give rise to a transition from their initial equilibrium distribution in the hot water component of the mixture to a distribution approaching that dictated by stoichiometric dissolution of the rock. Thus, potassium, calcium and, especially, magnesium tend to increase relative to sodium. The result is an increase in Na/K geothermometry temperature and a decrease in Na–K–Ca temperature. Silica concentrations may increase when the dilution effect of mixing is slight. This is due to enhanced dissolution of silica from the rock by the mixed acid water. It is, thus, clear that mixing processes do not invalidate the use of solute geothermometers only through dilution but also through water–rock interaction due to the relatively reactive characteristics of the mixed water.

Mixing of boiled geothermal water with cold groundwater does not produce acid and chemically reactive mixed water because such hot water has lost most of its dissolved carbon dioxide. It is, therefore, to be expected that mixed water that contains a boiled hot water component will not change much in composition by reactions with the rock subsequent to mixing, at least compared with unboiled waters.

It may not be safe to assume that variations in Cl concentrations in geothermal reservoirs, certainly if they are large, are due to mixing of two components in variable proportions of different Cl concentration. The variations may be due to variable supply of Cl to the water in different parts of the reservoir, whether its source is the rock with which the water has interacted or a gas phase

TABLE 11.1. DATA USED IN BOXES 11.1 TO 11.3 TO ESTIMATE SUBSURFACE TEMPERATURES BY THE CHLORIDE–ENTHALPY, SILICA–ENTHALPY WARM SPRING AND SILICA–CARBONATE MIXING MODELS. CONCENTRATIONS IN ppm.

Temperature (°C)	SiO_2	Na	K	CO_2	Cl	t_{qtz}	$t_{Na\text{-}K}$	Enthalpy[a] (kJ/kg)
94	210.2	263.0	11.6	200.5	106.2	174	131	737
82	258.4	252.6	35.3	307.0	280.3	190	218	343
94	207.1	363.6	17.3	534.7	11.4	173	135	732
45	160.6	151.6	14.0	192.0	99.1	155	181	188
95	271.8	413.9	16.1	416.0	68.7	194	124	825
94	145.4	208.2	9.0	149.8	68.6	149	160	628
94	299.1	291.9	15.1	264.4	38.3	203	140	866
59	186.0	65.4	13.0	51.8	153.4	165	255	247
24	81.8	57.6	8.7	79.3	19.9	115	225	101
58	165.5	70.8	14.5	49.8	183.9	157	259	243
10	36.9	17.9	3.5	13.6	56.3	75	253	42
45	173.1	61.7	13.4	45.0	127.1	160	266	188
93	265.4	278.9	13.6	280.3	52.3	192	137	816
96	297.3	273.4	22.6	274.6	24.5	202	172	861

[a] Based on the quartz equilibrium temperature for boiling hot springs (temperature ≥ 93°C) but on measured temperature for sub-boiling springs. The Na/K geothermometry temperatures tend to be highest for warm springs. It is assumed that the Na/K ratios in warm waters are determined by the ratio in which Na and K are dissolved from the rock and not by equilibration with secondary Na and K feldspars. Therefore, the Na/K geothermometer does not yield realistic values for these waters. For boiling hot springs, the quartz geothermometer gives higher temperatures than the Na/K geothermometer. All this is brought up here to emphasize that it is by no means a straightforward procedure to estimate the enthalpy of mixed waters and the selection can very significantly affect the resulting estimation of the temperatures of the hot water component. Experience indicates that, for dilute waters such as those at Landmannalaugar, re-equilibration in upflow zones with feldspars is more rapid than with quartz. Thus, the quartz geothermometer is preferred to the Na/K geothermometer in estimating the temperature (and enthalpy) of mixed water. Both geothermometers tend to yield unreliable results for warm waters because of lack of equilibration. Measured temperatures are considered to be the best choice for determining the enthalpy of such waters.

escaping from a magma heat source. To postulate mixing without, at least, envisaging a specific hydrological model for flow is not logical. When applying mixing models to hot spring discharges, it is generally not difficult to depict a hydrological model involving incursion of cold water into hot water aquifers due to the lower pressure of the latter.

When applying the chloride–enthalpy mixing model to mixing of two relatively hot components, difficulties rise in reliably estimating the enthalpy of the mixed fluid. Re-equilibration with respect to chemical geothermometers occurs rapidly at high temperatures and the water enthalpy indicated by the geothermometers is likely to be the actual enthalpy of that water rather than the enthalpy of the mixture. The geothermometry components cannot be taken to act as conservative at high temperatures during and after mixing.

Boxes 11.1 to 11.3 demonstrate how to construct the three kinds of mixing model and how to estimate the temperature of the hot water component in variably mixed waters. Data from the Landmannalaugar field in Iceland (Table 11.1), which is located in silicic volcanics, have been used for this demonstration.

BOX 11.1. THE CHLORIDE–ENTHALPY MIXING MODEL

The chloride–enthalpy mixing model allows estimation of the temperature of the hot water component in geothermal fluids from data on the composition of waters that have mixed and/or boiled to a variable extent. The diagram for the chloride–enthalpy mixing model is conveniently constructed as follows:

(1) Draw up enthalpy on the Y axis with 0 at the bottom and 1500 or 2000 kJ/kg at the top. Have Cl concentrations on the X axis equal to zero in the left corner. The highest Cl value should be somewhat higher than the highest Cl concentration measured in the hot spring waters.
(2) The next step is to select enthalpy values for individual samples. For boiling hot springs, it is common to use a geothermometer to estimate subsurface temperatures for each water sample. It is common to use both the quartz and Na/K geothermometers for this purpose. Subsequently, with the aid of steam tables, look up the enthalpy of liquid water at that temperature and use that value (see Box 12.1). It is best to use measured temperatures for cold waters and also for slightly thermal springs with high flow rates. It is not possible to give any general rules for the selection of temperature (and enthalpy) to be used in this model.
(3) When the enthalpy values have been estimated for individual samples, plot the data points on the diagram.
(4) Next draw a line between two points, one that has zero chloride and an enthalpy corresponding to that of saturated steam at 100°C (2676 kJ/kg), and the other one that will give the line with the least negative slope possible (the point with the highest chloride concentration relative to its enthalpy).
(5) Then draw two other lines, both originating at the points corresponding to local cold water in the area with slopes such that they form a triangle with the first line encompassing all the data points. The enthalpy of the parent hot water corresponds with the apex of the triangle. The temperature can be found with the aid of steam tables (see also Box 12.1), taking the enthalpy to be that of steam saturated water.

BOX 11.1. (cont.)

The upper line with positive slope and going through the local cold water point corresponds to waters that constitute a mixture of the parent hot water and the cold water. The lower line with positive slope corresponds to water that has boiled the most before mixing with cold water. Points falling within the triangle can be explained by a variable combination of boiling and mixing.

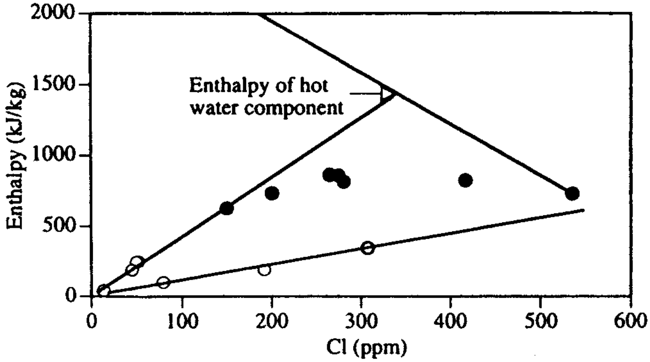

Enthalpy-chloride diagram for geothermal spring waters in the Landmannalaugar field, Iceland. For data points represented by dots (boiling springs) the enthalpy was estimated by the quartz geothermometer. For data points represented by circles measured temperature was used (warm springs) to obtain a value for the enthalpy. The enthalpy of the deep water component is estimated to be 1450 kJ/kg and its temperature 318°C.

BOX 11.2. SILICA–ENTHALPY WARM SPRING MIXING MODEL

This model handles non-boiled and boiled mixed waters separately, but not simultaneously like the the chloride–enthalpy mixing model.

(1) Choosing enthalpy as the X axis and aqueous silica concentration as the Y axis, draw up the solubility curve for quartz using the following quartz geothermometry equation:

$$t(°C) = -55.3 + 0.3659S - 5.3954 \times 10^{-4}S^2 + 5.5132 \times 10^{-7}S^3 + 74.360\log S$$

where S represents SiO_2 in ppm. Then convert temperature into enthalpy of liquid water, using the following equation:

$$h_{liquid} = 35.93 + 3.6053t + 2.3838 \times 10^{-3}t + 7.1004\exp(0.04t)$$

where h_{liquid} represents the enthalpy of liquid water in kJ/kg and t is the temperature in °C. Also convert values for measured temperatures of springs into liquid water enthalpy values.

(2) Plot the data points into the diagram. Draw a line through the data points and extrapolate it until it intersects the quartz solubility curve. The point of intersection represents the enthalpy of the hot water component in the mixture. As before, its temperature can be retrieved from steam tables.

It may be considered appropriate to assume that the hot water has boiled before mixing if the mixed water is low in carbonate, which is an indication of its degassing. When this is the case the line fitted through the data points is extrapolated to 100°C (419 J/mole), and from this point a horizontal line is drawn to the curve which represents quartz solubility corrected for steam loss by adiabatic boiling to 100°C (atmospheric pressure). The equation describing quartz solubility corrected for steam loss by adiabatic boiling to 100°C is given by:

$$t(°C) = -66.9 + 0.1378S - 4.9727 \times 10^{-5}S^2 + 1.0468 \times 10^{-8}S^3 + 87.841\log S$$

BOX 11.2. (cont.)

It is sometimes observed that the extrapolated line for non-boiled springs does not intersect the solubility curve (as in the diagram below). There may be two reasons for this. One is that the warm spring waters have cooled conductively without loosing silica, thus shifting the data points to the left on the diagram, making the line describing the silica–enthalpy relationship too steep. The other possibility is that the waters have boiled before mixing. If the waters are low in gas and have a relatively high pH (>8), they have, in all likelihood, boiled. If, on the other hand, they are gaseous with a relatively low pH (<7–8), they have most likely not boiled. If boiling is indicated, it is necessary to use the quartz solubility curve that takes into account steam loss by adiabatic boiling to 100°C.

Removal of silica from solution by precipitation of quartz has the opposite effect of conductive cooling after mixing. It tends to yield low temperature estimates for the hot water component. Dissolution of silica from the rock may, on the other hand, occur after mixing and lead to high estimates of subsurface temperatures.

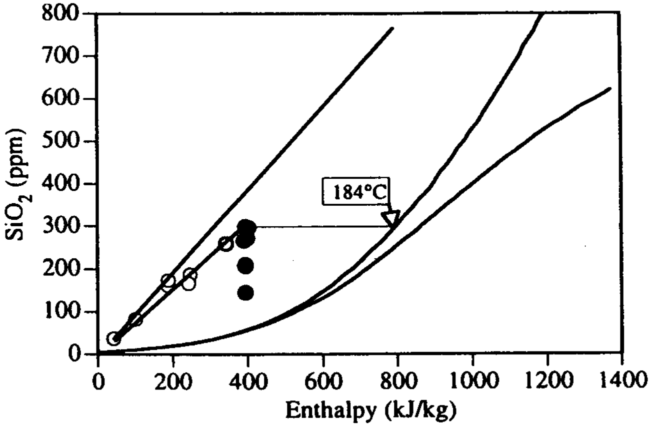

Silica–enthalpy warm spring mixing model. Data from Landmannalaugar. Dots: boiling hot springs; circles: warm springs rich in carbonate and, therefore, not degassed. If mixing occurs after boiling, the boiling hot spring waters indicate an enthalpy of 780 kJ/kg for the hot water component (184°C). A solution is not obtained for the non-boiled warm spring model (upper line) as there is no intersection between this line and the quartz solubility curve. Evidently, the reason is conductive cooling of the water before or after mixing.

BOX 11.3. THE SILICA–CARBONATE MIXING MODEL

This mixing model is based on the relationship between silica and total carbonate observed in many drilled geothermal reservoirs. It is further based on the assumption that practically all the silica in geothermal reservoir waters occurs as H_4SiO_4 and practically all the carbonate carbon as CO_2. This model not only serves to estimate the temperature of the hot water component in mixed waters but also to distinguish boiled and non-boiled waters. The diagram is constructed as follows:

(1) Use the temperature equations given below to draw a curve showing the relationship between silica (H_4SiO_4) and carbonate (CO_2) with silica on the Y axis:

$$SiO_2 = -15.433 - 151.60/T - 2.977 \times 10^{-6}T^2 + 5.464\log T$$
$$CO_2 = -1.09 - 3894.55/T + 2.532\log T$$

SiO_2 and CO_2 concentrations are in log moles while T is in kelvin.

(2) First select the temperature, e.g. at 25°C intervals from 0 to 300°C, then calculate the respective concentrations and convert them to ppm. Subsequently, draw up the curve where a particular SiO_2 value has a corresponding CO_2 value at each temperature.

(3) Plot your data points on the graph. Points plotted above the curve represent boiled, i.e. degassed, waters whereas points below the curve correspond to undegassed waters.

(4) Draw a line from a point corresponding to the silica and carbonate content of cold water through the data points for mixed unboiled waters. Extrapolate the line to find the point of intersection with the silica–carbonate curve. This point corresponds to the silica and carbonate content of the hot water component in the mixture.

(5) Use a geothermometry equation for quartz (see Box 10.1) to calculate the temperature of the hot water component.

BOX 11.3. (cont.)

Removal of silica from solution after mixing leads to high estimates for the temperature of the hot water component. Partial degassing or removal of carbonate (by calcite precipitation) from the water has the opposite effect.

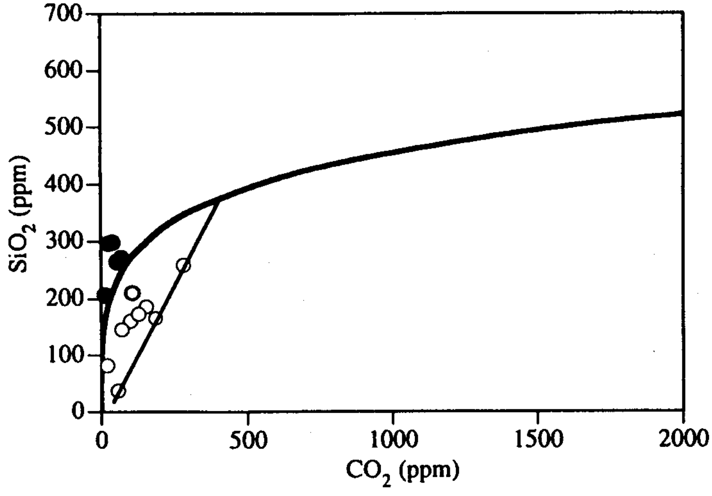

Plot of silica versus carbonate for thermal springs at Landmannalaugar, Iceland. Circles: Non-boiled water; dots: boiled and, therefore, degassed waters. The intersection of the line and curve gives the silica and carbonate concentration in the hot water component. For silica the value is about 380 ppm, which corresponds to 227°C.

12. ASSESSMENT OF RESERVOIR FLUID COMPOSITION FROM WET STEAM WELL DATA

Stefán Arnórsson

Wet steam wells discharge a mixture of water and steam. To calculate the chemical composition of the total well discharge it is necessary to collect samples of both water and steam at a measured separation pressure and calculate the water/steam ratio of the discharge from knowledge of the well discharge enthalpy. The total well discharge composition may or may not correspond to the composition of the initial reservoir fluid as discussed in this chapter.

For wells discharging only liquid water, hot or cold, it is obvious that the water discharged is representative of the aquifer or reservoir water. Cooling of the water though could bring about changes in the state of saturation of the water with respect to minerals. As a result, precipitation or dissolution of minerals could induce changes in the water composition. Reaction with the casing and pipe material could also occur. The situation is more complex with wet steam wells. Pressure drop created around producing wells leads to extensive boiling of the water in the aquifer. In the process the major part of the gases present in the undisturbed aquifer water are transferred to the steam phase. Solutes in the boiled water increase in concentration in proportion to the amount of steam formed.

The simplest case for assessing the total discharge composition of wet steam wells occurs when the level of first boiling is within the well. This means that only liquid water exists in the aquifer, even under producing conditions. In this case, it is reasonable to assume that both mass and heat of the fluid ascending in the well are conserved. Accordingly, the heat content of the total well discharge and its composition are the same as those of the water entering the well. In terms of thermodynamics, the well is regarded as an isolated system. For conservation of heat (enthalpy) we have

$$h^d = h^s_1 Y_1 + h^w_1(1 - Y_1) \qquad (12.1)$$

and for the mass of component i

$$m^d_{i,1} = m^s_{i,1} Y_1 + m^w_{i,1}(1 - Y_1) \qquad (12.2)$$

In Eq. (12.1), h^d stands for the enthalpy of the water entering the well, i.e. the total enthalpy of the system. h^s_1 and h^w_1 represent the enthalpy of steam and water, respectively, at a particular pressure P_1. Y_1 is the steam fraction at that pressure (and $1 - Y_1$ the water fraction). The super- and subscripts in Eq. (12.2) have the same meaning as in Eq. (12.1).

The enthalpy of saturated steam (steam in equilibrium with water) is equal to the enthalpy of boiling water plus its latent heat of vaporization (L), or

$$h_1^s = h_1^w + L_1 \tag{12.3}$$

Inserting the right hand side of Eq. (12.3) into Eq. (12.1) and rearranging yields

$$Y_1 = \frac{(h^d - h_1^w)}{L_1} \tag{12.1a}$$

After boiling has set in, the enthalpy of the aquifer water rising in the well splits between the two phases, the boiled water and the steam. The fraction of steam present at each point depends on the pressure. Consider, e.g., water at 250°C rising in a well. The enthalpy of this water is 1088 $\mathrm{kJ \cdot kg^{-1}}$ as can be deduced from the respective equation in Box 12.1. Consider that we want to operate a well at 6 bar abs. pressure. How can we calculate the steam fraction at this pressure? Look at the respective equations in Box 12.1 to obtain values for the enthalpy of liquid water and its latent heat of vaporization at a steam pressure of 6 bar abs. The values are 675 $\mathrm{kJ \cdot kg^{-1}}$ and 2085 $\mathrm{kJ \cdot kg^{-1}}$, respectively. By inserting all the enthalpy values into Eq. (12.1a) one obtains a value of 0.198 for the steam fraction Y_1.

Well discharge enthalpy can be measured by a variety of methods (Box 12.2) to yield a value for h^d. In the case discussed above for the level of first boiling in the well, it can simply be calculated from measurement of the temperature in the well below the level of first boiling. Having obtained a value for Y at a pressure corresponding to the sampling pressure of a particular sample, we are now in a position to calculate the concentrations of all chemical components in the aquifer water from analysis of steam and water samples, with the aid of Eq. (12.2). It is customary not to analyse components of dissolved solids in the steam phase nor of most gas components in water samples, in which case $m_{i,1}^s$ or $m_{i,1}^w$ in Eq. (12.2) are taken to be zero, respectively. For solute species, this equation reduces to

$$m_{i,1}^d = m_{i,1}^w(1 - Y_1) \tag{12.2a}$$

and for gaseous species, which are only analysed for in the steam phase, we have

$$m_{i,1}^{d} = m_{i,1}^{s} Y_1 \tag{12.2b}$$

Generally, all ionic components (Na, K, Ca, Mg, SO_4, Cl and F, and many trace components) as well as silica and boron are only analysed in the water sample. Non-condensable gases of low solubility in water (H_2, CH_4, O_2, N_2, Ar and others) are conventionally only determined in the steam sample. The only chemical components routinely determined in both water and steam samples are carbonate carbon, sulphide sulphur and ammonia. Deuterium and ^{18}O are sometimes determined in both phases, but sometimes only in one, either in the steam or in the water. When these isotopes are analysed only in one phase their concentration is calculated in the other phase from the known value of the fractionation coefficient, on the assumption that equilibrium is attained for these two isotopes between the water and steam phases. Such an assumption is apparently quite safe. However, it is always wiser to collect both phases, at least once for each well, in order to establish that equilibrium prevails.

Boiling by pressure drop in an isolated system leads to cooling. The water cools as it boils and at the same time makes heat available for vaporization. Cooling by boiling in wells may be very extensive, amounting to over 100°C. This cooling and changes in the chemical composition of the water associated with its degassing and steam formation can turn water initially at equilibrium strongly supersaturated with some minerals but undersaturated with others. When supersaturation results, the respective minerals tend to deposit from solution. The amount of deposition depends on the degree of supersaturation produced, the reaction rate and the initial composition of the water. Some minerals may not precipitate at all despite a high degree of supersaturation because of sluggish kinetics, as is the case with quartz. Calcite, on the other hand, deposits readily from supersaturated solution. If, at least, one of the components forming a mineral occurs in low concentration in the water, the quantity of the mineral deposited will be small and limited by the availability of the least abundant component forming that mineral. The concentrations of the low abundance component may change much between reservoir and surface, whereas the concentrations of the abundant components is least affected. This should always be borne in mind when interpreting data on trace elements in fluids from wet steam wells.

When boiling starts in the producing aquifer(s) of wells, it is sometimes more complex to calculate reservoir fluid compositions than when the first level of boiling is in the well. In considering initiation of boiling in the aquifer it becomes necessary to define precisely some terms frequently used in geothermics, such as aquifer temperature, aquifer fluid and reservoir fluid, aquifer/reservoir steam and aquifer/reservoir water.

Well measurements in many geothermal fields worldwide have shown that temperatures follow the boiling point curve with depth. Pressure measurements have shown that liquid water is continuous in most reservoirs, indicating that the steam phase must be discontinuous and constitutes only a very small fraction of the total fluid mass, even a small fraction in terms of volume. Production from 'boiling aquifers' enhances boiling by pressure drop. Enhanced boiling in producing aquifers is sometimes described as extensive boiling, which is to be contrasted with much more limited boiling under natural or undisturbed conditions. In other reservoirs, downhole pressures change little with depth, showing that the fluid volume is largely steam. Such reservoirs are said to be vapour dominated. Liquid water though is present in these reservoirs.

Extensive boiling in producing aquifers of liquid dominated reservoirs causes cooling of the flowing fluid. The extent of the zone of extensive boiling depends on:

(1) the permeability of the aquifer;
(2) the rate of mass withdrawn from the well;
(3) the length of time the well has been discharging;
(4) recharge into the aquifer.

The terms aquifer/reservoir water and aquifer/reservoir steam, as used here, correspond to the water and steam in the aquifer beyond the zone of depressurization around wells. The same applies to the term aquifer/reservoir fluid. Aquifer temperature is the temperature in the aquifer, or better the producing horizon, beyond the zone of depressurization. The term reservoir temperature is discouraged here. Geothermal reservoirs generally do not have uniform temperatures, like any large systems in nature. Temperatures vary across geothermal reservoirs.

When extensive boiling occurs in the producing aquifers of wells some of them have liquid enthalpy (the discharge enthalpy is the same as that of steam saturated water at the aquifer temperature), whereas others develop 'excess' enthalpy, i.e. the steam to water ratio in the discharge is higher than can be produced by pressure drop of the initial aquifer fluid.

As long as the well discharge enthalpy is close to that of water at the aquifer temperature, it is satisfactory to calculate the aquifer water composition with the aid of Eqs (12.1a) and (12.2) (see also Eqs. (12.2a) and (12.2b)). This is not, however, the case with 'excess' enthalpy wells. The method chosen to compute aquifer fluid compositions from analysis of water and steam samples collected at the wellhead depends on the model selected to explain the cause of the excess discharge enthalpy. As discussed in Chapter 15, there are essentially two processes that can lead to increased steam to water ratios of wet steam well discharges. One is flow of heat from the rock to the boiling water that flows through the zone of depressurization to the well. The other process is phase segregation: the steam flows into the well but the water is partly or totally retained in the aquifer. If the first process accounts for the 'excess' discharge enthalpy, the total discharge will be representative of the aquifer fluid. If, on the other hand, phase segregation has occurred, the discharge from the well differs compositionally from the reservoir fluid.

A simple method exists by which the importance of the two processes can be qualitatively assessed if chemical data are available for a well which has displayed variation in discharge enthalpy. It involves plotting the concentrations of an aqueous and a gaseous component against discharge enthalpy in (1) the total discharge and (2) the water phase for the aqueous component and in the steam phase for the gaseous component. Such plots are shown in Figs 12.1 and 12.2.

Phase segregation, if it occurs at a temperature close to the sampling temperature, will not affect the concentrations of solutes in the water phase and gases in the steam phase. Consequently, phase segregation will cause the aqueous solute concentrations to decrease but gas concentrations to increase in the total discharge (Fig. 12.1). If, on the other hand, the concentrations of both components remain constant in the total discharge despite changes in the discharge enthalpy, the cause of the 'excess' enthalpy is heat flow from the rock, not phase segregation, and the total well discharge chemical composition represents the reservoir fluid composition (Fig. 12.2). When the concentrations of chemical components in the total discharge of wells are not affected by changes in discharge enthalpy, the concentration of a solute in the aqueous phase will increase with rising discharge enthalpy, particularly when the discharge is approaching dry steam. On the other hand, the concentration of a gaseous component in the steam will decrease. This is demonstrated in Fig. 12.2.

Figure 12.3 depicts results for the sodium and hydrogen sulphide content of water and steam discharged from well 6 at Nesjavellir in Iceland. When initially discharged, the well had liquid enthalpy. It rose relatively rapidly in one

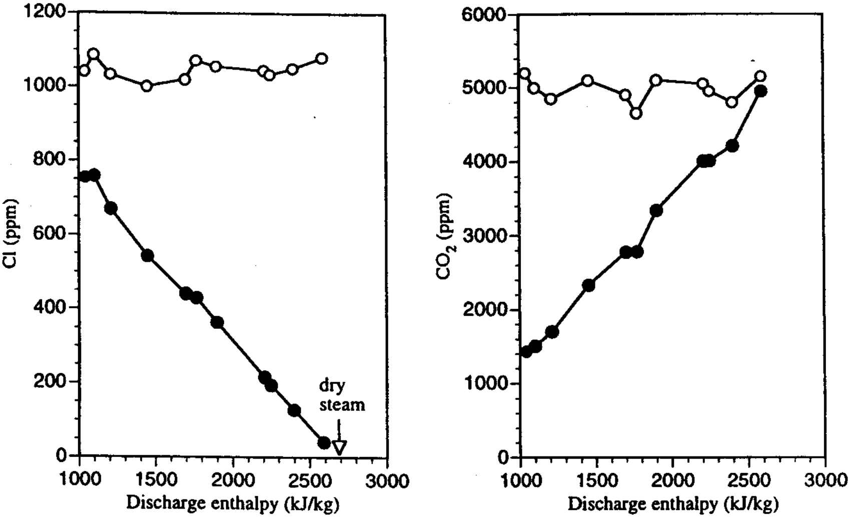

FIG. 12.1. Hypothetical example of chloride and carbon dioxide concentrations in water and steam samples collected from a wet steam well at atmospheric pressure (circles) and in the total discharge (dots) plotted against discharge enthalpy. The relationship indicates that the 'express' discharge enthalpy is produced by phase segregation in the aquifer.

week to about 2000 kJ·kg^{-1}, thereafter decreased to about 1800 kJ·kg^{-1} and then increased again to 2500 kJ·kg^{-1} after about four years of discharge (Fig. 12.4). As can be seen from Fig. 12.3, Na concentrations decrease in the total discharge with increasing discharge enthalpy and approach zero as the discharge enthalpy approaches that of dry steam (about 2800 kJ·kg^{-1}). On the other hand, the concentrations of Na in the water remain almost constant. These results indicate that the 'excess' enthalpy of well 6 at Nesjavellir is caused by phase segregation. The results for hydrogen sulphide are not conclusive, owing to much scatter.

The data for well 6 presented in Fig. 12.3 are based on flow tests in the period 1983–86. With continued production one could expect an increasing contribution to the 'excess' enthalpy of the well discharge of heat flowing from the rock. Long term production will tend to increase the zone of depressurization around the well. As a result, the water would have to move a longer distance through the disturbed pressure zone to the well and would, therefore, have a greater chance to pick up heat from the rock than during the early production history of the well.

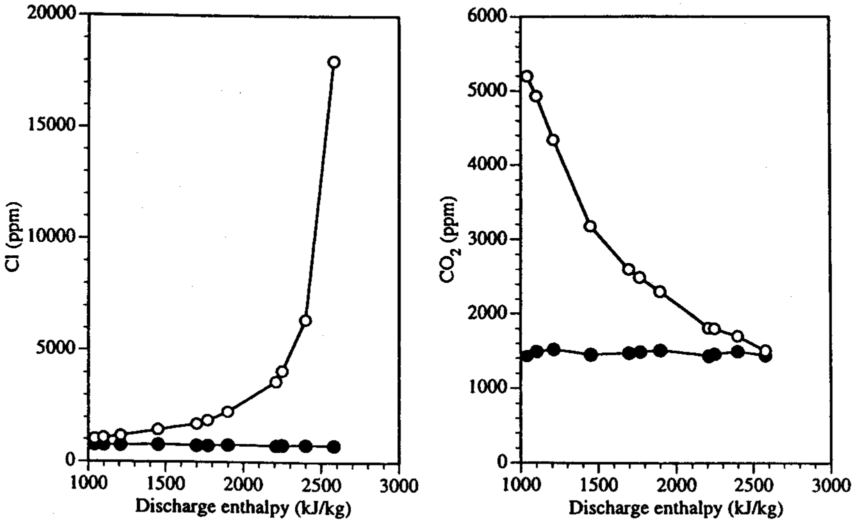

FIG. 12.2. Hypothetical example of chloride and carbon dioxide concentrations in water and steam samples collected from a wet steam well at atmospheric pressure (circles) and in the total discharge (dots) plotted against discharge enthalpy. The relationship indicates that the 'excess' discharge enthalpy is caused by heat flow from the rock to the fluid moving through the aquifer to the well.

Often, wells within a particular field do not show much variation in discharge enthalpy, even over a period of many years. However, there may be a large difference in the discharge enthalpy between wells in a particular field. When this is the case, and if it can be demonstrated that the reservoir fluid is quite homogeneous, diagrams such as those shown in Figs 12.1 and 12.2 may be used to assess the cause of 'excess' enthalpy in wells by plotting in a single diagram the data on discharge enthalpy and selected component concentrations.

The choice of components for evaluating causes of 'excess' well discharge enthalpy should be obvious. One should select a conservative component that can be precisely analysed. For water samples, Cl is the obvious choice. Yet, in the previous example from Nesjavellir, Na was selected instead of Cl. The reason is that the Nesjavellir water is very dilute, i.e. low in Cl, causing its analytical precision to be poorer than that of Na. The choice of gaseous components is more difficult. Most of them are reactive and may change in concentration in the well

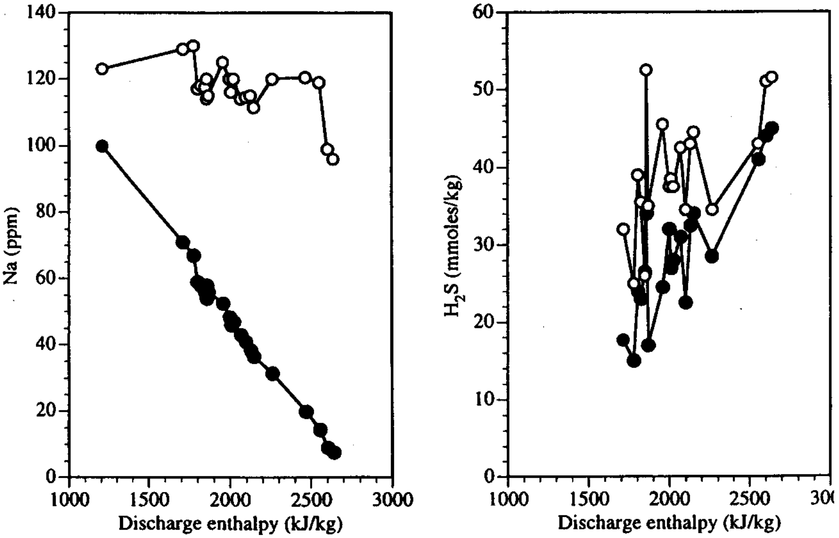

FIG. 12.3. Relationship between discharge enthalpy and sodium and hydrogen sulphide concentrations in water and steam discharged from well 6 at Nesjavellir in Iceland. Circles designate the concentrations of sodium and hydrogen sulphide in the water and steam phases, respectively, at bar abs. separation pressure, whereas dots represent concentrations in the total discharge. It is evident from the sodium data that the cause of the elevated discharge enthalpy is phase segregation in the aquifer. Because of the scatter of the hydrogen sulphide data, results are not conclusive, although one gets the impression that the hydrogen sulphide concentration stays almost constant in the steam phase but rises in the total discharge with increasing discharge enthalpy, a result which is consistent with that for Na.

discharge as a result of reactions in the zone of depressurization in producing aquifers. CO_2 or N_2 are probably the best. However, for N_2 there is always the risk that atmospheric contamination of the steam samples will affect the analysed N_2 levels. Besides, during the early discharge of a wet steam well, N_2 concentrations may be quite high when large amounts of cold water have been injected into the well during drilling and/or completion tests. For individual wells, it appears best to use CO_2 but this may not be acceptable when using a group of wells, at least if the CO_2 levels vary considerably between well discharges due to variable aquifer steam fractions and temperatures.

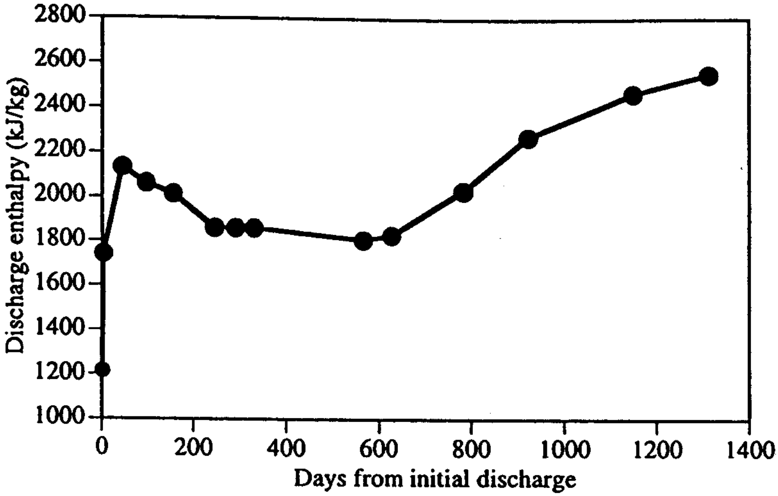

FIG. 12.4. Discharge enthalpy versus time for well 6 at Nesjavellir, Iceland.

If it can be demonstrated that the 'excess' enthalpy results from phase segregation, it is a satisfactory approximation to calculate Y from Eq. (12.1a) by taking h^d to be equal to that of liquid water at the aquifer temperature. If, on the other hand, heat flow from the rock in the aquifer is the sole cause of the 'excess' enthalpy, the h^d value chosen to calculate Y should be the measured one. In this case the total discharge composition is representative of the aquifer fluid (see Box 12.3).

In Chapter 15 we present a model which permits evaluation of the contribution of phase segregation and heat flow from the rock to the 'excess' enthalpy of well discharges. This model is based on the assumption of chemical equilibrium between specific mineral buffers and CO_2, H_2S and H_2.

BOX 12.1. EQUATIONS APPROXIMATELY DESCRIBING THE RELATIONSHIP BETWEEN TEMPERATURE, PRESSURE, ENTHALPY FOR STEAM AND SATURATED WATER AND ITS LATENT HEAT OF VAPORIZATION

The equations below are valid in the range 100–370°C at vapour saturation pressures. t is the temperature in °C and T in kelvin, P the pressure in bar abs., H_{liq} is the enthalpy of steam saturated water and L its latent heat of vaporization in kJ/kg:

$$H_{liq} = 35.9 + 3.6053t + 2.3838 \times 10^{-3}t^2 + 7.1004 \times \exp(0.004t)$$

$$L = 2384.1 - 0.3960t - 9.1537 \times 10^{-3}t^2 - 1.9416 \times \exp(0.004t)$$

$$P = \exp(18.2278 - 318.200/T^{0.5} + 9.0704 \times 10^7/T^3)$$

$$t = 99.69 + 0.12435P + 59.155\log P + 19.979\log P^2$$

$$H_{liq} = 412.2 + 2.6730P + 285.034\log P + 40.785\log P^2$$

$$\begin{aligned} L = {} & 2266.7 - 8.1861P + 3.5362 \times 10^{-2}P^2 \\ & - 1.3385\times 10^{-4}P^3 - 172.61\log P \end{aligned}$$

BOX 12.2. EASUREMENT OF THE ENTHALPY OF WELL DISCHARGES

There are several ways by which the enthalpy of wet steam well discharges can be measured. When testing wells, the Russel–James method is most often applied. This method is also called the critical lip pressure method. It involves measurement of critical lip pressure and water flow from an atmospheric silencer. The critical lip pressure is the pressure measured in a 1/4 in. diameter hole the centre of which is precisely 1/4 in. from the edge of the outflow pipe.

The critical lip pressure method is empirical. It is based on a measured relationship between critical lip pressure, discharge enthalpy and mass flow according to

$$M = \frac{1767\,420 P_c^{0.96} A}{(h^d)^{1.102}} \tag{1}$$

where M is the mass flow from the well in kg/s, P_c is the critical lip pressure in bar abs., A the cross-sectional area in m^2 of the flow pipe where P_c is measured, and h^d the dicharge enthalpy in kJ/kg.

By measuring P_c only, there are two unknowns in the equation above, discharge enthalpy and mass flow. It is most common to solve this by measuring the water flow from the well after steam separation at atmospheric pressure. We have

$$w = M(1 - Y) \tag{2}$$

where w represents water flow from the atmospheric silencer in kg/s and Y is the steam fraction in the discharge at atmospheric pressure given by Eq. (12.1a). Solving the two equations above together yields

$$w = \frac{1767\,420 P_c^{0.96} A(h_{atm}^s - h^d)}{L_{atm}(h^d)^{1.102}} \tag{3}$$

Here, h_{atm}^s and L_{atm} represent the enthalpy of steam and the latent heat of vaporization of water at atmospheric pressure, respectively. Their values can be obtained from the respective equations in Box 12.1. In the equation above, only h_d is unknown as P_c and w are both measured; so it can be solved.

BOX 12.2. (cont.)

The accuracy of the Russel–James method is about 10%. This method tends to yield high results for discharge enthalpy, at least, if steam and water are inadequately separated in the atmospheric silencer with the result that some of the water is carried off with the steam so the measured flow rate of water from the silencer is low. If water is swept into the air with the steam, this is easily observed as 'rain' from the steam leaving the atmospheric silencer.

During production the enthalpy of well discharges may be measured directly by recording separately steam and water flow as from wellhead separators. Alternatively, when two phase (water + steam) fluids are conveyed from wellhead to separator stations, discharge enthalpy may be measured with the Russel–James method by diverting the flow of individual wells into an atmospheric separator at the separator station.

During a flow test the critical pressure was measured as 2.2 bar abs., and the water flow from the atmospheric silencer as 4.5 L/s (~14 t/h). The diameter of the flow pipe was 20 cm, so its cross-sectional area is $0.1^2 \times \pi = 0.0314\ \text{m}^2$. We have:

$$4.5 = \frac{1767420(2.2)^{0.96} \times 0.034(2676 - h^d)}{2257(h^d)^{1.102}}$$

This equation must be solved by iteration. The solution yields 2250 J/mol. From Eq. (12.1a) we obtain a steam fraction of 0.811 and a steam flow at atmospheric pressure of 19.4 kg/s.

BOX 12.3. CALCULATION OF AQUIFER FLUID COMPOSITION (1) LIQUID DISCHARGE ENTHALPY

Below, there is an analysis of water and steam samples from a wet steam well at Hveragerdi, Iceland. The measured downhole temperature is 181°C at the level of the only producing horizon (as deduced from circulation loss during drilling). Downhole temperature logging during discharge shows that the first level of boiling is in the well. It is, therefore, safe to assume that only liquid water is present in the aquifer (the aquifer is sub-boiling). Thus, the enthalpy of the discharge, which corresponds to that of liquid water at 181°C, is 767 kJ/kg.

Water sample (ppm)		Steam sample (mmole/kg)	
pH/°C	8.82/20	CO_2	51.6
SiO_2	281.0	H_2S	4.69
B	0.62	NH_3	0.030
Na	153.3	H_2	1.24
K	13.4	CH_4	0.132
Ca	1.73	N_2	4.15
Mg	0.002	O_2	0
ΣCO_2	74.2	Ar	0.070
SO_4	43.7		
H_2S	19.2	**Physical parameters:**	
Cl	109.5	Discharge enthalpy (kJ/kg)	767 (calculated)
F	1.82	Sampling pressure (bar abs.)	5.8

For all aqueous and gaseous components, respectively, except CO_2 and H_2S, we have (Eqs (12.2a) and (12.2b))

$$m^d_{i,1} = m^w_{i,1}(1 - Y_1) \tag{12.2a}$$

and

$$m^d_{i,1} = m^s_{i,1}Y_1 \tag{12.2b}$$

For CO_2 and H_2S, Eq. (12.2) is used because these components are measured in both phases, or

$$m^d_{i,1} = m^s_{i,1}Y_1 + m^w_{i,1}(1 - Y_1) \tag{12.2}$$

BOX 12.3. (cont)

Before calculating the concentrations of all the components in the aquifer water, the steam fraction in the discharge at the sampling pressure must be obtained from Eq. (12.1a):

$$Y_1 = \frac{h^d - h_1^w}{L_1} \tag{12.1a}$$

Values for h_i^w and L_i were obtained from the respective equations in Box 12.1 as 669 and 2089 kJ/mol, respectively, giving a value for *Y* of 0.047.

Inserting this *Y* value into Eqs (12.2) to (12.2b) yields the following aquifer component concentrations:

Reservoir Water (ppm)

SiO_2	267.2	Mg	0.002	Cl	104.1	CH_4	0.103
B	0.59	ΣCO_2	181.8	F	1.73	N_2	5.69
Na	145.8	SO_4	41.6	NH_3	0.001	O_2	0
K	12.7	H_2S	26.1	H_2	0.12	Ar	0.123
Ca	1.65						

BOX 12.4. CALCULATION OF AQUIFER FLUID COMPOSITION (2) ‘EXCESS’ DISCHARGE ENTHALPY

Below, there is an analysis of water and steam samples from well 35 at Momotombo, Nicaragua.

Water sample (ppm)		Steam sample (% vol)		Steam sample (mmol/kg)
pH/°C	8.77/25	CO_2	93.52	268.1
SiO_2	864.5	H_2S	1.52	4.36
B	32.0	NH_3	0.12	0.34
Na	1838.0	H_2	0.25	0.72
K	342.6	CH_4	0.29	0.83
Ca	13.4	N_2	4.59	13.13
Mg	0.070	O_2	0	0
ΣCO_2	10.6	Ar	0.08	0.23
SO_4	6.7	L gas/ kg steam·°C	6.88/25	**Physical parameters:**
H_2S	1.9			Discharge enthalpy (kJ·kg^{-1}) 1654
Cl	3128.0			Sampling pressure (bar abs.) 1.0

First, we will calculate the composition of the total discharge. From the appropriate equations in Box 12.1, we see that the enthalpy of steam saturated water at the sampling pressure and its latent heat of vaporization are 417 and 2257 kJ·kg^{-1}, respectively. The steam fraction at the sampling pressure conditions can be obtained from Eq. (12.1a). We have

$$Y_s = \frac{1654 - 417}{2257} = 0.548$$

From this value for the steam fraction the total discharge composition is calculated as follows:

Total discharge composition (ppm)

SiO_2	390.8	Ca	6.1	CO_2	6469.0	CH_4	7.28
B	14.5	Mg	0.032	H_2S	82.1	N_2	201.5
Na	830.8	SO_4	21.1	NH_3	3.17	O_2	0
K	154.9	Cl	1414.0	H_2	0.80	Ar	4.54

The total discharge composition is the composition of the reservoir fluid if the ‘excess’ enthalpy is due to heat flow from the rock.

BOX 12.4. (cont.)

From the Na/K ratio of the discharge, the Na/K geothermometry temperature is calculated as 269°C. As may be seen from the respective equation in Box 12.1, the enthalpy of water at 269°C is 1182 $kJ \cdot kg^{-1}$. From this enthalpy value and the enthalpy of water at the sampling pressure (417 $kJ \cdot kg^{-1}$) and its latent heat of vaporization (2257 $kJ \cdot kg^{-1}$), a steam fraction value of 0.338 is obtained as well as the following composition for the reservoir fluid:

Reservoir water composition (ppm)

SiO_2	572.3	Ca	8.9	CO2	3994.0	CH_4	4.49
B	21.2	Mg	0.046	H_2S	51.4	N_2	124.3
Na	1217.0	SO_4	30.9	NH_3	1.95	O_2	0
K	226.8	Cl	2071.0	H_2	0.49	Ar	2.80

If the 'excess' enthalpy of well 35 is due to phase segregation in the aquifer, the numbers above give the correct solute concentrations in the aquifer but not those in the first part of this box.

BOX 12.5. WHAT DO WE DO WHEN WATER AND STEAM SAMPLES ARE COLLECTED AT DIFFERENT PRESSURES?

It is common to collect water samples from the weirbox at atmospheric pressure but steam samples under pressurized conditions from a pipeline conveying two phase flow or from wellhead separators. When this is so, it is considered convenient and satisfactorily accurate to calculate the gas content of the steam at atmospheric pressure by assuming that all the gas in the discharge occupies the steam phase and that progressive boiling with falling pressure simply adds pure steam to the higher pressure gaseous steam. Accordingly, we have:

$$m_i^d = m_{i,s}^s Y_s = m_{i,atm}^s Y_{atm}$$

where $m_{i,atm}^s$ and Y_{atm} represent the concentration of gas in steam at atmospheric pressure and the steam fraction, respectively. $m_{i,s}^s$ and Y_s are the corresponding values at sampling conditions. From the above relationship, we see that

$$m_{i,atm}^s = m_{i,s}^s \frac{Y_s}{Y_{atm}}$$

Having obtained a value for gas concentrations in steam at atmospheric pressure ($m_{i,atm}^s$), we may derive the aquifer fluid composition as explained in Boxes 12.3 or 12.4.

13. HYDROGEN AND OXYGEN ISOTOPE FRACTIONATION DURING BOILING

Franco D'Amore, Jane Gerardo-Abaya and Stefán Arnórsson

We have encountered isotopic fractionation in Chapters 5 and 10 and have acquired some understanding of the behaviour of isotopes with temperature changes. One important application of the concept of isotopic fractionation — and where one strength of isotopic studies of geothermal systems lies — is quantifying the processes in geothermal reservoirs, such as boiling, steam separation and condensation. Geothermal fluids undergo various physical and chemical changes during their ascent to the surface. These changes, such as cooling by conduction, mixing and boiling, are reflected in both their chemical and their isotopic constituents.

Steam tends to rise faster than liquid water in boiling zones of geothermal systems, because of its lower density and, therefore, to separate from its parent water. Steam separation has different effects on isotopic fractionation according to the mechanism of the steam loss. If the steam stays with the ascending water and then separates at one temperature, maximum isotopic fractionation is encountered. Such steam separation is termed one stage separation. At the other extreme, the process is continuous steam separation, i.e. the steam separates from the parent water as it forms. With this process, minimum isotopic fractionation occurs between the liquid water and vapour. An intermediate stage between these two is multistage steam separation. Fractionation of deuterium and ^{18}O by boiling leads to enrichment of the heavier isotopes in the water phase and corresponding depletion in the steam phase.

While isotopic data obtained from lakes, streams, rivers, springs and downhole samples are interpreted according to their analytical results, data obtained from samples collected from boiling springs and wet steam wells, whether of steam or of water, need to be calculated to reservoir conditions before they can be interpreted to account for effects of isotopic changes due to boiling and phase separation. To calculate the isotopic composition of the reservoir fluid from data on samples collected at the surface, conservation of mass and heat is generally assumed between reservoir and surface. By assuming conservation of heat, the boiling is not only adiabatic but also one stage. We have:

$$Y_c = \frac{h^d - h_c^w}{L_c} \qquad (12.1a)$$

where h^d represents the enthalpy of the reservoir water, and h_c^w and L_c the enthalpy of water at temperature c and its latent heat of vaporization at that temperature. Y_c is the steam fraction formed by adiabatic boiling from the temperature of the reservoir water to temperature c. Conservation of mass of isotopes is given by:

$$\delta_d = \delta_{A,c}(1 - Y_c) + \delta_{B,c}Y_c \tag{13.1}$$

where δ_d is the δ value for the isotope in the reservoir water and $\delta_{A,c}$ and $\delta_{B,c}$ are its δ values in the two phases, respectively, at temperature c. Isotopic fractionation between two phases, A and B, was given by the Eq. (5.8):

$$10^3 \ln \alpha_{A-B} = \delta_A - \delta_B$$

where α denotes the fractionation factor between phases A and B, and δ_A and δ_B represent the respective δ values in the phases denoted by the respective subscripts (see Box 13.1). Combination of Eqs (13.1) and (5.8) and elimination of δ_B yields:

$$\delta_d = \delta_{A,c} - Y_c \times 10^3\ \alpha_{(A-B),c} \tag{13.2}$$

For deuterium and ^{18}O fractionation between water and steam, Eq. (13.2) can be written as

$$(\delta^2H)_d = (\delta^2H)_{w,c} - Y_c \times 10^3 \ln \alpha(^2H)_{(w-s),c} \tag{13.2a}$$

and

$$(\delta^{18}O)_d = (\delta^{18}O)_{w,c} - Y_c \times 10^3 \ln \alpha(^{18}O)_{(w-s),c} \tag{13.2b}$$

The fractionation factors for deuterium and ^{18}O between water and steam are given in Table 13.1. Equations (13.2a) and (13.2b) allow calculation of the deuterium and ^{18}O content of geothermal reservoir waters from data on water and/or steam samples collected from the discharge of wet steam wells and boiling springs (Box 13.2).

Boiling in the aquifer of producing wet steam wells may be associated with some phase segregation (Chapter 15). When this occurs, and phase segregation is the sole cause of the excess enthalpy, it is appropriate to calculate a value for the steam fraction, on the assumption of adiabatic boiling from the initial aquifer

TABLE 13.1. DEUTERIUM (δ^2H) AND OXYGEN-18 ($\delta^{18}O$) FRACTIONATION FACTORS (10^3LN α), AND VALUES FOR INTEGRALS I FOR δ^2H AND $\delta^{18}O$ AT SELECTED TEMPERATURES. FROM TRUESDELL et al. (1977) AS REPORTED BY HENLEY et al. (1984)

	Deuterium		Oxygen-18	
t(°C)	$10^3\ln\alpha_{^2H}$	$I_{^2H}$	$10^3\ln\alpha_{^{18}O}$	$I_{^{18}O}$
0	106.0	0	11.20	0
20	81.5	3.021	9.54	0.349
40	61.3	5.377	8.17	0.651
60	46.4	7.197	7.03	0.916
80	36.1	8.640	6.07	1.150
100	27.8	9.792	5.24	1.350
120	21.5	10.710	4.53	1.542
140	16.3	11.443	3.91	1.707
160	11.7	12.008	3.37	1.855
180	7.4	12.414	2.90	1.989
200	3.5	12.654	2.48	2.110
220	0.1	12.739	2.10	2.219
240	–2.2	12.680	1.77	2.319
260	–3.6	12.509	1.46	2.410
280	–4.0	12.261	1.19	2.494
300	–3.4	11.986	0.94	2.571
320	–2.2	11.735	0.70	2.644
340	–1.3	11.536	0.45	2.710
360	–0.5	11.374	0.19	2.769
374	0	11.279	0	2.800

conditions to the sampling conditions, and to use the steam fraction value so obtained to retrieve values for the deuterium and ^{18}O content of the aquifer water with the aid of Eqs (13.2a) and (13.2b) rather than to use measured discharge enthalpy values to obtain Y. For excess enthalpy wells, the adiabatic boiling method yields numbers which are less negative than those of the total discharge (see Box 13.2).

The isotopic composition of the total discharge and that calculated assuming one stage adiabatic boiling from the initial aquifer temperature represent two extremes. The actual isotopic composition of the aquifer water may be intermediate, depending on the extent of phase segregation in the aquifer.

As discussed in Chapter 15, a model permitting evaluation of the contribution of phase segregation to the discharge enthalpy of wet steam wells has been developed (Box 13.3).

The deuterium and ^{18}O content of the fluid in producing aquifers of wells beyond the depressurization zone may change with time during the exploitation of geothermal reservoirs, as a result of enhanced recharge. This is the case with ^{18}O, if recharge of cold water with little or no oxygen shift is sufficiently rapid to prevent much exchange with the rock before entering wells. This is also the case for both isotopes when their δ values in the recharging fluid differ from that of the initial reservoir fluid.

An equation of continuous steam loss was given by Truesdell et al. (1977). The change in enthalpy and isotopic composition of boiling water of mass m is given by:

$$m\left(\frac{dh^w}{dm}\right) = h^w - h^s \tag{13.3}$$

and

$$m\left(\frac{d\delta_w}{dm}\right) = \delta_w - \delta_s \tag{13.4}$$

Dividing Eq. (13.4) by Eq. (13.3), we obtain

$$\left(\frac{d\delta_w}{dh^w}\right) = \frac{\delta_w - \delta_s}{h^w - h^s} \tag{13.5}$$

Using Eq. (5.8) to substitute for δ_s and integrating from initial (i) to final (f) conditions yields:

$$\ln\left(\frac{10^3 + \delta_{w,f}}{10^3 + \delta_{w,i}}\right) = \int_{h_i^w}^{h_f^w}\left(\frac{1/\alpha - 1}{h^s - h^w}\right)dh^w \tag{13.6}$$

Defining I as the integral from a reference state (r) to a specified state (s) leads to

$$I = \int_{h_r^w}^{h_s^w}\left(\frac{10^3(1-1/\alpha)}{h^s - h^w}\right)dh^w \tag{13.7}$$

and

$$\frac{10^3+\delta_{w,f}}{10^3+\delta_{w,i}}=\exp\left(\frac{I_i-I_f}{10^3}\right) \tag{13.8}$$

The numerical solution of the integral of Eq. (13.7) is given in Table 13.1. In upflow zones below boiling hot springs, steam loss may be intermediate between single step and continuous steam separation.

The following equations satisfactorily describe the changes of α and I with temperature, where t is in centigrades:

$$\begin{aligned}10^3\ln\alpha_{^2\mathrm{H}} = &-1.1726\times10^{-10}t^5+1.2817\times10^{-7}t^4-5.3583\times10^{-5}t^3\\ &+1.1547\times10^{-2}t^2-1.5197t+106.6\end{aligned}$$

$$\begin{aligned}I_{^2\mathrm{H}} = &-5.3742\times10^{-10}t^4+9.6594\times10^{-7}t^3-6.0423\times10^{-4}t^2\\ &+0.1485t+0.1705\end{aligned}$$

$$\begin{aligned}10^3\ln\alpha_{^{18}\mathrm{O}} = &\ 5.3482\times10^{-10}t^4-6.6028\times10^{-7}t^3-3.2091\times10^{-4}t^2\\ &-8.5382\times10^{-2}t+11.156\end{aligned}$$

$$I_{^{18}\mathrm{O}} = 3.9545\times10^{-8}t^3-3.9983\times10^{-5}t^2+1.6898\times10^{-2}t+0.02241$$

BOX 13.1 DERIVATION OF THE EQUATION:

$$10^3 \ln \alpha_{A-B} = \delta_A - \delta_B$$

$\ln \alpha_{A-B}$ is defined as:

$$\alpha_{A-B} = \frac{1000 + \delta_A}{1000 + \delta_B}$$

If δ_A and δ_B are small numbers, i.e. «100, $\alpha \approx 1$ and $\ln \alpha \approx 0$. We can, therefore, write

$$\ln \alpha_{A-B} \approx \alpha - 1$$

for $\alpha \approx 1$ and

$$\ln \alpha_{A-B} \approx \frac{1000 + \delta_A}{1000 + \delta_B} - 1$$

Rearranging and again taking δ_B « 100 yields

$$10^3 \ln \alpha_{A-B} \approx \delta_A - \delta_B$$

BOX 13.2. CALCULATION OF ISOTOPIC FRACTIONATION DURING ONE STEP ADIABATIC BOILING

Boiling hot springs

Water collected from a boiling hot spring has δ^2H and $\delta^{18}O$ values of –60‰ and –7.5‰, respectively. The quartz geothermometer indicates a subsurface temperature of 250°C. Calculate the isotopic composition of the aquifer water assuming one stage boiling from 250 to 100°C.

First calculate the steam fraction that forms by boiling (see Eq. (12.1a)). We have:

$$Y_{100} = \frac{h^d - h^w_{100}}{L_{100}}$$

where h^d and h^w_{100} stand for the enthalpy of the aquifer water and the steam saturated water at 100°C, respectively, and L_{100} is the latent heat of vaporization at 100°C. From steam tables or the respective equations in Box 12.2 we have

$$Y_{100} = \frac{1086 - 419}{2257} = 0.296$$

At 100°C, we see that the fractionation factors for ^2H and ^{18}O between water and steam are 5.24 and 27.8, respectively, or

$$10^3 \ln \alpha(^2H) = \delta(^2H)_l - \delta(^2H)_v = 27.8$$

and

$$10^3 \ln \alpha(^{18}O) = \delta(^{18}O)_l - \delta(^{18}O) = 5.24$$

From Eq. (13.2) we have

$$\begin{aligned}(\delta^2H)_d &= (\delta^2H)_{1,100} - Y_{100} \times 10^3 \ln \alpha(^2H)_{1-v} \\ &= -60 - 0.296 \times 27.8 = -68.2‰\end{aligned}$$

and

$$\begin{aligned}(\delta^{18}O)_d &= (\delta^{18}HO)_{1,100} - Y_{100} \times 10^3 \ln \alpha(^{18}O)_{1-v} \\ &= -7.5 - 0.296 \times 5.24 = -9.05‰\end{aligned}$$

BOX 13.2. (cont.)

Wet steam wells (total discharge)

It is common that samples of steam for analysis of deuterium and oxygen isotopes are collected from wet steam wells in order to calculate the isotopic composition of the total discharge. To demonstrate this, consider the following data from well 38 at Momotombo in Nicaragua: $\delta^2H = -51.5$ ‰ and $\delta^{18}O = -6.68$‰. The sampling pressure was 6.35 bar abs., and the discharge enthalpy is 1505 $kJ \cdot kg^{-1}$. From steam tables, we see that the temperature at a steam saturation pressure of 6.35 bar abs. is 161°C. From the physical data, we have:

$$Y_c = \frac{1505 - 680}{2078} = 0.397$$

where Y_c designates the steam fraction at the sampling pressure. The fractionation factors for deuterium and ^{18}O between water and steam at 161°C are 11.5 and 3.35, respectively. From Eq. (5.8) we have:

$$\delta(^2H)_l = \delta(^2H)_v + 10^3 \ln \alpha(^2H) = -51.5 + 11.5 = -40.00‰$$

and

$$\delta(^{18}O)_l = \delta(^{18}O)_v + 10^3 \ln \alpha(^{18}O) = -6.68 + 3.35 = -3.33‰$$

Then, from the steam fraction of 0.397 and Eqs (13.2a) and (13.2b), we have

$$\delta(^2H)_t = \delta(^2H)_l - Y_c 10^3 \ln \alpha(^2H) = -40 - 0.397 \times 11.5 = -44.6‰$$

and

$$\begin{aligned}\delta(^{18}O)_t &= \delta(^{18}O)_l - Y_c \times 10^3 \ln \alpha(^{18}O) \\ &= -3.33 - 0.397 \times 3.35 = -4.66‰\end{aligned}$$

Wet steam wells (aquifer water)

It is necessary to know the aquifer temperature to calculate the isotopic composition of aquifer water from samples collected from excess enthalpy wet steam wells, assuming that this excess enthalpy is due to phase

BOX 13.2. (cont.)

segregation in the aquifer. In the case of the Momotombo well considered in the example above, the average of the quartz, Na/K and Na/K/Ca geothermometry temperatures is 244°C. By selecting this value for the aquifer temperature, we obtain an enthalpy value of 1057 kJ·kg^{-1} for the aquifer water, and the steam fraction ($Y_{l,c}$) becomes:

$$Y_{l,c} = \frac{1057 - 680}{2078} = 0.181$$

Inserting this value of Y into Eqs (13.2a) and (13.2b) gives:

$$\begin{aligned}\delta(^2\mathrm{H})_d &= \delta(^2\mathrm{H})_l - Y_{l,c} \times 10^3 \ln \alpha(^2\mathrm{H}) \\ &= -40 - 0.181 \times 11.5 = -42.1‰\end{aligned}$$

and

$$\begin{aligned}\delta(^{18}\mathrm{O})_d &= \delta(^{18}\mathrm{O})_l - Y_{l,c} \times 10^3 \ln \alpha(^{18}\mathrm{O}) \\ &= -3.33 - 0.181 \times 3.35 = -3.95‰\end{aligned}$$

A comparison between the results of the last two exercises shows that the δ values of the total discharge are more negative than those of the aquifer water, assuming that phase segregation is the cause of the excess enthalpy.

BOX 13.3. CALCULATION OF AQUIFER WATER ISOTOPIC COMPOSITIONS FROM DATA ON WATER DISCHARGED FROM EXCESS ENTHALPY WET STEAM WELLS, TAKING INTO ACCOUNT THE EFFECT OF PHASE SEGREGATION

Model II in Chapter 15 deals with the calculation of the initial steam fraction in the producing aquifer of wet steam wells when both heat flow from the rock and phase segregation can contribute to the excess enthalpy of the discharge. For detailed information, the reader is referred to Chapter 15.

Basic data:

Discharge enthalpy:	1850 $kJ \cdot kg^{-1}$
Sampling pressure:	6.2 bar abs.
δ^2H (water):	–65.0‰
$\delta^{18}O$ (water):	–7.50‰
Aquifer temperature:	280°C

Temperature at which phase segregation and heat flow from rock occurs (t_s): 200°C

(1) Calculate the steam fraction (Y_c) at the sampling pressure:

$$Y_c = \frac{1850 - 676}{2081} = 0.564$$

(2) Calculate the isotopic composition of the total discharge ($\delta(A)_t$) (Eq. (13.2)):

$$\delta(^2H)_t = -65.0 - 0.564 \times 11.7 = -71.6‰$$
$$\delta(^{18}O)_t = -7.50 - 0.564 \times 3.37 = -9.40‰$$

(3) Calculate the isotopic composition of water at temperature t_s:

$$\delta(^2H)_{l,s} = -71.6 + 3.5 = -68.1‰$$
$$\delta(^{18}O)_{l,s} = -9.40 + 2.48 = -6.92‰$$

(4) Calculate the steam fraction which forms by adiabatic boiling from the aquifer temperature (t_0) to the phase segregation temperature (t_s):

BOX 13.3. (cont.)

$$Z_s = \frac{1237 - 852}{1939} = 0.199$$

(5) Calculate the isotopic composition of the aquifer water:

$$\delta(^2\mathrm{H})_d = -68.1 - 0.199 \times 3.5 = -68.8‰$$
$$\delta(^{18}\mathrm{O})_d = -6.92 - 0.199 \times 2.48 = -7.41‰$$

If phase segregation alone was responsible for the excess discharge enthalpy, the procedure given in Box 13.2 is appropriate. It gives $\delta(^2\mathrm{H})_d$ = 68.2‰ and $\delta(^{18}\mathrm{O})_d$ = –8.17‰.

BOX 13.4. CALCULATION OF ISOTOPIC FRACTIONATION DURING BOILING BY CONTINUOUS STEAM LOSS

Consider the isotopic data from the boiling hot spring given in the first example in Box 13.2. From Eq. (13.8), we have

$$\delta_{w,i} = \frac{10^3 + \delta_{w,f}}{\exp\left(\frac{I_i - I_f}{10^3}\right)} - 10^3$$

In this case, the subscript *i* refers to the unboiled aquifer water. Taking the initial temperature to be 250°C as in the previous example gives the following equations for deuterium and ^{18}O, respectively:

$$\delta(^2H)_{w,i} = \frac{10^3 - 60}{\exp\left(\frac{12.594 - 9.792}{10^3}\right)} - 10^3 = -62.6‰$$

and

$$\delta(^{18}\mathrm{O})_{w,i} = \frac{10^3 - 7.50}{\exp\left(\frac{2.364 - 1.357}{10^3}\right)} - 10^3 = -8.50‰$$

14. MINERAL SATURATION

Stefán Arnórsson

As was discussed earlier, particularly in Chapter 10 on geothermometry, it is common practice to assume specific mineral–solution equilibria when applying geochemistry to obtain an understanding of various physical features of geothermal systems. It cannot be overemphasized that the assumption of specific chemical equilibria may not be valid. Also, water and steam discharged from a well or a hot spring are inevitably a mixture of water originating at different sites in the aquifer so that the various components in the discharged fluid may have had significantly different temperatures. A fluid discharged from a well could be calculated to be out of equilibrium at any temperature, simply as a result of the mixing process. Yet, local equilibrium may have existed in various parts of the geothermal reservoir.

In chemical systems of a given composition and at overall equilibrium (i.e. all components are at equilibrium), there are no more than two independent variables, namely temperature and pressure. If some chemical components in the system have not equilibrated then the independent variables are temperature and pressure plus the number of non-equilibrated components. In the case of boiling geothermal systems, the independent variables are pressure and the number of non-equilibrated components. Here, the temperature depends on the pressure. In the case of a boiling system at overall equilibrium, one may select a value for pressure, which fixes temperature. Alternatively, one could also select a value for temperature that would in turn specify the pressure.

When studying the state of equilibrium between geothermal waters and specific minerals, or between components in the liquid phase, one must specify the temperature at which the system may be at equilibrium. If the fluid is mixed and its constituent components do not have the same temperature, it should be clear that there is no way of demonstrating equilibrium unless one could identify the composition and temperature of individual components in the mixture. This is not possible though to the best of our knowledge. It is always important to be aware of these limitations involved in evaluating solution–mineral equilibria in geothermal systems.

The thermodynamic properties of minerals and aqueous species change with temperature and pressure. The effect of temperature is much greater than the effect of pressure for the range of values that these variables take in groundwater systems, some 0–350°C for temperature and about 1–200 bar for pressure. For example, the apparent standard Gibbs energy of formation of albite changes by 33 500 J/mole in going from 0 to 350°C at 1 bar, but only by 2000 J/mole in going from 1 to 200 bar at 25°C and about the same at other temperatures. It is for this reason that the effect of pressure is often neglected when studying mineral–solution equilibria in groundwater systems. Certainly, in geothermal systems, the effect of pressure tends to be less than the uncertainty involved in selecting a value for the aquifer temperature.

There are essentially two steps involved in calculating the state of mineral saturation for the aquifer fluid of wet steam wells. The first step involves calculation of the chemical composition of the reservoir fluid from data on water and steam compositions at the wellhead. The other involves calculation of aqueous speciation for the aquifer fluid composition at a selected temperature. For single phase discharges, such as hot water wells or non-thermal waters, there is only one step — calculation of aqueous speciation. The analysed sample can safely be taken to represent the aquifer water.

Calculation of aqueous speciation requires the use of aqueous speciation computer programs. Such programs permit calculation of individual aqueous species activities. From these, reaction quotients can be obtained for individual minerals. Comparison between the reaction quotient and the equilibrium constant permits evaluation of the state of equilibrium. At equilibrium, $K = Q$; for supersaturated solution, $Q > K$ and for undersaturated solution, $Q < K$ (Chapter 3).

To explain further the derivation of a value for a specific reaction quotient, consider, e. g., the reaction between aqueous solution and epidote ($Ca_2Al_2FeSi_3O_{12}(OH)$), a mineral of rather complex composition which is common in geothermal systems, and calcite ($CaCO_3$), a mineral of simple composition. Reactions between these minerals and aqueous species can be written as follows:

$$CaCO_3 + 2H^+ = Ca^{2+} + CO_2 + H_2O \tag{14.1}$$

and

$$\begin{aligned} &Ca_2Al_2FeSi_3O_{12}(OH) + H^+ + 11H_2O \\ &\quad = 2Ca^{2+} + 2Al(OH)_4^- + Fe(OH)_4^- + 3H_4SiO_4^0 \end{aligned} \tag{14.2}$$

If the above reactions are read from left to right they represent dissolution; they describe, however, precipitation reactions when read from right to left. The reaction quotient for each reaction is given by

$$Q_{cal} = \frac{[\mathrm{Ca}^{2+}][\mathrm{CO}_2][\mathrm{H}_2\mathrm{O}]}{[\mathrm{CaCO}_3][\mathrm{H}^+]^2} \tag{14.3}$$

and

$$Q_{ep} = \frac{[\mathrm{Ca}^{2+}]^2[\mathrm{Al(OH)}_4^-]^2[\mathrm{Fe(OH)}_4^-][\mathrm{H}_4\mathrm{SiO}_4^0]^3}{[\mathrm{Ca}_2\mathrm{Al}_2\mathrm{FeSi}_3\mathrm{O}_{12}(\mathrm{OH})][\mathrm{H}^+][\mathrm{H}_2\mathrm{O}]^{11}} \tag{14.4}$$

where [i] stands for the activity of the i-th component/species and Q is the reaction quotient.

If the minerals involved in the reactions above are pure, their activity is equal to unity. If the aqueous solution is dilute (<1% dissolved solids), it is a good approximation also to take the activity of water to be 1. When this is the case, the reaction quotient according to Eqs (14.3) and (14.4) reduces to

$$Q_{cal} = \frac{[\mathrm{Ca}^{2+}][\mathrm{CO}_2]}{[\mathrm{H}^+]^2} \tag{14.3a}$$

and

$$Q_{ep} = \frac{[\mathrm{Ca}^{2+}]^2[\mathrm{Al(OH)}_4^-]^2[\mathrm{Fe(OH)}_4^-][\mathrm{H}_4\mathrm{SiO}_4^0]^3}{[\mathrm{H}^+]} \tag{14.4a}$$

In studying the state of equilibrium/disequilibrium according to a specific reaction, it does not matter which aqueous species are selected to represent the various dissolved components of the mineral. Testing of equilibrium has nothing to do with how the reaction occurs, i.e. the reaction path. One could, thus, express the reaction according to Eq. (14.1) above as

$$\mathrm{CaCO}_3 = \mathrm{Ca}^{2+} + \mathrm{CO}_3^{2-} \tag{14.1a}$$

It is considered advantageous to express mineral dissolution/precipitation reactions, as far as possible, in terms of the dominant aqueous species of individual components. This requires some feedback from the aqueous speciation calculations that reveal which, if any, aqueous species of a particular component predominates. An example is:

$$SiO_{2,qtz} + H_2O + OH^- = H_3SiO_4^- \tag{14.5}$$

It is, of course, possible to write a reaction involving dissolution/precipitation of quartz in terms of the ionized silica species and OH^-. In most geothermal waters, $H_4SiO_4^0$ is the dominant aqueous silica species, often over 99% of the total dissolved silica. It would, accordingly, be much simpler to express the quartz–solution reaction as

$$SiO_{2,qtz} + 2H_2O = H_4SiO_4^0 \tag{14.5a}$$

rather than presenting it as pH dependent according to reaction (14.5). Besides, by introducing OH^-(pH), an unnecessary error is introduced in the calculated value of the reaction quotient.

In dilute, neutral pH and alkaline waters (pH < 9), $Al(OH)_4^-$ is the predominant Al bearing aqueous species, and Na^+ and $H_4SiO_4^0$ are the dominant sodium and silica species. Albite ($NaAlSi_3O_8$) dissolution would, therefore, be best represented by

$$NaAlSi_3O_8 + 8H_2O = Na^+ + Al(OH)_4^- + 3H_4SiO_4^0 \tag{14.6}$$

In acid solution, Al^{3+} rather than $Al(OH)_4^-$ is the predominant Al species. In such solution it is logical to express albite dissolution as

$$NaAlSi_3O_8 + 4H^+ + 4H_2O = Na^+ + Al^{3+} + 3H_4SiO_4^0 \tag{14.6a}$$

Na^+ and $H_4SiO_4^0$ are the dominant bearing sodium and silica species in both acid and weakly alkaline solutions, i.e. at pH of less than about 9 when measured at 25°C.

According to reaction (14.6), the dissolution of albite is pH independent, whereas it is not according to Eq. (14.6a). In other words, if $Al(OH)_4^-$ is the dominant Al species (pH>7 at 25°C), dissolution or precipitation of albite is unaffected by pH, at least if $H_3SiO_4^0$ is not an important species. This is, however, not the case at lower pH values, particularly when below 5 (at 25°C) when Al^{3+} is the dominant Al bearing aqueous species. Dissolution of albite in acid solution consumes protons, and its precipitation from such solution releases H^+.

At very high pH (>9.5), some of the aqueous silica is ionized, leading to

$$NaAlSi_3O_8 + 7H_2O + OH^- = Na^+ + Al(OH)_4^- + 3H_3SiO_4^- \tag{14.6b}$$

With increasing pH above about 9, albite solubility increases.

Aqueous speciation programmes give values for the respective aqueous species activities but not for minerals nor for water. With few exceptions, it is a satisfactory approximation to take the activity of H_2O in geothermal waters to be equal to 1, because they are sufficiently dilute. The activity of any pure component in a phase of mixed composition is equal to its mole fraction in that phase. Thus, e.g., the activity of liquid water with 1% of dissolved constituents is 0.99.

Many minerals are often very pure, i.e. their composition is fixed. Examples include quartz, calcite and anhydrite. Other minerals have variable composition. The reason is that two or more ions of about equal size and charge can substitute for one another in the crystal lattice of such minerals. Substitution occurs, as a rule, more easily when minerals form at high temperature as compared to low temperature. This is caused by expansion of the crystal lattice as a response to increased volume by thermal expansion. Thus, for example, feldspars in igneous rocks have variable compositions, whereas feldspars precipitating under hydrothermal conditions are quite pure (K feldspar, albite). Yet, the composition of some hydrothermal minerals can be variable, depending on the composition of the parent rock and possibly also on the formation temperature. Examples include chlorite, epidote and prehnite.

When studying mineral–solution equilibria involving minerals that can have variable composition depending on their environment of formation, it is necessary to carry out a chemical analysis of that mineral from drill cuttings or drill cores in order to obtain a value for the activity of a pure end member component in it. Consider, e.g., the reaction between prehnite and solution:

$$\begin{aligned}&Ca_2Al_2Si_3O_{10}(OH)_2 + 10H_2O\\&\quad = 2Ca^{2+} + 2Al(OH)_4^- + 3H_4SiO_4^0 + 2OH^-\end{aligned} \tag{14.7}$$

Analysis of the prehnite gives $Ca_2Al_{1.5}Fe_{0.5}Si_3O_{10}(OH)_2$. The activity of pure prehnite (the Al end member component) in this particular prehnite is 1.5/2 = 0.75. The reaction quotient for prehnite is given by:

$$Q_{pre} = \frac{[Ca^{2+}]^2[Al(OH)_4^-]^2[H_4SiO_4^0]^3[OH^-]^2}{[Ca_2Al_2Si_3O_{10}(OH)_2][H_2O]^{10}} \tag{14.8}$$

By inserting the appropriate value for the a0ctivity of prehnite as well as that of the aqueous species, a value for Q is obtained. Comparison between the obtained Q value and the equilibrium constant (K) for reaction (14.7) permits an evaluation of the state of saturation of a water for prehnite with the composition given.

It was stated above that the activity of an end member component in a mineral solid solution is equal to its mole fraction. This is indeed the case for minerals with only one type of exchangeable energy site in the crystal lattice. The general relationship between activity and mole fraction is given by

$$a_i = X_i^n \qquad (14.9)$$

where X represents the mole fraction, a the activity and n the number of exchangeable sites in the unit cell formula. It is outside the scope of this book to expand on this in detail. The reader is referred to Nordstrom and Muñoz (1994) for more information.

Sometimes, it is of interest to study simultaneous equilibrium between solution and more than one mineral, a mineral buffer. In Box 14.1 a convenient methodology has been outlined for writing and balancing reactions involving mineral buffers.

By considering reactions between one mineral and solution, the number of aqueous species will be equal to the number of components in that mineral plus H^+ (or OH^-), if the solubility is pH dependent. Consider again prehnite: from reaction (14.7), it is seen that the number of components in prehnite is three (Ca, Al and Si) in addition to H (or OH). When it dissolves, the reaction cannot be expressed by less than four aqueous species. By involving another mineral in the reaction it is possible to describe the reaction by one less species, etc.

14.1. AQUIFER CHEMISTRY

Quantitative assessment of the chemistry of the fluid in the aquifer of discharging wells should be routinely carried out for any geothermal project. It serves basically four purposes:

(1) identification of the temperature of producing aquifers;
(2) evaluation whether mineral–solution equilibria are closely approached and, if so, identification of the minerals involved;
(3) calculation of steam to water ratio in the aquifer;
(4) relating the concentrations of conservative components in the aquifer fluid with the physical aquifer conditions as deduced from the reactive components.

By using both water and steam geothermometers, it is possible to deduce with some confidence the temperature of producing aquifers. If all geothermometers compare well, this can be taken as evidence that there is basically one feed zone or, if there are more, they have about the same temperature. If, on the other hand, individual geothermometers give different results, this can be attributed to contributions to the well discharge from more than one aquifer of significantly different temperatures. Specifically, if H_2 temperatures give high values compared to other geothermometers, this indicates the presence of a substantial amount of steam in the aquifer beyond the zone of depressurization around the well (aquifer steam). If the steam geothermometers yield higher values than the water geothermometers, this can be taken to indicate some extra inflow of steam from deeper and hotter levels in the reservoir in relation to the water inflow.

Geothermometry results for wet steam wells from two geothermal fields, Berlin, El Salvador, and Krafla, Iceland, are given in Box 14.2. If the geothermometers all yield about the same value for the aquifer temperature, it is safe to conclude that the discharge is predominantly derived from one aquifer and the geothermometers define the temperature in that aquifer beyond the zone of extensive boiling. Discrepancy between geothermometers, on the other hand, indicates flow from more than one aquifer of significantly different temperatures. It must not be forgotten that faulty geothermometry calibration may contribute to discrepancy in the geothermometry results.

When wells have been discharging over a long period of time (many years), partial re-equilibration for some geothermometers may have occurred in the zone of depressurization around the well but not for others. This would cause a discrepancy in geothermometry results. Monitoring studies of well discharge chemistry (Chapter 16) would reveal whether or not this was the cause of discrepancy for a particular sample. Recharge of deeper and hotter or cold shallow water into the aquifer could also produce discrepancy in geothermometry results.

14.2. EFFECTS OF BOILING AND COOLING

When a geothermal water above 100°C rises in a well, it will start to boil when the pressure has been sufficiently reduced to bring it to boiling point. Boiling causes essentially two changes in fluid composition: (1) degassing of the water and (2) an increase in its dissolved solids content. Two gases (CO_2 and

H_2S) which are invariably major components in geothermal fluids, at least, when above about 200°C, form weak acids when dissolved in water. Their removal from the water will cause its pH to increase.

Many minerals, such as calcite, hydroxides and all OH bearing silicates, have pH dependent solubility. Increase in the water pH and in the concentrations of dissolved solids upon boiling as well as cooling all lead to changes in the state of mineral saturation of the water.

Cooling without boiling, whether occurring in the wellbore, surface equipment or after disposal, also leads to changes in pH because the dissociation constants of the acids buffering geothermal water pH change with temperature. If boiling and/or cooling of a geothermal fluid results in supersaturation for specific minerals, these minerals tend to precipitate. This says, however, nothing about the rate of deposition.

Assessment of changes in mineral saturation upon boiling and cooling of geothermal waters has practical applications. It is useful to evaluate scaling tendencies, in production wells, injection wells, surface equipment and mineral deposition on the surface, if waste water is disposed of in such a way (Boxes 14.3 and 14.4). Such an assessment should always be made when geochemical data on fluid composition from exploration wells become available. The assessment should be updated as data from new wells become available and as more data accumulate during long term production.

14.3. ERRORS IN CALCULATION OF SATURATION INDICES

Calculating reaction quotients for specific reactions and comparing them with the equilibrium constants, one may virtually obtain the same value for both, in which case the conclusion to be made is obvious: equilibrium exists. It is, however, most common that the calculated $\log Q$ value differs somewhat from the $\log K$ value. The question often asked is: How much difference is significant? There is no simple answer to this question. The accuracy to which equilibrium constants are known differs much among minerals. The same applies to the reaction quotient. Although an aqueous speciation programme provides values for both reaction quotients and equilibrium constants, it says nothing about the errors involved in retrieving both of them. The program user must for himself judge the meaning of the numbers produced by the program.

There are many sources of error involved in the calculation of both $\log Q$ and $\log K$. They can be classified into several groups:

(1) Error in the thermodynamic database of the speciation program, both with respect to solubility constants and dissociational equilibria.
(2) Error in selected reference temperature (valid when one is trying to assess mineral–solution equilibria in producing aquifers of wells or hot springs).
(3) Error in the calculation of aquifer fluid composition from data on water and steam samples collected from wet steam wells. This is complex in cases when extensive boiling occurs in producing aquifers and an 'excess' discharge enthalpy results.
(4) Mixed water is discharged. Here the selection of a particular reference temperature is not valid. The selection of reference temperature is an approximation at its best.
(5) Error in chemical analysis.

It cannot be expected that the user of an aqueous speciation program is familiar with the thermodynamic database that goes into the program. The crude guidelines that are given below are only valid for the WATCH speciation program (Arnórsson et al., 1982) because one of us is familiar with the thermodynamic database in that program. For simple minerals such as calcite, quartz, chalcedony, fluorite and anhydrite, solubility is accurately known, within 0.1–0.2 log K units. Thus, if no other errors are involved, the conclusion of equilibrium existing is only safe if the difference between log Q and log K is within 0.1–0.2 log units. For complex Al silicates, uncertainties in calculated log K values are frequently of the order of 0.5 log units and even higher, which corresponds to about 3000 J/mole at 25°C.

The best way of analysing the influence of the selected reference temperature on the calculated saturation mineral is to calculate aqueous speciation over a range of temperatures in order to see how the results vary with the selected aquifer temperature. An example is given for anhydrite, calcite and quartz in Fig. 14.1. The same kind of approach is also valid for assessing errors in calculated aquifer water compositions and analytical imprecision. Let us first consider aquifer water compositions. It is frequently assumed that the 'excess' enthalpy of wet steam well discharges is caused by segregation of the water and steam flowing through the aquifer to the well (Chapter 15). When this is the case, it is a satisfactory approximation to calculate aquifer water compositions by assuming liquid enthalpy. If it is uncertain whether this is so and it is thought that the 'excess' enthalpy is partly or totally due to heat flow from the rock, a test can be run involving calculation of mineral saturation indices for a series of discharge

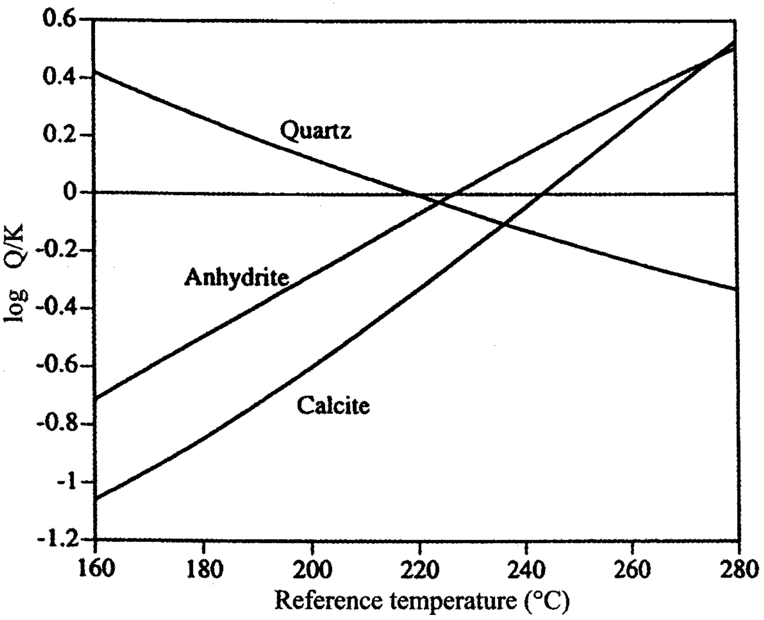

FIG. 14.1. Calculated state of saturation of quartz, calcite and anhydrite for water from well 23 at Momotombo, Nicaragua, as a function of the selected reference (aquifer) temperature.

enthalpy values. An example involving anhydrite, calcite and quartz is shown in Fig. 14.2.

The effect of analytical imprecision on log *Q* can be evaluated by simply modifying the concentration values for individual components. Generally, the parameter that is of most concern is pH but, to our knowledge, the values of gas concentrations in steam are also often of concern. Another method of studying this is to look at geochemical data from the same well that are bound to show some variation in analytical results and to see how the log *Q* values vary in relation to log *K* (Fig. 14.3).

The distribution of data points on a mineral saturation diagram for many waters from a particular area is useful to obtain an overall impression of the state of equilibrium of these waters with selected minerals. The overall picture obtained from this distribution may generate convincing results although it may not be

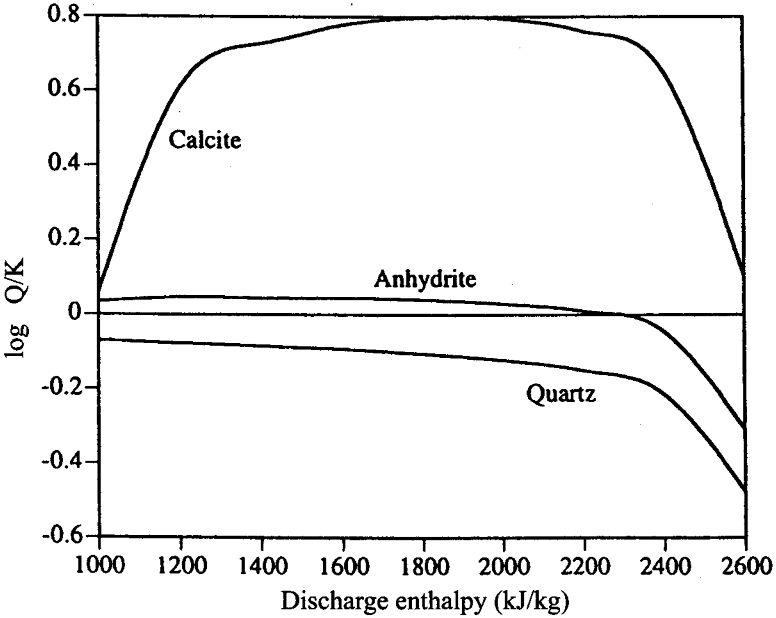

FIG. 14.2. Variation in calculated saturation state for calcite, anydrite and quartz in the aquifer of well 2 at Momotombo, Nicaragua, in relation to selected discharge enthalpy. It was assumed that the total discharge composition represents the reservoir fluid. The NaK geothermometer was taken to represent the aquifer temperature (229°C). It corresponds to an enthalpy of steam saturated water of 986 kJ/kg. The measured enthalpy of the well discharge is 2240 kJ/kg. The results suggest that the 'excess' enthalpy is largely due to phase segregation in the aquifer.

possible to conclude from chemical data on individual waters whether they are undersaturated, supersaturated or at equilibrium with specific minerals (Box 14.5).

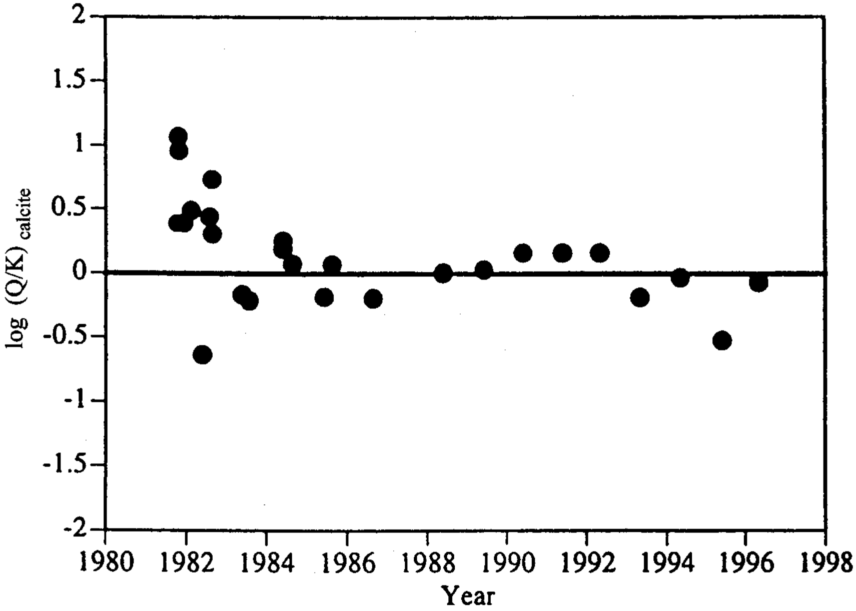

FIG. 14.3. Calculated state of calcite saturation in the aquifer of well 17 at Krafla, Iceland, for samples collected in the period of 1980 to 1996.

BOX 14.1. METHODOLOGY OF WRITING BALANCED REACTIONS INVOLVING MINERAL BUFFERS AND AQUEOUS SOLUTION

As an example, consider first a reaction involving clinozoisite, prehnite, quartz, calcite and solution. The procedure for writing a balanced reaction involves the following steps:

(1) Write the dissolution reaction for individual minerals. For the more complex silicates, this is done by
   (a) disproportionating the mineral into the chosen aqueous species;
   (b) adding H^+ to balance charges;
   (c) adding water on the left or right hand side to balance hydrogen;
   (d) finally, checking if oxygen balances (this should be so).

For clinozoisite, the reaction is:

$$\begin{aligned} &Ca_2Al_3Si_3O_{12}(OH) + H^+ + 11H_2O \\ &\quad = 2Ca^{2+} + 3Al(OH)_4^- + 3H_4SiO_4^0 \end{aligned} \tag{1}$$

Other mineral–solution reactions are:

$$\begin{aligned} &Ca_2Al_2Si_3O_{10}(OH)_2 + 2H^+ + 8H_2O \\ &\quad = 2Ca^{2+}2Al(OH)_4^- + 3H_4SiO_4^0 \end{aligned} \tag{2}$$

$$SiO_2 + 2H_2O = H_4SiO_4^0 \tag{3}$$

$$CaCO_3 + 2H^+ = Ca^{2+} + CO_2 + H_2O \tag{4}$$

(2) Eliminate the Al species by multiplying reaction (1) by 2 and reaction (2) by 3. Subtract the latter from the former. This yields:

$$\begin{aligned} &2Ca_2Al_3Si_3O_{12}(OH) + 2Ca^{2+} + 3H_4SiO_4^0 \\ &\quad = 3Ca_2Al_2Si_3O_{10}(OH)_2 + 4H^+ + 2H_2O \end{aligned} \tag{5}$$

(3) Eliminate aqueous silica by multiplying reaction (3) by 3 and adding it to reaction (5), which leads to:

$$\begin{aligned} &2Ca_2Al_3Si_3O_{12}(OH) + 3SiO_2 + 2Ca^{2+} + 4H_2O \\ &\quad = 3Ca_2Al_2Si_3O_{10}(OH)_2 + 4H^+ \end{aligned} \tag{6}$$

BOX 14.1. (cont.)

(4) Multiply reaction (4) by 2 and add it to reaction (6) to eliminate both calcium ion and H^+:

$$2Ca_2Al_3Si_3O_{12}(OH) + 3SiO_2 + 2CaCO_3 + 2H_2O$$
$$= 3Ca_2Al_2Si_3O_{10}(OH)_2 + 2CO_2 \qquad (7)$$

or

$$2\text{clinozoisite} + 3\text{quartz} + 2\text{calcite} + 2H_2O = 3\text{prehnite} + 2CO_2 \qquad (7a)$$

It may be read from reaction (6) that simultaneous equilibrium between clinozoisite, prehnite, quartz and solution fixes the activity ratio of calcium ion to protons. In other words, the equilibrium constant for a reaction involving clinozoisite, prehnite, quartz and solution is equal to the activity of Ca^{2+} divided by the activity squared of H^+. By adding calcite to the mineral buffer, reaction (7) shows that the equilibrium constant is equal to the activity of carbon dioxide in the second power, i.e. equilibration between this buffer and solution would fix the aqueous CO_2 activity.

Some reactions involve oxidation of some components and reduction of others. Consider now a reaction involving epidote, prehnite, pyrite and pyrrhotite. In epidote, iron is trivalent whereas in both pyrite and pyrrhotite it is divalent. Sulphur is monovalent in pyrite but divalent in pyrrhotite as well as in H_2S. Reactions involving these minerals, thus, involve reduction–oxidation of iron and sulphur:

(1) First write a half-cell reaction involving dissolution of pyrite and consumption of electrons, i.e. reduction of sulphur in pyrite to H_2S:

$$FeS_2 + 2e^- + 4H^+ = Fe^{2+} + 2H_2S \qquad (8)$$

The number of electrons is easily found by counting the number of atoms being reduced and multiplying by the change in the valence.

(2) Next write a half-cell reaction involving oxidation, in this case oxidation of divalent iron to trivalent, i.e. generation of electrons:

$$Fe^{2+} = Fe^{3+} + e^- \qquad (9)$$

BOX 14.1. (cont.)

(3) Adding up reactions (8) and (9) yields

$$FeS_2 + e^- + H^+ = Fe^{3+} + 2H_2S \qquad (10)$$

Reaction (10) is a half-cell reaction because it contains electrons. There are several possibilities to add another half-cell reaction to eliminate the electrons, thus retrieving an overall oxidation–reduction reaction. One could, e.g., add disproportionation of hydrogen gas into hydrogen ion and an electron. Here, we are interested in incorporating pyrrhotite. An appropriate half-cell reaction involving dissolution of that mineral would be

$$FeS + 2H^+ = Fe^{3+} + H_2S + e^- \qquad (11)$$

(4) By adding up the two half-cell reactions (10) and (11), an overall oxidation–reduction reaction involving pyrite and pyrrhotite is obtained:

$$FeS + FeS_2 + 6H^+ = 2Fe^{3+} + 3H_2S \qquad (12)$$

Mineral–solution reactions involving epidote and prehnite are given by

$$\begin{aligned}&Ca_2Al_2FeSi_3O_{12}(OH) + H^+ + 11H_2O\\ &\quad = 2Ca^{2+} + 2Al(OH)_4^- + Fe^{3+} + 3H_4SiO_4^0 \qquad (13)\end{aligned}$$

and

$$\begin{aligned}&Ca_2Al_2Si_3O_{10}(OH)_2 + 2H^+ + 8H_2O\\ &\quad = 2Ca^{2+} + 2Al(OH)_4^- + 3H_4SiO_4^0 \qquad (14)\end{aligned}$$

(5) Subtracting Eq. (14) from Eq. (13) eliminates the Al species, but also Ca and S, to give

$$\begin{aligned}&Ca_2Al_2Si_3O_{10}(OH)_2 + H_2O + Fe^{3+}\\ &\quad = Ca_2Al_2FeSi_3O_{12}(OH) + 3H^+ \qquad (15)\end{aligned}$$

To eliminate Fe^{3+}, multiply reaction (15) by 2 and add reaction (12) to it:

$$\begin{aligned}&FeS + FeS_2 + 2Ca_2Al_2Si_3O_{10}(OH)_2 + 2H_2O\\ &\quad = 2Ca_2Al_2FeSi_3O_{12}(OH) + 3H_2S \qquad (16)\end{aligned}$$

BOX 14.1. (cont.)

It can be read from reaction (15) that equilibrium between prehnite, epidote and solution fixes aqueous $Fe^{3+}/(H^+)^3$ ratios. Equilibrium between the mineral buffer pyrrhotite + pyrite + prehnite + epidote fixes aqueous H_2S activity.

From the following reaction involving pyrite and pyrrhotite

$$FeS_2 + H_2 = FeS + H_2S \qquad (17)$$

we see that pyrite–pyrrhotite equilibrium fixes aqueous H_2S/H_2 ratios.

(6) By multiplying reaction (17) by 3 and subtracting from reaction (16), H_2S is eliminated, giving

$$\begin{aligned} &4FeS + 2Ca_2Al_2Si_3OH_{10}(OH)_2 + H_2O \\ &\quad = 2FeS_2 + 2Ca_2Al_2FeSi_3O_{12}(OH) + 3H_2 \qquad (18) \end{aligned}$$

Thus, at equilibrium the same mineral buffer would control aqueous H_2 activity as H_2S activity.

BOX 14.2. EVALUATION OF AQUIFER TEMPERATURE

Selection of aquifer temperatures for aqueous speciation calculations should be based on evaluation of geothermometry results and temperature logging in wells. The required temperature logging data include measurements during heating-up in order to locate potential feed zones as well as measurements after thermal stabilization of the well.

The tables below show geothermometry results for wet steam wells from two geothermal fields: Berlin, El Salvador, and Krafla, Iceland.

Geothermometry results (°C) for wet steam wells at Berlin, El Salvador

Well	NaK[a]	NaK[b]	NaKCa	Qtz	CO_2	H_2S	H_2	Mean[c]	Meas[d]
TR-1	202	178	200	206	193	231	197	203	205
TR-2	295	286	293	271	236	276	227	284	295
TR-3	267	261	263	275	233	270	234	267	293
TR-5	308	297	333	287	232	271	244	291	302
TR-9	294	280	281	232	252	268	230	270	275
TR-10	261	255	246	227	269	247	241	247	276

[a] Fournier (1979).

[b] Arnórsson et al. (1983b).

[c] Average of all geothermometers.

[d] Measured temperature at inferred main feed zone. From Martínez (1997).

Inspection of the results for Berlin show rather good comparison between all the geothermometers and the measured aquifer temperature in two wells (TR-1 and TR-10). Generally, the water and the H_2S steam geothermometers give similar results. The CO_2 and H_2 temperatures tend to be lower. This can be explained by assuming the aquifer water to be a little degassed relative to equilibrium. Except for two wells (TR-3 and TR-10), the measured aquifer temperature and the average of the geothermometry temperatures compare well. When the geothermometers give lower values than the measured aquifer temperature, this is taken to indicate that the feed zone is truly cooler than the aquifer temperature inferred from logging.

BOX 14.2. (cont.)

Geothermometry results (°C) for wet steam wells at Krafla, Iceland

Well	NaK[a]	NaKCa	Qtz	CO_2	H_2S	H_2	Mean[b]	Meas[c]
5	207	197	218	215	217	204	210	205
9	237	219	238	237	231	215	230	240
11	263	236	259	283	271	275	264	325
12	277	290	263	330	300	315	296	300
13	238	222	240	292	282	344		310
14	249	236	243	307	287	331		310
15	285	252	290	314	305	331	289	325
17	273	266	273	305	302	347	284	290
19	268	268	229	327	288	330		310
20	296	278	279	377	309	342		300
21	252	229	250	291	293	324	263	260
24	186	187	213	211	222	180	200	200
25	220	200	220	229	227	193	215	185
26	301	275	297	330	310	325	306	320

[a] Arnórsson et al. (1983b).

[b] CO_2 and H_2 temperatures have not been included in the mean when yielding anomalously high temperatures because of degassing of the magma heat source or presence of reservoir steam, respectively.

[c] Measured temperature at inferred main feed zone.

For Krafla all geothermometers compare reasonably well internally for some wells (5, 9, 24, 25 and 26) as well as with the measured aquifer temperature. With one exception, these wells are all shallow and relatively cool. For others, there is either internal discrepancy or discrepancy with measured aquifer temperature, or both. When H_2 temperatures are significantly higher than any other temperature (wells 13, 14, 15, 17, 19, 20 and 21), this is taken to indicate the presence of equilibrium steam in the aquifer. Sometimes CO_2 temperatures are also anomalously high (in particular well 20). This is attributed to rapid transfer of this gas from the magmatic heat source. This is also considered to be a special case for Krafla. In 1975, a volcanic episode in the area started that lasted for almost ten years. The content of CO_2 rose as much as 100 times in well discharges and fumaroles shortly after the first

BOX 14.2. (cont.)

volcanic outbreak, which was assumed to be caused by the degassing of a new batch of magma that had intruded at 3–7 km depth under the geothermal reservoir.

For some of the Krafla wells the H_2S geothermometer gives higher temperatures than the water geothermometers (wells 12, 13, 14, 21 and to a lesser extent wells 17 and 19). This is considered to be due to a contribution to the well discharge from two feed zones, a deeper and hotter steam rich zone and a shallower and cooler water rich zone. When the aquifer temperature, as inferred from logging measurements, is significantly higher than both the water and H_2S geothermometer temperatures, it is assumed that a portion of the discharged fluid comes from feed zones at levels higher than that of the main aquifer according to logging results.

BOX 14.3. CHANGES IN MINERAL SATURATION UPON ADIABATIC BOILING OF GEOTHERMAL WATERS

Calcite scaling is common in geothermal production wells. Silica deposition is also of concern if geothermal waters cool sufficiently through boiling to make them amorphous silica supersaturated. Occasionally, anhydrite is also deposited in wells.

The figure below shows the state of saturation for anhydrite, calcite and amorphous silica as water entering well 3 at Zunil in Guatemala boils adiabatically. The reservoir water is taken to be at 270°C (dots in the figure). It can be seen from the figure that the reservoir water is somewhat calcite supersaturated but anhydrite and amorphous silica undersaturated.

In calculating the state of calcite saturation for the aquifer of wet steam wells it is common to obtain values which deviate by at least 0.3 log *Q/K* units from equilibrium. It is assumed that high temperature geothermal waters easily attain equilibrium with calcite and calculated departure from equilibrium is not real but due to various sources of error, such as that involved in selecting the aquifer temperature. Contribution to the well flow from more than one aquifer and the mechanism of boiling may also contribute.

Upon boiling, the well water from Guatemala becomes calcite supersaturated (see the figure below). The degree of supersaturation reaches a maximum at about 245°C. After this, cooling by further boiling leads to a diminishing degree of supersaturation, and below 150°C the water becomes undersaturated. An increasing degree of supersaturation during the early stages of boiling is due to CO_2 degassing, whereas decreasing supersaturation at lower temperatures and finally undersaturation results from the retrograde solubility of calcite. Degassing dominates during the early stages of boiling but after the water has been largely degassed increasing calcite solubility with decreasing temperature takes over.

The cooling, which results from boiling, causes the water to become progressively more anhydrite undersaturated, as a result of the retrograde solubility of this mineral. The reverse is true for amorphous silica because its solubility decreases with decreasing temperature. At 150°C, saturation is reached. Amorphous silica deposits rather easily from supersaturated solution. Thus, amorphous silica can be expected to deposit from the water from well 3 at Zunil if it cools by boiling below 150°C.

BOX 14.3. (cont.)

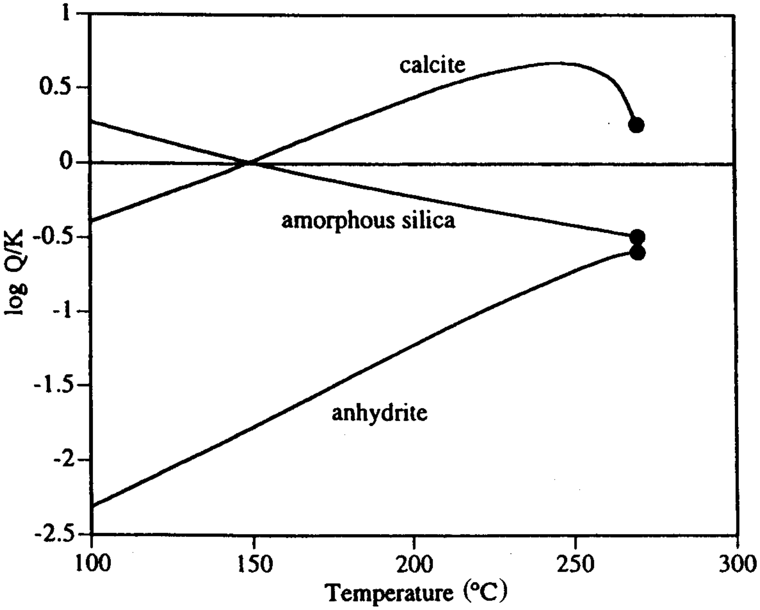

The state of saturation of water from well 3 at Zunil, Guatemala, with respect to anhydrite, calcite and quartz during adiabatic boiling.

BOX 14.4. CHANGES IN MINERAL SATURATION OF BOILED GEOTHERMAL WATER AS IT CONDUCTIVELY COOLS FURTHER OR GAINS HEAT

It is common practice to dispose of waste geothermal fluid by injection, either into shallow or deep drillholes. Such drillholes may be located within production wellfields or outside, even outside the geothermal field. If the water is disposed of by injection into shallow drillholes, it may be expected to cool further. On the other hand, if injected into deep wells, it may gain heat. The temperature changes may bring about supersaturation with respect to some minerals, thus creating a tendency for them to deposit from the water. It is important to assess the state of mineral saturation in waste geothermal fluid that is intended to be disposed of by injection in order to find out the optimum temperature for injection.

The first diagram in this box shows how the state of saturation for amorphous silica, calcite and anhydrite changes for the water injected into well RM-18 at Momotombo Geothermal Field, Nicaragua. The water to be disposed of has been separated in wellhead separators at a pressure of about 6 bar abs., which corresponds to a temperature of 160°C for steam saturated water. It is seen from this figure that the water is supersaturated with respect to amorphous silica below 120°C but undersaturated at higher temperatures. The situation is the reverse for calcite. The water reaches saturation when heated to 160°C. At lower temperatures, it is undersaturated, and the degree of undersaturation increases with falling temperature. The situations for amorphous silica and calcite are, therefore, opposite. This is due to the retrograde and prograde solubilities of calcite and amorphous silica, respectively.

Anhydrite behaves similarly to calcite because its solubility is also retrograde, i.e. the solubility increases with decreasing temperature. If the water is injected into hot rock so that it gains heat in excess of 210°C, anhydrite saturation is reached but below this temperature undersaturation prevails.

In the range of 120–160°C, the water is undersaturated with respect to all the minerals. An injection temperature in this range is, therefore, to be recommended.

BOX 14.4. (cont.)

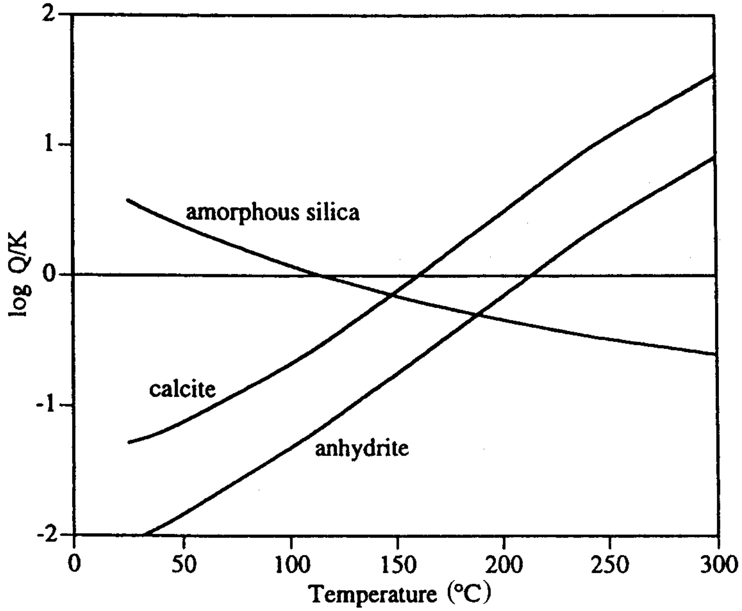

Mineral saturation versus temperature for water injected into well RM-18 at Momotombo.

BOX 14.4. (cont.)

The second diagram in this box shows the state of low albite saturation as a function of temperature. It is indicated that the water is strongly supersaturated with respect to this mineral except at the highest temperatures. This is not only the case at Momotombo, but the general rule for boiled high temperature geothermal waters. Yet, albite deposition is not known to be a problem in geothermal wells. The same applies to many other silicates and quartz. The reason is assumed to be slow kinetics for the deposition of these minerals. Amorphous silica, calcite and anhydrite, on the other hand, precipitate readily from supersaturated solution, at least when above about 100°C.

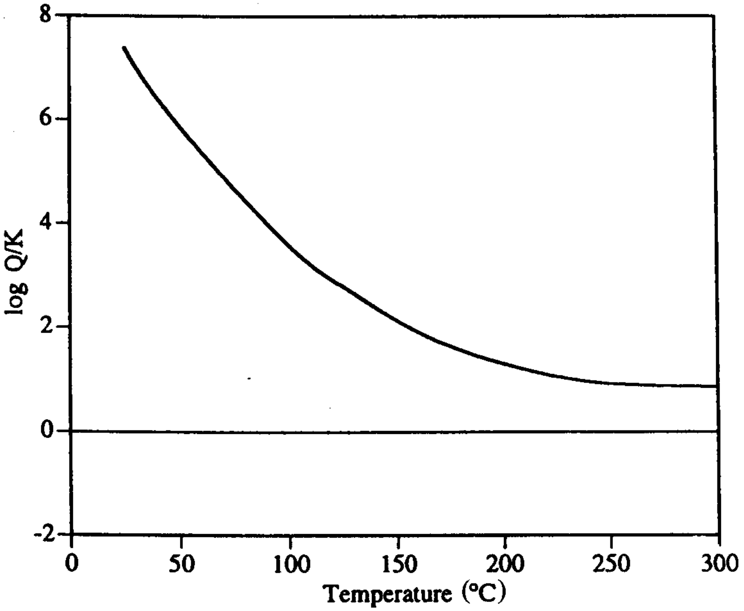

Albite saturation versus temperature for water injected into well RM-18 at Momotombo.

BOX 14.5. EVALUATION OF MINERAL–SOLUTION EQUILIBRIA

The calculated state of saturation for plagioclase of labradorite composition (60% anorthite), low albite and microcline is shown in the three figures in this box for natural waters from Skagafjördur, northern Iceland. All the waters are sub-boiling so that the evaluation of saturation involves water with the composition of the sample.

The overall pattern of the data indicates that the waters are undersaturated with labradorite, the plagioclase of the basaltic Miocene lava succession in this area. The results indicate that the plagioclase is unstable and would accordingly tend to dissolve in the water with which it is interacting. By contrast, the waters are supersaturated with low albite (the albite is stable at low temperatures), except for some river waters that have reacted with the soil and rock to a very limited extent. Low albite, a very common secondary mineral in geothermal systems, would tend to precipitate from waters that are supersaturated with respect to it. It appears that the degree of albite supersaturation is highest for the waters of the lowest temperature. Supersaturation decreases with rising temperature, which may be due to a kinetic effect. A higher degree of supersaturation builds up at lower temperatures because of lower rates of precipitation. The picture for microcline is just the same as that for low albite.

BOX 14.5. (cont.)

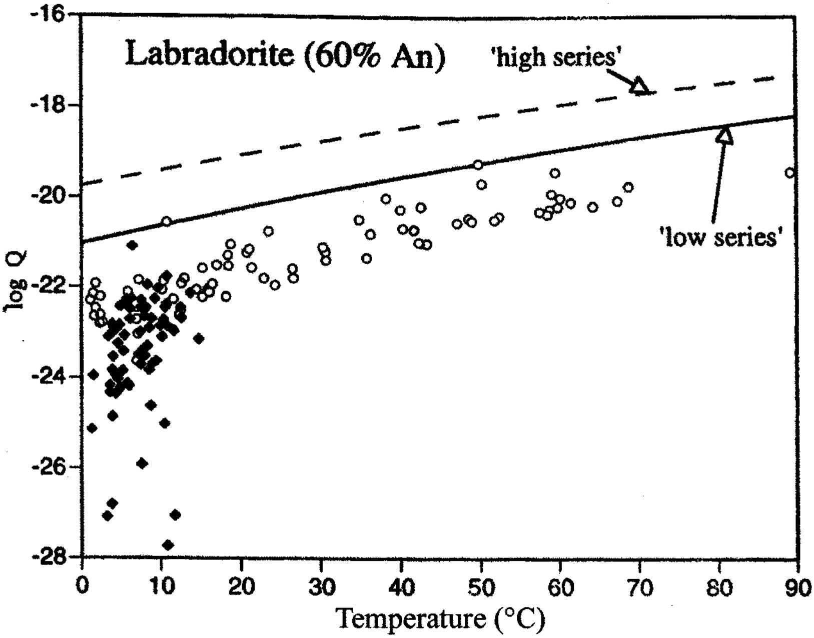

The state of plagioclase (labradorite) saturation in surface (diamonds) and groundwaters (circles) in natural waters in Skagafjödur, N. Iceland. 'High series' denotes disordered plagioclase and 'low series' partly ordered one (see text in this box).

15. ESTIMATION OF AQUIFER STEAM FRACTION

Stefán Arnórsson and Franco D'Amore

15.1. GENERAL REMARKS ON BOILING IN GEOTHERMAL SYSTEMS

In some geothermal systems liquid water forms a continuous phase. Such systems are said to be liquid dominated. Pressure in these systems is hydrostatic. In other systems the continuous fluid phase is vapour. Such systems are said to be vapour dominated. Pressure in these systems is hydrostatic. In other systems the continuous fluid phase is vapour. Such systems are said to be vapour dominated. Pressure is about constant in these systems because of the low density of the vapour. Vapour dominated systems are much less abundant than the liquid dominated ones, the ratio probably being 1 in 20 (White et al., 1971) .Evidence indicates that vapour fills the permeable fractures and cracks in vapour dominated systems but smaller pores are filled with liquid water. Under natural conditions, boiling in liquid dominated geothermal systems occurs by pressure drop. Rising fluid boils because its hydrostatic head is reduced but also because conductive heat loss is not sufficient to maintain subboiling conditions.

The temperature and enthalpy (steam to water ratios) of fluids in geothermal reservoirs not disturbed by exploitation is determined by the combined effects of two processes, the rate of heat transfer to the advecting fluid and the flow rate of this fluid through the system. If the heat transfer, in relation to the fluid flow, is high enough, the water will be heated to the boiling point and the reservoir fluid becomes two phase, i.e. both steam and water are present.

Two phase geothermal systems are hydrologically unstable. The steam tends to rise faster than the water because of its lower density (buoyant force). The extent of this gravity segregation depends on the rock permeability. Steady state develops when the amount of steam generation equals that of steam which rises to the surface. The steam fraction at each level in the reservoir depends on its rate of generation, condensation and permeability. Groundwater systems where hotter water underlies colder groundwater are also unstable; in this case, the hot water will tend to rise. The rate of advection depends on the geothermal gradient and permeability.

The temperature at which water boils increases with pressure (Fig. 15.1). At atmospheric pressure pure water boils at 100°C, as everybody knows. At the critical point (374°C), the boiling point is at 229 bar. Above the critical point only one fluid H_2O phase exists. In geothermal investigations it has been common

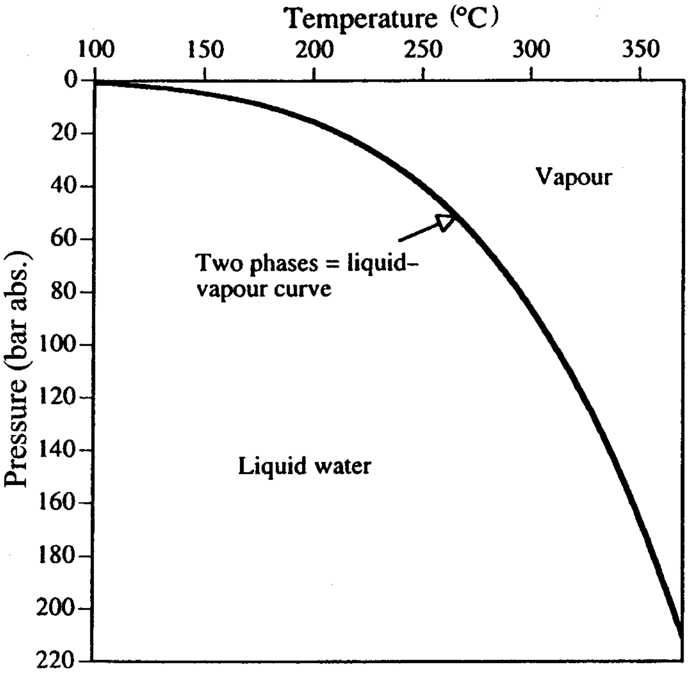

FIG. 15.1. Liquid–vapour curve for H_2O.

practice to express the pressure dependence of the boiling point in terms of depth (Fig. 15.2). In doing so, the pressure at each depth corresponds to that exerted by a water column which is at the boiling point at all depths. The curve is called the boiling point curve, occasionally the boiling point curve with depth or simply liquid–vapour curve.

In general, water boils when its 'internal' pressure equals the external pressure. In geothermal waters, the largest contribution to the internal pressure comes from the vapour pressure. However, gases dissolved in the liquid phase may also contribute to its internal pressure, thus decreasing the temperature of the boiling point at any external or hydrostatic pressure. In some geothermal systems which contain high gas, this effect of dissolved gases may be quite significant. Water salinity has the opposite effect by reducing vapour pressure at any temperature, thus increasing the temperature of the boiling point at any hydrostatic pressure (depth).

Geothermal systems with temperatures higher than the atmospheric boiling point temperature (100°C at 1 bar) will be two phase, down to a depth where the

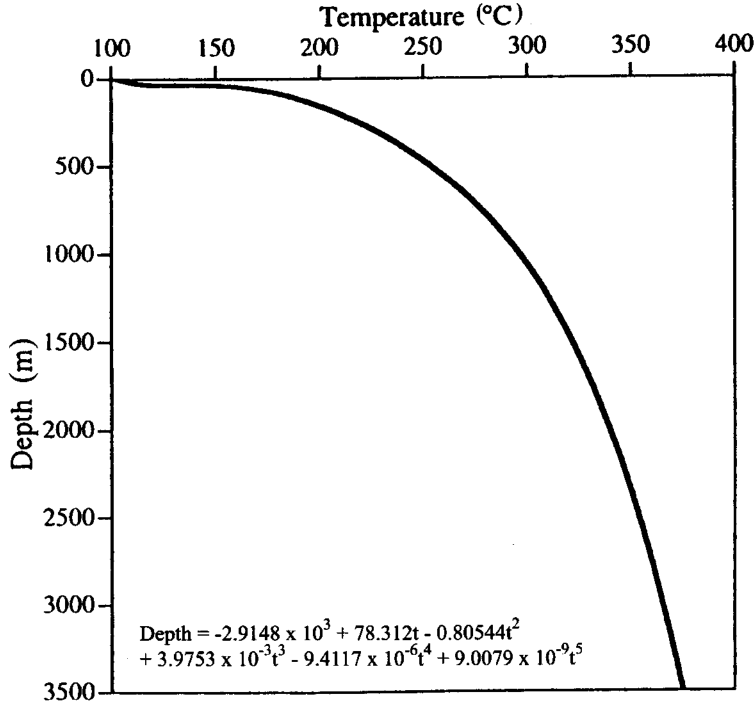

FIG. 15.2. Boiling point curve with depth. The equation in the figure describes well the curve in the range 150–370°C.

hydrostatic, or external, pressure becomes greater than the internal pressure. If the geothermal groundwater table coincides with the surface, Fig. 15.2 can be used to estimate the depth at which boiling starts for a given reservoir temperature. Geothermal systems may be two phase to the critical point. At temperatures below the critical point, temperature is dictated by pressure but above the critical point these two variables are independent.

Although boiling in the upflow of geothermal systems is considered to occur by pressure drop under natural conditions, this is not necessarily the case under highly disturbed conditions in the aquifer of discharging wells. When a well is discharged a pressure drop is induced in the formation around the well. The three dimensional shape of the pressure drawdown depends on the spatial distribution of permeability and may be very complex in fractured rocks with highly anisotropic permeability. Extensive pressure drop in the aquifer of a producing well causes cooling of the water and steam flowing through the aquifer towards the well. One can expect the aquifer rock to be hotter than the flowing fluid, thus creating a tendency for heat to flow from the rock to that fluid. Since the water in the fluid is boiling, any addition of heat to it will lead to enhanced vaporization, which is, of course, in addition to that caused by the pressure drop.

Water and steam have different flowing properties. Hence, water and steam flowing together towards a producing well may segregate; the water lags behind but the steam flows preferentially into the well. Phase segregation may cause the discharge of wells to turn into dry steam.

15.2. EQUILIBRIUM STEAM

Geochemical methods have been developed to estimate the steam to water ratios in geothermal reservoirs or, to be more precise, the steam to water ratio in the aquifer of producing wells beyond the zone of depressurization that forms as a result of mass withdrawal from the aquifer by the producing wells. The steam fraction beyond the depressurization zone, which corresponds to undisturbed or natural conditions, has been termed initial steam fraction to distinguish it from higher steam fractions at lower pressures within the depressurization zone. There are essentially two approaches. One assumes that the total discharge composition of wells is representative of the aquifer fluid (D' Amore and Celati, 1983). The other approach considers that both heat transfer from rock and phase segregation may contribute to the discharge enthalpy of wells (Arnórsson et al., 1990). If phase segregation occurs the composition of the total well discharge will differ from that of the initial aquifer fluid. The first model really assumes that 'excess' enthalpy of well discharges is only caused by heat flow from the rock to the fluid flowing into the well.

The initial steam fraction in the aquifer, or changes in it during production, provides various information on the reservoir characteristics. It is expected to be highest in major upflow zones. It may change in response to enhanced recharge into the reservoir as a result of exploitation. Together with porosity, estimation of initial steam fractions in aquifers of geothermal reservoirs, i.e. steam to water ratios, provide information required to evaluate the quantity of heat stored in a given volume of reservoir fluid. When interpreting data on the gas composition of well discharges it is generally assumed that equilibrium distribution of the gaseous component is attained in the aquifer between the liquid and vapour phases and that specific gas–gas or mineral–gas equilibria prevail in the aquifer beyond the zone of depressurization around producing wells. On the basis of these assumptions, the initial aquifer steam has been called equilibrium steam.

15.3. NOTATIONS ON GEOTHERMAL GAS CHEMISTRY

The mole fraction of gas i in steam, C_i^v, is defined as

$$C_i^v = \frac{n_i}{n_{H_2O} + n_i + \sum_j n_j} \tag{15.1}$$

where n_i and n_j stand for the number of moles of gas i and the jth gas in the steam and n_{H_2O} is the number of moles of steam. As the total number of moles of gases in geothermal steam is usually much smaller than the number of moles of H_2O, it is a satisfactory approximation to take

$$C_i^v \approx \frac{n_i}{n_{H_2O}} \tag{15.1a}$$

The mole fraction of a gas in liquid water is, of course, defined in the same way.

Gas solubility in water is described by Henry's law coefficient:

$$P_i = Kh_i C_i^l \tag{15.2}$$

TABLE 15.1. TEMPERATURE EQUATIONS FOR THE SOLUBILITY CONSTANTS ($K_{s,l}$) FOR COMMON GEOTHERMAL GASES.
See Eq. (15.2a) for the definition of $K_{s,i}$. (From Arnórsson et al. (1996).)

Gas	log K_s (T in kelvin)
CO_2	$-59.612 + 3448.59/T - 0.68640 \times 10^{-6}T^2 + 18.847\log T$
H_2S	$-68.775 + 3673.08/T - 4.07153 \times 10^{-6}T^2 + 22.561\log T$
H_2	$-25.260 + 1355.28/T + 4.11147 \times 10^{-6}T^2 + 6.966\log T$
CH_4	$-78.894 + 3962.05/T - 0.80325 \times 10^{-6}T^2 + 25.385\log T$
N_2	$-55.857 + 2947.41/T + 2.68428 \times 10^{-6}T^2 + 17.191\log T$
O_2	$-68.820 + 3412.65/T - 1.14239 \times 10^{-6}T^2 + 22.055\log T$
Ar	$-62.606 + 3136.06/T - 1.00993 \times 10^{-6}\mathrm{T}^2 + 19.931\log T$

where P_i denotes the partial pressure of gas i, C_i^l its mole fraction in the liquid water phase and Kh_i Henry's law coefficient. Sometimes Henry's law coefficient, i.e. the solubility constant for gas i, $K_{s,i}$, is defined as:

$$K_{s,i} = \frac{m_i}{P_i} \tag{15.2a}$$

where m_i represents the concentration of gas i dissolved in liquid water in moles/kg and P_i is the partial pressure of gas i as before. The units of $K_{s,i}$ are mole·kg^{-1}·bar^{-1}, whereas those of Kh_i are bar moles H_2O moles/gas. In the following discussion, we will use Kh_i unless otherwise indicated. The temperature equations for K_s for common geothermal gases are given in Table 15.1.

The distribution coefficient, B_i, for gas i between liquid water and steam is defined as:

$$B_i = \frac{C_i^v}{C_i^1} \tag{15.3}$$

where C_i^v and C_i^l have the same notations as in Eqs (15.1) and (15.2), respectively. By consideration of Raoult's law,

$$P_i = C_i^v \mathrm{P}_t \tag{15.4}$$

the relationship between B_i and Kh_i can be derived. P_t in Eq. (15.4) stands for the total pressure defined as

$$P_t = P_i + P_{\mathrm{H_2O}} + \sum_j P_j \tag{15.5}$$

The second and third terms on the right hand side of Eq. (15.5) stand for vapour pressure and the sum of the partial pressures of gases present in addition to gas i. Combination of Eqs (15.2) to (15.4) yields the following relationship between B_i and Kh_i:

$$B_i = \frac{Kh_i}{P_t} \tag{15.6}$$

In line with the approximation described by Eq. (15.1a), Eqs (15.4) and (15.6) should be expressed as

$$P_i = C_i^v P_{\mathrm{H_2O}} \tag{15.4a}$$

TABLE 15.2. TEMPERATURE EQUATIONS FOR DISTRIBUTION COEFFICIENTS (B_l) FOR SOME COMMON GEOTHERMAL GASES; B_l IS IN BARS MOLES H_2O MOLES/GAS; T REPRESENTS THE TEMPERATURE IN CENTIGRADES

(From D' Amore and Truesdell (1988).)

	Range
$\log B_{H_2S} = 4.04417 - 0.009798t$	150–320
$\log B_{CO_2} = 4.7695 - 0.010960t$	150–320
$\log B_{H_2} = 5.9681 - 0.013301t$	150–320
$\log B_{CH_4} = 6.0809 - 0.013875t$	150–320
$\log B_{N_2} = 6.3433 - 0.013753t$	150–320
$\log B_{NH_2} = 1.6019 - 0.004017t$	150–320
$\log B_{CO} = 6.2865 - 0.013729t$	150–320

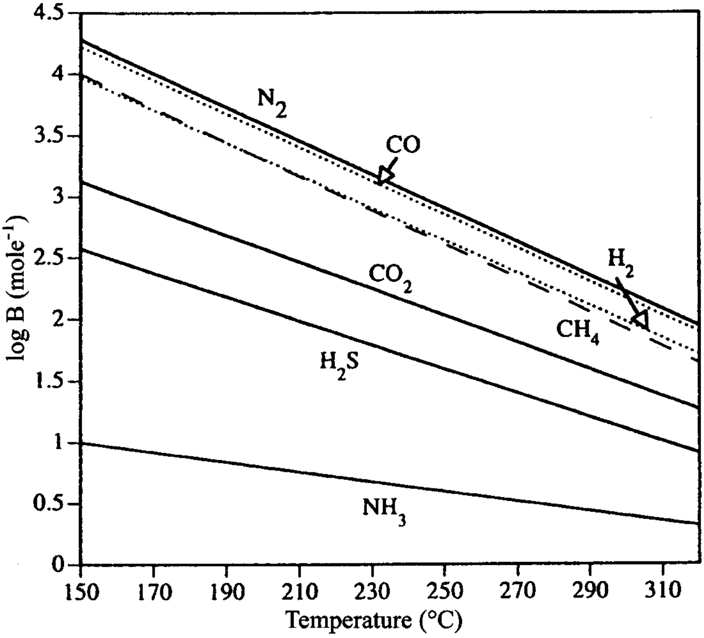

FIG. 15.3. Temperature dependence of the distribution coefficient, B, of some common gases in geothermal fluids.

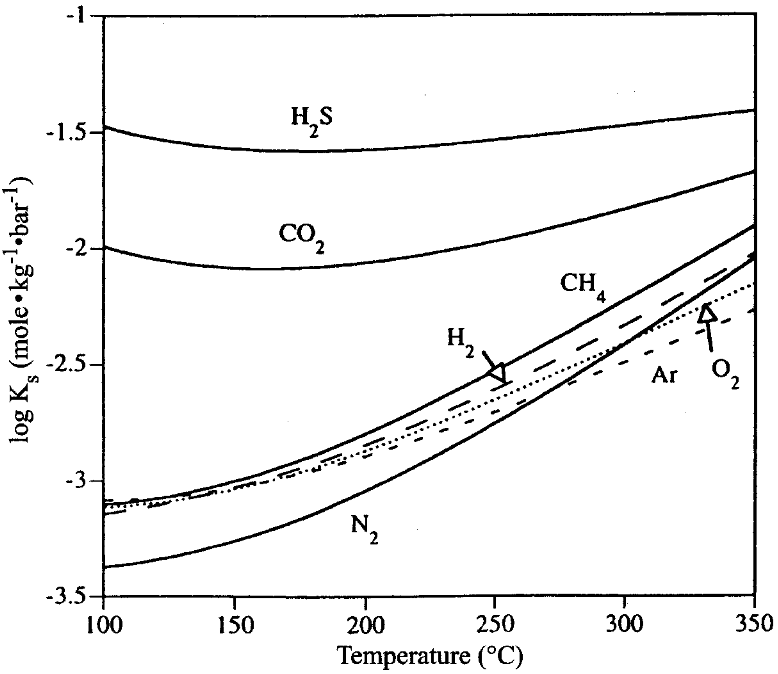

FIG. 15.4. Temperature dependence of the solubility constants (Henry's law coefficients) for some common gases in pure water (from Arnórsson et al. (1996)).

and

$$B_i = \frac{Kh_i}{P_{H_2O}} \tag{15.6a}$$

Values for B_i as defined by Eq. (15.6a) are given in Table 15.2 and depicted in Fig. 15.3. The temperature dependence of some gas solubility constants is shown in Fig. 15.4. The B_i values in Table 15.2 are not consistent with those given for K_s in Table 15.1, because they are based on a different temperature equation for K_{h_i}. The logarithm of the K_{h_i} values used by D' Amore and Truesdell (1988) to retrieve the B_i values in Table 15.2 can be obtained by subtracting from the respective log B_i equation the equation for P_{H_2O}, according to Eq. (6) in Table 15.4.

For non-ideal behaviour of water vapour, Eq. (15.6a) becomes

$$Kh_i = B_i P_v \Gamma = B_i \frac{RT}{V_v} \tag{15.6b}$$

and

$$B_i = Kh_i \frac{V_v}{RT} \tag{15.6c}$$

where P_v and V_v stand for vapour pressure and vapour volume, respectively, Γ is the fugacity coefficient, R the gas constant and T the temperature in kelvin. When P is in bar, V is in cm^3/g and T in kelvin, R becomes 4.5589 g·K/cm^3.

The steam fraction of the aquifer fluid of geothermal systems is defined as

$$y = \frac{n^s}{n^s + n^w} \tag{15.7}$$

where n^s and n^w represent the numbers of moles of steam and water, respectively. Gases in the fluid will partition between the steam and water phases in relation to their solubility in the water. It is the different solubility constants that lead to different partitioning or distribution coefficients, which forms the basis of using the gas composition of well discharges to calculate the initial steam to water ratio in the producing aquifer.

From mass balance considerations, we have

$$C_i^d = yC_i^v + (1 - y)C_i^l \tag{15.8}$$

where the superscripts d, v and l indicate aquifer fluid and the vapour and liquid phases, respectively, and y designates steam fraction (by mass) as defined by Eq. (15.7). In general,

$$C_i^d = Y_i C_i^v + (1 - Y_i)C_i^l \tag{15.8a}$$

where Y_j designates the steam fraction at any particular pressure, such as sampling pressure. Combination of Eqs (15.3) and (15.8) by eliminating C_i^l, taking also the mole fraction of gas i in the total discharge at the wellhead, C_i^{WH}, to be equal to C_i^d, leads to

$$C_i^{WH} = C_i^v \left[y + \frac{1-y}{B_i} \right] \tag{15.9}$$

The term in the brackets is symbolized as A_i, i.e.

$$A_i = y + \frac{1-y}{B_i} \tag{15.10}$$

Equation (15.10) is valid for $y > 0$. It can be demonstrated that, for $y < 0$ (irreversible steam loss from a liquid), A_i is given by

$$A_i = \frac{1}{B_i(1+y-yB_i)} \tag{15.10a}$$

When combined, Eqs (15.4a) and (15.9) yield

$$\log P_i = \log C_i^{WH} + \log P_{H_2O} - \log A_i \tag{15.11}$$

For $y > 0$, A_i is designated by Eq. (15.10), but for $y < 0$, A_i is given by Eq. (15.10a). Equation (15.11) is a general expression relating the partial pressure of gas i in the aquifer to its measured concentration in samples collected at the wellhead, steam pressure and initial steam fraction (y) in the aquifer. We observe that both B_i and P_{H_2O} are functions of the aquifer temperature.

As will be discussed later in this chapter, it is often convenient for calculation of initial steam fractions, y, and aquifer temperature to obtain the ratio of gas partial pressures to CO_2, which is invariably the most abundant gaseous component in geothermal fluids, because analytical data sometimes give relative gas concentrations only but not their concentration in the steam. From Eq. (15.11) we see that

$$\log\left(\frac{P_i}{P_{CO_2}}\right) = \log\left(\frac{C_i^{WH}}{C_{CO_2}^{WH}}\right) - \log\left(\frac{A_i}{A_{CO_2}}\right) \tag{15.12}$$

or

$$\log P_i = \log\left(\frac{C_i^{WH}}{C_{CO_2}^{WH}}\right) + \log P_{CO_2} - \log A_i + \log A_{CO_2} \tag{15.12a}$$

To explain this further, let us consider the following reaction:

$$CH_4 + 2H_2O = CO_2 + 4H_2 \tag{15.13}$$

The equilibrium constant K_{FT}, for this reaction expressed in terms of partial pressures, is given by

$$K_{FT} = \frac{P_{CO_2} P_{H_2}^4}{P_{CH_4} P_{H_2O}^2} \tag{15.14}$$

Substituting Eq. (15.12a) into Eq. (15.14) and rearranging yields

$$4\log C_{H_2}^{WH} - \log\left(\frac{C_{CH_4}^{WH}}{C_{CO_2}^{WH}}\right) = \log K_{FT} - 2P_{H_2O} + \log A_{CO_2} + 4\log A_{H_2} - \log A_{CH_4} \tag{15.15}$$

The derivation of Eq. (15.11) was based on the assumption that well discharge compositions represent the aquifer fluid. In general we have:

$$\log P_i = \log C_i^d + \log P_{H_2O} - \log A_i \tag{15.16}$$

By taking the ratio of i to CO_2 (see Eq. 15.12a), we have

$$\log P_i = \log\left(\frac{C_i^d}{C_{CO_2}^d}\right) + \log P_{CO_2} - \log A_i + \log A_{CO_2} \tag{15.17}$$

For positive and negative values of y, A_i is given by Eqs (15.10) and (15.10a), respectively.

TABLE 15.3. CALCULATED OXYGEN PARTIAL PRESSURES FROM VARIOUS MINERAL BUFFERS. THE VALUES GIVEN ARE AS log P_{O_2} IN BAR.

t(°C)	HM	SW	MF	DG
200	–40.6		–45.3	–42.0
250	–35.4	–35.4	–40.0	–37.6
300	–31.1	–31.7	–35.7	–34.0
350	–27.5	–28.7	–32.0	–31.2

HM: haematite–magnetite buffer; see Eq. (15.19). SW: Sato and Wright (1966); valid for volcanic systems. MF: magnetite–fayalite buffer; see Eq. (15.20). DG: D' Amore and Gianelli (1984); based on drillhole data.

15.4. CALCULATION OF AQUIFER GAS PARTIAL PRESSURES

In Eq. (15.11) there are three variables, the partial pressure of gas i, aquifer temperature and the initial aquifer steam fraction, y. We observe that the aquifer temperature fixes the vapour partial pressure and the value taken by the distribution coefficient. Aquifer temperatures can usually be assessed by geothermometry or by direct measurement. This leaves two unknowns in Eq. (15.11). As will be discussed below, in this section the partial pressures of H_2 and H_2S are fixed by the aquifer temperature. Thus, y values can be estimated from data on the mole fraction of either of these gases in steam collected at the wellhead. In Section 15.5 of this chapter, it is shown that simultaneous consideration of two gas–gas or mineral–gas reactions permits the calculation of a value for y from an analysis of relative gas concentrations in well discharges for preselected aquifer temperature values. Use of three reactions allows both y and aquifer temperature to be estimated from relative gas concentrations.

Studies of dry and wet steam well discharge compositions indicate that oxygen partial pressures in geothermal systems are fixed by temperature and, therefore, by specific temperature dependent chemical equilibria. The calculated oxygen pressures are very low and far from being measurable. However, the thermodynamically calculated values are meaningful. Another way to express this observation, which is probably more logical, is to use an equation describing the temperature dependence of hydrogen gas partial pressures. Experimentally, H_2 partial pressure is measured and the O_2 partial pressure is calculated, assuming equilibrium according to the following reaction:

$$H_2O = H_2 + \frac{1}{2} O_2 \tag{15.18}$$

The same approach is taken in correlating O_2 partial pressures to the aquifer temperature of wells.

D' Amore and Gianelli (1984) proposed a temperature equation describing O_2 partial pressures in aquifers of geothermal systems, which is valid up to 400°C. It is based on data on the gas composition of drillhole discharges and aquifer temperature in several geothermal fields. This equation yields O_2 partial pressures which do not differ much from those calculated from the haematite–magnetite and magnetite–fayalite oxygen buffers (Table 15.3), i.e. O_2 pressures calculated assuming equilibrium according to the following reactions:

$$3Fe_2O_3 = 2Fe_3O_4 + \frac{1}{2} O_2 \tag{15.19}$$

and

$$3Fe_2SiO_4 = 2Fe_3O_4 + SiO_2 + O_2 \qquad (15.20)$$

On the basis of drillhole data, Arnórsson and Gunnlaugsson (1985) concluded that aqueous H_2 aquifer concentrations and, therefore, H_2 partial pressures correlated with the aquifer temperature because they were regulated by temperature dependent equilibria with hydrothermal minerals. Arnórsson et al. (1998b) provide a temperature equation for H_2 aqueous concentrations based on equilibrium between solution and the mineral buffer epidote + prehnite + pyrite + pyrrhotite. The proposed temperature equations relating H_2 partial pressures to aquifer temperature have been drawn up in Fig. 15.5(a). As can be seen from this figure, conformity is rather poor. This may partly be caused by involvement of different mineral buffers, and, in the case of the curves of Arnórsson and Gunnlaugsson (1985), to very high partial pressures at high temperatures (>300°C) due to the presence of equilibrium steam in the aquifer that was not taken into account when deriving the temperature equation. Yet, the available evidence indicates that H_2 partial pressures in geothermal systems are regulated by close approach to equilibrium with hydrothermal mineral buffers.

Drillhole data also indicate that S_2 partial pressures are fixed by temperature dependent mineral solution equilibria (D'Amore and Gianelli, 1984). In strongly reducing systems, simultaneous equilibrium between pyrite and pyrrhotite appears to be involved:

$$FeS_2 = FeS + \frac{1}{2} S_2 \qquad (15.21)$$

but equilibrium between pyrite and magnetite in less reducing systems can be expressed as:

$$\frac{1}{3} Fe_3O_4 + S_2 = FeS_2 + \frac{2}{3} O_2 \qquad (15.22)$$

D'Amore and Gianelli (1984) have proposed two temperature equations to describe S_2 partial pressures. One is valid for strongly reducing systems and the other for less reducing systems (Table 15.4). From the following equation:

$$H_2S = H_2 + \frac{1}{2} S_2 \qquad (15.23)$$

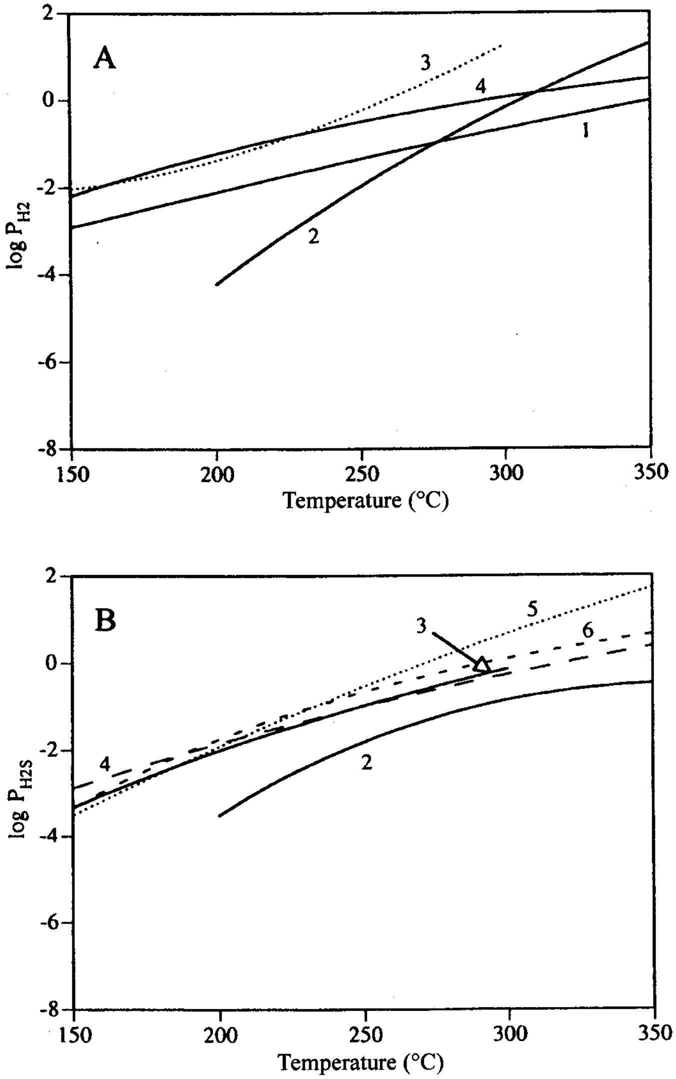

FIG. 15.5. Partial pressures of hydrogen and hydrogen sulphide versus aquifer temperature. (1) Amore and Gianelli (1984); (2) and (3) Arnórsson and Gunnlaugsson (1985); (2) is valid for all waters above 300°C and waters in the range of 200–300°C, if Cl > 500 ppm; (3) is valid for all waters below 200°C and waters in the range of 200–300°C, if Cl < 500 ppm; (4) Arnórsson et al. (1998); (5) and (6) D'Amore and Gianelli (1984) for very reducing and volcanic geothermal systems, respectively.

TABLE 15.4. TEMPERATURE EQUATIONS DESCRIBING THE PARTIAL PRESSURES OF O_2 AND S_2 IN HIGH TEMPERATURE EQUILIBRATED GEOTHERMAL FLUIDS

Reaction
(1) Reaction not known. Based on drillhole data.
(2) Reaction not known. Volcanic systems.
(3) $FeS_2 = FeS + \frac{1}{2} S_2$
(4) Reaction not known. Based on drillhole data.

Equation (T in kelvin)		Source
(1) $\log P_{O_2}$	$= -3.808 - 13\,708.3/T - 2.075 \times 106/T^2$	D' Amore and Gianelli (1984)
(2) $\log P_{O_2}$	$= 6.48 - 21\,900/T$	Sato and Writght (1966)
(3) $\log P_{S_2}$	$= 13.42 - 14\,360/T$	D' Amore and Gianelli (1984)
(4) $\log P_{S_2}$	$= -18.68 + 14\,727/T - 6\,139\,625/T^2$	D' Amore ad Gianelli (1984)
(5) $\log P_{H_2O}$	$= -5.51 - 2048/T$	Valid in the range 150–325°C

we see that H_2S partial pressures must be a function of temperature as both H_2 and S_2 are. We have

$$\log P_{H_2S} \log P_{H_2} + \tfrac{1}{2} \log S_2 - \log K_s \tag{15.24}$$

where K_S represents the equilibrium constant for the reaction of Eq. (15.23). From the temperature equations in Table 15.4 for $\log P_{O_2}$ (Eq. (1)) and $\log P_{S_2}$ (Eqs (4) and (5)) and the temperature equations for $\log K_S$ and $\log K_H$ in Table 15.6 the following temperature equations have been derived for H_2S partial pressures:

$$\log P_{H_2S} = 13.641 - 10791.6/T + 1.038 \times 10^6/T^2 + 0.979 \log T \tag{15.25}$$

and

$$\log P_{H_2S} = -2.409 + 3752.2/T - 2.122 \times 10^6/T^2 + 0.979 \log T \tag{15.26}$$

These equations are plotted in Fig. 15.5(b).

TABLE 15.5. TEMPERATURE EQUATIONS FOR THE AQUEOUS CONCENTRATIONS OF H_2, H_2S AND CO_2 IN GEOTHERMAL FLUIDS ACCORDING TO ARNÓRSSON AND GUNNLAUGSSON (1985) AND ARNÓRSSON et al. (1998B)

Gas		Temperature equations for gas concentrations as log mole/kg. (T in kelvin)	Temperature range (°C)	Source
(1)	H_2	$11.98 + 0.08489T + 82.54.09/T - 27.587\log T$		(1)[a]
(2)	H_2	$-3.04 - 10763.54/T + 7.003\log T$		(1)[b]
(3)	H_2	$17.370 - 4587.39/T + 0.00547\,T - 5.356\log T$	>150	(2)[c]
(4)	H_2S	$-1.24 - 4691.84/T + 2.830\log T$		(1)[a]
(5)	H_2S	$-11.80 - 0.6035T - 17\,691.09/T + 27.163\log T$		(1)[b]
(6)	H_2S	$-16.555 - 3635.08/T + 0.00839T - 6.074\log T$	>150	(2)[c]
(7)	CO_2	$-1.09 - 3894.55/T + 2.532\log T$	100–330	(1)
(8)	CO_2	$3.236 - 4606.63/T - 0.00537T + 2.386\log T$	>100	(2)[d]

(1): Arnórsson and Gunnlaugsson (1985). (2): Arnórsson et al. (1998). [a] Applicable to all waters below 200°C and waters in the range of 200–300°C if Cl in the aquifer is <500 ppm. [b] Applicable to all waters above 300°C and water in the range of 200–300°C if Cl in the aquifer is >500 ppm. [c] Calculated from equilibrium between aqueous H_2 and the mineral assemblage epidote + prehnite + pyrite + pyrrhotite, taking the activity of epidote to be 0.7, but that of other minerals equal to unity (see Box 10.5). [d] Based on the same mineral assemblage as the H_2 and H_2S equations of Arnórsson et al. (1998) above at temperature >200°C but on drillhole data at lower temperatures.

On the basis of drillhole data, Arnórsson and Gunnlaugsson (1985) concluded that aqueous H_2S concentrations in the aquifer of geothermal systems could be described by two temperature equations: one is valid for aquifer Cl concentrations of <500 ppm and the other for Cl concentrations of >500 ppm. These curves have been drawn up in Fig. 15.5(b). In general, conformity is relatively good for the proposed H_2S partial pressure–temperature equations, indicating that the partial pressure of this gas is indeed regulated by temperature dependent equilibria in geothermal reservoirs.

The concentrations of CO and H_2 in steam can be used to estimate CO_2 partial pressures, assuming equilibrium according to the reaction

$$CO_2 + H_2 = CO + H_2O \qquad (15.27)$$

From the equilibrium constant for this reaction,

TABLE 15.6. TEMPERATURE EQUATIONS FOR EQUILIBRIUM CONSTANTS FOR GAS–GAS AND MINERAL–GAS REACTIONS USED TO CALCULATE INITIAL AQUIFER STEAM FRACTIONS IN GEOTHERMAL AQUIFERS. THE EQUILIBRIUM RELATIONS ARE EXPRESSED IN TERMS OF GAS PARTIAL PRESSURES IN BAR.

	Reaction	K_i	Temperature equation for log K_i (T in kelvin)
(1)	$CH_4 + 2H_2O = CO_2 + 4H_2$	K_{FT}	$-4.33 - 8048.8/T + 4.635\log T$
(2)	$\frac{3}{2}\,FeS_2 + H_2 + 2H_2O = 3H_2S + \frac{1}{2}\,Fe_3O_4$	K_{PM}	$6.234 - 6222.2/T - 0.412\log T$
(3)	$\frac{1}{3}\,Fe_3O_4 + S_2 = FeS_2 + \frac{2}{3}\,O_2$	K_{MP}	$-4.54 - 3747.7/T$
(4)	$CO_2 + H_2 = CO + H_2O$	K_{CO}	$5.019 - 2240.44/T - 0.979\log T$
(5)	$3CO_2 + CH_4 = 4CO + 2H_2O$	K_{COC}	$4.73 - 12\,913.8/T + 0.719\log T$
(6)	$H_2O = H_2 + \frac{1}{2}\,O_2$	K_H	$-0.483 - 12\,513.7/T + 0.979\log T$
(7)	$H_2S = H_2 + \frac{1}{2}\,S_2$	K_S	$-0.132 - 4394.5/T + 0.791\log T$
(8)	$C + O_2 = CO_2$	K_{CC}	$0.0437 + 20\,590.7/T$
(9)	$N_2 + 3H_2 = 2NH_3$	K_N	$-0.784 + 1304/T$

$$K_{CO} = \frac{P_{CO}P_{H_2O}}{P_{CO_2}P_{H_2}} \tag{15.28}$$

and the relationship of Eq. (15.11), we have

$$\begin{aligned}\log P_{CO_2} &= -\log K_{CO} + \log\left(\frac{C^d_{CO}}{C^d_{H_2}}\right) + \log P_{H_2O} \\ &\quad - \log A_{CO} + \log A_{H_2}\end{aligned} \tag{15.29}$$

Inserting the temperature equations for log K_{CO} and P_{H_2O} into Eq. (15.29) (see Eq. (4) in Table 15.6 and Eq. (5) in Table 15.4) yields

$$\begin{aligned}\log P_{CO_2} &= 0.491 + 192.44\,/\,T + 0.979\log T + \log\left(\frac{C^d_{CO}}{C^d_{H_2}}\right) \\ &\quad - \log A_{CO} + \log A_{H_2}\end{aligned} \tag{15.29a}$$

In the temperature range of 100–350°C the value of the equilibrium constant of the reaction of Eq. (15.29a) is almost constant, 3.53 ± 0.01. If the last two terms of Eq. (15.29a), which incorporate y, are ignored and C_i^d is taken to be equal to C_i^{WH}, we have

$$\log P_{CO_2} \cong 3.53 + \log\left(\frac{C_{CO}^{WH}}{C_{H_2}^{WH}}\right) \tag{15.30}$$

From Eq. (15.30)we see that measurement of CO and H_2 of well and fumarole discharges allows estimation of CO_2 partial pressures in the producing aquifer. The effect of considering a pure liquid phase in the aquifer ($y = 0$) will increase $\log P_{CO_2}$ by about 0.2 units (1.6 bar) as a result of the difference in the solubilities of CO and H_2. For $y = 1$, Eq. (15.30) is exact, i.e. $\log A_i = 0$.

Arnórsson and Gunnlaugsson (1985) concluded that aqueous CO_2 concentrations in geothermal reservoirs were controlled by temperature dependent mineral equilibria. For high temperature geothermal reservoirs (>220°C), a likely mineral assemblage is epidote + prehnite + quartz + calcite. In some fields, particularly if the aquifer temperature is low, CO_2 concentrations may be externally fixed, i.e. by the sources of supply to the geothermal fluid. High flux of CO_2 to the geothermal fluid from the magma heat source may also prevent attainment of equilibrium between CO_2 and hydrothermal minerals, as seems e.g. to be the case at Krafla in Iceland. Temperature equations for CO_2 aqueous concentrations in equilibrated geothermal fluids are shown in Table 15.5. The temperature curves are shown in Fig. 15.6.

15.5. ESTIMATION OF INITIAL AQUIFER STEAM FRACTIONS AND AQUIFER GAS PRESSURES

15.5.1. Model I

This model assumes that the gas composition of total well discharges is representative of the aquifer fluid. In was developed by D'Amore and Celati (1983) and later expanded by D'Amore and Truesdell (1985). Various gas–gas and gas–mineral equilibria have been assumed to obtain values for y and the aquifer temperature, as will be discussed below. On the basis of this model, the initial aquifer steam fraction (y) can be estimated from:

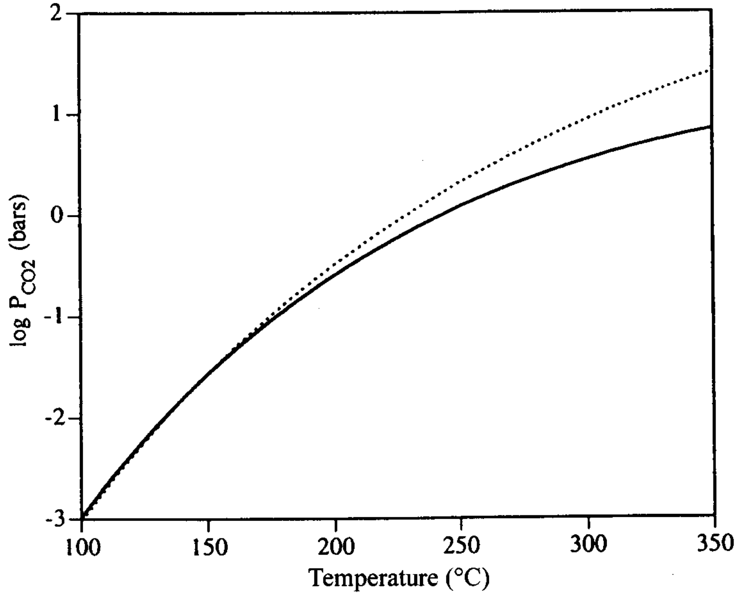

FIG. 15.6. Carbon dioxide partial pressures versus aquifer temperature. The upper curve is based on Arnórsson and Gunnlaugsson (1985) and the lower one on Arnórsson et al. (1998b).

(1) either measured H_2 or H_2S concentrations in steam samples because the aquifer partial pressures of these gases are fixed by equilibria with specific mineral buffers;

(2) the assumption of equilibrium for a single gas–gas or mineral–gas reaction and measurement of the mole fraction of the respective gases in the steam, provided the aquifer temperature is known [Eqs (15.37a) and (15.38a)];

(3) the assumption of equilibrium for two gas reactions, data on the relative amount (vol.%) of the respective gases in the well discharge and a preselected value for aquifer temperature [Eqs (15.37c) and (15.38c)].

(4) the assumption of equilibrium for three gas reactions and data on the relative amount (vol.%) of the respective gases. In this case, the aquifer temperature is evaluated together with y (Eq. (15.40)).

If the analytical data on the mole fraction of gas in steam are available, case (3) permits simultaneous estimation of both initial steam fraction and aquifer temperature.

For wet steam wells, gas concentrations are generally obtained from an analysis of steam samples collected at the wellhead with the aid of an equation in the form of (12.2b):

$$C_i^v Y_c = C_i^{WH} = C_i^d \tag{15.31}$$

where C_i^v represents the mole fraction of gas i in the discharged steam and Y_c is the steam fraction of the discharge at the pressure at which the steam sample was collected. C_i^{WH} and C_i^d denote the concentrations of gas i in the total discharge and the aquifer fluid, respectively. Sometimes only the relative gas concentrations are reported, i.e. the mole percentage (= vol.%) of the gases associated with the steam. This is, however, seldom the case with CO_2 and H_2S because these gases partition significantly into the phase of condensed steam.

It can be read directly from Eq. (15.11) that y can be estimated from this equation on the basis of the mole fraction of H_2 and H_2S in well discharges at a selected value for the aquifer temperature, as the aquifer partial pressure of these gases is a function of the aquifer temperature. To demonstrate the principles involved with cases (2) and (3) above, the following two reactions are considered:

$$CH_4 + 2H_2O = CO_2 + 4H_2 \tag{15.32}$$

and

$$H_2 + \tfrac{3}{2}\,FeS_2 + 2H_2O = 3H_2S + \tfrac{1}{2}\,Fe_3O_4 \tag{15.33}$$

For case (4) above, the reaction

$$N_2 + 3H_2 = 2NH_3 \tag{15.34}$$

has also been included.

The equilibrium constants for reactions (15.32) and (15.33) are:

$$K_{FT} = \frac{P_{CO_2} P_{H_2}^4}{P_{CH_4} P_{H_2O}^2} \tag{15.35}$$

and

$$K_{HSH} = \frac{P^3_{H_2S}}{P_{H_2} P^2_{H_2O}} \qquad (15.36)$$

Inserting Eq. (15.11) into Eqs (15.35) and (15.36) leads to

$$\begin{aligned} \log K_{FT} &= 2\log P_{H_2O} - \log A_{CO_2} - 4\log A_{H_2} + \log A_{CH_4} \\ &\quad + 4\log C_{H_2} - \log\left(\frac{C_{CH_4}}{C_{CO_2}}\right) \end{aligned} \qquad (15.37)$$

and

$$\log K_{HSH} = 3\log C^{WH}_{H_2S} - \log C^{WH}_{H_2} - 3\log A_{H_2S} + \log A_{H_2} \qquad (15.38)$$

Inserting the temperature equations for $\log K_{FT}$, $\log K_{HSH}$ and, $\log P_{H_2O}$, expressing the mole fraction, C_i, as given in Eq. (15.1a) and rearranging leads to

$$\begin{aligned} 4\log\left(\frac{n_{H_2}}{n_{H_2O}}\right) - \log\left(\frac{n_{CH_4}}{n_{CO_2}}\right) &= -15.35 - 3952.8/T + 4.635\log T \\ &\quad + 4\log A_{H_2} + \log A_{CO_2} - \log A_{CH_4} = FT \end{aligned} \qquad (15.37a)$$

and

$$\begin{aligned} 3\log\left(\frac{n_{H_2S}}{n_{H_2O}}\right) - \log\left(\frac{n_{H_2}}{n_{H_2O}}\right) &= 6.231 - 6222.2/T - 0.412\log T \\ &\quad + 3\log A_{H_2S} - \log A_{H_2} = HSH \end{aligned} \qquad (15.38a)$$

The terms on the left hand side of Eqs (15.37a) and (15.38a), *FT* and *HSH*, respectively, are obtained by analysing the mole fractions of H_2, CH_4, CO_2 and H_2S in steam discharged from wells. In these equations, n_i stands for number of moles of gas *i* or steam. Thus, both terms on the left hand side of Eq. (15.38a) and the first term on the left hand side of Eq. (15.37a) represent mole fractions of H_2 and H_2S, whereas the second term on the left hand side of Eq. (15.37a) represents the molal ratio of CH_4 to CO_2. The unknowns on the right hand side of these equations are temperature and *y* (the initial steam fraction in the aquifer incorporated in the A terms (see Eq. 15.10 for the definition of A_i). By selecting a value for the aquifer temperature either of the above equations can be used to calculate y (Box 15.3).

Instead of solving Eqs (15.37a) and (15.38a) numerically, it is convenient to use a grid diagram. The analytical parameters *FT* and *HSH* are presented as co-ordinates while the physical parameters, temperature and steam fraction, produce a grid inside the diagram. The graphical solution of the system given by Eqs (15.37a) and (15.38a) generates a plot like the one shown in Fig. 15.7. In this figure, the ranges of temperatures and y values are, respectively, 125–350°C and from –0.05 (5% steam depleted liquid water) to 1 (pure steam). Use of the diagram in Fig. 15.7 permits derivation of common y and aquifer temperature values from the respective reactions.

When gas analysis is given as volume or mole percentage of the total gas rather than as mole fraction of H_2O, it is convenient to take the ratio of all the gases to CO_2 and solve Eqs (15.37a) and (15.38a) together in order to retrieve a value for y. By taking the ratio of gases to CO_2 , the equations are modified as follows:

$$4\log\left(\frac{n_{H_2}}{n_{CO_2}}\right)-\log\left(\frac{n_{CH_4}}{n_{CO_2}}\right)=CC=-15.35-3952.8/T+4.635\log T \qquad (15.37b)$$
$$+4\log P_{H_2O}+4\log A_{H_2}-3\log A_{CO_2}-\log A_{CH_4}-4\log P_{CO_2}$$

and

$$3\log\left(\frac{n_{H_2S}}{n_{CO_2}}\right)-\log\left(\frac{n_{H_2}}{n_{CO_2}}\right)=HS=6.231-6222.2/T-\log T \qquad (15.38b)$$
$$+2\log P_{H_2O}+3\log A_{H_2S}-\log A_{H_2}-2\log A_{CO_2}-2\log P_{CO_2}$$

Finally, by inserting the temperature equation for the H_2O partial pressure, as given in Eq. (6) in Table 15.6, we obtain:

$$4\log\left(\frac{n_{H_2}}{n_{CO_2}}\right)-\log\left(\frac{n_{CH_4}}{n_{CO_2}}\right)=CC=6.69-12\,144.8/T+4.635\log T \qquad (15.37c)$$
$$+4\log A_{H_2}-3\log A_{CO_2}-\log A_{CH_4}-4\log P_{CO_2}$$

and

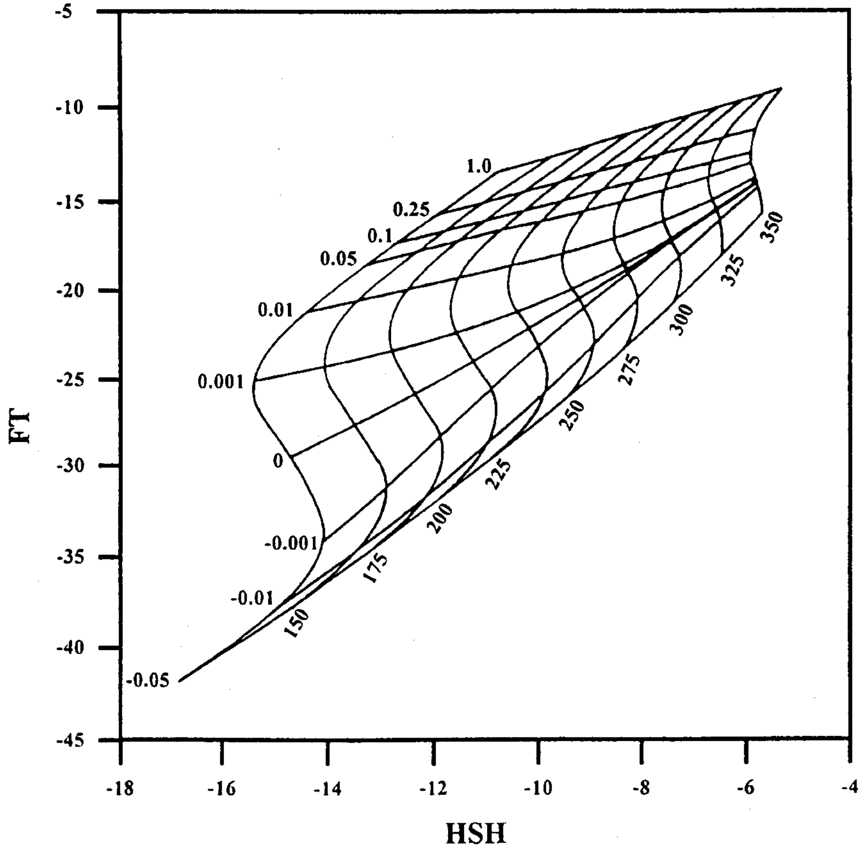

FIG. 15.7. Grid diagram of the FT versus HSH chemical parameters for selected values of temperature (°C) and initial steam fraction, y. $FT = 4\log(n_{H_2}/n_{H_2O}) - \log(n_{CH_4}/n_{CO_2})$, $HSH = 3\log(n_{H_2S}/n_{H_2O}) - \log(n_{H_2}/n_{H_2O})$. See Eqs (15.37a) and (15.38a) in the text.

$$3\log\left(\frac{n_{\mathrm{H_2S}}}{n_{\mathrm{CO_2}}}\right) - \log\left(\frac{n_{\mathrm{H_2}}}{n_{\mathrm{CO_2}}}\right) = HS = 17.251 - 10\,318.2/T - 0.412\log T \qquad (15.38c)$$
$$+\,3\log A_{\mathrm{H_2S}} - \log A_{\mathrm{H_2}} - 2\log A_{\mathrm{CO_2}} - 2\log P_{\mathrm{CO_2}}$$

Multiplying Eq. (15.38c) by 2 and subtracting it from Eq. (15.37c) eliminates $P_{\mathrm{CO_2}}$, giving

$$CC - 2HS = -27.812 + 8491.4/T + 5.459\log T + \log A_{\mathrm{CO}^2} - A_{\mathrm{CH}^4} + 8\log A_{\mathrm{H}^2} - 6\log A_{\mathrm{H}^2\mathrm{S}} \qquad (15.39)$$

There are two variables in Eq. (15.39), temperature and y (incorporated in the A_i term; see Eq. (15.10)). By selecting a value for the aquifer temperature, a value for y can be obtained from analysis of the relative abundances of CO_2, CH_4, H_2 and H_2S in the discharge of a dry or wet steam well (Box 15.4). Eq. (15.39) is representative for case (3) above. A value for the initial steam fraction according to case (3) could, of course, be calculated by considering another pair of gas reactions, e.g. the one involving N_2 and NH_3 (Eq. (15.34)) and H_2 and H_2S (Eq. (15.33)). This yields the following relationship:

$$3\log\left(\frac{n_{\mathrm{H_2S}}}{n_{\mathrm{CO_2}}}\right) + 2\log\left(\frac{n_{\mathrm{NH_3}}}{n_{\mathrm{CO_2}}}\right) - 4\log\left(\frac{n_{\mathrm{H_2}}}{n_{\mathrm{CO_2}}}\right) - \log\left(\frac{n_{\mathrm{N_2}}}{n_{\mathrm{CO_2}}}\right) = 5.45 - 4918.2/T - 0.412\log T + 3\log A_{\mathrm{H_2S}} + 2\log A_{\mathrm{NH_3}} - 4\log A_{\mathrm{H_2}} - \log A_{\mathrm{N_2}} \qquad (15.40)$$

By considering three gas reactions, e.g. those of Eqs (15.32) to (15.34), aquifer temperature and initial steam fraction values can both be evaluated. Simultaneous solution of three reactions is numerically quite complex and will not be demonstrated here.

15.5.2. Model II

This model, which was developed by Arnórsson et al. (1990), evaluates boiling processes in the producing aquifers of 'excess' enthalpy wet steam wells using data on the concentrations ratios of CO_2/H_2 or H_2S/H_2 in the discharged steam. The model permits calculation of the initial steam fraction as well as of the extent to which water and steam separate in the producing aquife, and of the amount of enhanced evaporation due to heat flow from the rock to the boiling water. If phase segregation occurs in producing aquifers, the total well discharge composition is not the same as that of the initial aquifer fluid. In other words, $C_i^{WH} \neq C_i^{l}$ (see Eq. (15.9)). In this respect, this model differs from Model I described in the previous section, but otherwise the two models are basically the same. The basic equation for calculating the initial aquifer steam fraction by Model II is:

$$y_{\mathrm{HS}} = \frac{A_{\mathrm{H}} - A_{\mathrm{S}}}{\frac{55.51}{P}\left[\frac{A_{\mathrm{S}}}{K_{\mathrm{H_2}}} - \frac{A_{\mathrm{H}}}{K_{\mathrm{H_2S}}}\right] + (A_{\mathrm{H}} - A_{\mathrm{S}})} \tag{15.41}$$

The symbols in this equation and the next three equations below are explained in Box 15.5; the derivation of these equations is given as well. The nomenclature is the same as in the original publication on this model (Arnórsson et al., 1990), except for mole fraction because in Model I the number of moles has the same symbol, n_i. This is considered more convenient than adopting the same nomenclature for both models here because it allows an easy reference to the original publication, which gives greater detail about the method than is given here.

The fraction of steam in the total discharge generated by enhanced evaporation due to heat flow from the rock, X_e, is given by

$$X_e = X_c\left(\frac{1}{1-Z_{s,c}} - RZ_s\right) - \frac{Z_{s,c}}{1-Z_{s,c}} \tag{15.42}$$

and the relative masses of aquifer water which has boiled to yield steam into wells, and the relative mass of boiled water retained in the aquifer, are given by respectively,

$$V^f = X_c\frac{m^v_{g,c}}{m^f_g} \tag{15.43}$$

and

$$V^l_r = V^f + X_e - 1 \tag{15.44}$$

An example for the calculation of initial steam fraction by Model II is given in Box 15.6. In general, it is assumed that H_2S/H_2 ratios give more reliable estimates of y than CO_2/H_2 ratios, largely because there is larger difference in solubility between H_2S and H_2 than there is between CO_2 and H_2. The reliability of the results obtained for the initial steam fraction and the boiling parameters, X_e, V^f and V^l_r by Model II depends on various factors including:

(1) The selected values for the aquifer temperature, t_0, and the temperature of phase segregation, t_s;

(2) Chemical reactions between gases and with minerals in the aquifer in the zone of depressurization, i.e. after extensive boiling has started in producing aquifers;

(3) Departure from equilibrium in the initial aquifer fluid;

(4) Inaccuracy of the equations used to describe gas solubilities;

(5) Inaccuracy in the equations used to describe the aqueous concentrations of CO_2, H_2S and H_2 in the undisturbed aquifer.

Analyses of data from many wells indicate that the selection of values for t_s within reasonable limits will not affect the results substantially. There is evidence that gas reactions are in general limited between undisturbed aquifer conditions and wellhead, and gas solubility is quite well known from experimental work in the temperature range of interest. Aquifer temperatures can usually be evaluated with reasonable confidence. Unreliable estimates of aquifer temperature may, however, result when there is contribution to the well discharge from more than one aquifer of significantly different temperatures (>20°C). It is assumed that the main error involved in calculating y and the boiling parameters lies in item (5) above. The selection of an equation describing the temperature dependence of aqueous gas concentrations should, as far as possible, be based on data on alteration mineralogy in the geothermal system in question and on a calculation of the equilibrium constant for the respective gas–mineral reaction from the thermodynamic properties of the gases and minerals involved. The equation describing the temperature dependence of the equilibrium constant is the temperature equation to be used.

15.6. DISCUSSION

The basic equation relating gas partial pressures and gas composition of geothermal fluids to the initial aquifer steam fraction is Eq. (15.11):

$$\log P_i = \log C_i^d + \log \mathrm{H_2O} - \log\left(y + \frac{1-y}{B_i}\right)$$

According to Model I, it is assumed that the total well discharge composition is the same as that of the initial or source aquifer fluid, in which case the mole fraction of gas i in the aquifer fluid is equal to that of the total well discharge, i.e. $C_i^d = C_i^{WH}$, so that

$$\log P_i = \log C_i^{WH} + \log \mathrm{H_2O} - \log\left(y + \frac{1-y}{B_i} \right) \tag{15a}$$

In contrast, Model II assumes that phase segregation may occur in the producing aquifer. Accordingly, the mole fraction of a gas in the aquifer fluid may not be the same as that of the total well discharge, or $C_i^d \neq C_i^{WH}$. This is the essential difference between the two models. The validity of each model should be assessed, as far as data permit, for each field and each well when interpreting data on the gas composition of well discharges with respect to initial steam fractions. For wet steam wells with high discharge enthalpy it is specifically recommended to compare quartz, Na/K and Na/K/Ca geothermometry temperatures using the silica content of the total discharge to compute the quartz equilibrium temperature. If this temperature so calculated is similar to the Na/K and Na/K/Ca temperatures, it is likely that the basic assumption of Model I is valid, namely that the total discharge composition is representative of the initial aquifer fluid. If, on the other hand, the quartz equilibrium temperature, as calculated from the total discharge composition, is much lower than the Na/K temperature but similar if adiabatic boiling is assumed, it is assumed likely that phase segregation is largely responsible for the elevated discharge enthalpy, in accordance with Model II.

Both models rely on the assumption of specific gas equilibria in the reservoir. In the case of Model II, specific gas–mineral equilibria are considered but in the case of Model I gas–gas equilibria are also taken. Drillhole data have also been used to derive empirical relationships between aquifer gas partial pressures or aqueous gas concentrations with aquifer temperature. Both simple and complex minerals, compositionally speaking, have been considered. A difficulty may arise in using compositionally complex minerals to obtain an equilibrium relationship between gas partial pressures and temperature because these minerals often form solid solutions such as chlorite, epidote and prehnite. The composition of these minerals will be affected by the composition of the rock with which the water reacts and, as a result, the rock composition will affect gas partial pressures at equilibrium at any temperature even if the same minerals are involved. In this case it is always the task of the geochemist, when interpreting data on geothermal fluid compositions, to estimate initial aquifer steam fractions, to provide evidence for and against the assumption of specific gas–gas or mineral–gas equilibria and to discuss the validity of the gas temperature equations used. It is logical to select hydrothermal minerals identified in the rock of the geothermal system under study. If data on alteration mineralogy are not available, the second best choice is to assume equilibrium with minerals known to occur in other geothermal systems hosted in the same type of rock. In calculating y values it is considered useful to use all the proposed equations, then compare the results and discuss which assumptions of equilibrium, if any, are considered most appropriate.

Both models assume equilibrium distribution of gases between liquid water and vapour. Neither model assumes conservation of heat between undisturbed aquifer and wellhead. Model I assumes conservation of mass but Model II considers the system to be open, allowing phase segregation to occur in the aquifer. However, both models assume that no reactions take place in the depressurization zone around wells that would affect the composition of the flowing fluid.

In deriving Eq. (15.11), the simplification was made to take vapour pressure in the aquifer to be equal to total pressure. This approximation is quite reasonable for most geothermal fluids because the sum of the partial pressures of all gases is small compared with the vapour pressure. However, in some geothermal reservoirs the gas content of the aquifer fluid is high enough to cause the gas partial pressures to be ≥10% of the total pressure. This can also be the case for fields of relatively low gas content, when the initial aquifer steam fraction is low. The values of the distribution coefficients (B_i) given in Table 15.2 were derived on the basis of the simplification that vapour pressure is equal to total pressure. For an exact presentation of Eq. (15.11), the mole fraction of gas i in the total discharge, the vapour pressure and the gas distribution coefficients must be based on Eqs (15.1), (15.4), (15.5) and (15.6).

By Model I it is possible to calculate the initial aquifer steam fraction from knowledge of the H_2 or H_2S mole fractions in the well discharge. However, since the mole fraction for either of these gases cannot be taken to be the same in the aquifer fluid and the total well discharge by Model II, this is not possible by this model. Analytical data on the mole fraction of two gases are required to calculate a value for y by this model. Model II does not exclude that 'excess' discharge enthalpy is solely caused by heat flow from the rock, in which case phase segregation does not contribute to this enthalpy. In that sense Model I may be regarded as a special case of Model II.

Both models assume a single aquifer temperature. When well discharges are a mixture of fluid from two or more aquifers with significantly different temperatures (>20°C), neither model is truly valid. The reliability of the results depends on the relative contribution from the different aquifers and their temperature differences. To assess the source of the fluid discharged from wells, it is considered of value to study circulation losses during drilling and temperature logging during heating-up of wells, as well as water geothermometry results. The first two provide information on the level of potential aquifers. Water geothermometry indicates which of these potential aquifers, if any, dominates the discharge.

Calculated values of initial steam fractions as well as values for the boiling parameters may change during exploitation as a result of recharge into the producing aquifers, either of cold water or of deeper and hotter geothermal fluid. In particular, recharge of cold water may cause the fluid entering wells to become depleted in gases because of their insufficient supply and upset gas–gas and gas–mineral equilibria that are conventionally assumed for calculation of y. When this happens, changes in calculated y values are not real. For this reason, it is considered important always to study time variations in gas concentration in the steam phase and total discharge of wells and relate any such changes to changes in calculated y values.

In two phase geothermal systems, the fluid reserves are determined by the porosity of the reservoir rock, the temperature and the volume fraction of liquid water in the pores. Fluid reserves decrease rapidly with increasing vapour fraction. The relationship between liquid (S^l) and vapour (S^v) saturation is given by

$$S^l = 1 - S^v \tag{15.45}$$

where

$$S^v = \frac{yV^v}{yV^v + (1-y)V^l} \tag{15.46}$$

Here, V^v and V^l stand for the specific volumes of vapour and liquid water, respectively, both of which are temperature dependent. y refers to initial vapour fraction as before. Figure 15.8 shows the relationship between S^l and y at three different temperatures. In this context it is of particular importance to estimate the initial steam fractions in vapour dominated geothermal reservoirs, since the range of values taken by these fractions may be such that it strongly affects the fluid reserves in the reservoir.

BOX 15.2. CALCULATION OF H_2, H_2S AQUIFER PARTIAL PRESSURES

With the aid of the equation

$$H_2O = H_2 + \frac{1}{2} O_2$$

H_2 partial pressure can be calculated at a preselected temperature from the equilibrium constant of this reaction and the known value of the oxygen partial pressure. The equilibrium constant, K_H, is defined as

$$\log K_H = \log P_{H_2} + \frac{1}{2} \log P_{O_2} - \log P_{H_2O}$$

A temperature equation for the equilibrium constant for the above reaction is given in Table 15.6 and equations for the temperature dependence of O_2 partial pressures in Table 15.4 (Eq. (1)). By selecting the analysis for H_2 in Box 15.1 and an aquifer temperature of 250°C we have from Eq. (1) in Table 15.4 that $\log P_{O_2} = -37.59$, and from this value and the value for the equilibrium constant for the dissociation of water (–21.74, Eq. (6) in Table 15.6) a value of –1.34 is obtained for $\log P_{H_2}$, or $P_{H_2} = 0.046$ bar.

Having estimated H_2 partial pressures, the H_2S aquifer partial pressures can be estimated from the following reaction:

$$H_2S = H_2 + \frac{1}{2} S_2$$

and Eq. (4) in Table 15.4, relating S_2 to temperature. From the equilibrium constant for the above reaction, it follows that

$$\log P_{H_2S} = -\log K_S + \log P_{H_2} + \frac{1}{2} \log P_{S_2}$$

Let us fix the temperature at 250°C as in the previous example. Equation (4) in Table 15.4 yields a value for $\log P_{S_2} = -12.96$. From Eq. (7) in Table 15.6, a value of –6.38 is obtained for $\log K_s$. As $\log P_{H_2} = -1.34$, the above reaction gives $\log P_{H_2S} = -1.44$ or 0.036 bar.

BOX 15.3. CALCULATION OF INITIAL STEAM FRACTION BY MODEL I. CONSIDERATION OF ONE GAS REACTION, SELECTION OF AQUIFER TEMPERATURE AND USING DATA ON GAS MOLE FRACTIONS IN STEAM

The gas analysis given in Box 15.1 gives the following gas mole fractions (C_i):

CO_2	7.41×10^{-3}
H_2S	0.133×10^{-3}
H_2	0.088×10^{-3}
CH_4	0.178×10^{-3}

By inserting the appropriate gas mole fractions into Eqs (15.37a) and (15.38a), the following values are obtained for FT and HSH:

FT = −14.60
HSH = −7.57

Next select an aquifer temperature of 250°C. From the equations for the distribution coefficients (B_i) in Table 15.2, we obtain:

$\log B_{CO_2} = 2.0295$ $\quad B_{CO_2} = 107.0$
$\log B_{H_2S} = 1.5947$ $\quad B_{H_2S} = 39.3$
$\log B_{H_2} = 2.6428$ $\quad B_{H_2} = 439.3$
$\log B_{CH_4} = 2.6122$ $\quad B_{CH_4} = 409.4$

From Eq. (15.37a) we see that this leads to

$$-10.30 + 4\log\left(y + \frac{1-y}{439.3}\right) + \log\left(y + \frac{1-y}{107.0}\right) - \log\left(y + \frac{1-y}{409.4}\right) = -14.60$$

It is easiest to solve this equation by iteration, i.e. guessing the y value until the right and left hand sides of the equation are equal. This gives a y value of 0.08.

Similarly, for Eq. (15.38a), we have

$$-6.78 + 3\log\left(y + \frac{1-y}{39.3}\right) - \log\left(y + \frac{1-y}{439.3}\right) = -7.57$$

Solution of this equation yields a y value of 0.38. In this example, the HSH reaction yields a considerably higher y value than the FT reaction. There may be several reasons for this, such as lack of equilibration for either of the two reactions or both of them.

BOX 15.4. CALCULATION OF INITIAL STEAM FRACTION BY MODEL I. CONSIDERATION OF TWO GAS REACTIONS, SELECTION OF AQUIFER TEMPERATURE AND USING DATA ON RELATIVE GAS CONCENTRATIONS IN STEAM

Let us use the gas analysis in Box 15.1:

Gas	vol.%
CO_2	92.2
H_2S	1.66
H_2	1.10
CH_4	2.21

First calculate CC and HS from the gas analysis (see Eqs (15.37c) and (15.38c)):

$$CC = 4\log\left(\frac{n_{H_2}}{n_{CO_2}}\right) - \log\left(\frac{n_{CH_4}}{n_{CO_2}}\right) = -6.073$$

and

$$HS = 3\log\left(\frac{n_{H_2S}}{n_{CO_2}}\right) - \log\left(\frac{n_{H_2}}{n_{CO_2}}\right) = -3.311$$

Next calculate the values for the respective temperature equation for the equilibrium constants in Eq. (15.39), taking the aquifer temperature to be 250°C (T = 523.15 K):

$$-27.812 + 849.4/T + 5.49\log T = 3.260$$

and

$$-12.644 = \log A_{CO_2} - \log A_{CH_4} + 8\log A_{H_2} - 6\log A_{H_2S}$$

By inserting the appropriate B_i values into the A term, iteration yields $y = 0.082$, which is practically the same value as that obtained by assuming equilibrium according to the Fischer–Tropsch reaction and by using Eq. (15.37a) to describe the temperature dependence of aquifer H_2 partial pressures (see Box 15.3).

BOX 15.5. DERIVATION OF EQUATIONS FOR CALCULATING BOILING PROCESSES IN PRODUCING AQUIFERS AND INITIAL STEAM FRACTIONS BY MODEL II

NOMENCLATURE

A_H	$m^{v}_{\mathrm{H_2}}/m^{f,l}_{\mathrm{H_2}}$
A_S	$m^{v}_{\mathrm{H_2S,c}}/m^{f,l}_{\mathrm{H_2S}}$
C^g	mole fraction of gas g in steam phase (kg/s)
h	enthalpy of discharge (kJ/kg)
h^f	enthalpy of initial aquifer fluid (kJ/kg)
$h^{f,l}$	enthalpy of initial aquifer water (kJ/kg)
$h^{t,c}$	enthalpy of boiled water at temperature t_c (kJ/kg)
$h^{t,i}$	enthalpy of boiled water at temperature t_i (kJ/kg)
$h^{t,s}$	enthalpy of boiled water at temperature t_s (kJ/kg)
K_s	gas solubility constant for gas g (mol·kg^{-1}·bar^{-1}) $K_s = m^f_g/P_g$
L^c	latent heat of vaporization of water at temperature t_c (kJ/kg)
L^i	latent heat of vaporization of water at temperature t_i (kJ/kg)
L_s	latent heat of vaporization of water at temperature t_s (kJ/kg)
m^f_g	concentration of gas g in initial aquifer fluid (mol/kg)
$m^{f,l}_g$	concentration of gas g in initial aquifer water (mol/kg)
P	total pressure (bar abs.)
P_g	partial pressure of gas g (bar abs.)
R	constant defined by Eq. (9a) in this box
t_c	temperature of fluid at wellhead at which a sample is collected (°C)
t_i	temperature of fluid at inflow into well (°C)
t_0	temperature of initial aquifer fluid (°C)
t_s	temperature of partial separation of water and steam in aquifer (°C)
V^f	M^f/M. Relative mass of aquifer fluid which boils to yield steam into well
V^l_r	M^l_r/M. Relative mass of boiled water retained in the aquifer
X_c	M^v_c/M. Mass fraction of steam in well discharge at temperture t_c
X_e	M^v_e/M. Mass fraction of steam in well discharge formed by enhanced vaporization of water due to heat flow from rock
X_i	M^v_i/M. Mass fraction of steam entering a well at temperature t_c

BOX 15.5. (cont.)

$m_g^{f,v}$	concentration of gas g in initial aquifer steam (mol/kg)
m_g^t	concentration of gas g in total well discharge (mol/kg)
$m_{g,c}^v$	concentration of gas g in saturated steam at temperature t_c
M	mass flow of water and steam flowing into a well (kg/s)
M^f	mass flow of aquifer fluid affected by the well (kg/s)
$M^{f,v}$	mass flow of initial aquifer steam affected by the well (kg/s)
M_r^l	mass flow of boiled aquifer water which separates from the steam flowing into the well (kg/s)
M_e^v	mass flow of steam formed by vaporization of water in aquifer due to heat flow from rock (kg/s)
M_c^v	mass flow of steam discharged from well at temperature t_c (kg/s)
M_i^v	mass flow of steam entering a well (kg/g)
y	$M^{f,v}/M^f$. Mass fraction of initial aquifer steam in aquifer fluid
y_{HS}	mass fraction of initial aquifer steam obtained from the H_2 and H_2S content of the discharged steam
y_{HC}	mass fraction of initial aquifer steam obtained from the H_2 and CO_2 content of the discharged steam
Z_s	(defined by Eq. (4) in this box) Mass fraction of initial aquifer water which has vaporized by adiabatic boiling from temperature t_0 to temperature t_s
$Z_{s,i}$	(defined by Eq. (5) in this box) Mass fraction of water which has vaporizated by adiabatic boiling from temperature t_s to temperature t_c
$Z_{s,c}$	(defined by Eq. (6) in this box) Mass fraction of water which has vaporized by adiabatic boiling from temperature t_s to temperature t_c

BOX 15.5. (cont.)

DERIVATION OF EQUATIONS

The mass flow of water and steam, M, entering a wet steam well can be divided into components as follows:

$$M = M^f - M^l_r + M^v_e \tag{1}$$

Expressing Eq. (1) in terms of relative mass gives

$$1 = V^f - V^l_r + X_e \tag{2}$$

The mass flow of steam entering a well, M^v_i, can be divided into the following three components:

$$M^v_i = M^f Z_s + M^v_e + [M^f(1 - Z_s) - M^l_r]Z_{s,\mathrm{i}} \tag{3}$$

The first term on the right hand side of Eq. (3) represents steam formed by adiabatic boiling of the initial aquifer fluid from temperature t_0 to temperature t_s, which is the temperature at which phase segregation may occur. The second term designates steam entering the flowing fluid at temperature t_s because of enhanced evaporation of the water with the aid of the heat flow from the rock. The third term represents steam formed by adiabatic boiling between temperature $\mathrm{t_s}$ and the well inflow temperature t_i. Z_s is the fraction of the aquifer fluid M^f that occurs as steam after adiabatic boiling to temperature t_s, or

$$Z_s = \frac{h^f - h^{l,s}}{L^s} \tag{4}$$

$Z_{s,i}$ represents the mass fraction of water which has vaporized by adiabatic boiling from temperature t_s to temperature t_i, or

$$Z_{s,i} = \frac{h - h^{l,i}}{L^i} - \frac{h - h^{l,s}}{L^s} \tag{5}$$

and, correspondingly, $Z_{s,c}$ symbolizes the steam fraction formed by adiabatic boiling from t_s to the temperature at which a steam sample is collected at the wellhead, t_c:

$$Z_{s,c} = \frac{h - h^{l,c}}{L^c} - \frac{h - h^{l,s}}{L^s} \tag{6}$$

When $Z_{s,i}$ is replaced by $Z_{s,c}$ in Eq. (3), M^v_i should be replaced by M^v_c.

BOX 15.5. (cont.)

Converting mass flow of steam (Eq. (3)) into relative mass flow entering a well gives

$$X_i = V^f Z_s + X_e + [V^f(1 - Z_s) - V_r^l]Z_{s,i} \tag{7}$$

at the inflow into the well, Similarly, for the steam fraction at the wellhead collection temperature t_c we have

$$X_c = V^f Z_s + X_e + [V^f(1 - Z_s) - V_r^l]Z_{s,c} \tag{8}$$

Assuming that all gas in the initial aquifer fluid occupies the steam phase at temperature t_s and at a lower temperatures gives

$$X_c m^v_{g,c} = m^t_g = V^f m^f_g \tag{9}$$

The total mass of gas in the reservoir fluid is split between the water and steam phases in accordance with the following equation:

$$m^f_g = m^{f,l}_g(1 - y) + m^{f,v}_g y \tag{10}$$

From Henry's law ($m^{f,l}_g = K_g P_g$) and Raoult's law ($P_g = C_g P$), it follows that

$$\frac{m^{f,l}_g}{m^{f,v}_g} = \frac{K_g P}{55.51} \tag{11}$$

Combining Eqs (10) and (11) by eliminating $m^{f,v}_g$ yields

$$m^f_g = m^{f,l}_g \left[y\left(\frac{55.51}{K_g P} - 1 \right) + 1 \right] \tag{12}$$

$$m^v_{g,c} = m^f_g \frac{V^f}{X_c} = m^f_g R \tag{9a}$$

From Eqs (12) and (9a) we see that

$$R = \frac{m^v_{g,c}}{m^{f,l}_g} \left[y\left(\frac{55.51}{K_g P} - 1 \right) + 1 \right]^{-1} \tag{13}$$

i.e. $R = V^f/X_c$. When writing Eq. (13) for two gases, e.g. H_2 and H_2S, we obtain

BOX 15.5. (cont.)

$$R = \frac{m^{v}_{\mathrm{H_2},c}}{m^{f,l}_{\mathrm{H_2}}}\left[y\left(\frac{55.51}{K_{\mathrm{H_2}}P}-1\right)+1\right]^{-1}$$

$$= \frac{m^{v}_{\mathrm{H_2}s,c}}{m^{f,l}_{\mathrm{H_2S}}}\left[y\left(\frac{55.51}{K_{\mathrm{H_2S}}P}-1\right)+1\right]^{-1} \tag{14}$$

Isolating y and rearranging yields

$$y_{\mathrm{HS}} = \frac{A_{\mathrm{H}} - A_{\mathrm{S}}}{\frac{55.51}{P}\left[\frac{A_{\mathrm{S}}}{K_{\mathrm{H_2}}} - \frac{A_{\mathrm{H}}}{K_{\mathrm{H_2S}}}\right] + (A_{\mathrm{H}} - A_{\mathrm{S}})} \tag{15}$$

Inserting X_cR for V^f into Eq. (8) [see Eq. (9a)] and $V^f + X_e - 1$ for V^l_r [Eq. (2)] yields

$$X_c = X_c RZ_c + X_e + (1 - X_c RZ_s - X_e)Z_{s,c} \tag{16}$$

Isolating X_e and rearranging gives

$$X_e = X_c\left(\frac{1}{1-Z_{s,c}} - RZ_s\right) - \frac{Z_{s,c}}{1-Z_{s,c}} \tag{17}$$

Finally

$$V^f = RX_c \tag{9b}$$

and

$$V^l_r = V^f + X_e - 1 \tag{2a}$$

Equations (16), (17), (9b) and (2a) allow calculation of the desired parameters. They are:

(1) The initial steam fraction (y) in the aquifer;

(2) The mass fraction of steam in the well discharge formed by enhanced vaporization of water due to heat flow from rock;

(3) Relative mass of aquifer fluid which boils to yield steam into the well;

(4) Relative mass of boiled water separated from the steam that flows into the well.

BOX 15.6. CALCULATION OF THE INITIAL AQUIFER STEAM FRACTION AND THE VARIOUS BOILING PARAMETERS BY MODEL II

The following gas analysis and well data are from well 10 at Okkaria in Kenya:

gas	mol %
CO_2	72.13
H_2S	11.09
H_2	14.41

mmole total gas/kg steam: 66.2
sampling pressure: 5.3 bar abs.
aquifer temperature: 269°C
inflow temperature: 192°C
discharge enthalpy: 2289 kJ/kg

To calculate the initial aquifer steam fraction, adopt the following procedure:

(1) Calculate the concentrations of H_2S and H_2 in the initial aquifer water at the selected aquifer temperature. We suggest using Eqs (4) and (1) in Table 15.5:

$$\log (m^{fl}_{H_2S}) = -1.24 - 46.91/T + 2.83\log T = -2.157$$
$$\log (m^{fl}_{H_2}) = 11.98 + 0.08489T + 8254.09/T - 27.587\log T = -2.198$$

(2) Calculate gas concentrations as mole/kg steam:

$$H_2S\text{: } \frac{11.09}{100} \times 66.2 \times 10^{-3} = 7.34 \times 10^{-3}$$
$$H_2\text{: } \frac{14.41}{100} \times 66.2 \times 10^{-3} = 9.54 \times 10^{-3}$$

(3) Obtain values for the gas solubility constant given in Table 15.1:

$$\log K_{s,H_2S} = -66.775 + 3448.59/T - 0.68640 \times 10^{-6}T^2 + 18.847\log T = -1512$$
$$\log K_{s,H_2} = -25.260 + 1355.28/T + 4.11147 \times 10^{-6}T^2 + 6.966\log T = -2.506$$

(4) From steam tables, we see that the vapour pressure at 269°C is 54.2 bar abs. (see the respective equation in Box 12.1).

BOX 15.6. (cont.)

(5) Obtain values for A_S and A_H:

$$A_s = \frac{7.34 \times 10^{-3}}{10^{-2.157}} = 1.054$$

$$A_H = \frac{9.54 \times 10^{-3}}{10^{-2.198}} = 1.505$$

(6) Insert the values obtained under items (1) to (5) above into Eq. (15.41) to obtain a value for the initial aquifer steam fraction (y):

$$y_{HS} = \frac{1.505 - 1.054}{\frac{55.51}{54.2}\left[\frac{1.054}{10^{-2.506}} - \frac{1.505}{10^{-1.512}}\right] + (1.50 - 1.054)} = 0.0015$$

(7) Calculate the steam fraction in the well discharge at the sampling pressure, using the measured discharge enthalpy value:

$$X_c = \frac{h - h^{l,c}}{L^c} = \frac{2289 - 654}{2099} = 0.779$$

(8) Calculate Z_s snd $Z_{s,c}$ with the aid of Eqs (4) and (6) in Box 15.5, respectively. Take the temperature at which phase segregation has occurred, t_s, to be equal to the temperature of the inflow into the well (t_i = 192°C):

$$Z_s = \frac{h^f - h^{l,s}}{L^s} = \frac{1182 - 816}{1970} = 0.186$$

$$Z_{s,c} = \frac{h - h^{l,c}}{L^c} - \frac{h - h^{l,s}}{L^s} = \frac{2289 - 654}{2099} - \frac{2289 - 816}{1970} = 0.031$$

(9) Next obtain a value for R which is defined by Eq. (13) in Box 15.5:

$$R = \frac{m^v_{g,c}}{m^{f,l}_g}\left[y\left(\frac{55.51}{K_g P} - 1\right) + 1\right]^{-1}$$

$$= \frac{9.54 \times 10^{-3}}{10^{-2.198}}\left[0.0015\left(\frac{55.51}{10^{-2.506} \times 54.2} - 1\right) + 1\right]^{-1} = 1.009$$

BOX 15.6. (cont.)

(10) Finally, using the values obtained from items (7) to (9) above, calculate the mass fraction of steam in the well discharge which has formed by enhanced vaporization of water due to heat flow from rock (X_e), using Eq. (15.42):

$$X_e = X_c\left(\frac{1}{1-Z_{s,c}} - RZ_s\right) - \frac{Z_{s,c}}{1-Z_{s,c}}$$

$$= 0.779\left(\frac{1}{1-0.031} - 1.009\times 0.186\right) - \frac{0.031}{1-0.031} = 0.626$$

(11) With the aid of Eq. (9b) in Box 15.5, calculate the relative mass of aquifer fluid which has boiled to yield steam into the well (V^f);

$$V^f = RX_c = 1.009 \times 0.779 = 0.786$$

(12) Lastly, calculate the fraction of boiled liquid water retained in the aquifer (V_r^l) with the aid of Eq. (2a) in Box 15.5:

$$V_r^l = V^f + X_e - 1 = 0.786 + 0.626 - 1 = 0.412$$

Summary of results:

$y = 0.0015$
$X_e = 0.626$
$V^f = 0.786$
$V_r^l = 0.412$

These results indicate a very small initial aquifer steam fraction and that most of the steam discharge from the well (0.626 out of 0.779, or 80%) is generated by heat flow from the rock. Phase segregation is limited; the fraction of the water retained in the aquifer is 0.412, relative to the discharge.

16. MONITORING OF RESERVOIR RESPONSE TO PRODUCTION

by Stefán Arnórsson and Franco D'Amore

16.1. RESPONSE OF GEOTHERMAL RESERVOIRS TO PRODUCTION LOAD

Rocks always have limited permeability. As a result, drillings and withdrawal, in excess of the natural throughflow rate or natural discharge rate, of fluids, whether hot or cold water or steam from an underground fluid reservoir, will cause a decline in fluid pressure in that reservoir. The magnitude of this pressure drawdown depends on the rock permeability and on the rates of fluid extraction and recharge. A complicated situation arises in boiling geothermal reservoirs. The fluid volume increases much by steam formation that results from the pressure drop; it is not constant but a function of pressure. The increase in volume by extensive boiling enhances the pressure drop. Also, water and steam have different flowing properties, and their relative mobility depends on their volume fraction, the so-called relative permeability. As a result, they may separate, at least partly, as they flow along the pressure gradient through the zone of depressurization towards a well. The steam flows preferentially into wells when it dominates the volume.

The way a geothermal reservoir changes with time as a result of its exploitation has been described as the response of the reservoir to the production load. The main effects of the pressure drawdown are increased recharge of water into the reservoir, from above, below or laterally, and enhanced boiling in the case of reservoirs with temperatures in excess of 100°C. Pressure drawdown by itself may cause wells to become unproductive but cold water recharge may also do so by condensing steam and, thus, reducing boiling.

Geothermal energy is often considered to be a renewable resource. It is not. In exploited geothermal fields, hot fluid is always extracted at a rate higher than it is produced. Yet, it is justifiable to describe geothermal resources as semi-renewable, because even if a geothermal reservoir has been abandoned after excessive pressure drawdown, it may, within a period of a few years to a few decades, become productive again. It is considered appropriate to look at geothermal reservoirs as mines of heat. The heat content of the mine depends on its volume, temperature, the proportion of rock to fluid in it (its porosity) and the steam to water ratio. Water contains more heat per unit volume than steam and at any temperature about three times more heat than rock. Therefore, the highest quantity of heat is stored in a unit volume of a geothermal reservoir when the temperature and porosity are highest and when steam constitutes an insignificant fraction of the fluid.

It is straightforward to monitor reservoir pressure drawdown and cooling in single liquid phase reservoirs. Monitoring only involves measuring the temperature of the water discharged from wells, whether artesian or pumped, and recording the water level in special monitoring wells. This is, on the other hand, not the case with boiling geothermal reservoirs. Temperatures at wellheads are controlled by the wellhead pressure, which is in turn adjusted at a particular level to suit the required inlet pressure to the power station. For the same reason, measurement of pressure in discharging wells provides information that is of little value to reservoir pressure drawdown. On the other hand, measurement of water level in non-productive wells in boiling geothermal systems provides information on drawdown in reservoir pressure. This is not the case with shut-in wells if they form a steam cap.

Chemical and isotopic data on water and steam from wells sunk into a boiling geothermal reservoir provide useful information on the response of the reservoir to the production load as regards recharge and enhanced boiling. Such data have also proved valuable to map cold water recharge into single liquid water reservoirs. The chemical data gathered by the monitoring studies also provide information on the quality of the fluid for the use in question, including any changes in scaling and corrosion tendencies.

16.2. INJECTION

During the development of the Ahuachapán geothermal field in El Salvador in the late 1960s it was considered for the first time that injection of the waste brine from producing wells was a viable method of disposal, both for economic and environmental reasons. Injection has now been adapted as the general method of disposal in most geothermal projects worldwide. The reason for injection is twofold. It is feasible environmentally and helps maintain reservoir pressures, at least, if the waste fluid is injected through special wells back into the reservoir.

For injection, either special wells must be drilled or non-productive wells must be used for that purpose. If an injection well is located within the field of producing wells, there is always the risk that relatively cold water from the injection well will flow rapidly into the aquifer of a producing well, thus deteriorating its performance or even killing it. In the long run, injection of waste brine into a producing reservoir may have some negative effects. When the same water is recycled, successive steam loss will increase its salinity, which may in turn lead to scaling problems. In the Palinpinon geothermal field in the Philippines, where waste fluid has been injected for some years, reinjection return into production wells has already occurred as indicated by an increase in the salinity of the water produced. It is, therefore, clear that chemical and isotopic monitoring is required for studying the fate of the injected waste brine because such an injection affects the characteristics of the reservoir. Specifically, geochemical studies are required to assess the temperature dependence of scaling tendencies from waste fluids and to identify the optimum temperature for injection. This topic was discussed in Chapter 14 (see Box 14.5).

Special tracer studies have been carried out in many wellfields to map the subsurface flow of the injected fluid. They involve injection of an isotope or a chemical into one well and analyses over a period of time for that isotope or element in producing wells in order to map flow rates and see how much of the tracer is returned. Chemical compounds which have been used as tracers include various halogen alkaes, sodium fluorescein, rhodamin-WT and halogen salts of potassium and magnesium. Iodine-125 and iodine-131 as well as tritium have also been used as artificial tracers (Adams, 1995).

16.3. FREQUENCY OF SAMPLING FOR MONITORING STUDIES AND THE SELECTION OF CHEMICAL AND ISOTOPIC COMPONENTS FOR ANALYSIS

Chemical and isotopic monitoring studies of exploited geothermal reservoirs require regular sampling of the discharged fluid. More frequent sampling is required for dry and wet steam wells than for hot water wells. Generally, the frequency of sampling is highest during the early stages of discharge of each well. Occasionally, samples should be taken for analysis of all major components in both water and steam samples but otherwise partial analysis is considered sufficient. Box 16.1 summarizes which components should be analysed for partial and complete major element and isotopes.

Each of the components provides its information on changes in reservoir conditions as discussed in the following sections of this chapter. Specifically, decreases in the concentrations of the incompatible components Cl and B in the liquid water phase of well discharges, at a particular separation pressure, are indicative of cold water recharge. Changes in reactive component concentrations or ratios can be due to reactions in the depressurization zone in the aquifer of producing wells, recharge of shallow cold water into that aquifer or recharge of deeper hotter water. Changes in deuterium and ^{18}O may reflect recharge from a different source into producing aquifers. Recharge of injected waste brine can be expected to be reflected in increasing Cl concentrations and increasing δ values for deuterium and ^{18}O in the fluid discharged from producing wells. Further, rapid recharge of shallow cold water may show up in measurable tritium in discharged fluids.

16.4. PRESENTATION OF MONITORING DATA

The principal variable for monitoring studies is time. It is, therefore, convenient to present chemical and isotopic data from discharged fluids as plots against time where time is on the x-axis and the respective chemical or isotopic component concentration or ratio on the y-axis. Both primary data and derived data should be plotted. The primary data include analytical concentrations or ratios whereas derived data include such parameters as geothermometry temperatures and initial aquifer steam fraction values. It is important to plot together with the chemical and isotopic data discharge enthalpies and steam flows because variations in discharge enthalpy can be the cause of variations in chemical and isotopic compositions of well discharges. It is also important to relate the chemical and isotopic variations to steam flow, both for the same well and between wells. Drawdown not only affects steam flow rates from wells; it may also affect the chemistry of the discharged fluid. When drawdown is extensive, the water/steam mixture takes longer time to flow through the depressurization zone as compared to limited drawdown and has, therefore, more time to react and change its chemistry under the new temperature and pressure conditions in this zone. Accordingly, poor producing wells are more likely to change their chemistry with time than highly productive wells.

There are two possibilities for representing time variations in the concentrations of chemical and isotopic components in well discharge fluids. One is to select the total discharge composition. The other is to show concentration variations in the discharged water (aqueous components) and steam (gaseous components) phases, respectively.

The extent to which liquid water vaporizes during pressure drop does not only depend on this drop but also on the ratio of liquid water to vapour and the absolute pressure values. Steam has maximum enthalpy at 236°C (35 bar), and in the range of 180–270°C (10–55 bar) the enthalpy of steam varies little with temperature (Fig. 16.1). In this range, vaporization of water as a result of pressure drop has little dependence on the ratio of liquid water to vapour. At temperatures below about 180°C and above 270°C this is, however, not the case. This means that the concentrations of aqueous and gaseous components in samples of water and steam collected at pressures below 180°C depend not only on their concentrations in the aquifer fluid but also on the enthalpy of the discharge (Box 16.2). To minimize as much as possible the effect of variations in discharge enthalpy on the concentrations of aqueous and gaseous components in the water and steam phases of the discharge, these concentrations should be calculated from the measured discharge enthalpy at a temperature where the steam enthalpy varies little with temperature. The temperature should, however, not be higher than the inflow temperature of wells because boiling processes in the aquifer can affect the enthalpy of the flowing fluid to the point of entrance into the well. It appears that a value of 180°C is a convenient choice for many geothermal fields.

It is advisable to occasionally draw maps for wellfields of equal concentrations for a partial element or isotope, or a ratio, to reflect changes with time. Comparison of maps representing different points in time facilitates evaluation of the spatial distribution of changes and helps in locating where recharge into an exploited reservoir may be occurring.

16.5. CONSERVATIVE COMPONENTS

An account of conservative components was given in Chapter 4. These components are particularly useful in mapping recharge into exploited geothermal reservoirs. The highly mobile components, although not strictly conservative, as well as the radioactive isotope tritium are also useful in this respect. The most widely used natural chemical and isotopic components to trace recharge into geothermal reservoirs are chloride and deuterium. Other components, such as B and ^{18}O, have also been used. Cold water recharge may neither cause immediate cooling of producing aquifers nor of the discharged fluid because the recharging water gains heat by contact with the hot reservoir rock on passage to discharging wells. Thus, cold water recharge may be particularly

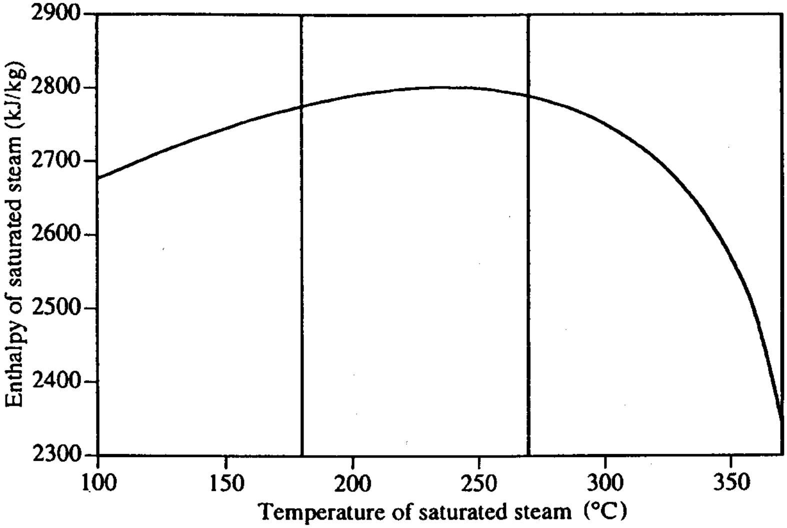

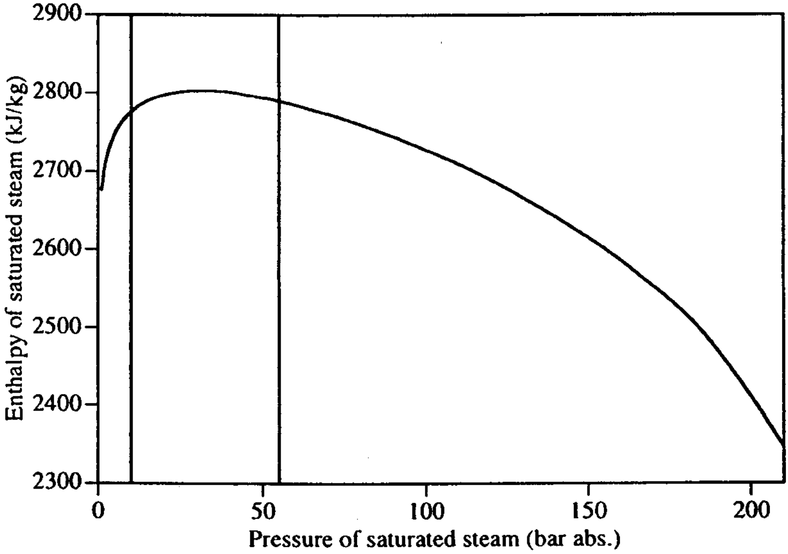

FIG. 16.1. Relationship between enthalpy, temperature and pressure of saturated steam. The enthalpy of steam is about constant within the ranges marked by the vertical lines, 180–270°C and 10–55 bar abs., respectively.

difficult to detect in boiling reservoirs. However, changes in the chemical and isotopic composition of the fluid discharged from wells with respect to conservative components may reflect recharge of cold water and act as a signal that cooling could take place in the future.

The decreasing chloride concentrations in water discharged from wells at the Momotombo geothermal field in Nicaragua are indicative of cold water recharge into the reservoir. Initially chloride levels in water boiled to atmospheric pressure were at about 4000 ppm, but in 10–15 years these concentrations have decreased to less than 2000 ppm in some wells. Concentrations in water at vapour pressure of 10 bars abs. show a little less decline (Fig. 16.2). This decrease has been accompanied with a drop in steam output (Fig. 16.3). During their early production history, some wells had excess discharge enthalpy whereas others had liquid enthalpy. The enthalpy of the excess enthalpy wells has gradually decreased with decreasing chloride concentrations in the discharged

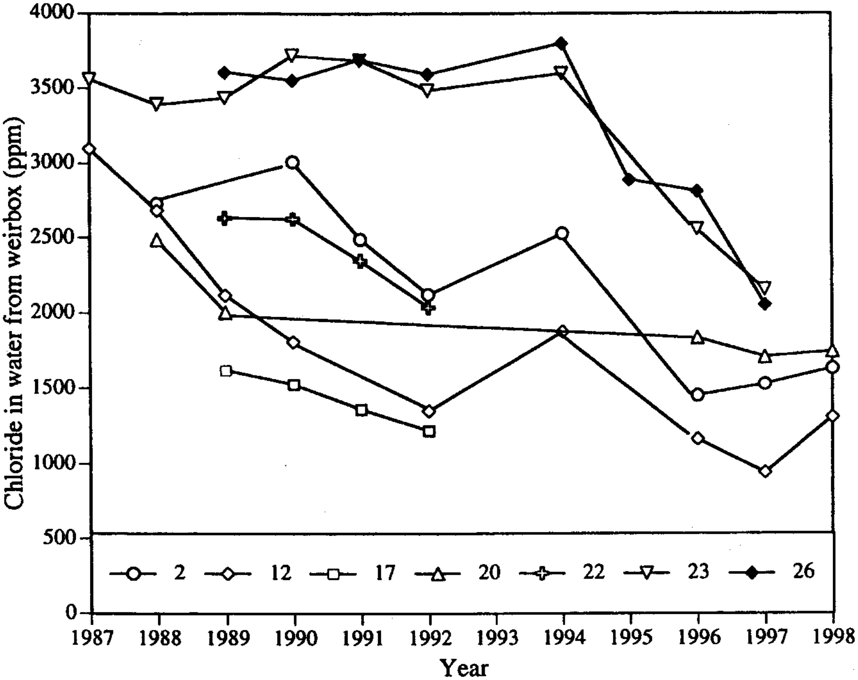

FIG. 16.2. Chloride concentrations in water at 10 bar abs. from wells 2, 12, 17, 20, 22, 23 and 26 at Momotombo, Nicaragua. From Arnórsson (1998).

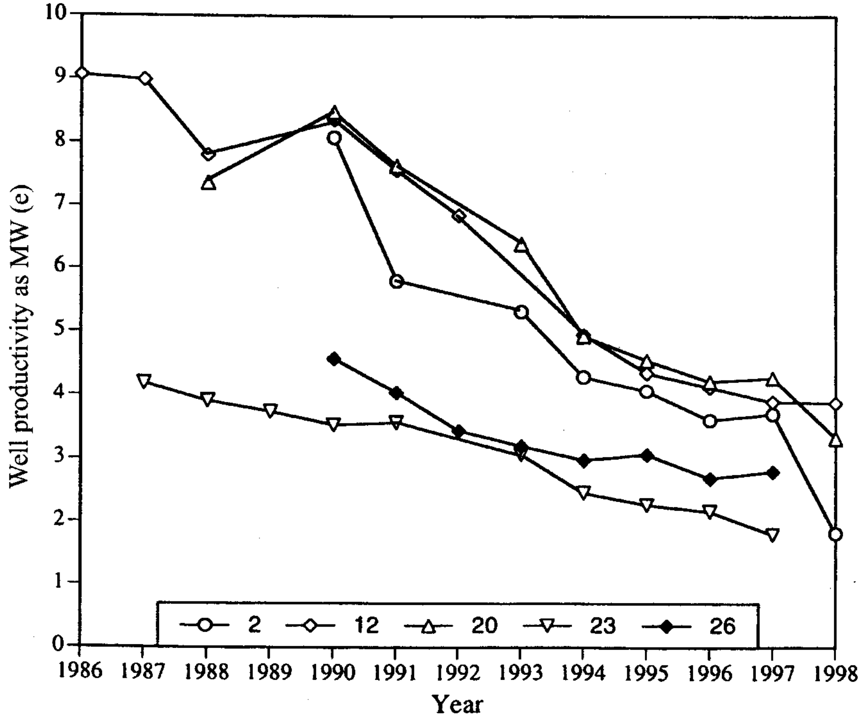

FIG. 16.3. Steam discharge (expressed as MW(e)) of wells 2, 12, 20, 22, 23 and 26 at Momotombo, Nicaragua, in the period 1987–1998. 1 MW(e) ≈ 2 kg/s of steam at 6 bar abs. From Arnórsson (1998).

water (Fig. 16.4). Some of these wells have become unproductive at a time when their enthalpy was approaching that of liquid enthalpy for the respective aquifer temperature.

As is the case at Momotombo, some well discharges in the Krafla field in Iceland display decreasing chloride concentrations, indicating cold water recharge, whereas others do not (Fig. 16.5). Well 9, the results for which are depicted in Fig. 16.5, shows both constant chloride concentrations and discharge enthalpy, this enthalpy being equal to that of liquid water in the aquifer (Fig. 16.6). Its steam flow decreased in the period 1978–1984 but has stayed constant since (Fig. 16.7). By contrast, the chloride concentrations of wells 13 and 21 have decreased substantially (Fig. 16.5). For well 13 they decreased rapidly up to 1984 but since then have stayed constant at a level very similar to that of

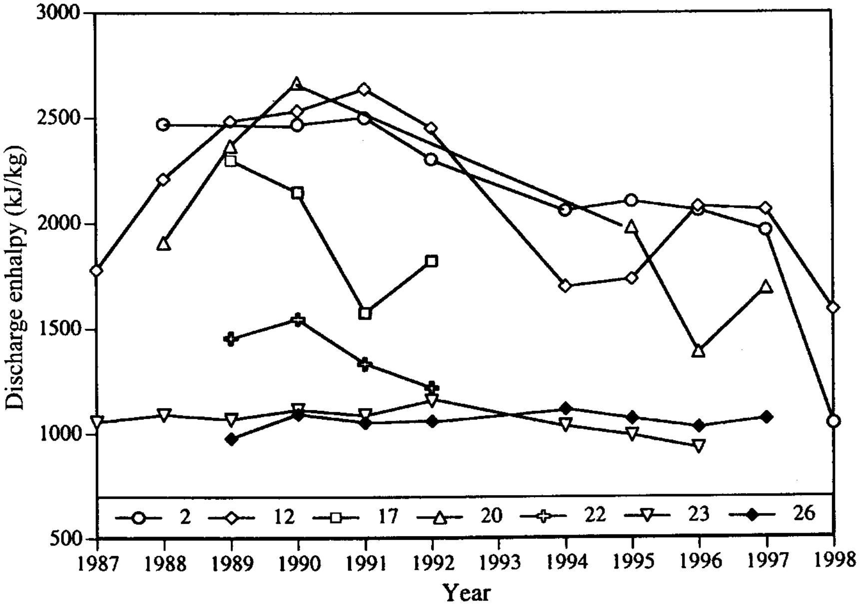

FIG. 16.4. Discharge enthalpy of wells 2, 12, 17, 20, 22, 23 and 26 at Momotombo, Nicaragua, in the period 1987–1998. From Arnórsson (1998).

well 9. In the water discharged from well 21, chloride levels have decreased about linearly with time (Fig. 16.5). The discharge enthalpy of well 13 has decreased gradually but at the same time its steam flow rate has increased (Figs 16.6 and 16.7). In the case of well 21, discharge enthalpy was about constant until 1988, after which it has increased (Fig. 16.6). The same applies to its steam flow (Fig. 16.7). These examples from Krafla show that there need not be any correlation between cold water recharge and well performance (discharge enthalpy and steam flow rate) and that individual wells within the same field can behave differently. The improved yield of wells 13 and 21 could be due to widening of fractures by thermal contraction of the aquifer rock due to cooling. This cooling could be caused either by depressurization or cold water recharge, or both. As will be discussed in the following section, there is no evidence from geothermometry that the improved yield is caused by recharge from deeper and hotter levels in the reservoir.

The idea that more attention should be given to Ar for monitoring studies has been put forward. Argon can easily and accurately be determined by gas

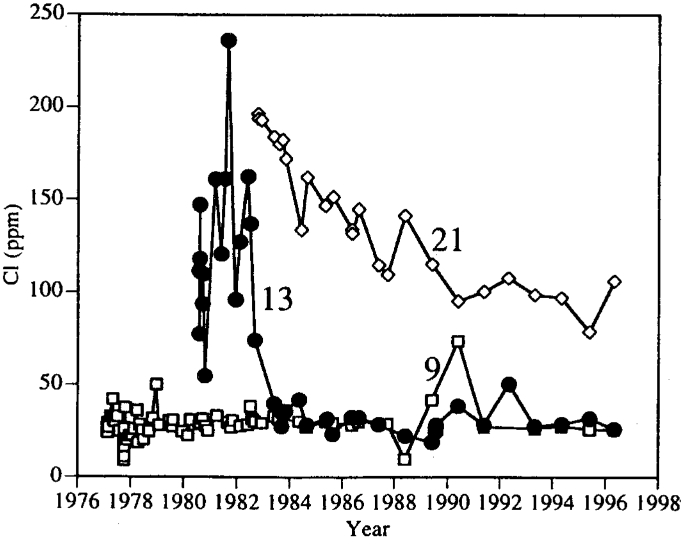

FIG. 16.5. Variations in chloride concentrations with time in water at 10 bar abs. vapour pressure discharged from wells 9, 13 and 21 at Krafla, Iceland. From Gudmundsson and Arnórsson (1997).

chromatography by using double separation columns that eliminate interference from oxygen. The sole source of argon in groundwater is the atmosphere. The levels of Ar in geothermal aquifer fluids are expected to furnish information on recharge. Decrease in argon concentrations with time below those of air saturated water are indicative of progressive boiling of water in the formation, whereas an increase in argon bears witness to flow of early formed steam into wells. Boron should also be given more attention because of its high volatility even at moderate temperatures. The distribution of boron between liquid water and vapour and its concentration changes in water discharged from wet steam wells in relation to variations in discharge enthalpy may provide useful information on the boiling mechanisms responsible for excess enthalpy well discharges. At relatively high temperatures (>250°C), a significant fraction of the B in the fluid partitions into the steam phase. If phase segregation occurs at high temperature in the aquifer of a discharging well in such a way that the steam to water ratio of the flowing fluid increases, later pressure drop and, therefore, cooling of the flowing fluid will cause the B in the steam to dissolve in the flowing water. Since the fraction of this flowing water has decreased as a result of phase segregation, B can be substantially enriched in the water that enters the well. A decrease in the Cl/B ratio

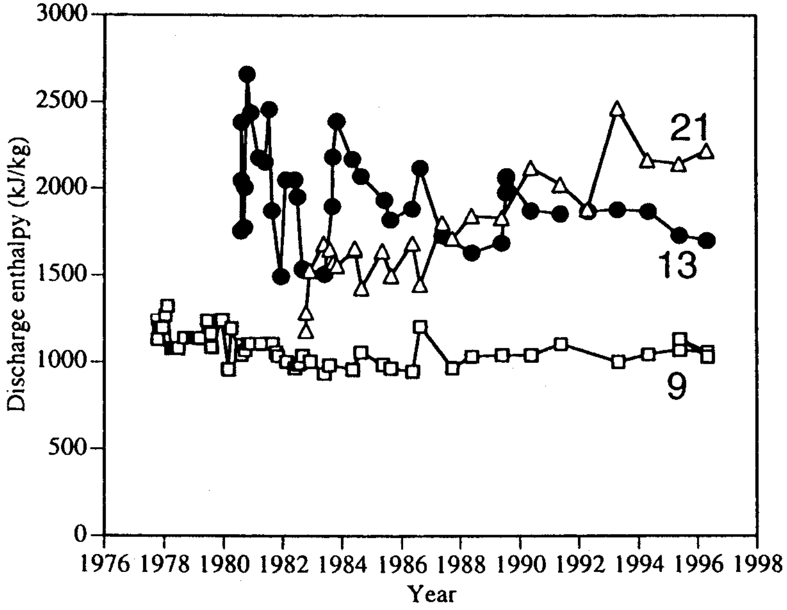

FIG. 16.6. Discharge enthalpy versus time for wells 9, 13 and 21 at Krafla, Iceland. From Gudmundsson and Arnórsson (1997).

of well discharges that relates to increases in discharge enthalpy is expected to be due to transport of B into high pressure steam and back into the water at lower pressures.

16.6. REACTIVE AQUEOUS COMPONENTS

Cold water recharge into exploited geothermal reservoirs will not only tend to change the concentrations of the conservative components in the produced fluids but will also tend to change those of the reactive components. However, the reactive components will react between themselves and/or with minerals in the rock towards equilibrium as the recharging water gains heat. How closely

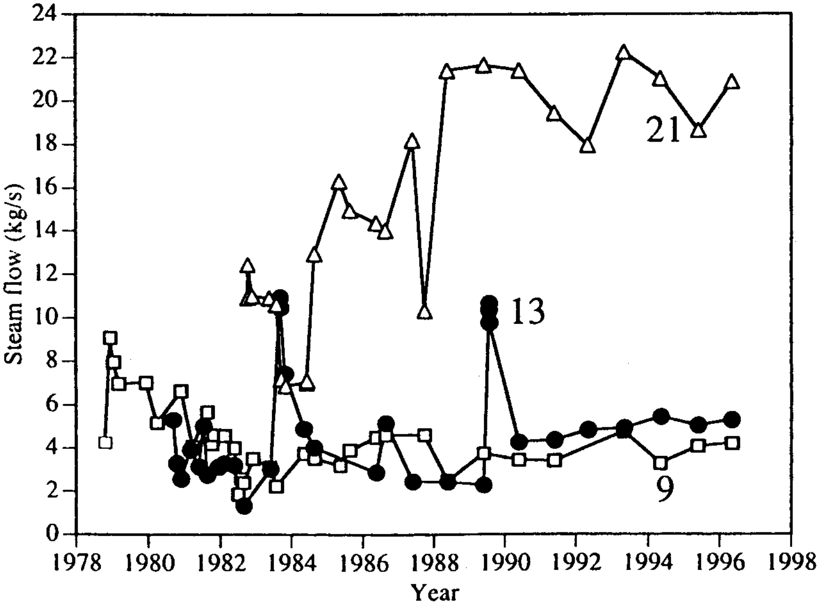

FIG. 16.7. Steam flow wells 9, 13 and 21 at Krafla, Iceland. From Gudmundsson and Arnórsson (1997).

equilibrium is approached for any particular component depends on the rate of recharge, the path of heating, the reaction rate for that component and the surface area between the water and minerals with which this component reacts.

Cooling by depressurization boiling upsets the state of mineral–solution equilibria in producing aquifers of wet steam wells, as well as the slates involving aqueous component concentrations only. Degassing of the aquifer water, which accompanies the boiling, has the same effect. Changes in the equilibrium state by cooling and degassing tend to cause modification of the activities of the reactive components through reactions towards equilibrium under the new conditions. Reactions involving minerals are relatively slow, as are many redox reactions involving aqueous species and gases. Many aqueous component reactions can, on the other hand, be regarded as instantaneous, such as those involving CO_2, bicarbonate or cation hydrolysis.

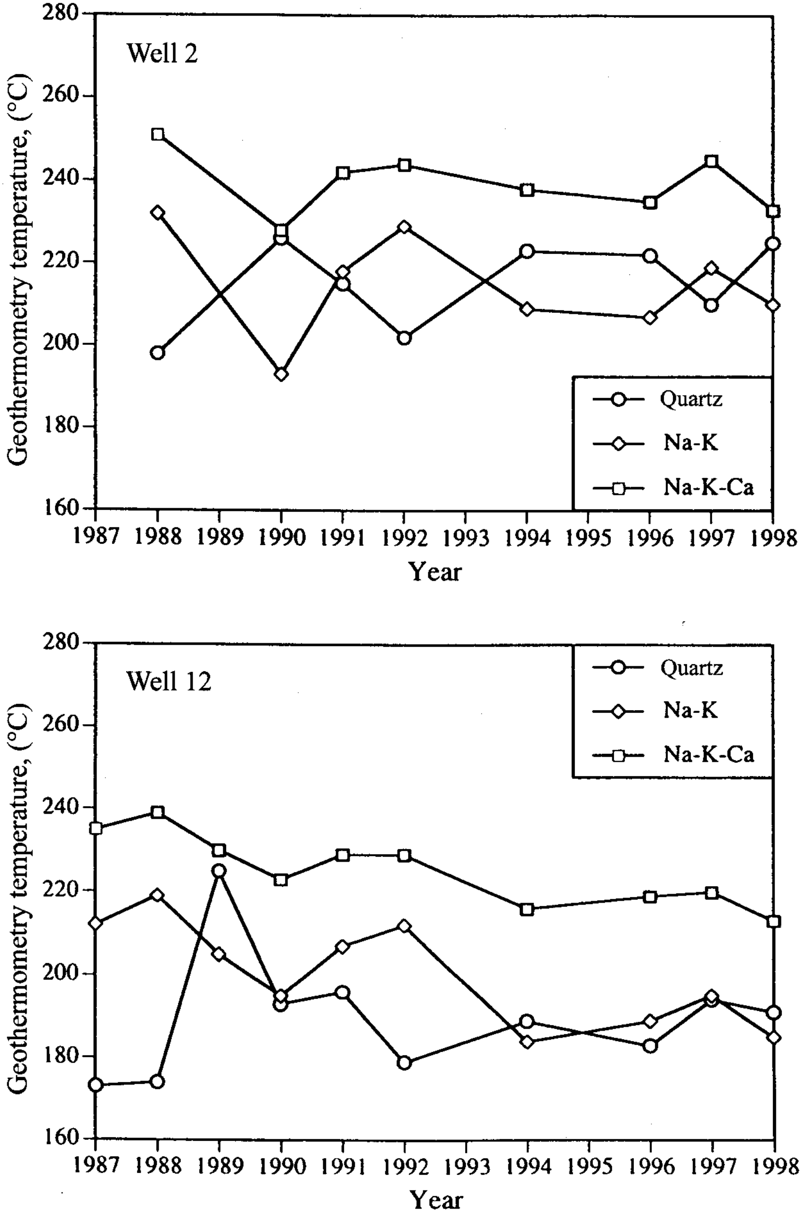

FIG. 16.8. Geothermometry results for wells 2 and 12 at Momotombo, Nicaragua. From Arnórsson (1998).

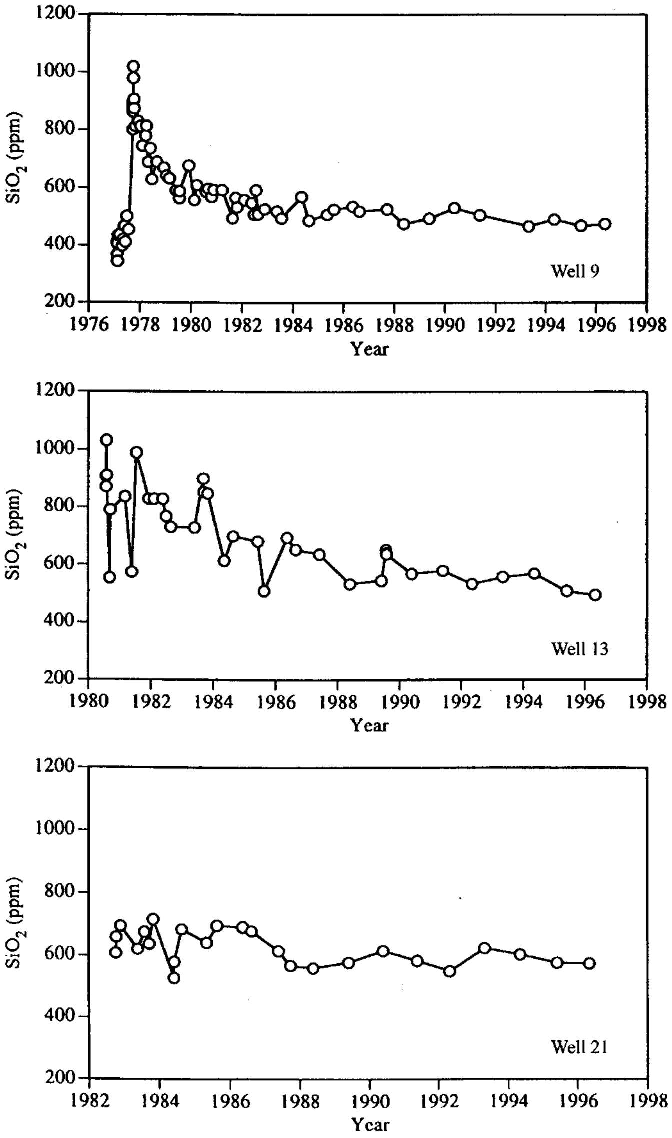

FIG. 16.9. Variation of silica concentrations with time in water at 10 bar abs. vapour pressure from wells 9, 13 and 21 at Krafla, Iceland. From Gudmundsson and Arnórsson (1997).

In the previous example from Momotombo, geothermometry temperatures have not decreased significantly with time for most of the wells (Arnórsson, 1998). This is exemplified for two wells in Fig. 16.8. No decline is observed for well 2 but some decline for well 12. The results for well 2 suggest two things: first, the recharging cold water has closely approached equilibrium at the prevailing aquifer temperature and, secondly, the recharge is not directly into the depressurization zone around the well where the initial aquifer fluid has cooled by boiling. If this were the case, one would expect geothermometry temperatures to become maximally equal to those existing in this zone. In the case of well 12, either recharge into the depressurization zone or partial re-equilibration in this zone, or both, could be responsible for the declining quartz and Na/K geothermometry temperatures. For the Momotombo wells, quartz equilibrium and Na/K temperatures compare quite well, whereas those of the Na/K/Ca geothermometer are higher. This could be due to inadequate calibration of this geothermometer with respect to the Momotombo waters. However, loss of calcium from the water, which accompanies calcite precipitation, when the water boils, leads to an increase in the calculated Na/K/Ca temperature, which could be, at least partly, the cause of the discrepancy.

The picture for the Krafla wells is quite different. In the wells selected for discussion in the previous section (Nos 9, 13 and 21), silica concentrations have decreased with time (Fig. 16.9), and at the same time the Na/K ratios have increased (Fig. 16.10). In the case of well 9, the initial low silica concentrations and the high Na/K ratios represent samples taken before the well had been drilled to full depth. The aquifer producing at this time was later cased off and the well deepened. During this later drilling, a deeper and hotter aquifer that produces into the well was struck.

Decrease in silica and increase in Na/K ratios cause the quartz and Na/K geothermometry temperatures to decrease with time (Fig. 16.11). These geothermometers yield different values for well 9, the quartz temperature being higher, particularly during the first few years of discharge, but subsequently about constant at approximately 20°C variation. By contrast, quartz and the Na/K temperatures are very similar for wells 13 and 21 during the first few years of discharge, but subsequently the Na/K temperatures decrease more than the quartz temperatures. In a twenty year period the decrease in the Na/K temperatures amounts to 11°C and 54°C for wells 9 and 13, respectively. A continuous decrease is not observed for well 21. Before 1987, geothermometry temperatures stayed constant, at about 265°C. After this time they also stayed about constant but at a lower level, at about 235°C in the case of the Na/K geothermometer and

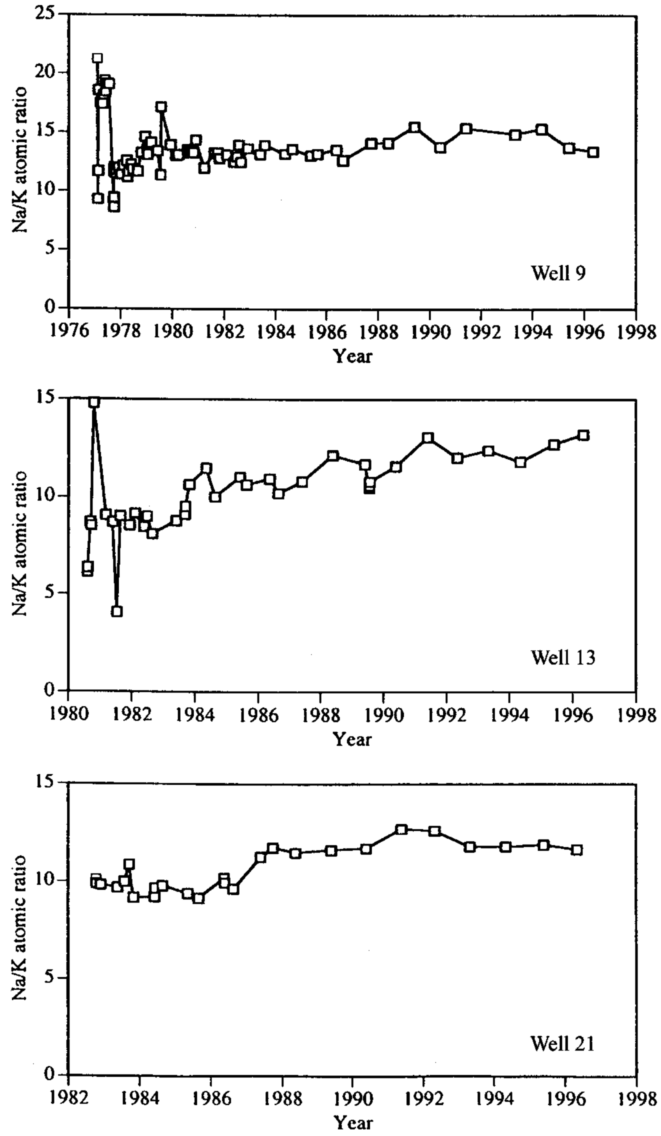

FIG. 16.10. Na/K ratios versus time for selected wells at Krafla, Iceland. From Gudmundsson and Arnórsson (1997).

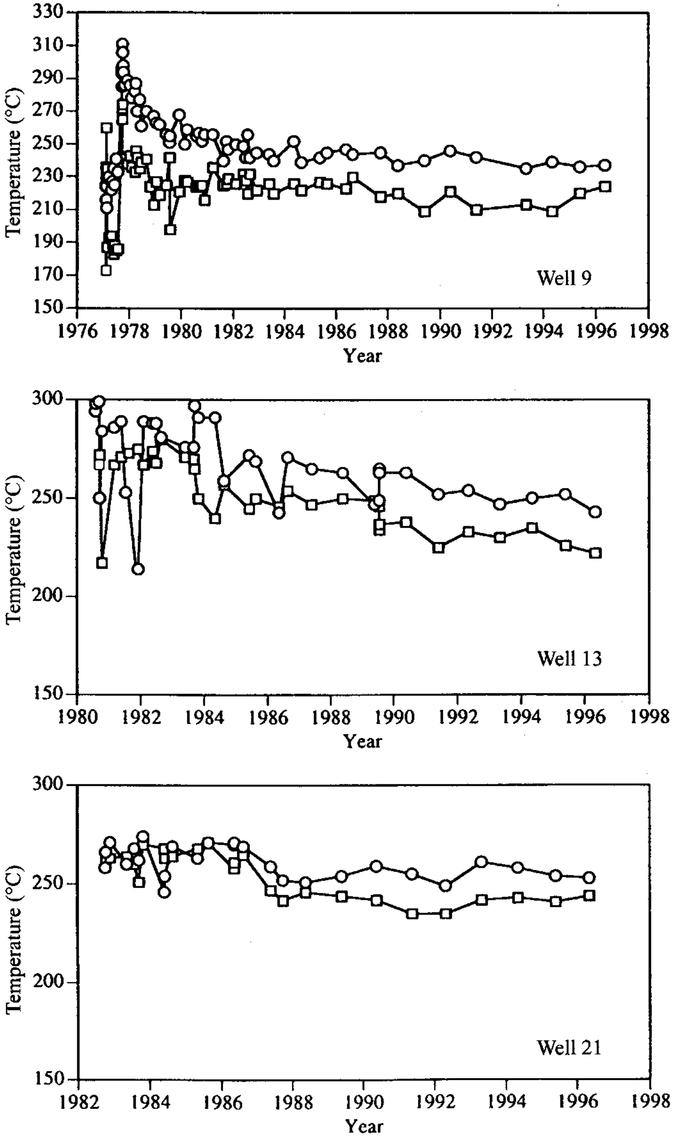

FIG. 16.11. Quartz equilibrium (circles) and Na/K (squares) temperatures for selected wells in the Krafla field, Iceland. From Gudmundsson and Arnórsson (1997).

at about 255°C for the quartz geothermometer. The change in the geothermometry temperatures can be correlated with a change towards an increase in both steam flow and discharge enthalpy. Together, these results are considered to be indicative of opening up, or widening, of a colder aquifer than the one producing before 1987.

When calculating the quartz equilibrium temperatures for the wells from Momotombo and Krafla discussed previously, a one stage adiabatic boiling was assumed. If the silica content of the total discharge had been used instead, lower quartz equilibrium temperatures would have been obtained. Many of the wells in question have excess enthalpy. One stage adiabatic boiling really assumes that phase segregation is responsible for the excess enthalpy. Using the silica in the total discharge for calculating the quartz equilibrium temperature implies, on the other hand, that one assumes the excess well discharge enthalpy to be produced by heat flow from the rock to the flowing fluid in the depressurization zone. In contrast to the quartz geothermometer, the Na/K geothermometer is independent of the boiling mechanism in the aquifer because it is based on an elemental ratio rather than on concentration. The discrepancy between the results of these two geothermometers is largest for well 9, which has liquid enthalpy. For that reason, it seems unlikely that the high quartz equilibrium temperatures, as compared with those of Na/K, can be due to the faulty assumption of one stage adiabatic boiling when calculating the quartz temperature.

Quartz and Na/K geothermometry results should always be compared in order to infer the boiling mechanism responsible for excess enthalpy wells. To be able to do this with confidence, precise analysis is required and, if liquid enthalpy wells exist in the area under study, quartz and Na/K temperatures must compare well. If they do not, either the analysis is imprecise or the calibration used is faulty. Alternatively, a possible cause of the discrepancy could be yield from more than one aquifer of significantly different temperatures into the liquid enthalpy well in question.

Sulphate is controlled by anhydrite solubility in many geothermal fluids. Some such fluids, though, may be anhydrite undersaturated. In the latter case, the sulphate could be incompatible or controlled through a redox equilibrium with H_2S. It is observed that sulphate levels tend to be low in very hot geothermal waters and increase with decreasing temperature. This is the case at Momotombo and Krafla. Deep and hot wells (>250°C) have aqueous sulphate concentrations running in few tens of ppm, whereas shallower and less hot wells (<250°C) have aqueous sulphate concentration of a few hundreds of ppm. For many of the Krafla wells, sulphate concentrations have increased with time when chloride

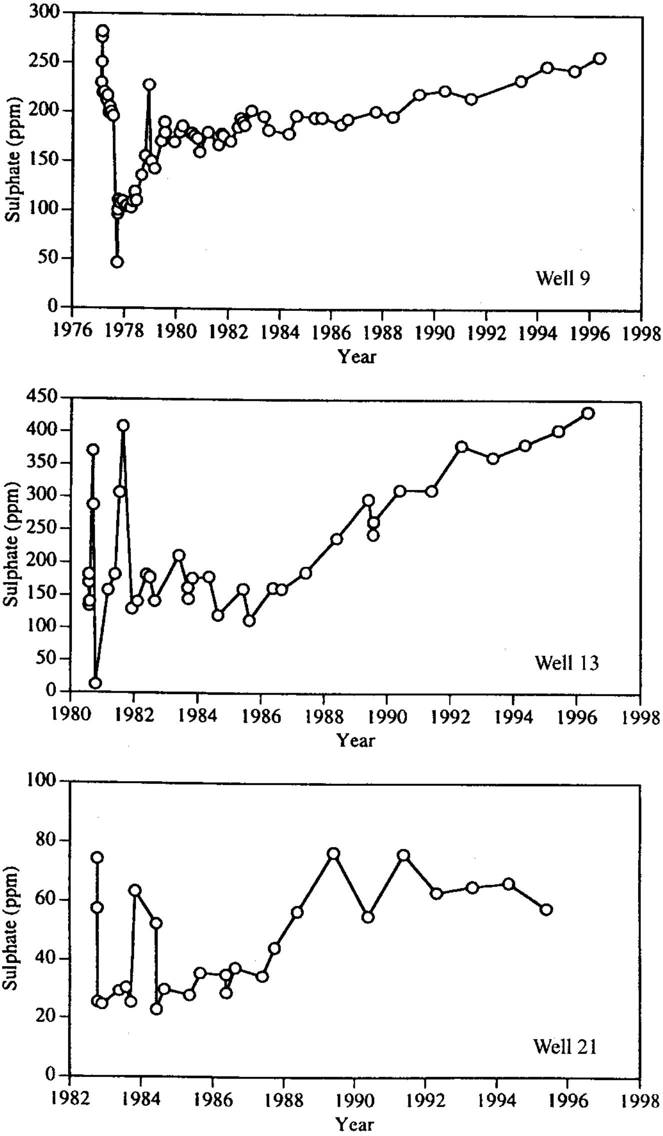

Fig. 16.12. Variation in sulphate concentrations in water (at 10 bar abs. vapour pressure) discharged from wells at Krafla, Iceland. From Gudmundsson and Arnórsson (1997).

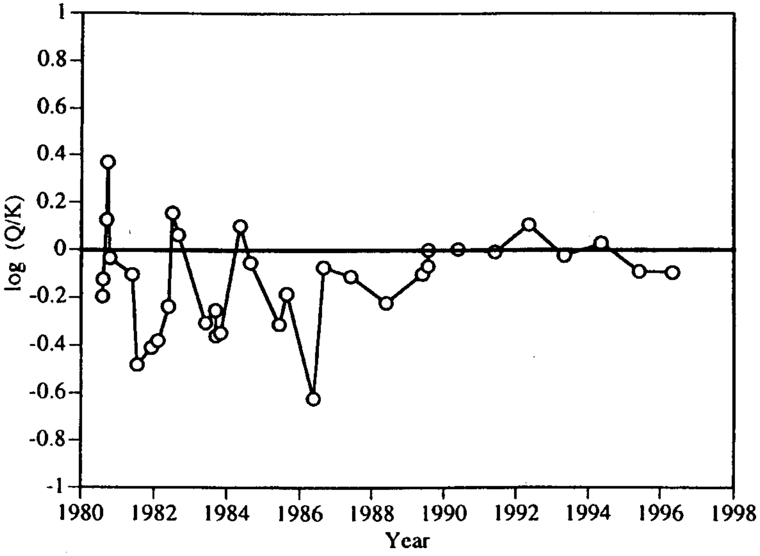

FIG. 16.13. Anhydrite saturation in the aquifer of well 13 at Krafla.

concentrations have decreased (Fig. 16.12). This is particularly the case for well 13, which has suffered the most cooling. For well 21, sulphate concentration jumped to a higher value in 1987 when an aquifer having a lower temperature as indicated by geothermometry fed the well. However, sulphate levels are generally constant before 1987 and at a later stage (Fig. 16.12). The aquifer waters of all these wells at Krafla are close to being anhydrite saturated as depicted in Fig. 16.13 for well 13. Anhydrite has retrograde solubility. Increased sulphate concentrations in the well discharges are, therefore, the result of cooling, either because of cold recharge or cooling by boiling in the depressurization zone around wells.

16.7. REACTIVE GASEOUS COMPONENTS

Gaseous components may be used to study the response of geothermal reservoirs to the production load. CO_2, H_2S and H_2, as well as various gas–gas equilibria, are considered to be of particular interest in this respect. Studies by the authors, which were discussed in Chapter 15, indicate that aqueous H_2S and H_2 concentrations are fixed by aquifer temperature through equilibria with minerals. CO_2 also appears to be controlled by mineral solution equilibria, at least in some reservoirs. In other words, the concentrations of these gases can be used as geothermometers. H_2S is very soluble in water compared to H_2. For this reason steam fraction values, when low, do not significantly affect the H_2S content of reservoir fluids and wet steam well discharges. When H_2 geothermometry temperatures are significantly higher than those of H_2S, this can be taken as an evidence of the presence of equilibrium steam in the producing aquifer. Increases in H_2 temperatures in the steam of well discharges in excess of H_2S temperatures are indicative of an increasing initial, or equilibrium, steam fraction in the aquifer, and visa versa.

Figures 16.14 to 16.16 depict monitoring results for CO_2, H_2S and H_2 in the steam of three wells in the Krafla field in Iceland. During the first few years of discharge, steams from all the wells show considerable scatter in gas levels, after which they stabilize. After the stabilization period, CO_2 levels in well 9 are constant. They have increased a little in well 20, but decreased about five times in well 11, most likely because of decreasing contribution from magma having intruded into the roots of the geothermal system in the period, of 1975 to 1984 (Ármannsson et al., 1982; Arnórsson, 1995a). The pattern for H_2S in wells 9 and 20 is similar to that for CO_2. In well 11, H_2S levels have remained constant since 1982. The variations in H_2S concentrations in the steam discharged from the wells in the Krafla field reflect changes in the aquifer temperature of these wells (Fig. 16.17).

H_2 concentrations have not changed significantly in the steam discharged from well 9 at Krafla. Considerable increase is, on the other hand, observed for well 11. As H_2S has remained constant for this well, the increase in H_2 is considered to result from an increased initial steam fraction in the discharge, possibly due to additional contribution to the well flow from a deeper horizon in the reservoir. In well 20 there also appears to be a slight increase in the initial steam fraction in the aquifer.

Changes in estimated initial steam fraction values, *y*, have been observed to vary, both laterally and vertically, across geothermal reservoirs such as at the Geysers in California. Time variations have also been observed, such as at Larderello, Italy. Here, the *y* values initially increase with time until well flow rates stabilize. Simultaneously, gas to steam ratios increase. Later, *y* values begin to decrease, which is to be correlated with an increase in the HCl content of the

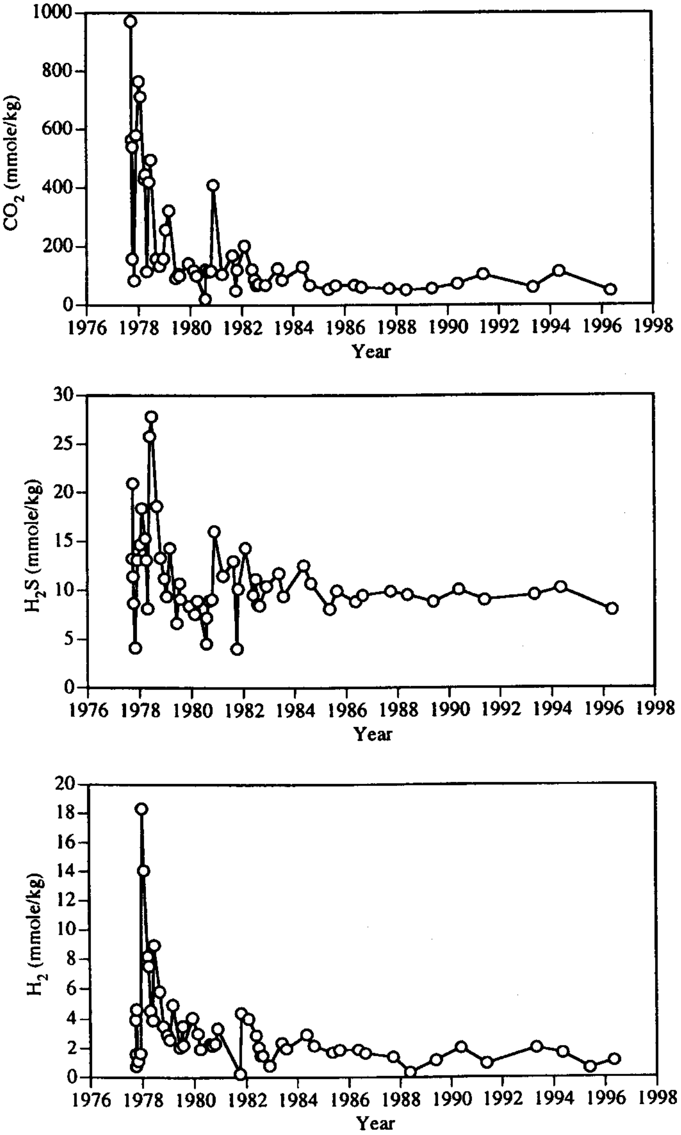

FIG. 16.14. Variations in gas concentrations in steam at 10 bar abs. pressure from well 9 at Krafla, Iceland. Based on Gudmundsson and Arnórsson (1997).

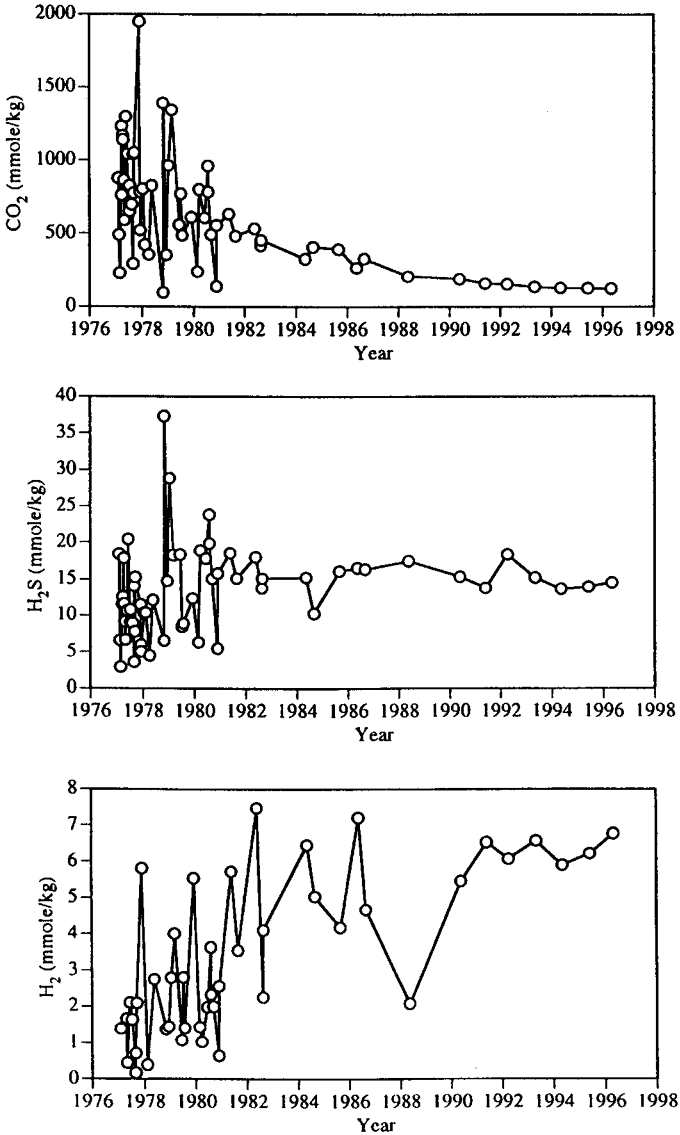

FIG. 16.15. Variations in gas concentrations in steam at 10 bar abs. pressure from well 11 at Krafla, Iceland. Based on Gudmundsson and Arnórsson (1997).

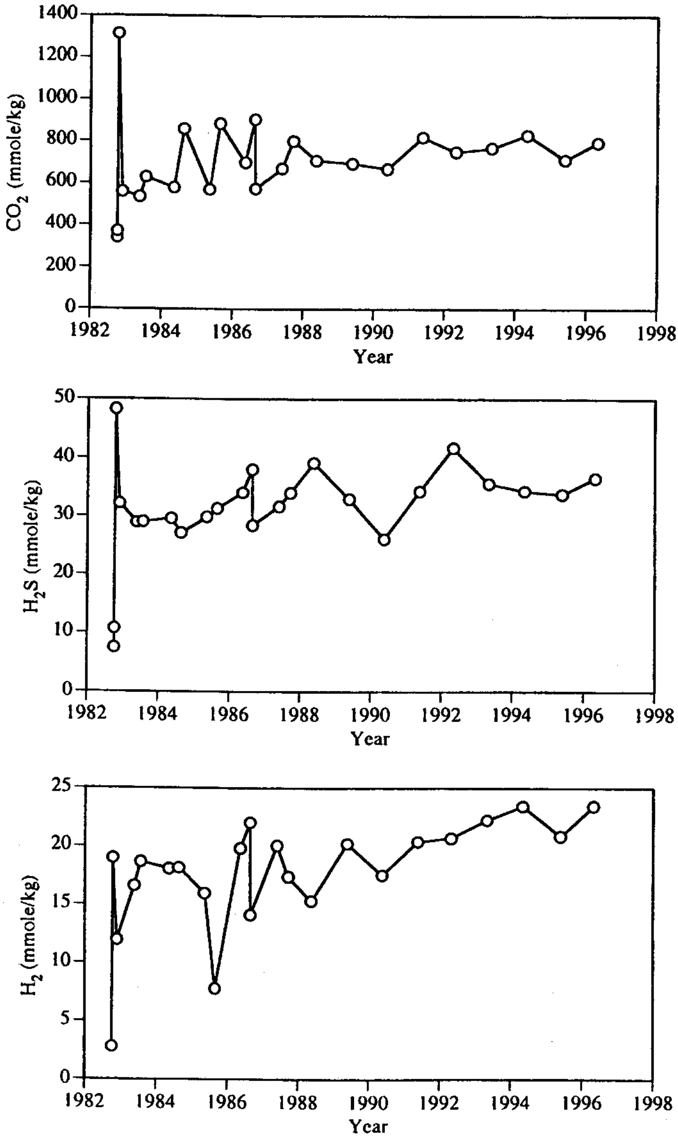

FIG. 16.16. Variations in gas concentrations in steam at 10 bar abs. pressure from well 20 at Krafla, Iceland. Based on Gudmundsson and Arnórsson (1997).

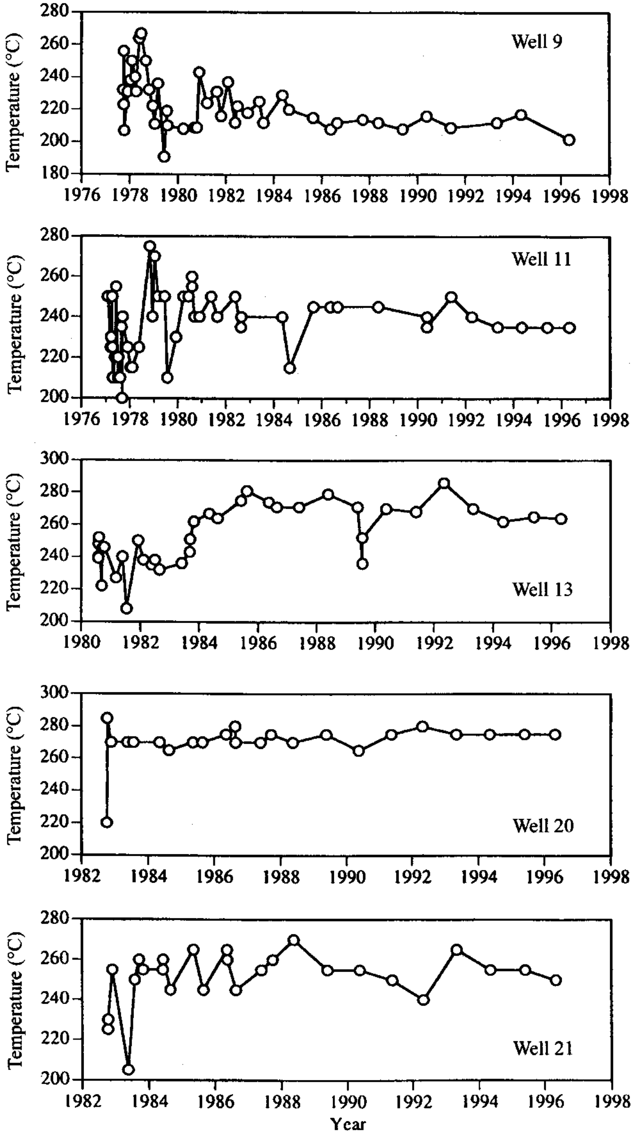

FIG. 16.17. H_2S temperatures in selected Krafla wells.

steam. This increase in HCl is considered to be due to boiling of deep hot brine, which has a low initial steam fraction value.

16.8. DEUTERIUM AND ^{18}O

The deuterium and ^{18}O compositions, either one of them or both, of fluids discharged from wells may change with time during exploitation. There can be several causes for such changes. First, the exploitation may lead to rapid recharge of local groundwater, which differs in its deuterium content from the initial geothermal fluid in the reservoir, owing to a distant origin of the latter. Altitude and/or inland effects would be the cause of the difference in the deuterium content of the local groundwater and the initial reservoir fluid. Second, the recharging water may not develop equal ^{18}O shift as the initial water, because of enhanced fluid circulation through the system. Third, the original geothermal fluid may contain a significant magmatic component, but with enhanced circulation through the system in response to the production load, the relative amount of this magmatic component may decrease and the meteoric component increase correspondingly. Fourth, injected water can be responsible, which, as a result of steam loss, has deuterium and ^{18}O contents different from these of the initial reservoir fluid. Fifth and last, exploitation may alter the boiling mechanism in producing aquifers.

In some geothermal fields, such as the vapour dominated fields of Larderello and the Geysers, spatial variations in δ^{18}O are observed across the fields. The least negative values are associated with major upflow zones, and more negative values away from the upflow have been linked to condensation of steam flowing laterally towards the margins of the fields. Decreasing (more negative) δ^{18}O values are associated with increasing gas content of the steam but decreasing boron content. This is due to concentration of the gases in the remaining steam and partitioning of the boron into the condensate. Injection at Larderello of water with about 0‰ (δ^{18}O and δ^{2}H values) is reflected in an increase in the δ^{18}O and δ^{2}H of steam discharged from wells and a decrease in its gas content (Fig. 16.18), showing that the injected water is rapidly vaporized, at least partly, and that δ^{18}O serves well in this field as a tracer for the injected water.

Monitoring studies of the Palinpinon field, Philippines, indicate that the exploitation of the geothermal resource has led to mixing of the initial reservoir

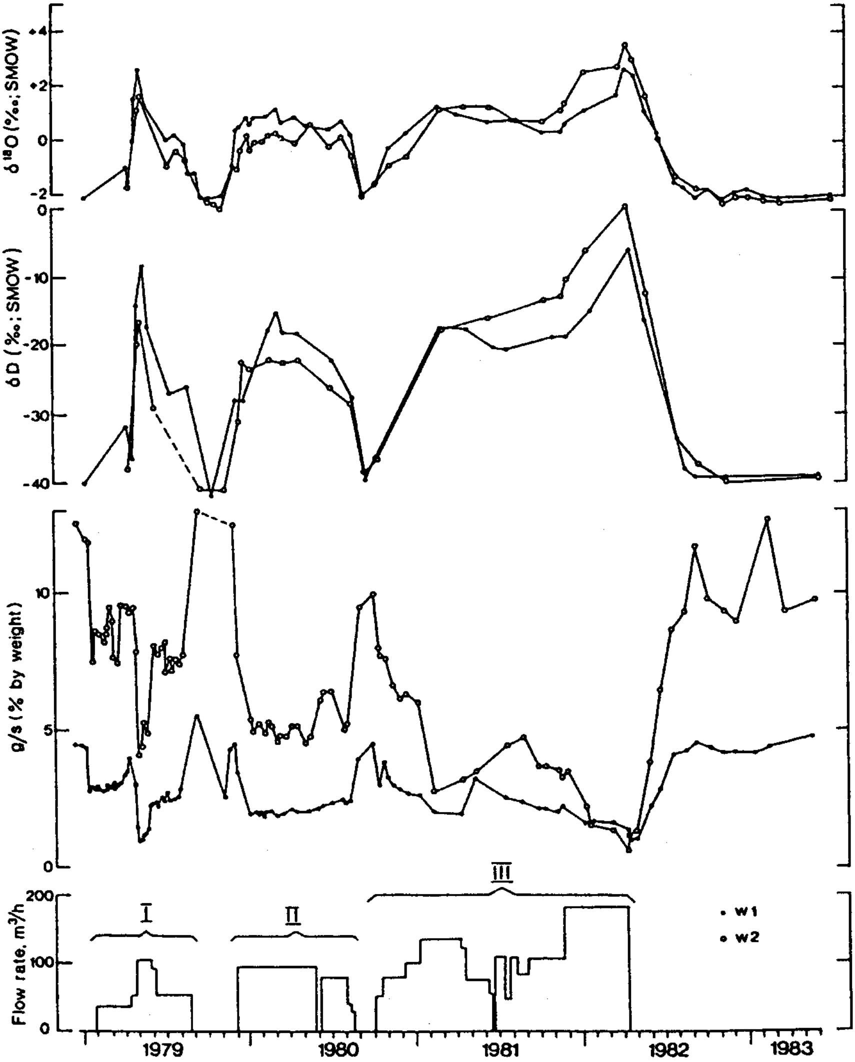

FIG. 16.18. Variations in gas, deuterium and ^{18}O in relation to injection at Larderello, Italy. Different injection periods are indicated by I, II and III.

fluid with fluids of several origins, i.e. meteoric water, magmatic water, injected waste brine and acid sulphate water (Fig. 16.19) (Gerardo et al., 1993; D'Amore et al., 1995; Seastres et al., 1995). Point B in this Fig. 16.9 represents the initial

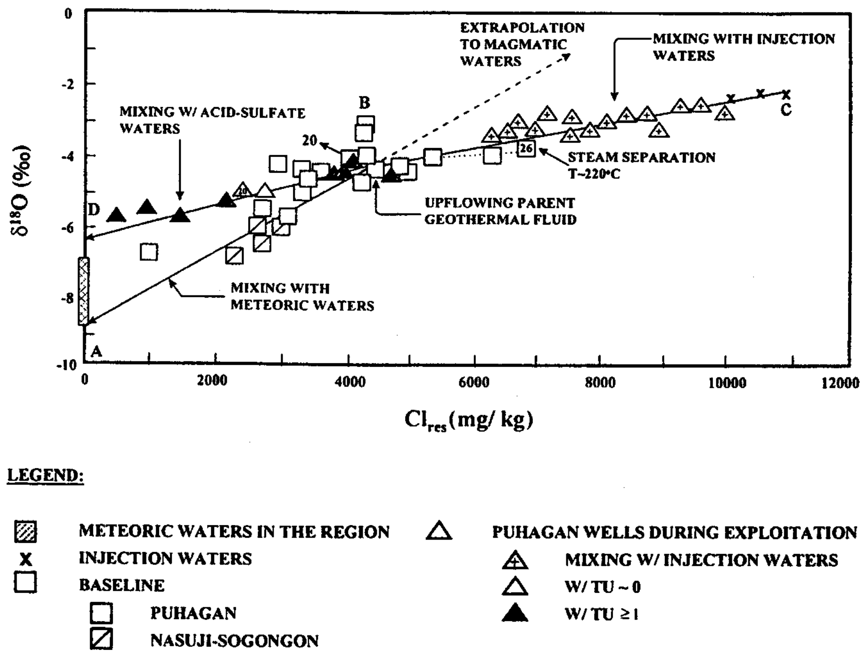

Fig. 16.19. Effects of injection and mixing on the isotopic composition of well discharges at the Palinpinon geothermal field, Philippines. Point B corresponds to the initial geothermal reservoir fluid. Line A–B represents mixing with meteoric water, line B–C refers to mixing of the original reservoir fluid with injected boiled waste brine and line B–D designates mixing with acid sulphate waters.

reservoir fluid. Trend A–B corresponds to mixing with meteoric water, and trend B–C is a mixing line between the initial reservoir fluid and injected boiled waste brine. The high $\delta^{18}O$ value of the acid sulphate waters and their low Cl content have been taken as evidence of their surface origin. Accordingly, these waters represent acid sulphate surface waters which have infiltrated back into the reservoir. Another hypothesis of the origin of the deep acid sulphate waters is that they owe their formation to SO_2 degassing of the magma heat source. If this was true, it implies that the gaseous phase from the heat source is rather low in Cl, with a high $\delta^{18}O$ value.

Figure 16.20 represents a conventional δ^2H–$\delta^{18}O$ diagram for geothermal well fluids and local surface and non-thermal groundwaters at Momotombo,

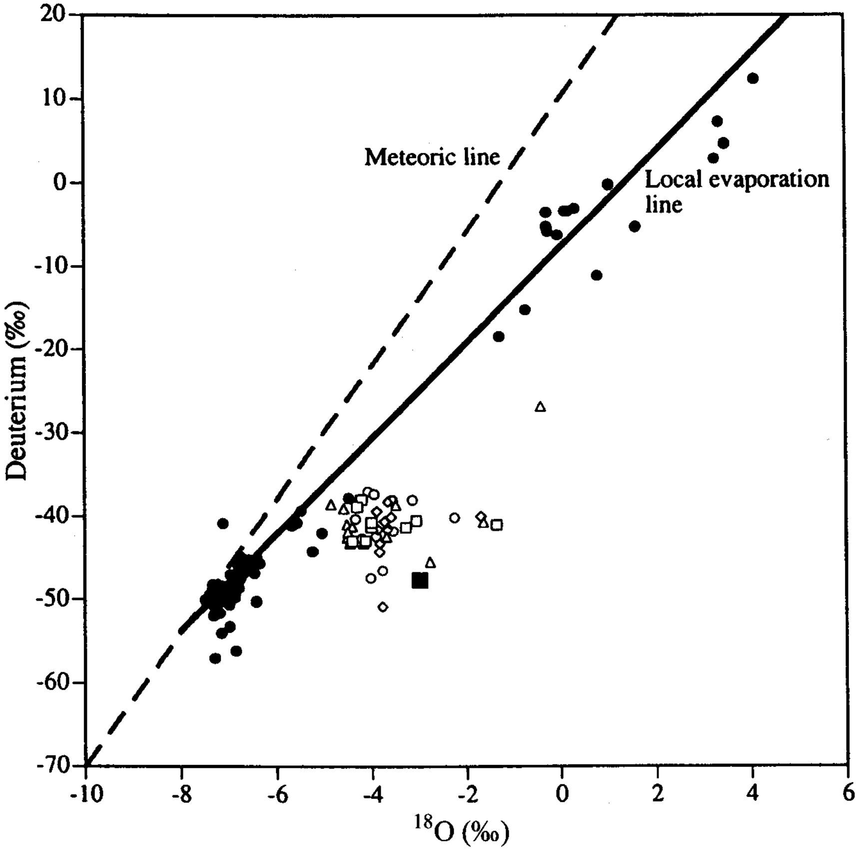

FIG. 16.20. δ^2H–$\delta^{18}O$ relationship in surface waters, cold groundwaters and geothermal reservoir waters from Momotombo wells. Dots: non-thermal waters. Circles, diamonds, triangles and squares denote the isotopic composition for aquifer water of Momotombo wells collected in January 1996, November 1996, May 1997 and November 1997, respectively. The large filled square designates anticipated initial reservoir water isotope composition as based on a sample collected before exploitation. From Arnórsson (1998).

Nicaragua. Most of the surface and non-thermal groundwaters are a little displaced from the meteoric line, and some are displaced even quite significantly, defining a local evaporation line. The aquifer fluids for the wet steam wells at Momotombo have deuterium values less negative by 5–10‰ than most of the local non-thermal waters. This relationship has been taken to indicate that the geothermal water is a mixture of local meteoric water and magmatic water ('andesitic water') (Giggenbach, 1992). However, in view of the observation that many of the local waters have been enriched in the heavy isotopes of deuterium and ^{18}O through evaporation, the possibility exists that water of meteoric origin, which infiltrates the Momotombo geothermal reservoir, has been enriched in deuterium through surface evaporation and that mixing with magmatic water is not required to explain the difference in the δ^{2}H content of local meteoric water and the Momotombo geothermal reservoir water. Despite the evidence from decreasing Cl concentrations in well discharges of cold water recharge into the Momotombo reservoir, a change towards less δ^{18}O shift with time has not been observed. Such a shift has, however, been observed for other geothermal fields, such as Cerro Prieto, Mexico (Truesdell, 1991). It is possible that the lack of observable δ^{18}O shift at Momotombo is due to too short a time of observation (two years).

BOX 16.1. RECOMMENDED FREQUENCY OF SAMPLING FOR PARTIAL AND FULL ANALYSIS DURING MONITORING STUDIES

Frequency of sampling

As a general rule for dry and wet steam wells which are discharged for the first time, it is recommendable that samples for full analysis should be collected weekly for the first month, thereafter bimonthly for a year and subsequently during production for about three times a year. For hot water wells, less frequent sampling is generally required, or about monthly to bimonthly for the first year and thereafter annually. Samples for partial analysis of water and steam should be collected bimonthly after one year of discharge, i.e. every other sample should be fully analysed and every other sample partially analysed for certain constituents.

It is anticipated that no specific recommendations as to the frequency of sampling can be given. The final decision must be taken by the expert responsible for the monitoring studies. If the concentrations of the chemical and isotopic components show much fluctuations or rapid changes, more frequent sampling is required than in the case of discharges with stable chemical and isotopic composition.

Partial analysis

Water samples:	SiO_2, B, Na, K, Ca, SO_4 and Cl
Steam samples:	CO_2, H_2S, H_2, CH_4, N_2, O_2 and Ar

Full analysis

Water samples:	pH, SiO_2, B, Na, K, Ca, Mg, CO_2, SO_4, H_2S, Cl, F, δ^2H and $\delta^{18}O$
Steam samples:	CO_2, H_2S, NH_3, H_2, CH_4, N_2, O_2 and Ar

BOX 16.2. CONCENTRATIONS OF AQUEOUS AND GASEOUS COMPONENTS IN WATER AND STEAM FROM WET STEAM WELLS — DEPENDENCE ON DISCHARGE ENTHALPY

Three sets of samples of water and steam were collected from a wet steam well at atmospheric pressure (1 bar). The total discharge enthalpy at the time of sampling was also measured. The results for Cl in the water and CO_2 in the steam are as follows:

	Cl (ppm)	CO_2 (mmole/kg)	Discharge enthalpy (kJ/kg)
(1)	1150	235	1300
(2)	1230	300	2000
(3)	2500	380	2600

Calculate the concentrations of Cl and CO_2 in the water and steam phases at 10 bars abs. saturated steam pressure (equivalent to 180°C).

Steam fractions (Y) are given by:

$$Y_i = \frac{h^t - h_i^w}{L_i}$$

where h^t represents the enthalpy of the total discharge and h_i^w and L_i the enthalpy of steam saturated water and its latent heat of vaporization at the temperature (or pressure) conditions, indicated by the subscript. For samples (1), (2) and (3), the steam fractions are as follows at 100°C (1 bar abs.) and 180°C (10 bar abs.), respectively:

	Y_{100}	Y_{180}
(1)	0.390	0.267
(2)	0.700	0.614
(3)	0.966	0.912

Equations (12.2a) and (12.2b) describe the concentrations of Cl and CO_2 in the water and steam phases at any temperature. Accordingly, we have:

BOX 16.2. (cont.)

$$m^t_{\mathrm{Cl}} = m^w_{\mathrm{Cl},180}\,(1 - Y_{180}) = m^w_{\mathrm{Cl},100}\,(1 - Y_{100})$$

and

$$m^t_{\mathrm{CO_2}} = m^s_{\mathrm{CO_2},180} Y_{180} = m^s_{\mathrm{CO_2},100} Y_{100}$$

With the aid of these equations, the following concentrations at 180°C are obtained:

	Cl (ppm)	CO_2 (mmole/kg)
(1)	957	343
(2)	956	342
(3)	966	359

BIBLIOGRAPHY

ADAMS, M.C. (1995), "Vapor, liquid, and two phase tracers for geothermal systems", Proceedings of the World Geothermal Congress, Florence, Italy, 1875–1880.

ARAÑA, V., PANICHI, C. (1974), Isotopic composition of steam samples from Lanzarote, Canary Island, Geothermics **3**, 142.

ARANGO, E., BUITRAGO, A.J., CATALDI, R., FERRARA, G.C., PANICHI, C., VILLEGAS, V.G. (1970), Preliminary study on the Ruiz geothermal project (Columbia), Geothermics (Special Issue 2) **2**, 43.

ÁRMANNSSON, H., GÍSLASON, G., HAUKSSON, T. (1982), Magmatic gases in well fluids aid the mapping of flow pattern in a geothermal system, Geochim. Cosmochim. Acta **46**, 167–177.

ÁRMANNSSON, H., GUDMUNDSSON, Ás., STEINGRÍMSSON, B.S. (1987), Exploration and development of the Krafla geothermal area, Jökull **37**, 13–30.

ÁRNASON, B. (1977a), Hydrothermal systems in Iceland traced by deuterium, Geothermics **5**, 125–151.

ÁRNASON, B. (1977b), The hydrogen and water isotope thermometer applies to geothermal areas in Iceland, Geothermics **5**, 75–80.

ARNÓRSSON, S. (1998), Interpretation of Chemical and Isotopic Data on Fluids Discharged from Wells in the Momotombo Geothermal Field with Notes on Gas Chromatography Analysis, Rep. IAEA (Project NIC/8/008-05), June 1998, 28 p.

ARNÓRSSON, S. (1995b), Geothermal systems in Iceland: Structure and conceptual models. I. High-temperature areas, Geothermics **24**, 603–629.

ARNÓRSSON, S. (1995a), Geothermal systems in Iceland: Structure and conceptual models. II. Low-temperature areas, Geothermics **24**, 561–602.

ARNÓRSSON, S. (1991), "Geochemistry and geothermal resources in Iceland", Applications of Geochemistry in Geothermal Reservoir Development (Coordinator: D'AMORE, F.), UNITAR publication, Rome, 145–196.

ARNÓRSSON, S. (1986), The chemistry of gases associated with geothermal activity and volcanism in Iceland, J. Geophys. Res. **91**, 12, 261–12, 268.

ARNÓRSSON, S. (1985), The use of mixing models and chemical geothermometers for estimating underground temperatures in geothermal systems, J. Volc. Geothermal Res. **23**, 299–335.

ARNÓRSSON, S. (1984), Germanium in Icelandic geothermal systems, Geochim. Cosmochim. Acta **48**, 2489–2502.

ARNÓRSSON, S. (1975), Application of the silica geothermometer in low-temperature hydrothermal areas in Iceland, Am. J. Sci. **275**, 763–784.

ARNÓRSSON, S., ANDRÉSDÓTTIR, A. (1995), Processes controlling the chemical composition of natural waters in the Hreppar-Land area in southern Iceland, IAEA-TECDOC-788, IAEA, Vienna 21–43.

ARNÓRSSON, S., STEFÁNSSON, A. (1998), Assessment of feldspar solubility in water in the range 0–350°C at P_{sat}, submitted to Am. J. Sci.

ARNÓRSSON, S., SVAVARSSON, H. (1985), Application of chemical geothermometry to geothermal exploration and development, Geotherm. Resources Council Trans. **9**, 293–298.

ARNÓRSSON, S., GUNNLAUGSSON, E. (1985), New gas geothermometers for geothermal exploration — Calibration and application, Geochim. Cosmochim. Acta **49**, 1307–1325.

ARNÓRSSON, S., ANDRÉSDÓTTIR, A., GUNNARSSON, I., STEFÁNSSON, A. (1998a), "New calibration for the quartz and Na/K geothermometers — valid in the range 0–350°C", Proc. Geoscience Society of Iceland Annual Meeting, April 1994, 42–43 (in Icelandic).

ARNÓRSSON, S., BJÖRNSSON, S., MUNA, Z.W., OJIAMBO, S.B. (1990), The use of gas chemistry to evaluate boiling processes and initial steam fractions in geothermal reservoirs with an example from the Olkaria field, Kenya, Geothermics **19**, 497–514.

ARNÓRSSON, S., FRIDRIKSSON, Th., GUNNARSSON, I. (1998b), "Gas chemistry of the Krafla geothermal field, Iceland", Water–Rock Interaction, Proc. Int. Symp. Auckland, New Zealand, 613–616.

ARNÓRSSON, S., GEIRSSON, K., ANDRÉSDÓTTIR, A., SIGURDSSON, S. (1996), Compilation and Evaluation of Thermodynamic Data on Aqueous Species and Dissociational Equilibria in Aqueous Solution. I. The Solubility of CO_2, H_2S, H_2, CH_4, N_2, O_2 and Ar in Pure Water, Science Institute Rep. 20–95, 20 pp.

ARNÓRSSON, S., GUNNLAUGSSON, E., SVAVARSSON, H. (1983b), The chemistry of geothermal waters in Iceland. III. Chemical geothermometry in geothermal investigations, Geochim. Cosmochim. Acta **47**, 567–577.

ARNÓRSSON, S., GUNNLAUGSSON, E., SVAVARSSON, H. (1983a), The chemistry of geothermal waters in Iceland. II. Mineral equilibria and independent variables controlling water compositions, Geochim. Cosmochim. Acta **47**, 547–566.

ARNÓRSSON, S., SVEINBJÖRNSDHÓTTIR, Á.E., ANDRÉSDÓTTIR, A. (1995), "Processes influencing δ^2H, $\delta^{18}O$, B and Cl distribution in cold and thermal waters in the NW-Peninsula and in the Southern Lowlands, Iceland", Isotope and Geochemical Techniques Applied to Geothermal Investigations, IAEA-TECDOC-788, IAEA, Vienna, 45–61.

ARNÓRSSON, S., SIGURDSSON, S., SVAVARSSON, H. (1982), The chemistry of geothermal waters in Iceland. I. Calculation of aqueous speciation from 0° to 370°, Geochim. Cosmochim. Acta **46**, 1513–1532.

BAERTSCHI, P. (1976), Absolute ^{18}O content of Standard Mean Ocean Water, Earth Planet. Sci. Letter **31**, 341.

BECKER, R.H., CLAYTON, R.N. (1976), Oxygen isotope study of a Precambrian banded iron formation, Hamerley Range, Western Australia, Geochim. Cosmochim. Acta **40**, 1153–1165.

BJÖRNSSON, A., SAEMUNDSSON, K., EINARSSON, P., TRYGGVASON, E., GRÖNVOLD, K. (1977), Current rifting episode in north Iceland, Nature **266**, 318–323.

BJÖRNSSON, S., ARNÓRSSON, S., TÓMASSON, J. (1972), Economic evaluation of the Reykjanes thermal brine area, Iceland, Bull. Am. Assoc. Petrol. Geol. **56**, 2380–2391.

BÖDVARSSON, G. (1982), Glaciation and geothermal processes in Iceland, Jökull **32**, 21–28.

BOTTINGA, Y. (1969), Calculated fractionation factors for carbon and hydrogen isotope exchange in the system calcite–carbon dioxide–graphite–methane–hydrogen–water vapor, Geochim. Cosmochim. Acta **33**, 49.

BOWERS, T.S., JACKSON, K.J., HELGESON, H.C. (1984), Equilibrium Activity Diagrams for Coexisting Minerals and Aqueous Solutions at Pressures and Temperatures to 5 kb and 600°C, Springer-Verlag, New York.

CRAIG, H. (1961), Standards for reporting concentrations of deuterium and oxygen-18 in natural waters, Science **133**, 1833–1834.

CRAIG, H., BOATO, G., WHITE, D.E. (1956), "Isotope geochemistry of thermal waters", Nuclear Processes in Geologic Settings (Proc. 2nd Conf. National Academy of Sciences — National Research Council), paper 400, 29–38.

CRAIG, H. (1966), Isotopic composition and origin of the Red Sea and Salton Sea geothermal brines, Science **154**, 1544.

CRAIG, H. (1963), "The isotopic geochemistry of water and carbon in geothermal areas", Nuclear Geology in Geothermal Areas, Consiglio Nazionale delle Ricerche, Laboratorio di Geologia Nucleare, Pisa, Italy, 17–53.

CRAIG, H. (1975), Oral presentation to the IAEA Advisory Group on the application of nuclear techniques to geothermal studies, Pisa, Italy, 8–12 September 1975.

CRERAR, D.A., ANDERSON, G.M. (1971), Solubility and solvation reactions of quartz in dilute hydrothermal solutions, Chem. Geol. **8**, 107–122.

D'AMORE, F., CELATI, C. (1983), Methodology for calculating steam quality in geothermal reservoirs, Geothermics **12**, 129–140.

D'AMORE, F., GIANELLI, G. (1984), Mineral assemblages and oxygen and sulphur fugacities in natural water–rock interaction processes, Geochim. Cosmochim. Acta **48**, 847–857.

D'AMORE, F., PANICHI, C. (1980), Evaluation of deep temperatures in hydrothermal systems by a new gas geothermometer, Geochim. Cosmochim. Acta **44**, 549–556.

D'AMORE, F., TRUESDELL, A.H. (1989), "A review of solubilities and equilibrium constants for gaseous species of geothermal interest", Sci. Geol. Bull. **41**, 309–332.

D'AMORE, F., TRUESDELL, A.H. (1985), Calculation of geothermal reservoir temperatures and steam fractions from gas compositions, Geotherm. Resources Council Trans. **9**, 305–310.

D'AMORE, F., GERARDO, J., SEASTRES, J., CALVI, E. (1995), "Fluid isotopic composition in the Palinpinon 1 geothermal system (Philippines)", Water Resources Management (Proc. Int. Symp. Vienna, 1995) 423.

FRANZSON, H. (1988), Nesjavellir, borehole geology and permeability in the reservoir. National Energy Authority Rep. OS-88046/JHD-09 (in Icelandic, with an English summary).

EINARSSON, P. (1978), S-wave shadows in the Krafla caldera in NE-Iceland, evidence for a magma chamber in the crust, Bull. Volcanol. **43**, 1–9.

ELLIS, A.J., MAHON, W.A.J. (1964), Natural hydrothermal systems and experimental hot water/rock interactions, Part I, Geochim. Cosmochim. Acta **28**, 1323–1357.

ELLIS, A.J., MAHON, W.A.J. (1967), Natural hydrothermal systems and experimental hot water/rock interactions, Part II, Geochim. Cosmochim. Acta **31**, 519–538.

ELLIS, A.J., WILSON, S.H. (1960), The geochemistry of alkali metals ions in the Wairakei hydrothermal system, N. Z. J. Geol. Geophys. **3**, 593–617.

EPSTEIN, S., MAYEDA, T. (1953), Variation of ^{18}O content of waters from natural sources, Geochim. Cosmochim. Acta **4**, 213–224.

FLÖRKE, O.W., JONES, J.B., SCHMINKE, H.U. (1976), A new microcrystalline silica from Gran Canaria, Z. Kristallogr. **143**, 156–165.

FOUILLAC, R., MICHARD, S. (1981), Sodium/lithium ratio in water applied to geothermometry of geothermal reservoirs, Geothermics **10**, 55–70.

FOURNIER, R.O. (1960), Solubility of quartz in water in the temperature interval from 25°C to 300°C, Geol. Soc. Am. Bull. **71**, 1867–1868.

FOURNIER, R.O. (1979), A revised equation for the Na/K geothermometer, Geotherm. Resources Council Trans. **3**, 221–224.

FOURNIER, R.O. (1991), "Water geothermometers applied to geothermal energy", Applications of Geochemistry in Geothermal Reservoir Development (Coordinator: D'AMORE, F.), UNITAR publication, Rome, 37–69.

FOURNIER, R.O. (1977), Chemical geothermometers and mixing models for geothermal systems, Geothermics **5**, 41–50.

FOURNIER, R.O., POTTER, R.W.II, (1982), A revised and expanded silica (quartz) geothermometer, Geotherm. Res. Council Bull. **11**, 3–9.

FOURNIER, R.O., POTTER, R.W.II, (1979), Magnesium correction to the Na–K–Ca chemical geothermometer, Geochim. Cosmochim. Acta **43**, 1543–1550.

FOURNIER, R.O., TRUESDELL, A.H. (1973), An empirical Na–K–Ca geothermometer for natural waters, Geochim. Cosmochim. Acta **37**, 1255–1275.

FRANZSON, H. (1988), Nesjavellir, borehole geology and permeability in the reservoir, National Energy Authority Rep. OS-88046/JHD-09 (in Icelandic, with an English summary).

FRIDLEIFSSON, I.B. (1996), Present status and potential role of geothermal energy in the world, World Renewable Energy Congress IV, Denver, Colorado, 15–21 June.

FRIEDMAN, I. (1953), Deuterium content of natural water and other substances, Geochim. Cosmochim. Acta **4**, 89–103.

GERARDO, J.Y., NUTI, S., D'AMORE, F., SEASTRES, J.S., GONFIANTINI, R., (1993), Isotopic evidence for magmatic and meteoric water recharge and the processes affecting reservoir fluids in the Palinpinon geothermal system, Philippines, Geothermics **22**, 521–533.

GIGGENBACH, W.F. (1992), Isotopic shifts in waters from geothermal and volcanic systems along convergent plate boundaries and their origin, Earth Planet. Sci. Lett. **113**, 495–510.

GIGGENBACH, W.F. (1991), "Chemical techniques in geothermal exploration", Application of Geochemistry in Geothermal Reservoir Development (D'AMORE, F., Ed.), UNITAR/UNDP Centre on Small Energy Resources, Rome, 119–144.

GIGGENBACH, W.F. (1988), Geothermal solute equilibria, Geochim. Cosmochim. Acta **52**, 2749–2765.

GIGGENBACH, W.F. (1984), Mass transfer in hydrothermal alteration systems, Geochim. Cosmochim. Acta **48**, 2693–2711.

GIGGENBACH, W.F. (1981), Geothermal mineral equilibria, Geochim. Cosmochim. Acta **45**, 27–27.

GIGGENBACH, W.F. (1980), Geothermal gas equilibria, Geochim. Cosmochim. Acta **44**, 2021–2032.

GÍSLASON, S.R., HEANEY, P.J., OELKERS, E.H., SCHOTT, J. (1997), Kinetic and thermodynamic properties of moganite, a novel silica polymorph, Geochim. Cosmochim. Acta **61**, 1193–1204

GÍSLASON, S.R., unpublished data.

GONFIANTINI, R., BORSI, S., FERRARA, G., PANICHI, C. (1973), Isotopic composition of waters from the Danakil Depression, Earth Planet. Sci. Lett. **18**, 13.

GUDMUNDSSON, B.Th., ARNÓRSSON, S. (1997), Krafla: Compilation of Chemical Analysis of Water and Steam Discharged from Wells and Proposed for Further Data Interpretation, Rep. RH 16-97, The National Power Company and The Science Institute.

GUNNARSSON, I., ARNÓRSSON, S. (1998), Amorphous silica solubility and the thermodynamic properties of aqueous silica in the range 0–350°C, to be submitted to Geochim. Cosmochim. Acta.

GUNNLAUGSSON, E. (1977), The Origin and Distribution of Sulphur in Fresh and Geothermally Altered Rocks in Iceland, PhD thesis, Univ. Leeds.

GUNTER, B.D., MUSGRAVE, B.C. (1971), New evidence on the origin of methane in hydrothermal gases, Geochim. Cosmochim. Acta **35**, 113–118.

HAGEMANN, R., NIEF, G., ROTH, E. (1970), Absolute isotope scale for deuterium analysis of natural waters. Absolute D/H ratio for SMOW, Tellus **22**, 712.

HELGESON, H.C., DELANY, J.M., NESBITT, H.W., BIRD, D.K. (1978), Summary and critique of the thermodynamic properties of rock-forming minerals, Am. J. Sci. **278A**, 1–229.

HELGESON, H.C., KIRKHAM, D.H. (1974), Theoretical prediction of the thermodynamic behavior of aqueous electrolytes at high pressures and temperatures: I. Summary of the thermodynamic/electrostatic properties of the solvent, Am. J. Sci. **274**, 1089–1198.

HEMLEY, J.J., MONTOYA, J.W., MARINENKO, J.W., LUCE, R.W. (1980), Equilibria in the system $A_{12}O_3$–SiO_2–H_2O and some general implications for alteration/mineralization processes, Econ. Geol. **75**, 210–653.

HENLEY, R.W., TRUESDELL, A.H., BARTON, P.B., Jr., WHITNEY, J.A. (1984), Fluid–mineral equilibria in hydrothermal systems, Reviews in Economic Geology, Vol. 1, Society of Economic Geologists, The Economic Geology Publishing Company, El Paso, Texas.

HOEFS, J. (1997), Stable Isotope Geochemistry, Springer-Verlag, Berlin.

HULSTON, J.R., McCABE, W.J. (1962), Mass spectrometer measurement in the thermal areas of New Zealand. Part I. Carbon dioxide and residual gas analysis, Geochim. Cosmochim. Acta **26**, 383–397.

INTERNATIONAL ATOMIC ENERGY AGENCY (1983), Guidebook on Nuclear Techniques in Hydrology, Technical Reports Series No. 91, IAEA , Vienna.

INTERNATIONAL ATOMIC ENERGY AGENCY (1981), Stable Isotope Hydrology, Technical Reports Series No. 210, IAEA , Vienna.

KENNEDY, G.C. (1950), A portion of the system silica–water, Econ. Geol. **45**, 629–653.

KHARAKA, Y.K., MARINER, R.H. (1988), "Chemical geothermometers and their application to formation waters from sedimentary basins", Thermal History of Sedimentary Basins (NASER, N.D., McCOLLIN, T.H., Eds), Springer-Verlag, New York, 99–117.

KHARAKA, Y.K., LICO, M.S., LAW, L.M. (1982), Chemical geothermometers applied to formation waters, Gulf of Mexico and California Basins, Am. Assoc. Petrol. Geol. Bull. **66**, 538.

KITAHARA, S. (1960a), The solubility of quartz in the aqueous sodium chloride solutions at high temperatures and high pressures, Rev. Phys Chem. Jpn. **30**, 115–121.

KUSAKABE, M. (1974), Sulphur isotope variations in nature. 10: Oxygen and sulphur isotope study of Wairakei geothermal well discharges, N. Z. J. Sci. **17**, 183.

LLOYD, R.M. (1968), Oxygen isotope behaviour in the sulfate–water system, J. Geophys. Res. **73**, 6099.

LYON, G.L. (1974), "Geothermal gases", Natural Gases in Marine Sediments (KAPLAN, I.R., Ed.), Plenum Press, New York.

LYON, G.L., HULSTON, J.R. (1984), Carbon and hydrogen isotope compositions of New Zealand geothermal gases, Geochim. Cosmochim. Acta **44**, 161–171.

MACKENZIE, F.T., GEES, R. (1971), Quartz: Synthesis at earth surface conditions, Science **173**, 533–535.

MIZUTANI, Y., RAFTER, T.A. (1969), Oxygen isotope composition of sulphates. Oxygen isotope fractionation in the bisulphate ion–water system, N. Z. J. Sci. **12**, 54.

MOREY, G.W., FOURNIER, R.O., ROVE, J.J. (1962), The solubility of quartz in water in the temperature interval from 25 to 300°C, Geochim. Cosmochim. Acta **26**, 1029– 1043.

MIYASHIRO, A. (1994), Metamorphic Petrology, ULC Press, London.

NAKAI, N. (1968), Geochemical estimation of temperature and state of H_2O at the bottom of geothermal wells, Bull. Jpn. Geothermal Eng. Assoc. **17**, 45.

NEHRING, N.L., D'AMORE, F. (1984), Gas chemistry and thermometry of the Cerro Prieto, Mexico, geothermal field, Geothermics **13**, 75–89.

NIEVA, D., NIEVA, R. (1987), Developments in geothermal energy in Mexico, Part 12. A cationic geothermometer for prospecting of geothermal resources, Heat Recovery Systems & CHP **7**, 243–258.

NORDSTROM, D.K., MONOZ, J.L. (1994), Geochemical thermodynamics, Blackwell Scientific Publications, Cambridge, MA.

NUTI, S. (1991), "Isotope techniques in geothermal studies", Applications of Geochemistry in Geothermal Reservoir Development (Co-ordinator: D'AMORE, F.), UNITAR publication, Rome, 215–251.

NUTI, S., CAPRAI, A., NOTO, P. (1985), Hypothesis on the origin of steam and on the deep temperatures of the fluids of Pozzuoli Solfatara (Campania, Italy), paper presented at 1985 Int. Symp. Geothermal Energy, 9th Annual Meeting, Geothermal Resources Council.

PACES, T. (1975), A systematic deviation from the Na–K–Ca geothermometer below 75°C and above 10^{-4} atm. P_{CO_2}. Geochim. Cosmochim. Acta **39**, 541–544.

PANICHI, C., NUTI, S., NOTO, P. (1979), "Use of isotopic geothermometers in the Larderello geothermal field", Isotope Hydrology 1978 (Proc. Int. Symp. Neuherberg 1978), Vol. 2, IAEA, Vienna (1979) 613–630.

PANICHI, C., GONFIANTINI, R. (1976), "Environmental isotopes in geothermal studies", Energía Geotérmica en América Latina (Proc. Symp. Guatemala City, 1976) 29–70.

PANICHI, C., CELATI, R., NOTO, P., SQUARCI, P., TAFFI, L., TONGIORGI, E. (1974), "Oxygen and hydrogen isotope studies of the Larderello geothermal system", Isotope Techniques in Groundwater Hydrology (Proc. Symp. Vienna, 1974), Vol. 2, IAEA, Vienna, 3.

POREDA, R.J., CRAIG, H., ARNÓRSSON, S., WELHAN, J.A. (1992), Helium isotopes in Icelandic geothermal systems: I. ^{3}He, gas chemistry, and ^{13}C relations, Geochim. Cosmochim. Acta **56**, 4221–4228.

REED, M., SPYCHER, N. (1984), Calculation of pH and mineral equilibria in hydrothermal waters with application to geothermometry and studies of boiling and dilution, Geochim. Cosmochim. Acta **48**, 1479–1492.

REYES, A.G. (1991), Mineralogy, distribution and origin of acid alteration in Philippine geothermal systems, Geol. Surv. Jpn. Rep. **277**, 59–66.

RICHET, P., BOTTINGA, Y., JAVOY, M. (1977), A review of hydrogen, carbon, nitrogen, oxygen, sulfur and chlorine stable isotope fractionation among gaseous molecules, Ann. Reg. Earth Planet. Sci. **5**, 65–110.

RIMSTIDT, J.D. (1997), Quartz solubility at low temperatures, Geochim. Cosmochim. Acta **61**, 2553–2558.

SEASTRES, J.S., HERMOSO, D.Z., CANDELARIA, M.N., GERARDO, J.Y. (1995), Application of geochemical techniques in evaluating the reservoir response to exploitation at Palinpinon geothermal field, Philippines, Proc. 1995 World Geothermal Congress, Florence, Italy.

SHAW, D.M., STURCHIO, N.C. (1992), Boron–lithium relationships in rhyolites and associated thermal waters of young silicic calderas with comments on incompatible element behaviour, Geochim. Cosmochim. Acta **56**, 3723–3731.

SIEVER, R. (1962), Silica solubility 0–200°C, and the diagenesis of siliceous sediments, J. Geol. **70**, 127–150.

STEINGRÍMSSON, B., FRIDLEIFSSON, G.Ó., SVERRISDÓTTIR, G., TULINIUS, H., SIGURDSSON, Ó., GUNNLAUGSSON, E. (1986b), Nesjavellir, Well NJ-15. Drilling, Investigations and Production Characteristics, National Energy Authority Rep. OS-86029/JHD-09 (in Icelandic).

SVEINBJÖRNSDÓTTIR, Á.E., JOHNSEN, S.J., ARNÓRSSON, S. (1995), The use of stable isotopes of oxygen and hydrogen in geothermal studies in Iceland, World Geothermal Congress, Florence, Italy, 1043–1048.

SVEINBJÖRNSDÓTTIR, Á.E., HEINEMEIER, J., ARNÓRSSON, S. (1995), Origin of ^{14}C in Icelandic groundwater, Radiocarbon **37**, 551–565.

THORSSANDER, P. (1986), Origin of volcanic sulfur in Iceland. A sulfur isotope study, Meddelanden från Stockholms Universitets Geologiska Institution, No. **269**.

TÓMASSON, J., KRISTMANNSDÓTTIR, H. (1972), High temperature alteration minerals and thermal brines, Reykjanes, Iceland, Contrib. Mineral. Petrol. **36**, 123–134.

TONANI, F. (1980), Some remarks on the application of geochemical techniques in geothermal exploration, Proc. Adv. Eur. Geoth. Res., 2nd Symp. Strasbourg, 428–443.

TRUESDELL, A.H., NATHENSON, M., RYE, R.O. (1977), The effects of subsurface boiling and dilution on the isotopic composition of Yellowstone geothermal waters, J. Geophys. Res. **82**, 3694–3704.

TRUESDELL, A.H., FOURNIER, R.O. (1977), Procedure for estimating the temperature of a hot water component in a mixed water using a plot of dissolved silica vs enthalpy, US Geol. Survey J. Res. **5**, 49–52.

TRUESDELL, A.H. (1991), "Effects of physical processes on geothermal fluids", Application of Geochemistry in Geothermal Reservoir Development (D'AMORE, F., Ed.), UNITAR/UNDP Centre on Small Energy Resources, Rome, 71–92.

TRUESDELL, A.H., HULSTON, J.R. (1980), "Isotope evidence on environments of geothermal systems", Handbook of Environmental Isotope Geochemistry (FRITZ, P., FONTES, Ch.J., Eds) **1**, 179–226.

TRUESDELL, A.H. (1976), Summary of Section III. Geochemical Techniques in Exploration, Second United Nations Symposium on the Development and Use of Geothermal Resources, San Francisco, 53–79.

UNITAR (1991), Application of Geochemistry in Geothermal Reservoir Development (Co-ordinator: DÓAMORE, F.), UNITAR publication, Rome.

VAN LIER, J.A., DE BRUYN, P.L., OVERBEEK, J.T.G. (1960), The solubility of quartz, J. Phys. Chem. **64**, 1675–1682.

WALTHER, J.V., HELGESON, H.C. (1977), Calculation of the thermodynamic properties of aqueous silica and the solubility of quartz and its polymorphs at high pressures and temperatures, Am. J. Sci. **277**, 1315–1351.

WHITE, D.E. (1970), Geochemistry applied to the discovery, evaluation, and exploitation of geothermal energy resources, Geothermics, Special Issue 2, **1**, 58–78.

WHITE, D.E., MUFFLER, L.J.P., TRUESDELL, A.H. (1971), Vapour-dominated hydrothermal systems compared with hot water systems, Econ. Geol. **66**, 75–97.

No. 11, June 2000

WHERE TO ORDER IAEA PUBLICATIONS

In the following countries IAEA publications may be purchased from the sources listed below, or from major local booksellers. Payment may be made in local currency or with UNESCO coupons.

AUSTRALIA
Hunter Publications, 58A Gipps Street, Collingwood, Victoria 3066
Telephone: +61 3 9417 5361 • Fax: +61 3 9419 7154 • *E-mail: jpdavies@ozemail.com.au*

BELGIUM
Jean de Lannoy, avenue du Roi 202, B-1060 Brussels • Telephone: +32 2 538 43 08 • Fax: +32 2 538 08 41
E-mail: jean.de.lannoy@infoboard.be • Web site: http://www.jean-de-lannoy.be

BRUNEI
Parry's Book Center Sdn. Bhd., 60 Jalan Negara, Taman Melawati, 53100 Kuala Lumpur, Malaysia
Telephone: +60 3 4079176, 4079179, 4087235, 4087528 • Fax: +60 3 407 9180
E-mail: haja@pop3.jaring.my • Web site: http://www.mol.net.my/~parrybook/parrys.htm

CANADA
Renouf Publishing Company Ltd., 1-5369 Canotek Rd., Ottawa, Ontario, K1J 9J3
Telephone: +613 745 2665 • Fax +613 745 7660
E-mail: order.dept@renoufbooks.com • Web site: http://www.renoufbooks.com

CHINA
IAEA Publications in Chinese: China Nuclear Energy Industry Corporation, Translation Section, P.O. Box 2103, Beijing

DENMARK
Munksgaard Direct, Postbox 173, DK-1005 København K
Telephone: +45 77 33 33 33 • Fax: +45 77 33 33 77
E-mail: direct@munksgaarddirect.dk • Web site: http://www.munksgaarddirect.dk

FRANCE
Nucléon, Immeuble Platon, Parc les Algorithmes,F-91194 Gif-sur-Yvette, Cedex
Telephone: +33 1 69 353636 • Fax +33 1 69 350099 • *E-mail: nucleon@wanadoo.fr*

GERMANY
UNO-Verlag, Vertriebs- und Verlags GmbH, Am Hofgarten 10, D-53113 Bonn
Telephone: +49 228 94 90 20 • Fax: +49 228 94 90 222
E-mail: unoverlag@aol.com • Web site: http://www.uno-verlag.de

HUNGARY
Librotrade Ltd., Book Import, P.O. Box 126, H-1656 Budapest
Telephone: +36 1 257 7777 • Fax: +36 1 257 7472 • *E-mail: books@librotrade.hu*

INDIA
Allied Publishers Limited, 1-13/14, Asaf Ali Road, New Delhi 110002
Telephone: +91 11 3233002, 004 • Fax: +91 11 3235967
E-mail: aplnd@del2.vsnl.net.in • Web site: http://www.alliedpublishers.com

ISRAEL
YOZMOT Ltd., 3 Yohanan Hasandlar St., P.O. Box 56055, IL-61560 Tel Aviv
Telephone: +972 3 5284851 • Fax: +972 3 5285397

ITALY
Libreria Scientifica Dott. Lucio di Biasio "AEIOU", Via Coronelli 6, I-20146 Milan
Telephone: +39 2 48 95 45 52 or 48 95 45 62 • Fax: +39 2 48 95 45 48

JAPAN
Maruzen Company, Ltd., P.O. Box 5050, 100-3191 Tokyo International
Telephone: +81 3 3275 8539 • Fax: +81 3 3275 0657
E-mail: journal@maruzen.co.jp • Web site: http://www.maruzen.co.jp

MALAYSIA
Parry's Book Center Sdn. Bhd., 60 Jalan Negara, Taman Melawati, 53100 Kuala Lumpur,
Telephone: +60 3 4079176, 4079179, 4087235, 4087528 • Fax: +60 3 407 9180
E-mail: haja@pop3.jaring.my • Web site: http://www.mol.net.my/~parrybook/parrys.htm

NETHERLANDS
Martinus Nijhoff International, P.O. Box 269, NL-2501 AX The Hague
Telephone: +31 793 684 400 • Fax: +31 793 615 698 • *E-mail: info@nijhoff.nl • Web site: http://www.nijhoff.nl*

Swets and Zeitlinger b.v., P.O. Box 830, NL-2160 SZ Lisse
Telephone: +31 252 435 111 • Fax: +31 252 415 888 • *E-mail: infoho@swets.nl • Web site: http://www.swets.nl*

POLAND
Ars Polona, Book Department/Import, P.O. Box 1001, PL-00-950 Warsaw
Telephone: +48 22 826 1201 ext. 147, 151, 159, 167 • Fax: +48 22 826 4763
E-mail: ksiazki@arspolona.com.pl • books119@arspolona.com.pl • Web site: http://www.arspolona.com.pl

SINGAPORE
Parry's Book Center Pte. Ltd., 528 A MacPherson Rd., Singapore 1336
Telephone: +65 744 8673 • Fax: +65 744 8676
E-mail: haja@pop3.jaring.my • Web site: http://www.mol.net.my/~parrybook/parrys.htm

SLOVAKIA
Alfa Press, s.r.o, Račianska 20, SQ-832 10 Bratislava • Telephone/Fax: +421 7 566 0489

SPAIN
Díaz de Santos, S.A., c/ Juan Bravo, 3A, E-28006 Madrid
Telephone: +34 91 781 94 80 • Fax: +34 91 575 55 63 • *E-mail: compras@diazdesantos.es • carmela@diazdesantos.es*
barcelona@diazdesantos.es • julio@diazdesantos.es • Web site: http://www.diazdesantos.es

UNITED KINGDOM
The Stationery Office Ltd, International Sales Agency, 51 Nine Elms Lane, London SW8 5DR
Telephone: +44 171 873 9090 • Fax: +44 171 873 8463
E-mail: Orders to: book.orders@theso.co.uk • Enquiries to: ipa.enquiries@theso.co.uk
Web site: http://www.the-stationery-office.co.uk

UNITED STATES OF AMERICA
Bernan Associates, 4611-F Assembly Drive, Lanham, MD 20706-4391, USA
Telephone: 1-800-274-4447 (toll-free) • Fax: (301) 459-0056 / 1-800-865-3450 (toll-free)
E-mail: query@bernan.com • Web site: http://www.bernan.com

Renouf Publishing Company Ltd., 812 Proctor Ave., Ogdensburg, New York, 13669
Telephone: +888 551 7470 (toll-free) • Fax +888 568 8546 (toll-free)
E-mail: order.dept@renoufbooks.com • Web site: http://www.renoufbooks.com

Orders and requests for information may also be addressed directly to:

Sales and Promotion Unit, International Atomic Energy Agency
Wagramer Strasse 5, P.O. Box 100, A-1400 Vienna, Austria
Telephone: +43 1 2600 22529 (or 22530) • Facsimile: +43 1 2600 29302
E-mail: sales.publications@iaea.org • Web site: http://www.iaea.org/worldatom/Books

INTERNATIONAL ATOMIC ENERGY AGENCY
VIENNA
ISBN 92–0–101600–X